CRANFIELD UNIVERSITY

REZA SALAMAT

GAS PATH DIAGNOSTICS FOR COMPRESSORS

SCHOOL OF ENGINEERING

PhD THESIS

Supervisor: Dr. Yiguang Li
May 2012

CRANFIELD UNIVERSITY

SCHOOL OF ENGINEERING

PhD THESIS

2004-2012

REZA SALAMAT

Gas Path Diagnostics for Compressors

Supervisor: Dr. Yiguang Li

May 2012

Abstract

The use and application of compressors cannot be overemphasized in the aeronautical and oil & gas industries. Yet research works in sufficient depth has not been conducted previously to analyze their actual behaviour under degraded or even new conditions in operation.

For the purpose of degradation modeling and simulation, a compressor model was set up using thermodynamic equations and affinity laws representing the characteristics of a clean compressor. HYSYS was used for degradation modeling analysis by implanting known linear and nonlinear degradation trends for an operating point and taking the compressor measurement changes. It was then assumed the degradation levels are unknown and these were established by applying the compressor health indices to the new compressor map. A diagnostic method for compressors was developed where the prediction in degradation levels were compared for diagnostic purposes.

By applying a unique “successive iteration method” to a real gas site compressor data at various speeds, a compressor performance adaptation technique has been developed in this thesis which maps out the actual performance of the compressor shows the errors in performance prediction has been reduced from 5-15% to a minimum. This performance adaptation method allows the compressor performance map to be adapted against field data of a compressor for a range of speeds. All data were corrected to a common datum and GPA Indices were utilised for the evaluation of confidence in the established method.

By observing the centrifugal compressor performance data from 2006 to 2010, the actual compressor degradation was quantified and modeled by trending techniques for diagnostic and prognostic purposes so that the operator can plan ahead for maintenance by knowing an estimate for the actual health of the compressor at any time.

The major conclusions are that the performance adaptation developed for the site compressor and the diagnostic technique by data trending has been successful. And estimation of degradation in health indicators (throughput, pressure ratio and efficiency drops) by scaling the measurable parameters is a useful tool for diagnostic purposes.

Acknowledgement

My sincere gratitude and appreciation go to my supervisor Dr. Li who helped and supported me with his knowledge and vision throughout these valuable years.

I would also extend my thanks to Professor Pilidis, Professor Alexander (Korakianitis), Ted Gresh, Dr. Ramsden and Dr. Mba for their assistance and support as well as Dr. A. Zohrabian and Dr. J. Howard for their input.

Finally I salute my family for their patience, encouragement and support right from the start in these hard but rewarding times.

I dedicate this thesis to my wife, Nayereh.

Table of Content

List of Figures

List of Tables, Graphs and Charts

Notation

Subscripts

0	Stanation conditions (static plus velocity terms)
ac	Actual
ad	Adiabatic
c	Compressor
clean	Compressor at un-degraded conditions
C_p	Specific Heat Capacity, J/kg/K
D_c	Tip Diameter, meters
deg	Compressor at degraded conditions
ex	Exit
F_h	Hub to Tip ratio of 1st stage
g_{w3}	Compressor external losses
h	heat transfer
in	Inlet
it	Isothermal
p	Polytropic
P	Power
Q_L	Labyrinth seal flow
Q_i	Impeller flow
ref	Referred value of temperature or pressure
s/1	Compressor suction condition
d/2	Compressor discharge condition
s	Isentropic
st	Static conditions
t_0	Initial time
th	Thermal
T_b	Blade temperature
ts	Stagnation-to-static efficiency
ΔT_{stage}	Average total temp rise between each compressor stage, K
z	Vertical direction above a datum

Symbols

a	Velocity of sound
A	Area available for flow
A, B	Constants of mass throughput deterioration
b	Blade height
Y	Ratio of specific heats
C	Absolute flow velocity
Cl	Blade tip /Labyrinth clearance
C_p	Specific heat at constant pressure
C_v	Specific heat at constant volume
d	Derivative operator
δ	Dimensionless component inlet pressure

δ	Small difference operator (thermodynamics)
Δ	Finite difference operator
$\sum$	Summation operator
E	General energy
©	Hypothetical specified conditions
θ	Dimensionless component inlet temperature
g	Gravitational constant
g_c	Unit matching constant in Newton's law
G_p/PWR	Absorbed power (gas power)
h	Head
h	Enthalpy per unit mass
H	Influence Coefficient Matrix (ICM)
H^{-1}	Fault Coefficient Matrix (FCM)
M	Mach Number
m/w	mass flow rate through the compressor
N	Compressor RPM
n	Polytropic index
n	Number of kmoles of gas
η/EEP	Efficiency
p	Pressure
Q	Volumetric flow rate
Q	Heat transfer rate
q	Compressor volumetric Inlet Flow rate, actual
q	Heat per unit mass transferred
ρ	Gas Density
R	Universal Molar Gas Constant (8.314 kN.m/ kmole K)
R_w	Gas constant based on mass of gas
r_C	Compressor pressure ratio
s	Entropy per unit mass
S	Entropy
t	Time
T	Temperature
u	Internal thermal energy per unit mass
v	Volume per unit mass
W	Work or power transfer rate
$\vec{x}$	An independent vector in GPA analysis
$\vec{z}$	A dependent (measurable) vector in GPA analysis
z	Gas compressibility factor
z	Height above a datum

Acronyms

AE	Acoustic Emission
CFD	Computational Fluid Dynamics

CNDF	Compressor Non-dimensional Flow
CNDS	Compressor Non-dimensional Speed
CMT	Condition Monitoring Techniques
DE	Drive End
DOD	Domestic Object Damage
ECT	Exit Cone Temperature
EEP	Polytropic Efficiency
EGT	Exhaust Gas Temperature
FOD	Foreign Object Damage
FOH	Total forced outage hours
GPA	Gas Path Analysis
ISF	Index of Compressor Sensitivity to Fouling
M	Gas Molecular Weight
MMBtu	Million British Thermal Units
MW	Mega Watts energy
N	Compressor Speed (rpm)
NDE	Non Drive End
OEM	Original Equipment Manufacturer
OLM	On-line Monitoring
OPM	Online Performance Monitoring
P	Pressure
PH	Period hours
PR	Pressure Ratio
PTFE	A type of Teflon
PW	Power
RCM	Reliability Centred Maintenance
SFEE	Steady-flow energy equation
VIGV	Variable Inlet Guide Vane
VSV	Variable Stator Vane

1. Introduction

Compressors raise the pressure of a gas stream by the required magnitude and pass it along to the downstream equipment or facilities. They form a very critical and expensive part of oil & gas and aerospace industries with hundreds of billions of dollars invested so far globally in purchases, research & development and these trends will continue into the foreseeable future. Performance-based compressor diagnostics is a pertinent part of this research and development.

Good performance of gas turbine axial compressors and process compressors are of paramount importance in maintaining revenue for these companies. Performance deterioration in gas turbine compressors during operation will result running gas turbine at higher turbine temperatures for the given power output. This will use the creep life more rapidly resulting in increased number of overhauls and increased operating costs. Performance deterioration in process compressors results in increased power demand for a given compressor duty. Performance deterioration will therefore result in increased maintenance activity and increased maintenance costs. Suitable performance monitoring systems can prevent major deterioration and expensive secondary damage. It would detect the problem and prevent this damage resulting in saving in increased maintenance cost and lost operating production. Most performance diagnostic systems available are unable to determine faults accurately which give rise to these performance deterioration. A successful diagnostic system must be able to detect the performance short fall and highlight the components that are failing.

The performance data supplied by the original equipment manufacturer (OEM) are for a specific set of defined inlet gas properties and environmental conditions. Furthermore, these data are for a fleet of compressors rather than the particular compressor supplied to the operator due to manufacturing tolerances (PTC10- Ref. 45). Therefore seldom the compressor at site behaves as promised by OEM. Hence once the compressor has moved to site, the actual performance map of the particular compressor in operation needs to be established as a base line performance based on real site parameters and actual gas. Once into the operation, generation of compressor health indices at selected intervals give snapshots of compressor performance and compared with the established baseline performance gives the compressor diagnostics. It is important to recognize that the base line performance is not a constant expectation and need to be updated with time to ensure maximum compressor performance availability and reduction of operational costs.

In order to diagnose the compressor correctly, the model set up for the site compressor must be highly accurate because, for the same environmental condition, differences between expected and actual measurable parameters such as pressure ratio are the lump sum of actual degradation and any errors due to inaccurate modeling and parameter readings. This thesis describes how measured data reading errors are made diminishingly small at site by regular calibrations and noise reduction. This principally leaves out any performance modeling errors that could be mistaken for degradation. When an accurate performance model is set up for the compressor, the operator can be certain that any deviation from the expected performance (i.e., base line) is principally due to compressor degradation.

As operation time progresses, it is usually expected that degradation will also propagate. In order to investigate the relationship between degradation and time, the health parameters or degradation indices will be established at various times during compressor operation. By developing the degradation or health indices for the compressor at regular intervals it will provide snapshots of the compressor real performance. Therefore, developing a method for generating health indices for compressors by on line monitoring is best way forward for the compressors. It will be noted that when evaluation intervals are too small then the derived data will virtually overlap thus some suitable time interval should be considered for performance evaluation. Figure 1 [developed from Ref 33] demonstrates the expected normal profile of a compressor health and how it degrades with time. It demonstrates the detection and quantification of degradation (degraded performance) at present time in relation to a reference point (un-degraded performance) is diagnostics. It also shows how the maintenance strategies fit in with the health profile of the compressor. Figure 2 [Ref. 33] shows the overall cycle of performance data analysis and maintenance advice based on diagnosis derived from compressor performance simulation as a part of gas turbine.

The actual centrifugal compressor data at site from 2006 onwards are used by the Author to develop a unique performance adaptation by “successive iteration technique” that structures the actual performance of a clean compressor for a range of speeds. For this purpose, the compressor health parameters defined as pressure ratio, polytropic efficiency and throughput obtained from 2006 onwards which are considered as degraded health parameters are compared with the un-degraded or clean health parameters obtained from site tests. The degradation indices are established at various times and these parameter trends are recorded on graphs for validation, analysis and development of diagnostic technique by the Author.

The main objectives of this thesis are to develop:

(i) An adaptation technique for a centrifugal compressor by successive iteration and compressor diagnostics by the generation of degradation indices on measurable or independent parameters (pressure ratio, polytropic efficiency and mass throughput). The proposed adaptation technique will be validated by evaluating errors in predicted measurements before and after the performance adaptation. The methodology for diagnostics will be substantiated by the application Gas Path Analysis (GPA) Indices over several years of site operational data.

(ii) A diagnostic technique to estimate the health of a centrifugal compressor by taking the measured compressor parameters under degraded condition and gauging them with those when the compressor was un-degraded or clean. To accomplish this objective, representative performance maps for a clean compressor will be developed from thermodynamic and proportionality principles and then fed to compressor simulation programme, HYSYS, where the degraded compressor will be modeled and the performance measurements analysed and scaled to estimate the degradation in throughput, efficiency and pressure ratio.

In addition to the above developed techniques using site measurements, the following are covered in this thesis:

1) A comprehensive literature review covering the qualitative principles of thermodynamic laws and efficiency types in compressors, the principles and advances in both centrifugal and axial compressor degradations, mechanisms of degradation and the state of the art compressor online monitoring and diagnostic techniques.
2) Introduction of the advanced compressor simulation package HYSYS with its unique capability of allowing the operator to mimic the near exact compressor measurable input/output under clean and degraded conditions.
3) Sensitivity analysis on the effect of degradation on measurable parameters.

The results are discussed in depth and conclusions made based on the established results.

The diagnostics design tools developed in this thesis can be used as a decision making tool to achieve minimum capital and operating costs for new gas transmission system design or upgrade/expansion of an existing transmission system, upstream and downstream of oil and gas facilities.

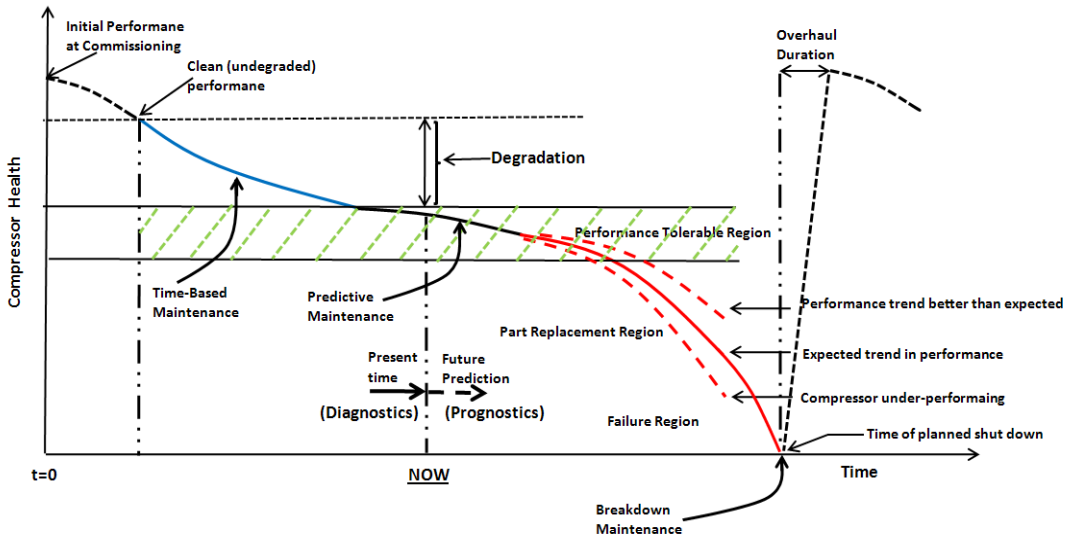

Figure 1. The normal profile of compressor's health with time (developed from Ref. 33)

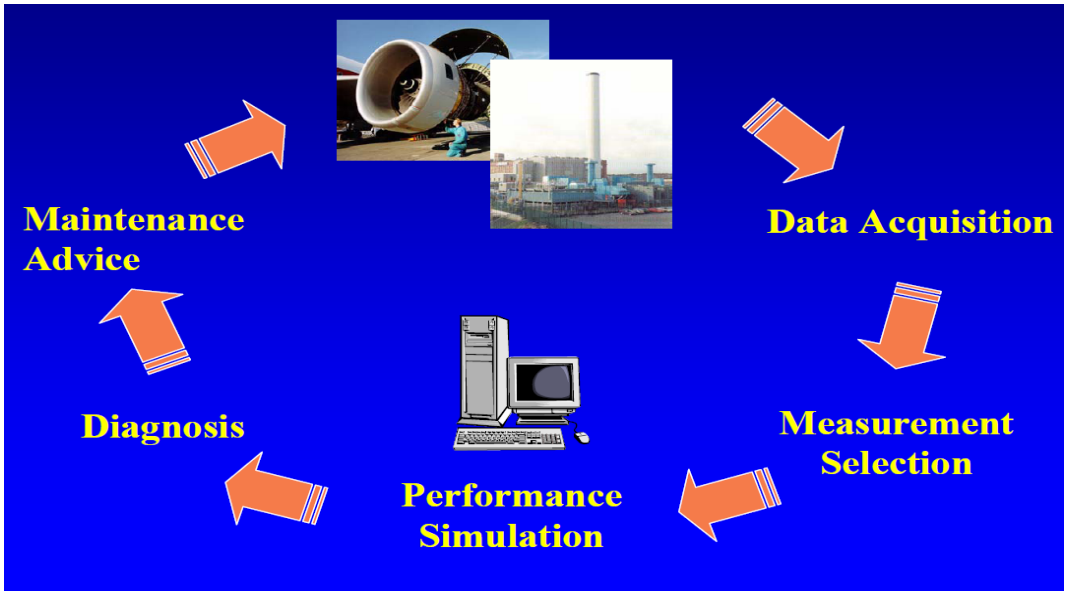

Figure 2. The cycle of rotating equipment on-line performance monitoring [Ref. 33]

2. Literature

2.1 Compressor Operation

Centrifugal and axial compressors respectively find extensive use in the oil & gas and aerospace industries. Optimum design of compressors with highest possible efficiencies has been the prime goal of compressor designers. Reference to Figure 3A, thank to the superior design by the application of CFD, better materials of construction and ever tighter clearances between moving and stationery parts, the polytropic efficiencies of centrifugal compressors has increased by nearly 20% over the past 5 decades from 75% in 1950s to well over 88% in 2000 [Refs 36, 59]. High reliabilities and availabilities are necessary to ensure compressors remain online to perform their duty as expected and maintained as necessary. There are different definitions of efficiency and types in compressor design and operation and these should be well understood by the asset holder and the designer alike to avoid unexpected performance or power demand when in operation. These factors as well the thermodynamic principles are discussed in the following subsection.

The components of a typical centrifugal process compressor are shown in Figures 3B and 3C. Figure 3D shows a gas turbine with its axial compressor component.

Reference to Figures 3B, 3F and 3G on centrifugal compressors, the stationery part of the compressor is the diaphragm which forms a face of the upstream diffuser, part of the return bend, all of the return channel and a face of the downstream diffuser. Each impeller requires a diaphragm. After the gas passes through the first impeller, it enters the diffuser, which systematically reduces the velocity of the gas by increasing the flow area radially. With reference to Figure 3H, the kinetic energy imparted to the gas by the impeller is converted to the pressure rise as a consequence of this velocity reduction in the diffuser. After leaving the diffuser, the gas enters the return bend which guides the gas into the return channel and finally into the next impeller. The return channel includes guide vanes which eliminate swirl in the gas caused by rotation of the preceding impeller. After the gas passes through the last diffuser, it enters the discharge volute which directs the gas to the discharge nozzle and into the piping system.

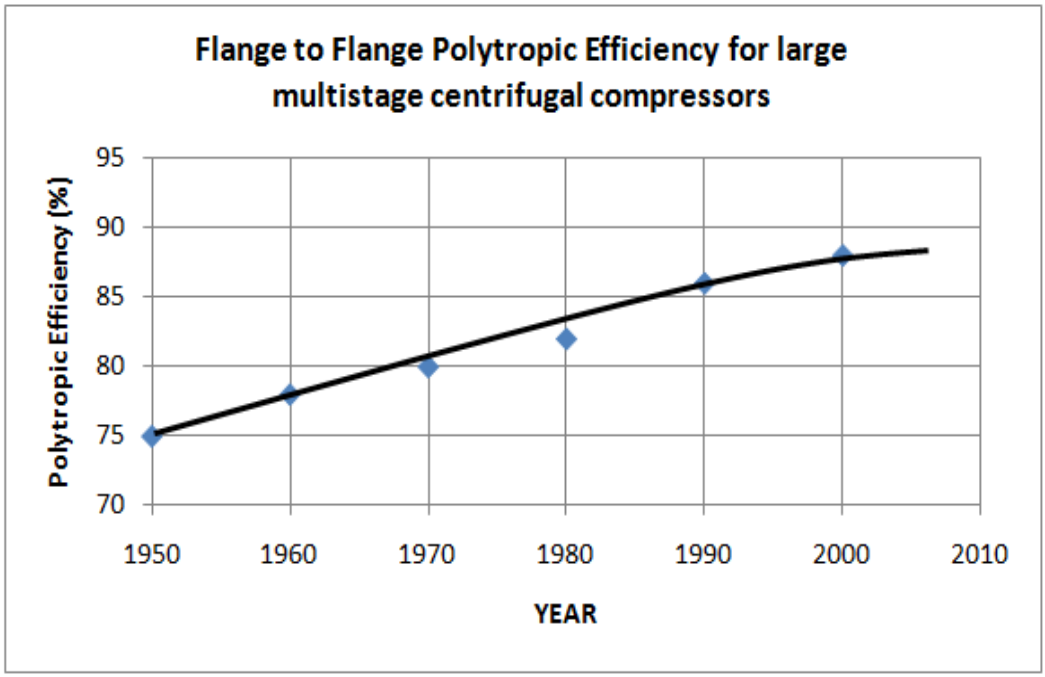

Figure 3A. The increasing trend in compressor efficiency over the past 50 years [Ref. 59]

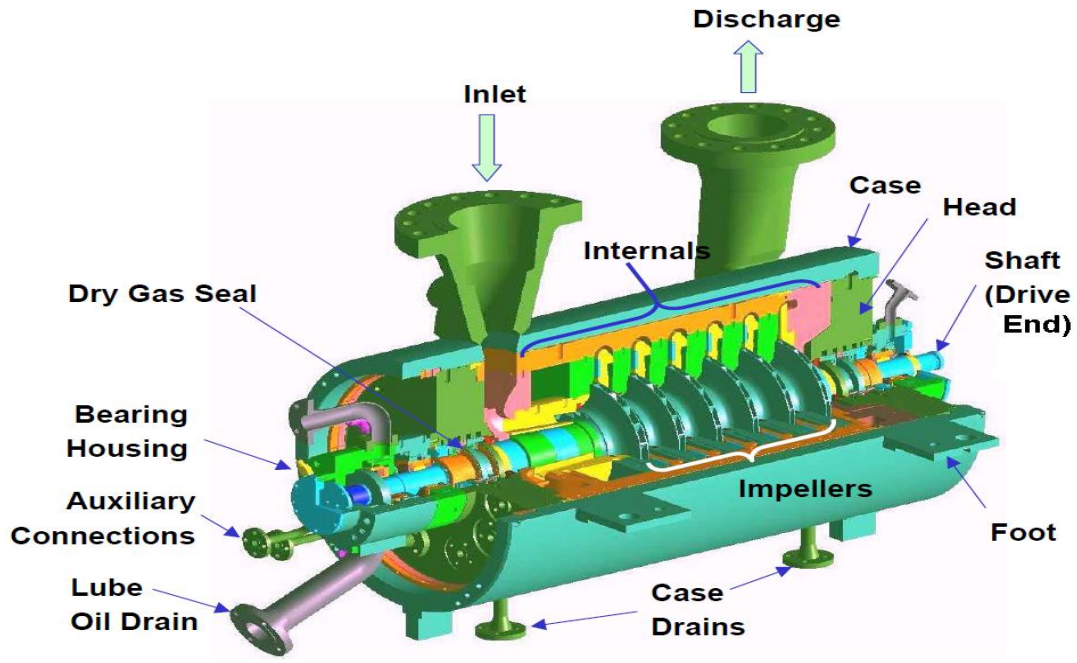

Figure 3B. A typical compressor components used in the process industry [Ref. 27]

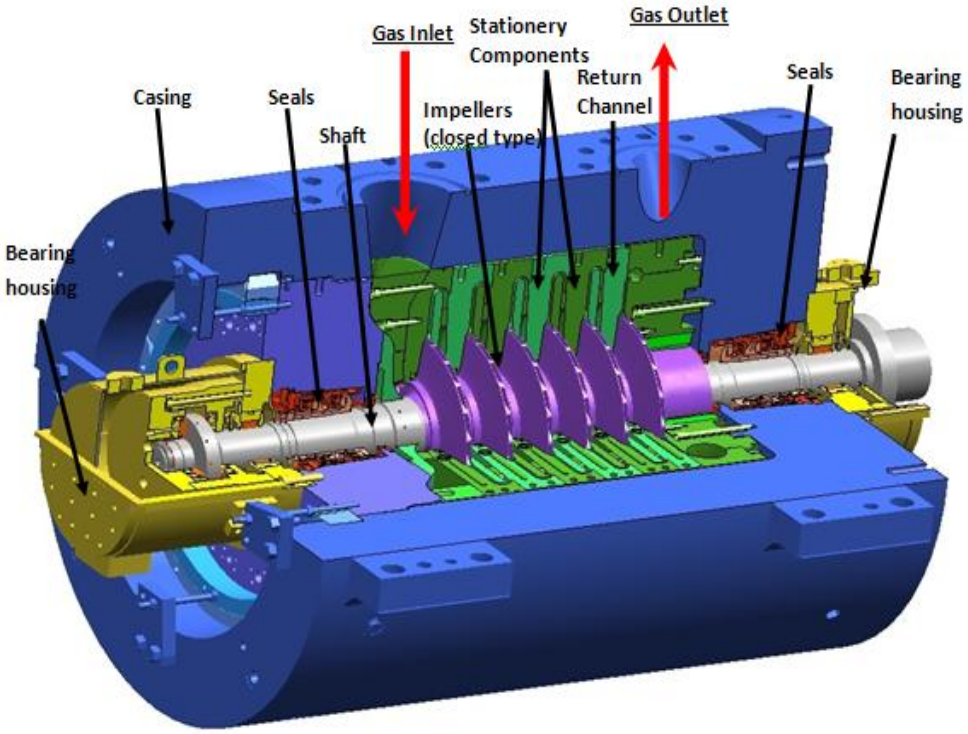

Figure 3C. A close up to the internal parts of a centrifugal (barrel type) compressor [Ref. 60]

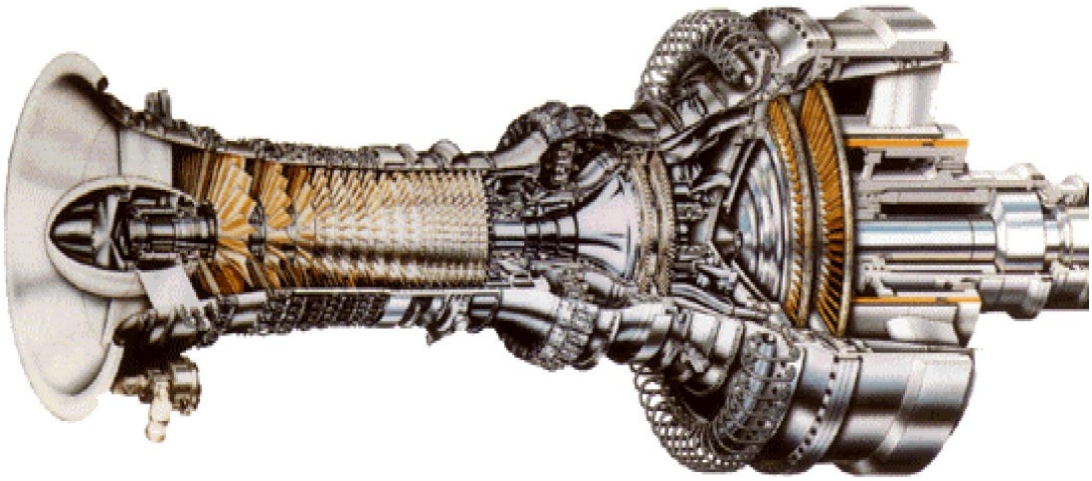

Figure 3D. A gas turbine (LM2500+) showing the compressor part at the intake on the left [Ref. 61]

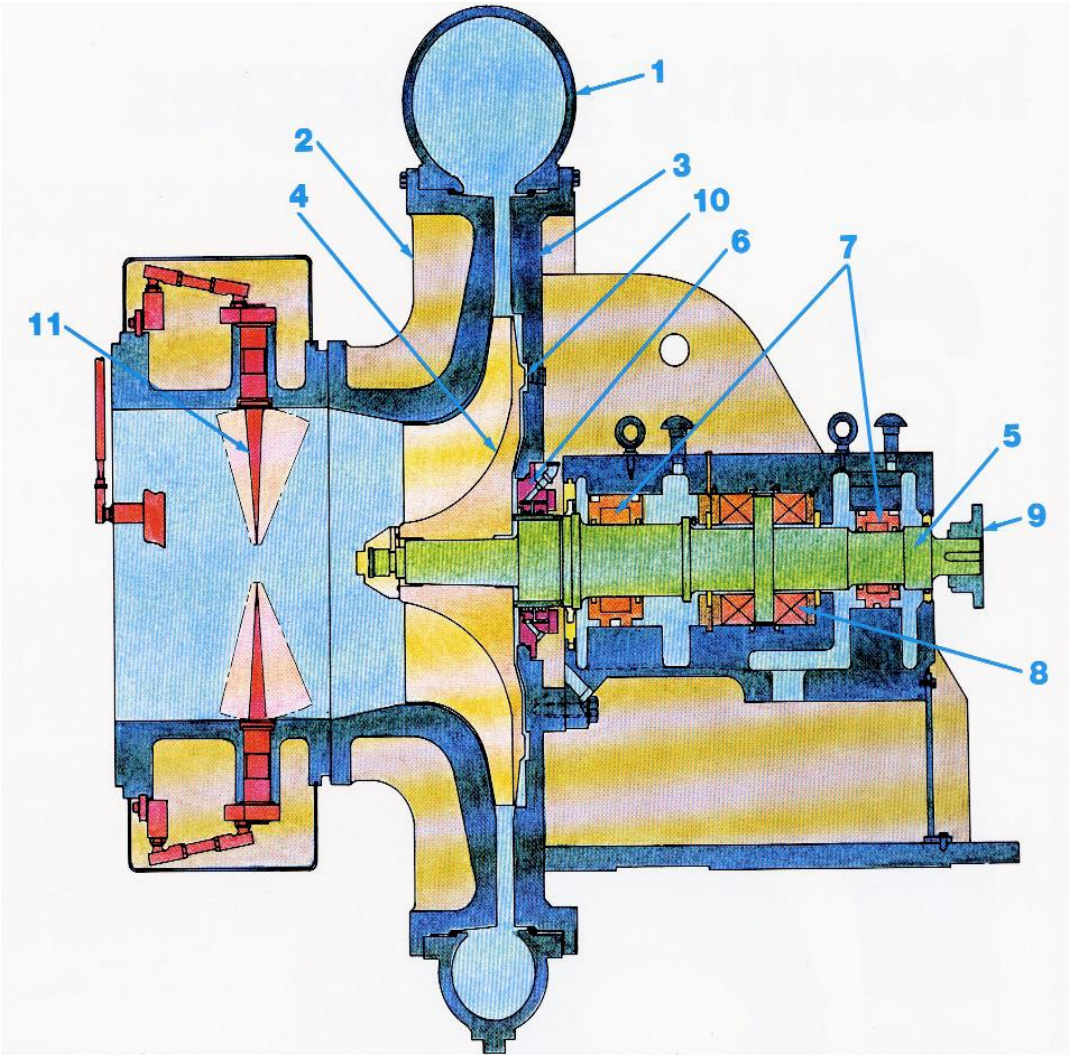

Figure 3E. Single stage compressor internal details: (1) discharge volute, (2) casing, (3) diffuser, (4) impeller, (5) shaft, (6) seal, (7) radial bearings, (8) trust or axial bearing, (9) coupling, (10) wear rings (protects the impeller), (11) inlet guide vanes (IGVs) [Ref. 60]

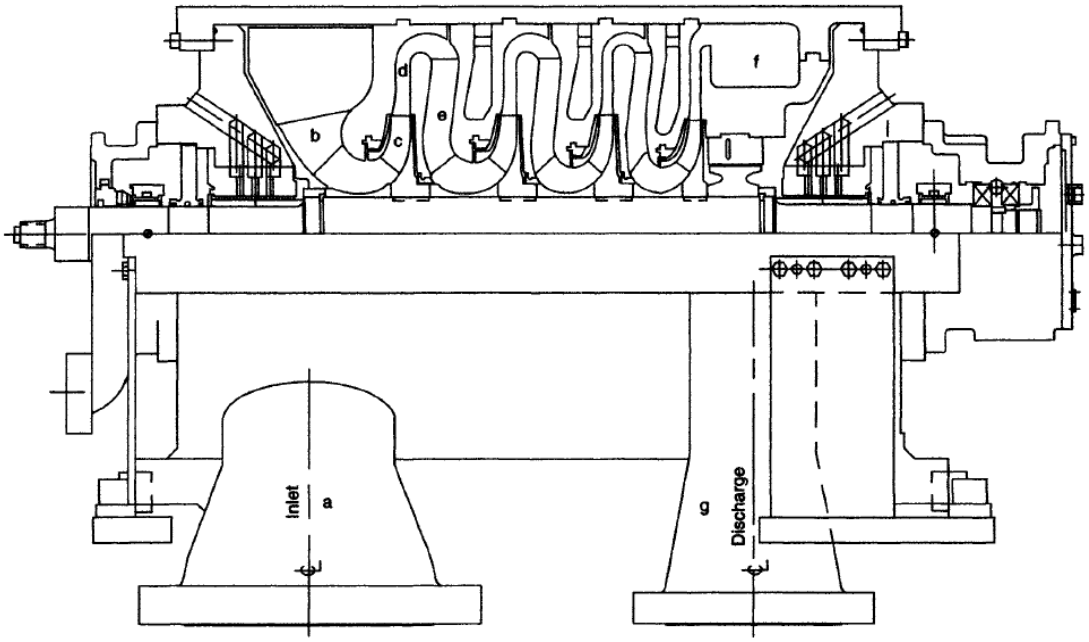

Figure 3F. Multistage centrifugal compressor : (a) the inlet nozzle, (b) inlet guide vanes, (c) impeller, (d) radial diffuser, (e) return channel, (f) collector volute, and (g) discharge nozzle [Ref. 28]

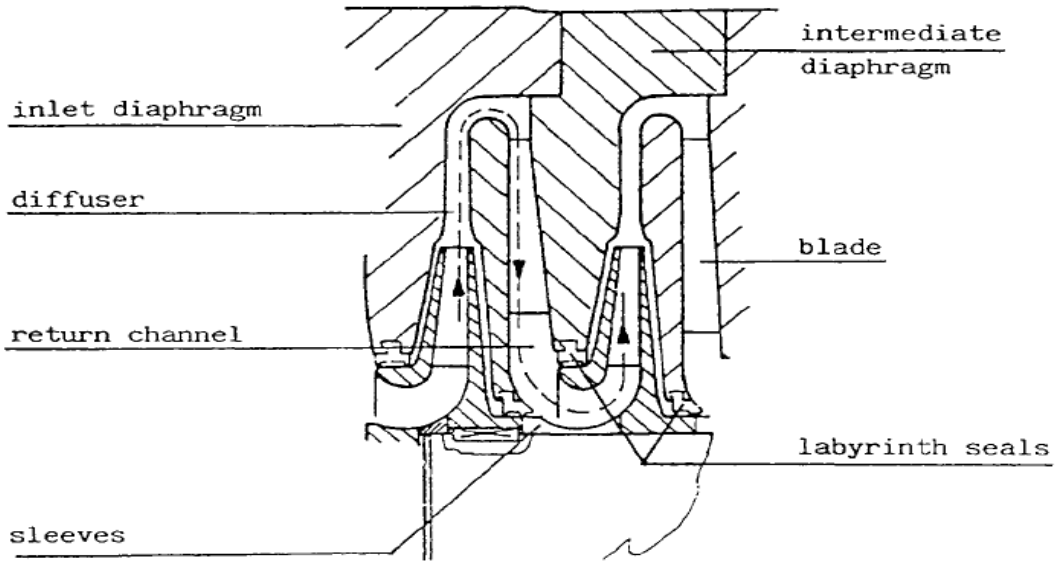

Figure 3G. The internals and the flow path in a centrifugal compressor [Ref. 28]

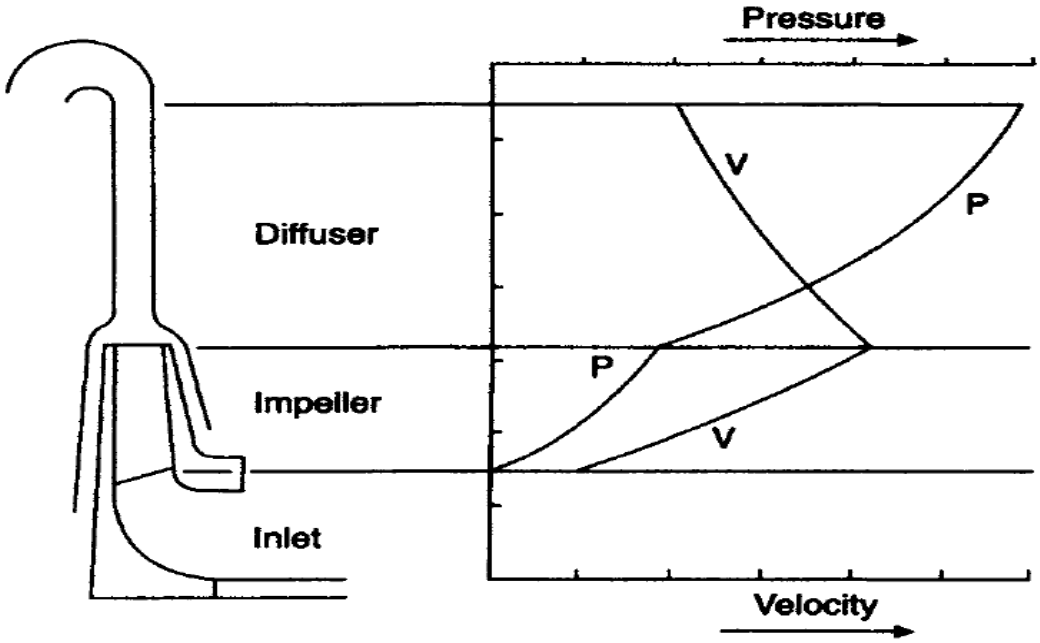

Figure 3H. Velocity/pressure development in a centrifugal compressor [Ref. 28]

2.1.1 Thermodynamic laws principles and turbomachinery efficiency definitions

Compressor design with high efficiency is a major source of fluid mechanics challenge in turbomachinery. Prior to 1900s, the compressor efficiency was less than 50%. A major pioneering work was by Auguste Rateau in 1902 when he designed a turbocompressor giving a pressure ratio of 1.5 at 12000 rpm giving an efficiency of 56% and in later years he continued to improve the efficiency. In certain industries such as aircraft, each fraction of improvement in efficiency translates into appreciable savings. In order to achieve these improvements, a detailed analytical and experimental methods need to be implemented or adopted on the analysis of flow and stress as well as the vibration predictions.

A turbomachinery produces a change in enthalpy in a stream of fluid passing through it and transfers work through a rotating shaft. Compressors absorb shaft work from a “driver” defined as power turbine.

The content of this section is not exhaustive as it forms the foundation knowledge for further readings and analysis [Ref. 67 provides detailed description of thermodynamics and efficiencies upon which this section is based]. The principles of thermodynamic laws defining the energy-enthalpy relations are defined and various forms and types of machinery efficiencies are clearly discussed to help the researcher choose an appropriate definition of efficiency depending on the objective and type of machinery being

designed or used in order to avoid possible implications later on during operation including a higher power demand than expected.

2.1.1.1 A Review of Thermodynamics

The first and second laws of thermodynamics are applied to the flow systems of turbomachinery to derive the energy-enthalpy relations. However these equations must be used with caution, for example, an isentropic (i.e., conditions under which the entropy remains essentially constant under enthalpy change) flow function should not be employed to relate upstream to downstream conditions in a frictional flow as in a frictional flow some of the useful work is dissipated as unwanted heat and entropy can not be considered constant. A review of first and second laws of thermodynamics are covered in the following subsections.

First Law

This is the law of the conversation of energy. This can be stated as “The energy passing into a given mass of material in a given time is equal to the energy passing out of the material plus the energy stored within it”. The referred material could be any form of molecule collection such as solid, liquid or gas. In symbolic terms this could be referred as the following equation in a positive displacement machinery where boundaries are well defined:

$$\delta q = \mathrm{d}\, E_A + \delta w \qquad \text{Eq. 2.1}$$

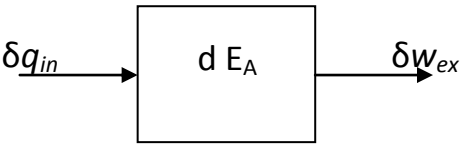

Figure 3I. Energy Flow and Storage [Ref. 67]

Where,

δq ($=\delta q_{in}$) is the heat transferred per unit mass in the process (as a convention, this is positive for heat transfer into the material);

$\mathrm{d}\, E_A$ is the increase of energy level of the material inside the system “A”, termed as “internal” energy; and,

δw ($=\delta w_{ex}$) is the work transferred per unit mass out of the material to the surroundings (as a convention, this is positive for work done by the material on the surroundings).

In turbomachinery application, however, Figure 3I is less applicable because the material (working fluid) crosses control volume boundaries. Here the first

law of thermodynamics is adapted to the material-crossing-boundary known as “flow” system. A space or “control volume” in which the flow process takes place can be modeled and the fluid is analysed for mass and energy as it moves in and out of the fixed boundaries of the control volume in a time increment of δt.

With reference to Figure 3J, the control volume has a single inlet (Station 1) and single outlet flow (station 2). The rate of heat transfer entering and exiting the control volume are ($\delta q_{in}/dt$) and ($\delta q_{ex}/dt$) respectively. Likewise, power transfer entering and exiting the control volume are ($\delta w_{in}/dt$) ($\delta w_{out}/dt$). The average fluid velocity is C perpendicular to area A.

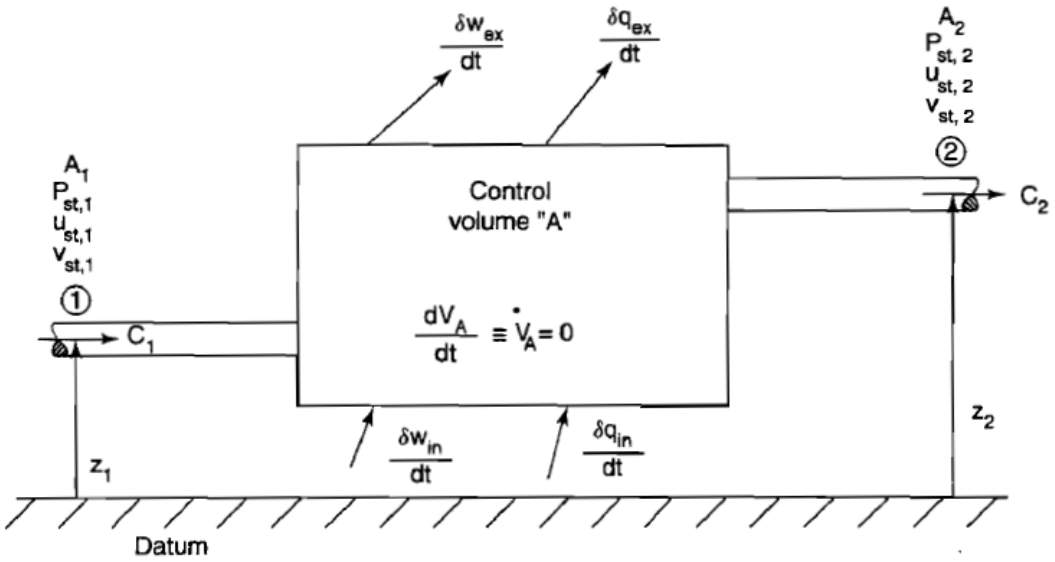

Figure 3J. Energy flows for a steady stream of fluid passing through a control volume [Ref. 67]

For flow-process control volumes it is just not the heat and work transfers through the surfaces of control volume but the various categories of energy that the material takes with it as it passes through the inlet and outlet of the control volume. These principle categories include kinetic (the effect of high velocity as material or fluid passes through the control volume). Another category accounts for the displacement of mass through the port at pressure p. Another category accounts for potential energy changes between ports due to changes of elevation z with respect to an arbitrary datum level.

When the energy balances are applied to turbomachinery, the subscript st (static) denotes property values that do not include the effects of kinetic or potential energy terms. The subscript 0 (stagnation) denotes property values that include effects of kinetic energy but not the effects of potential energy and subscript T (total) denotes the property values that include the effects of kinetic energy as well as the potential energy.

Perfect or semi-perfect gases have different static and stagnation temperatures, pressures and densities (T_{st}, T_0, p_{st}, p_0, ρ_{st} and ρ_0) and the mass flow rate is given by $m= \rho_{st}AC$.

From the principle of conservation of energy, at steady state the energy flows in and out of the control volume in Figure 3J may be represented as:

$$W_{ex} + Q_{ex} + m_2 (u_{st,2} + p_{st,2} v_{st,2} + C_2^2/2g_c + gz_2/g_c)$$

$$= W_{in} + Q_{in} + m_1 (u_{st,1} + p_{st,1} v_{st,1} + C_1^2/2g_c + gz_1/g_c) \quad \text{Eq. 2.2}$$

Where,

W is work transferred
Q is heat transferred
C is the velocity of material
g_c is unit matching constant in Newton's law
v is specific volume at static conditions (i.e., measured at the speed of the flowing materials) and it is the reciprocal of ρ_{st}
u is the internal thermal energy per unit mass
p_{st} is the static pressure
z is height above datum

Subscripts "in" and "ex" denote the inlet and exit to and from the control volume, and,
1, 2 denote stations 1 and 2 on Figure 3J

The above equation is known as the "steady-flow energy equation", (SFEE) and it may be applied widely for the analysis of turbomachinery and associated steady flow processes as the characteristic response time of flow in turbomachinery are orders of magnitude shorter than the characteristic response time of the overall transient encounter meaning that most flow analysis cases may be completed by examining a series of steady-state conditions in which there is no storage of mass or energy inside the control volume.

The combined static properties of (u_{st} + $p_{st}v_{st}$) can be given the name as "static enthalpy" or h_{st} and this may be defined as:

$$h_{st} \Xi u_{st} + p_{st} v_{st} \quad \text{Eq. 2.3}$$

In this equation, h_{st} can be measured only from a defined datum state as the internal thermal energy can only be measured from a defined datum whilst p and v are measurable quantities.

It may be noted that enthalpy in the above equation has the subscript “st” or static (i.e., stream). This is because these are the conditions measured with instruments that are “static” or stationery with respect to the fluid and this is difficult task at high speed flows. The stagnation properties are measured by probes that are shielded to reduce heat transfer by radiation and conduction (Figure 3K). Thus reference to Figure 3J, for a horizontal stream ($z_2=z_1$) and assuming that the flow velocity within the probe (C_2) is vanishingly small, then at any flow station:

$$H_0 \equiv h_{st} + C^2/2g_c \quad \text{Eq. 2.4}$$

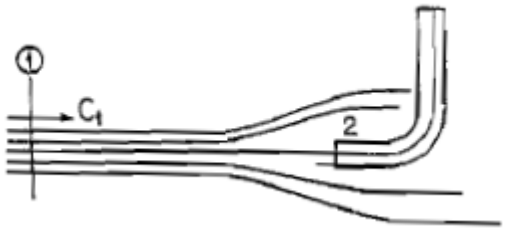

Figure 3K. Isentropic flow into a Pitot tube

Thus difference between static and stagnation is established and appropriate types of properties and should be used in flow analysis. When motion is slow, for instance, the static properties equal the stagnation properties. In thermodynamics relationships, stagnation conditions should be used throughout.

In air and gas turbomachinery, changes of height have a negligible effect on enthalpy change and the general form of steady-flow energy equation (Equation 2.2) can be written as

$$(Q_{in} + W_{in} - Q_{ex} - W_{ex}) / m = \Delta_1^2(h_0) = h_{0,2} - h_{0,1} \quad \text{Eq. 2.5}$$

Where,

Δ is finite difference operator and it is the property difference between outlet station 2 and inlet station 1.

The steady-flow energy equation (SFEE) is conveniently simplified for component of turbomachinery. For instance, in compressors where there is a good thermal isolation, the heat transfer is negligible and the process undergoes an adiabatic change ($Q_{in} = Q_{ex} = 0$). In other turbomachinery components there is considerable heat transfer but no work transfer (i.e., W=0), such as in combustor chambers and heat exchangers. In other turbomachinery components such as nozzles and diffusers there is neither heat nor work transfers. Figure 3L summarizes how Equation 2.2 is used in components with gas, vapour or liquid and how the restricted SFEE of

Equation 2.5 is in used in components with gas, vapour or liquid in horizontal flow.

	W	Q	$\Delta_1^2 h_0$
Nozzles	0	0	0
Valves	0	0	0
Throttles	0	0	0
Ducts, pipes, diffusers	0	0	0
Boilers	0		$\dot{Q}_{in}/\dot{m}$
Heat exchangers	0		$\dot{Q}/\dot{m}$
Combustion chambers	0		$\dot{Q}_{in}/\dot{m}$
Compressors, pumps, etc.		0(?*)	$\dot{W}_{in}/\dot{m}$
Turbines		0(?*)	$\dot{W}_{ex}/\dot{m}$

Figure 3L. Applicability of the steady-flow energy equation (SFEE) [Ref. 67].

* denotes case to case basis: a compressor may incorporate intercooler or turbine blade may incorporate cooling circuit.

Second Law of Thermodynamics

The second law of thermodynamics is stated in various forms. One common form is “Heat cannot pass from cooler to a warmer body without the expenditure of work”. This gives rise to the entity of “entropy” or degree of disorder within the fluid structure which in general has the tendency to increase. The general equation for entropy known as the Gibbs equation for a simple substance in the absence of energy storage due to motion, gravity, electricity, magnetism and capillary is:

$T\,ds = du + p\,dv$ Eq. 2.6

The Gibbs equation apply to any ideal or non ideal changes. For a simple reversible process,T ds = δq and p dv = δw in the first law of thermodynamics (Equation 2.1) and hence the equations are identical under simple reversible conditions.

A perfect gas may be defined as the one which has constant values of C_v (specific heat capacity at constant volume) and C_p (specific heat capacity at constant pressure). A semi-perfect gas may be defined as the one which C_v and C_p are functions of temperature (T) only. Both perfect and semi-perfect gases obey the equation of state as follows:

$pV = nRT = m R_w T$ Eq. 2.7

Where, n is the number of kmoles of gas, R is the universal molar gas constant (8.313 kJ/kmol/K), m is the mass flow rate of gas and R_w is the gas constant based on unit mass of the gas under analysis (0.287 kJ/kg/K for Air).

The above equation of state dictates that the specific internal energy and specific enthalpy of perfect and semi-perfect gases also obey the following relations:

$dh = C_p\, dT$ Eq. 2.8

$du = C_v\, dT$ Eq. 2.9

Where the ratio of specific heat capacities, γ, is defined as

$\gamma \equiv C_p/C_v = C_p/(C_p\text{-}R)$ Eq. 2.10

By the application of 2nd law of thermodynamics (Eq. 2.6) and equation of state (Eq. 2.7) one may obtain the velocity of small pressure wave propagation as:

$$a_{st} = \sqrt{g_c \gamma R T_{st}} = \sqrt{\frac{g_c C_p T_{st}}{(C_p/R) - 1}} \qquad \text{Eq. 2.11}$$

Where,

a_{st} is the actual velocity of sound (static) and T_{st} is appropriately the static temperature

For a perfect gas the entropy change between any two states 1 and 2 may be given by

$$s_2 - s_1 = C_v \ln\frac{T_2}{T_1} + R \ln\frac{v_2}{v_1} \qquad \text{Eq. 2.12}$$

For a semi-perfect gas the entropy change can be calculated by above with a suitably averaged value of C_p over the temperature range between T_2 and T_1. For an isentropic process where entropy stays the same, $S_2 – S_1 = 0$, and the above equation becomes:

$$\frac{T_2}{T_1} = \left(\frac{p_2}{p_1}\right)^{\frac{R}{C_p}} = \left(\frac{\rho_2}{\rho_1}\right)^{\frac{R}{C_v}} = \left(\frac{v_1}{v_2}\right)^{\frac{R}{C_v}} \qquad \text{Eq. 2.13}$$

Many flow issues in the design of turbomachinery involve the specification of the stagnation pressure and temperature, p_0 and T_0 and either the absolute

velocity C or the mass flowrate m and characteristic area A. If the Mach number can be found, all the actual and static properties are immediately calculable. Applying Eq. 2.4 to an adiabatic system for a perfect gas the following ratio is obtained:

$$\frac{T_0}{T_{st}} = 1 + \frac{C^2}{2g_c C_p T_{st}} = 1 + \frac{C^2}{2\left(\frac{C_p}{R} - 1\right) a_{st}^2}$$

Eq. 2.14

And, substituting for ast in equation Eq. 2.11, and defining Mach number M as M= C/a_{st} , will yield the following equation which is the fundamental equation for one-dimensional compressible flow based on first law and adiabatic (no heat transfer) process:

$$\frac{T_0}{T_{st}} = 1 + \frac{M^2}{2\left(\frac{C_p}{R} - 1\right)} = 1 + \left(\frac{\gamma - 1}{2}\right) M^2$$

Eq. 2.15

Combining equation 2.15 with equation 2.13 will yield the following equations for isentropic flows in terms of stagnation to static ratios:

$$\frac{p_0}{p_{st}} = \left[1 + \frac{M^2}{2\left(\frac{C_p}{R} - 1\right)}\right]^{(C_p/R)} = \left[1 + \left(\frac{\gamma - 1}{2}\right) M^2\right]^{\frac{\gamma}{\gamma - 1}}$$

Eq. 2.16

$$\frac{\rho_0}{\rho_{st}} = \frac{v_{st}}{v_0} = \left[1 + \frac{M^2}{2\left(\frac{C_p}{R} - 1\right)}\right]^{[(C_p/R)-1]} = \left[1 + \left(\frac{\gamma - 1}{2}\right) M^2\right]^{\frac{1}{\gamma - 1}}$$

Eq. 2.17

2.1.1.2 Turbomachinery efficiency definitions

The overall energy efficiency of turbomachines compares the actual work transfer with that which would occur in an ideal process. If the machine is using energy such as the compressor, the work transfer in an ideal process is in the numerator. If the machine is energy producing, then the ideal process work transfer is in the denominator.

Efficiencies must be defined with sufficient precision and seldom this is the case. Hence here these are well defined.

If the efficiency of a compressor is defined as follows: [power transfer in ideal process from an inlet stagnation pressure and temperature to a defined outlet stagnation pressure] / [the actual compressor power], or,

$\eta_c = W_{in, ie}/W_{in, ac}$ Eq. 2.18

Then, (i) The ideal process must be identified where the principle choices are isentropic, polytropic and isothermal, (ii) The inlet and specifically the outlet plane must be identified, (iii) The outlet pressure should be stated whether it is actual or static, (iv) The actual work transfer include or exclude the losses in seal friction, bearings and disk.

Each of the above definitions is described below.

Ideal Processes

The two principle ideal processes used are isentropic for adiabatic processes and the isothermal for gas compression when intercooling is employed.

The isentropic efficiency for a compressor ($\eta_{s, c}$) is best defined as:

$$\eta_{s,c} = \frac{h^{\otimes}_{0,ex,s} - h_{0,in}}{h_{0,ex} - h_{0,in}} = \frac{T^{\otimes}_{0,ex,s} - T_{0,in}}{T_{0,ex} - T_{0,in}} = \frac{r_c^{R/C_p} - 1}{\frac{T_{0,ex}}{T_{0,in}} - 1}$$ Eq. 2.19

Where,

$h^{\otimes}_{0,ex,s}$ = Enthalpy after an isentropic process from h0, in and T0, in to $T^{\otimes}_{0,ex,s}$

r_c = Compression ratio

It is important to note that the term "R/C_p" is used rather than "Y" because the latter leads the user to find a value of C_p appropriate for temperature but to take Y as constant with temperature which leads to errors and inconsistencies in precise calculations. The equation 2.19 above in terms of temperature differences and r_c are exact for perfect gases and approximation for semi-perfect gases.

The isothermal power required for perfect and semi-perfect gases is obtained by Equation 2.20 below:

$$\left(\frac{W_{in} - W_{ex}}{m}\right)_{it} = TR \ln \frac{p^{\otimes}_{0,ex}}{p_{0,in}}$$ Eq. 2.20

The actual work transfer in the process is given by the steady-flow energy equation (SFEE) as:

$$\left(\frac{W_{in} - W_{ex}}{m}\right) + \left(\frac{Q_{in} - Q_{ex}}{m}\right) = \Delta^{ex}_{in} h_0 = (h_{0,ex} - h_{0,in})$$ Eq. 2.21

The above equation is a general and exact expression for the actual work transfer where no significant change in fluid height is experienced meaning the work transfer between the fluid and the machine's rotor(s), stator(s) and ducts. In many evaluations of energy efficiencies this equation (Eq. 2.21) is used and it gives the measure of the quality of the aerodynamic and thermodynamic design. The "external" energy losses resulting from friction in bearings and labyrinths must be added or subtracted from the process energy.

Turbomachines are generally adiabatic ($Q_{in} = Q_{ex} = 0$). In certain cases where intercooling is involved, heat transfer is significant.

Figure 3M shows the general types of turbomachine efficiencies. W_{g3} indicate "group 3" or external losses (i.e., shaft power losses through friction, the energy from which is dissipated away from the working fluid such as friction losses in bearings and seals) and these power losses appear as increases in compressor power requirements.

Efficiency	Compressor or pump	Expander or turbine
Isentropic, general fluid, η_s	$\dfrac{h^{\otimes}_{0,ex,s} - h_{0,in}}{h_{0,ex} - h_{0,in} + \dot{W}_{g3}/\dot{m}}$	$\dfrac{h_{0,in} - h_{0,ex} - \dot{W}_{g3}/\dot{m}}{h_{0,in} - h^{\otimes}_{0,ex,s}}$
Isentropic, perfect gas, η_s	$\dfrac{(p^{\otimes}_{0,ex}/p_{0,in})^{(R/C_p)} - 1}{(p^{\otimes}_{0,ex}/p_{0,in})^{n'} - 1 + \frac{\dot{W}_{g3}}{(\dot{m}h_{0,in})}}$	$\dfrac{1 - (p^{\otimes}_{0,ex}/p_{0,in})^{n'} - \frac{\dot{W}_{g3}}{(\dot{m}C_pT_{0,in})}}{1 - (p^{\otimes}_{0,ex}/p_{0,in})^{(R/C_p)}}$
Isentropic, incompr. liquid, η_s	$\dfrac{(H^{\otimes}_{0,ex} - H_{0,in})(g/g_c)}{\dot{W}_{in}/\dot{m}}$	$\dfrac{\dot{W}_{in}/\dot{m}}{v(p_{0,in} - p^{\otimes}_{0,ex}) + (z_{in} - z_{ex})(g/g_c)}$
Isothermal, general gas, η_{it}	$\dfrac{h^{\otimes}_{0,ex} - h_{0,in}}{\dot{W}_{in}/\dot{m}}$	$\dfrac{\Delta^{ex}_{in}h_0 - T\Delta^{ex}_{in}s_0 - \dot{W}_{g3}/\dot{m}}{\Delta^{ex}_{in}h_0 - T\Delta^{ex}_{in}s_0}$
Isothermal, perfect gas, η_{it}	$\dfrac{RT\ln(p^{\otimes}_{0,ex}/p_{0,in})}{C_p\Delta^{ex}_{in}T_0 - T\Delta^{ex}_{in}s_0 + \dot{W}_{g3}/\dot{m}}$	Not used for expanders

Figure 3M. Types of turbomachine efficiencies

Polytropic Efficiency

The isentropic efficiency is a function of pressure ratio and losses. Isentropic efficiency has a serious disadvantage if it is used as a measure of the quality of the aerodynamic design, or as a measure of losses, in an adiabatic machine. To avoid the influence of pressure ratio on isentropic efficiency, the limiting value of the isentropic efficiency for a given polytropic process can be used as the pressure ratio approaches unity. This is known as the “polytropic” efficiency and for compressors this is represented as:

$\eta_p \equiv (\eta_s)_r \longrightarrow_{1.0} = (R/C_p)/((n-1)/n))$ Eq. 2.22

Where n=polytropic index (a unique number advised by the manufacturer based on fluid composition and properties). For perfect gases Eq. 2.22 leads to the useful equation of the following:

$$\frac{T_{0,ex}}{T_{0,in}} = r_c^{\left[\left(\frac{R}{C_p}\right)\frac{1}{\eta_{p,c}}\right]}$$ Eq. 2.23

Equation 2.23 enables the adiabatic work to be obtained directly from pressure ratio. However, which value of $p^{®}_{0,\,ex}$ to use is a subject of debate and depends on the objective(s). When $p^{®}_{0,\,2}$ is defined as static pressure, the efficiency obtained is termed a “stagnation-to-static” efficiency, η_{0s}. When $p^{®}_{0,2}$

is a stagnation pressure, the efficiency obtained is “stagnation to stagnation”, η_{00}. Thus there is no unique “one” definition of efficiency but whichever is chosen should be well identified and defined [Ref. 67]. The type of efficiency used is application dependent. For instance, the appropriate definition of $p^{®}_{0,2}$ for the efficiency of a compressor in a turbojet engine is the static pressure at the end of compressor diffuser at the boundary between the compressor and the combustor because the dynamic pressure at the point cannot be used by the combustor. If stagnation pressure is used, undesirable consequences would result since actual losses would be increased if the diffuser were eliminated. Whereas, in the case of the turbine of a turbojet engine, the appropriate $p^{®}_{0,2}$ to use in the turbine-efficiency definition is the stagnation pressure upstream of the propulsion nozzle that produces the jet. It is to be noted that the actual work is unaffected by the choice of useful outlet pressure, $p^{®}_{0,2}$ and only the ideal work is affected since from the SFEE the actual (internal) work is the difference in stagnation enthalpy from inlet to outlet and this work remains constant at ($h_{0,\,ex} – h_{0,\,in}$) regardless of how the outlet pressure is defined.

In removing the effect of pressure ratio, the polytropic efficiency is useful in the sense it enables machines of different pressure ratios to be reliably compared, regardless of number of stages.

The relationship between polytropic and isentropic efficiencies for perfect gases may be defined as in Eq. 2,24 below and therefore knowing one type of efficiency, the other may be calculated:

$$\eta_{s,c} = \frac{r^{R/C_p} - 1}{r^{(R/C_p)\eta_{p,c}} - 1}$$

$$\eta_{p,c} = \frac{\ln\left(r^{R/C_p}\right)}{ln\left[\left(r^{R/C_p} - 1\right)/\eta_{s,c} + 1\right]} \quad \text{Eq. 2.24}$$

2.2 Compressor and Driver: Interface Losses and Environmental Effects on Performance

On oil and gas projects, the process discipline group is usually the first to commence plant design and often the process is designed by the process engineer without sufficient consideration for compression equipment. At a later stage, when mechanical engineers come onboard, they frequently find that they have to search the market for a compression unit that satisfies the process requirements as at this stage it is virtually impossible to change the process conditions. It is of paramount importance, therefore, that the

engineers across the disciplines know what factors affect the compressor power demand and the profile of power requirement during the life cycle of the compressor such that suitable gas turbine drivers are supplied from the beginning to keep the availability and reliability at high levels.

The conditions of environment, process and fluid properties entering the compressor vary with time over the life cycle of a project and as such, it must be ensured that at the very early stage all these variations and their effects on compressor performance as well as the gas turbine driving the compressor are accounted for, so that critical conditions such as power supply shortfall from the gas turbine(s) driving the compressor(s) do not happen at any time during the entire expected life time of the compressor(s) thus keeping the compressor online in operation at the highest availability.

The power demand profile from the compressor is evaluated taking into account all the environmental losses and process changes as well as identification of sources and quantification for supply power losses, then finding a suitable driver. Once the power demand profile over the entire life expectancy is determined, suitable cascade of choices for the gas turbine driver shall be the next step. Determination of a suitable gas turbine driver is an important task which should be determined by the compressor operator considering all the losses throughout the life cycle of the project.

2.3 Causes and Mechanisms of Performance Deterioration in Compressors

2.3.1 Compressor performance deterioration

In an axial compressor as a part of the gas turbine, the performance deterioration of the compressor results from the deterioration of one or more of the engine sub-components. The deterioration of these sub-components results in changes in their characteristics. The interaction of these deteriorated component characteristics lead to a change in compressor shaft power demand, efficiency and engine measurable parameters such as pressure, temperatures speeds and flows. Likewise, in the centrifugal compressors used in the process industries, the performance deteriorates due degradation resulting in changes in its performance maps.

Many factors affect the compressor performance and include the following:

- Compressor Fouling
- Variable Inlet Guide Vane (VIGV) and Variable Stator Vane (VSV) problems for axial type
- Blade Tip Rubs
- Vibrations in the shaft, indicator of rotor problems
- Tip seal and labyrinth seal Wear & Damage

- Foreign Object Damage (FOD) & Domestic Object Damage (DOD)
- Erosion
- Corrosion

The effect of rubs is discussed separately in the following section. Fouling is the most common cause of performance deterioration. Even with the best filtration system, dirt, salt (offshore), sand etc. will get through the filtration system and deposit on the compressor blading. Compressor fouling will increase surface roughness as well as reducing the flow area (capacity) and efficiency. The first effect will be lowering the performance curves and the second will shift the curves to the left. Vibration is usually an indication of compressor deterioration rather than the cause. However, vibration can also be due to operating in region of choke of the compressor, where vibrations may increase as the compressor becomes fouled. Axial displacement is also another key indication of performance deterioration of the compressor thrust piston condition.

There are two kinds of turbo machinery performance deterioration: recoverable and non recoverable. The performance degradation associated with widening clearances between the moving and stationery parts of the compressor are “non-recoverable”. The only remedy for non-recoverable degradation is an overhaul. Compressor fouling is a “recoverable” degradation in that it can be alleviated by periodic on-line and/or off-line compressor washing. Off-line washing may fully recover the performance loss of compressor. It is essential to develop maintenance schedules based on the characteristics of the compressor (see Figures 1 and 4) or its operating environment and/or cycle in order to balance the maintenance costs with lost revenues resulting from the loss of production. Compressor washing mitigates compressor fouling and the shift in these running lines may be used to determine compressor washing frequency. Optimizing compressor washes is more complex and has to take into account many factors such as downtime for washing, costs and revenue [Ref 41], see Figure 4 developed for a demonstration of optimized wash periods based on running hours for the compressor of a gas turbine. Arebi [Ref 37] has discussed the compressor washing in detail and Jordal [Ref 25] and Hovland [Ref 46] have arrived at formulas for optimum compressor washing intervals.

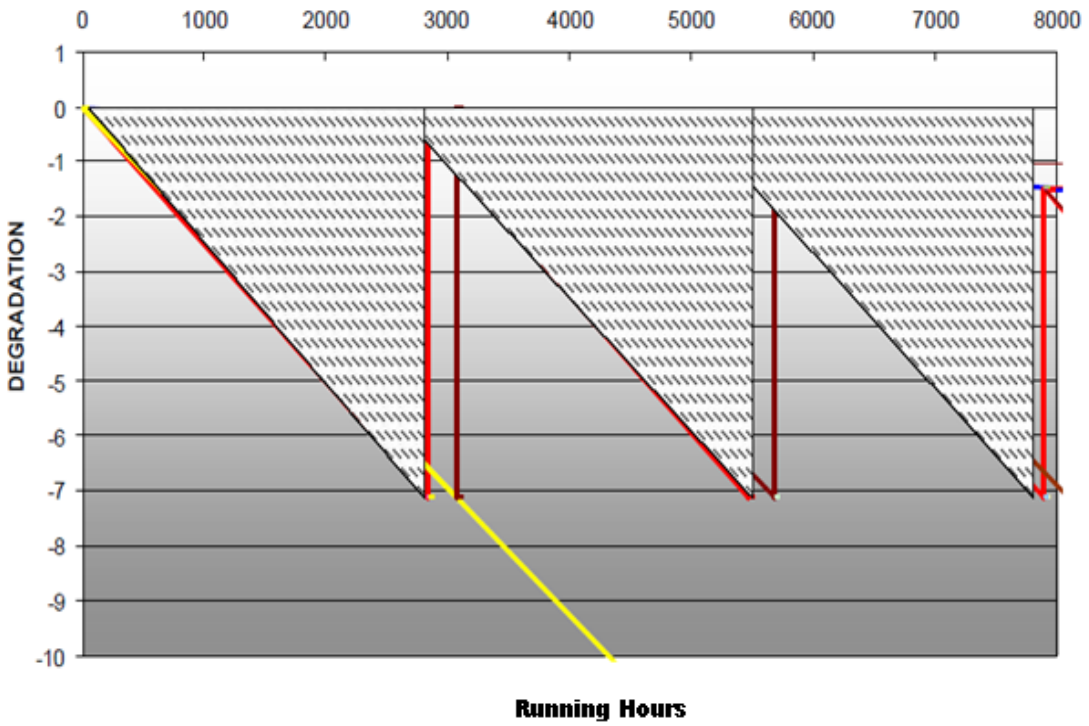

Figure 4. A compressor wash programme developed for a station [Ref 37]

In the proceeding subsections, the significant causes and forms of compressor performance deterioration are discussed and these are tip seal damage, labyrinth seal wear and/or damage, fouling due to adherence of dirt particles on the surface of materials, erosion which is the abrasive removal of compressor coatings and materials and corrosion which is the removal of compressor materials due to chemical reaction between the gas medium and compressor components.

2.3.2 Effect of Seals on Compressor Performance

Due to the pressure rise across successive compression stages seals are required at the impeller eye and shaft to prevent back flow from discharge to the inlet end of the casing. Therefore the conditions of these seals directly affect the compressor performance. These seals are normally labyrinth seals and if they are clogged with dirt and worn with increased clearances allow larger leaks (see Figures 6A and 7A). This will affect operation and also the compressor efficiency. Calculations and field performance data have shown that wiped interstage seal reduce efficiency as much as 7% or more.

In axial compressors the labyrinth seal reduces internal leakage between the discharge and suction side of the compressors and turbines. Damage to these seals increases the internal leakage and result in reduced compressor and turbine performance. Labyrinth seal damage reduces component efficiency rather than flow capacity.

The fall in efficiency due to rob and wear is not a recoverable process. The rub and wear causes a direct drop in efficiency and pressure ratio curves; it does not shift the curves from left to right like fouling. Having said that, however, if the tip clearances open up in a open face impeller, more flow will migrate causing an increase in viscous losses but it will also impact the loading on the impeller blades. This could be seen as reduction in capacity of the stage as well as reduction in the range of operation (stall point moves). It should also be noted that a high degree of varying flow angle coming out of the impeller will negatively impact diffuser vane performance.

Figures 6A-6C show the position of seals within the compressor.

The effect of blade tip clearance in centrifugal as well as axial compressors is shown on Figure 5. For an open centrifugal impeller the efficiency loss is about one-third of a point for each percent of tip clearance ratio at the impeller outer diameter.

For axial compressor the clearance between the compressor rotor and the casing must be kept small in order to reduce secondary loss. Increase in compressor clearance reduces compressor flow capacity and efficiency. Increase in clearance normally occurs when running an engine with high vibration. Erosion also increases the rotor tip clearance. Significant increase in axial compressor clearance can result in the surging of the compressor. The compressor efficiency is reduced by 2 percentage points for each percent of tip clearance ratio [Ref. 28].

For a closed centrifugal impeller with labyrinth seals at the eye, the efficiency loss is about one percentage point for each percentage increase in impeller flow as a result of the leak (see Figure 5).

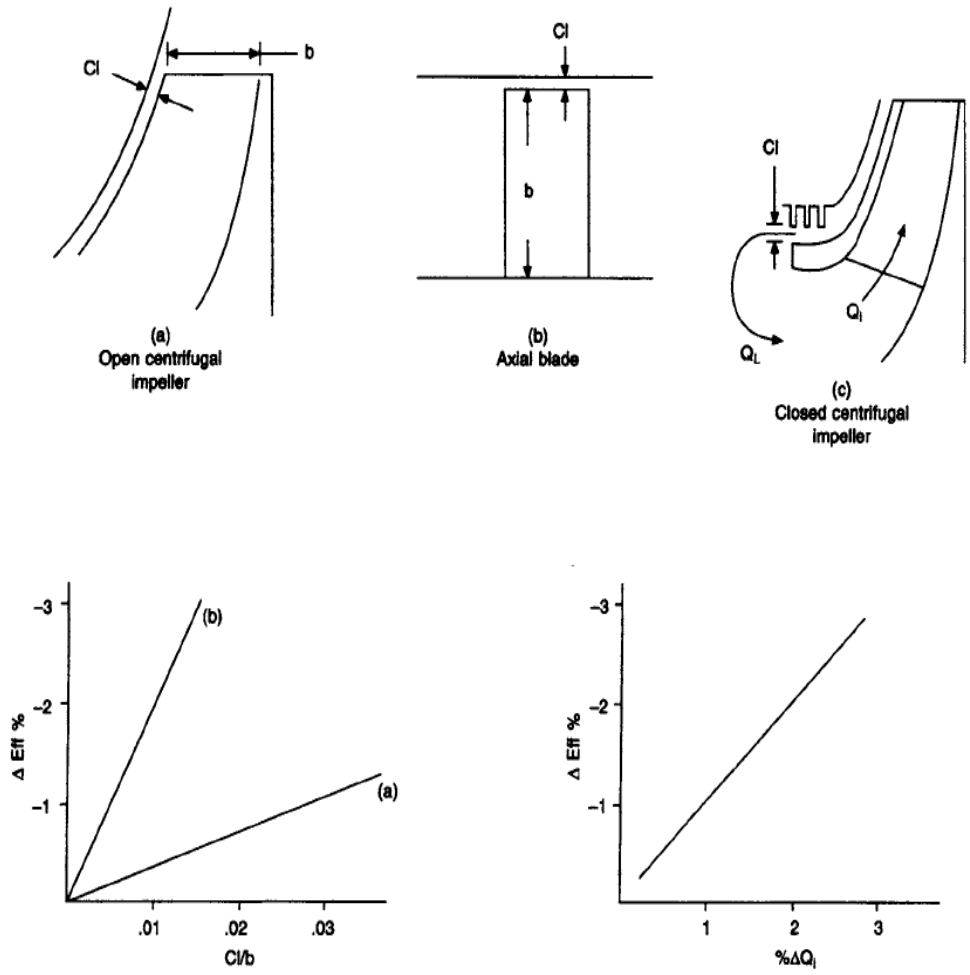

Figure 5. The effect of blade tip clearance on efficiency in centrifugal as well as axial compressors [Refs 50, 51]

Seals also avoid process gas inside the casing leak outboard. A typical seal arrangement to accomplish this objective is shown on Figure 6A. The location of shaft seals is clearly shown on Figures 6B and 6C.

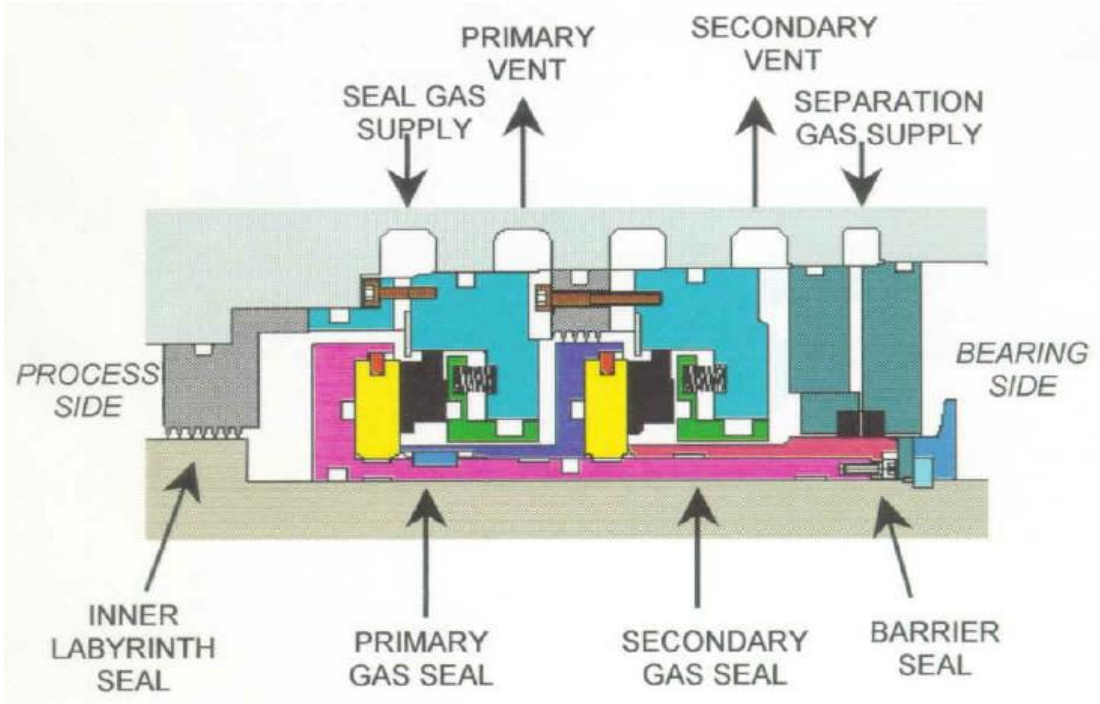

Figure 6A. Typical seal arrangement in centrifugal compressors for leakage avoidance [Ref.62]

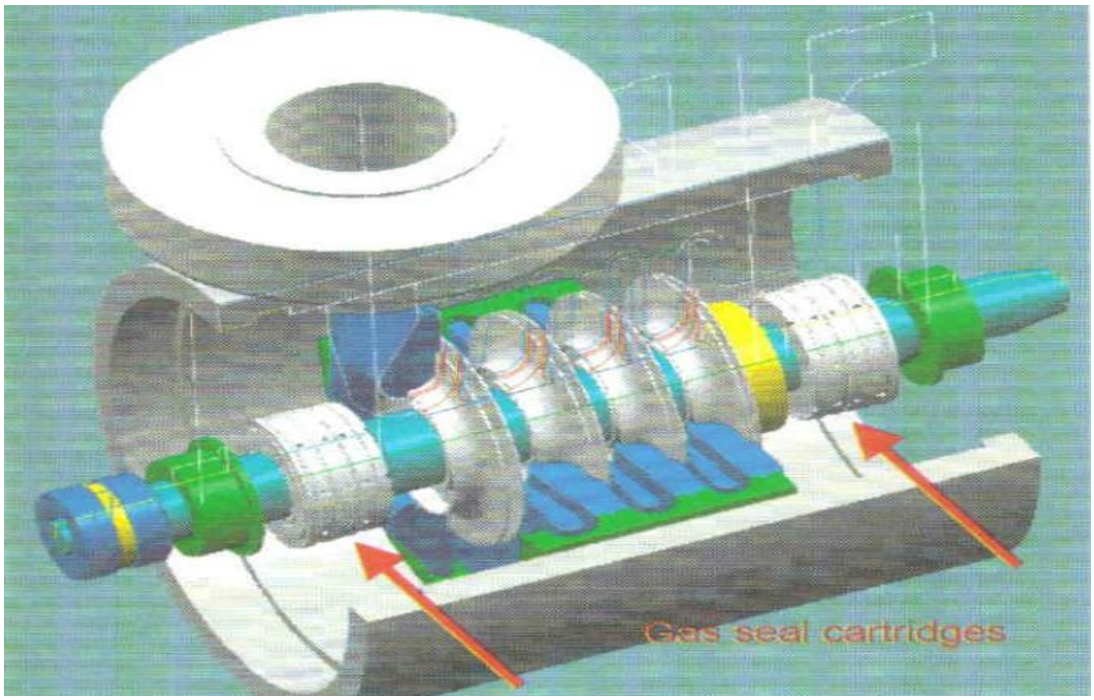

Figure 6B. Location of shaft seals in the compressor [Ref.62]

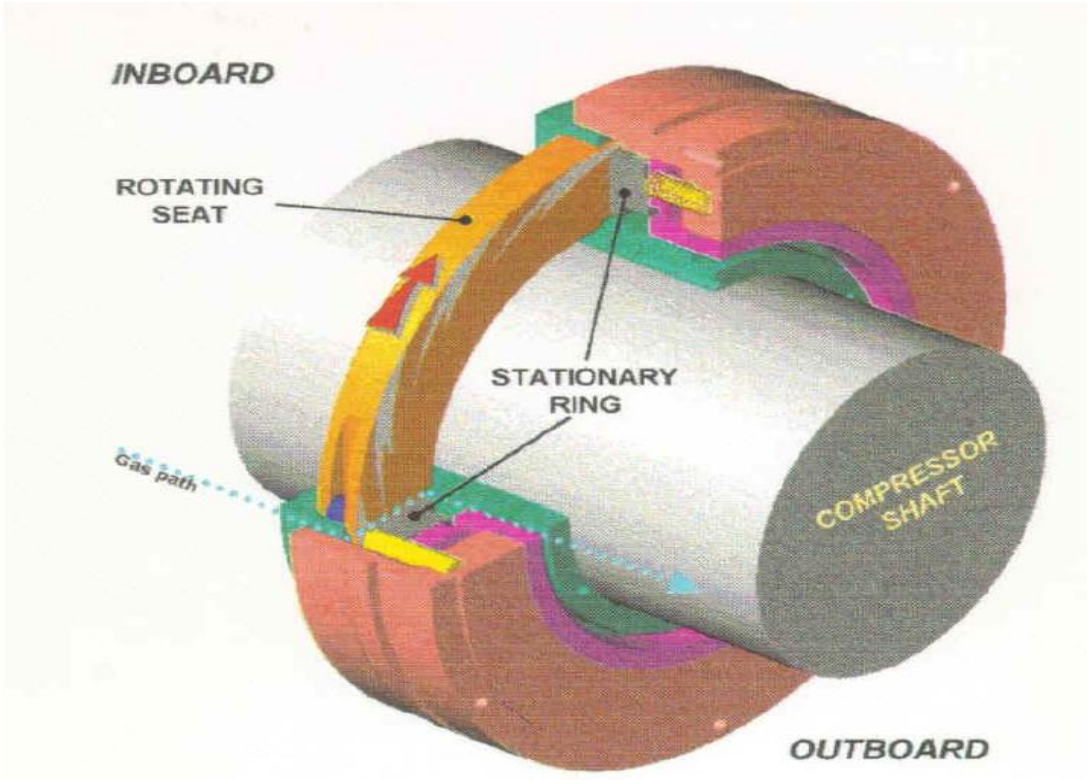

Figure 6C.Gas seal component in the compressor [Ref.62]

2.3.3 Compressor degradation, degradation modeling and Gas Path Analysis

With reference to Figures 7A-7H, a compressor performance falls with time or degrades via fouling (adherence of particles) and erosion (abrasive removal of compressor materials and hence the increase of surface roughness) mechanisms. The removal of compressor materials by chemical reaction(s) between it and the transported gas will result in corrosion in which the material surface also ends up in increased roughness and ultimately material failure.

In compressors the degradation causes an increase in tip clearance, change in airfoil geometry and quality. The first two are irrecoverable (part replacement is necessary) and the 3rd type is partially recoverable through compressor washing. The effect of on-line/offline washing on the recovery of compressor performance is shown in Figure 8 [Ref. 57]. It is seen here that effective washing brings back a noticeable part of the lost performance due to degradation.

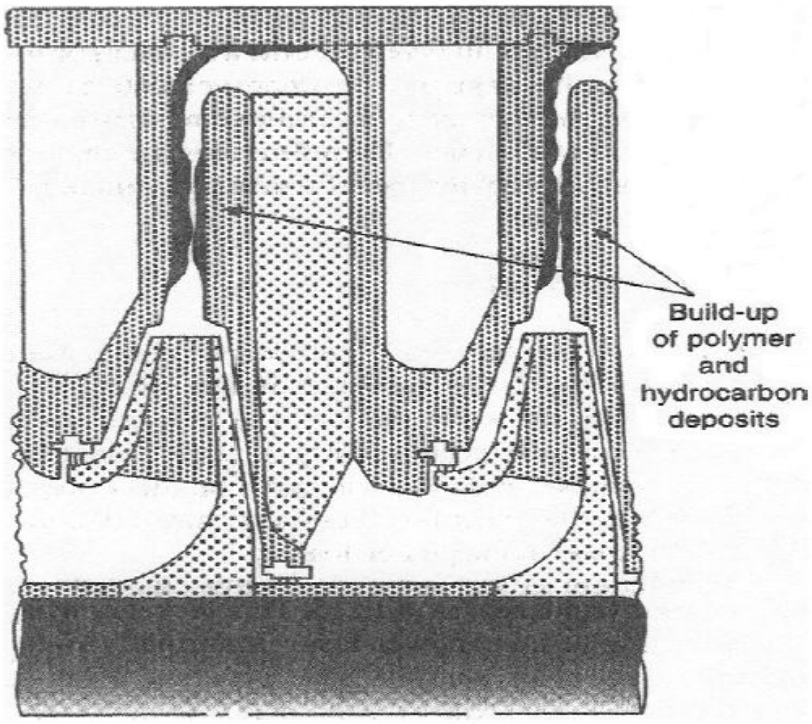

Figure 7A. Dirt or polymer buildup in the diffuser passage of the centrifugal compressor [Ref 28]

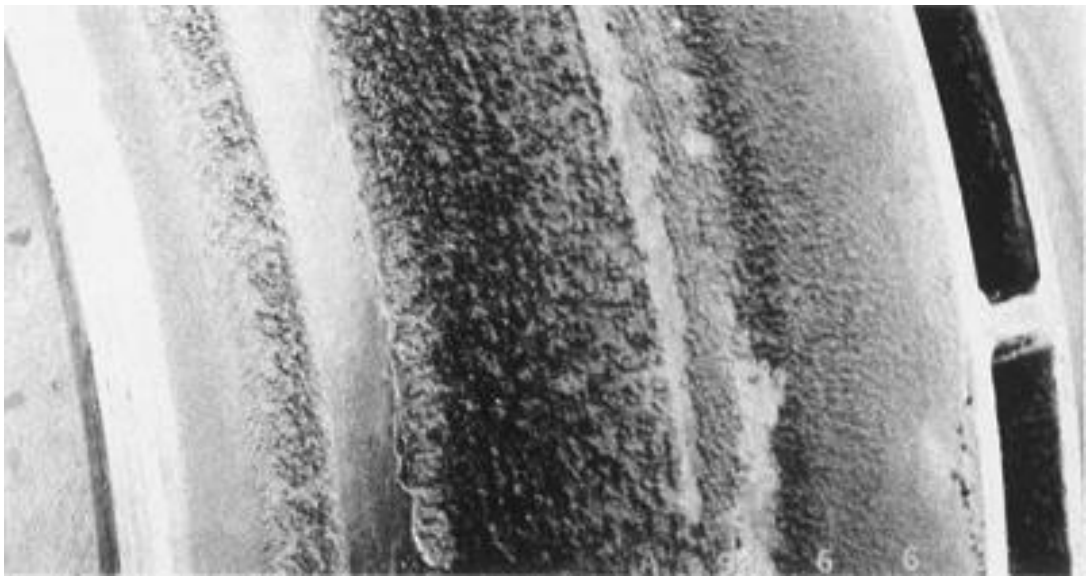

Figure 7B. Impeller fouling of a centrifugal compressor [Ref.60]

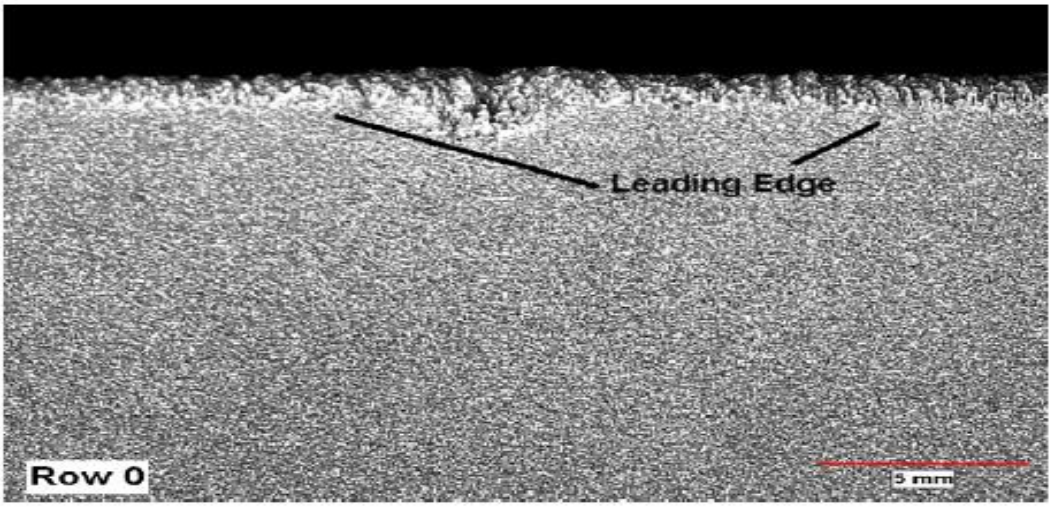

Figure 7C. Eroded leading edge of a rotor blade of a first stage of a compressor. The picture shows the mid-span of a first stage compressor (axial) rotor [Ref 16]

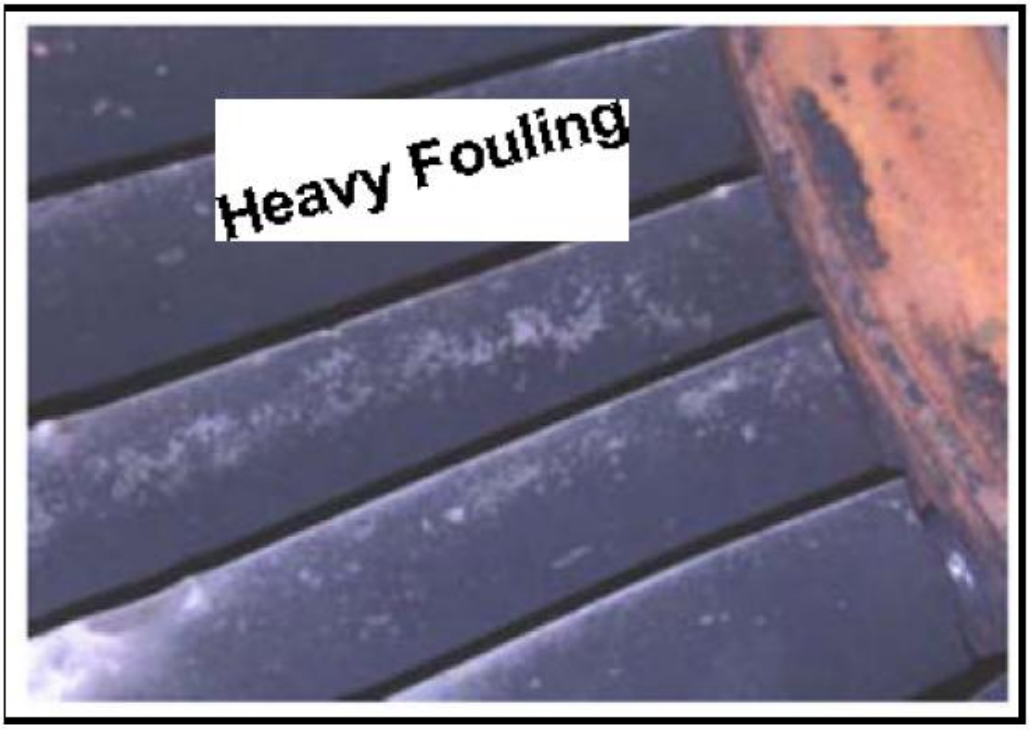

Figure 7D. Axial compressor blade fouling [Ref 37]

Figure 7E. Compressor blade corrosion [Ref 37]

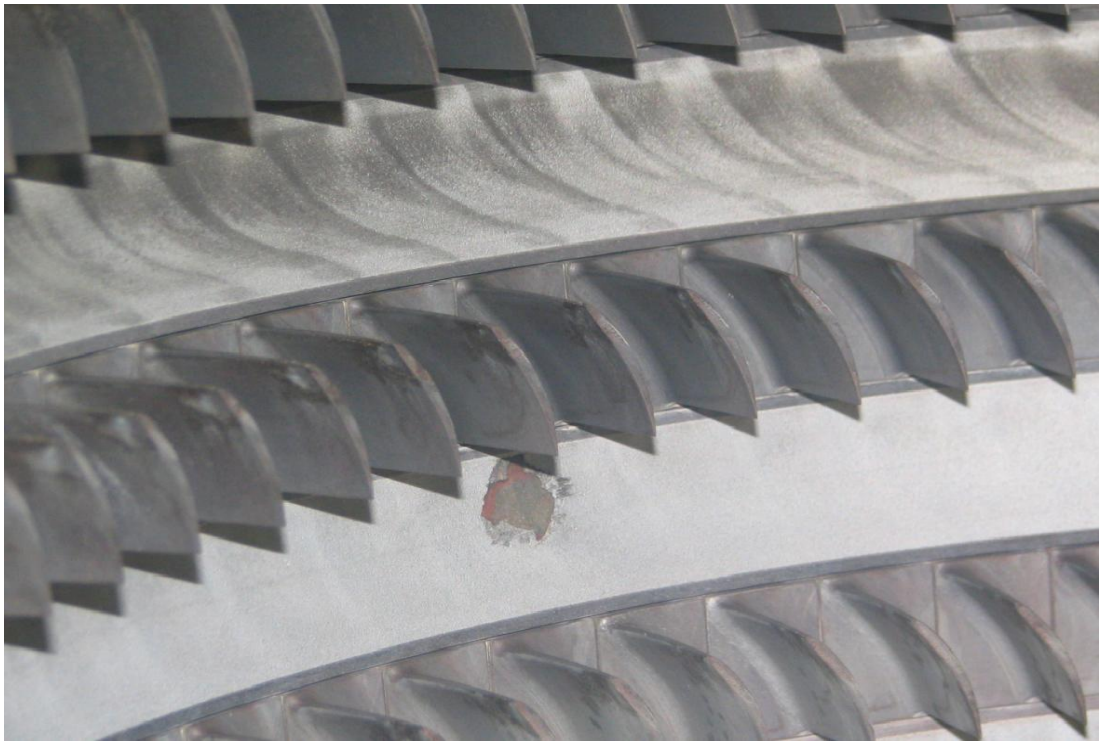

Figure 7F. Damage to the casing coating [Ref. 60]

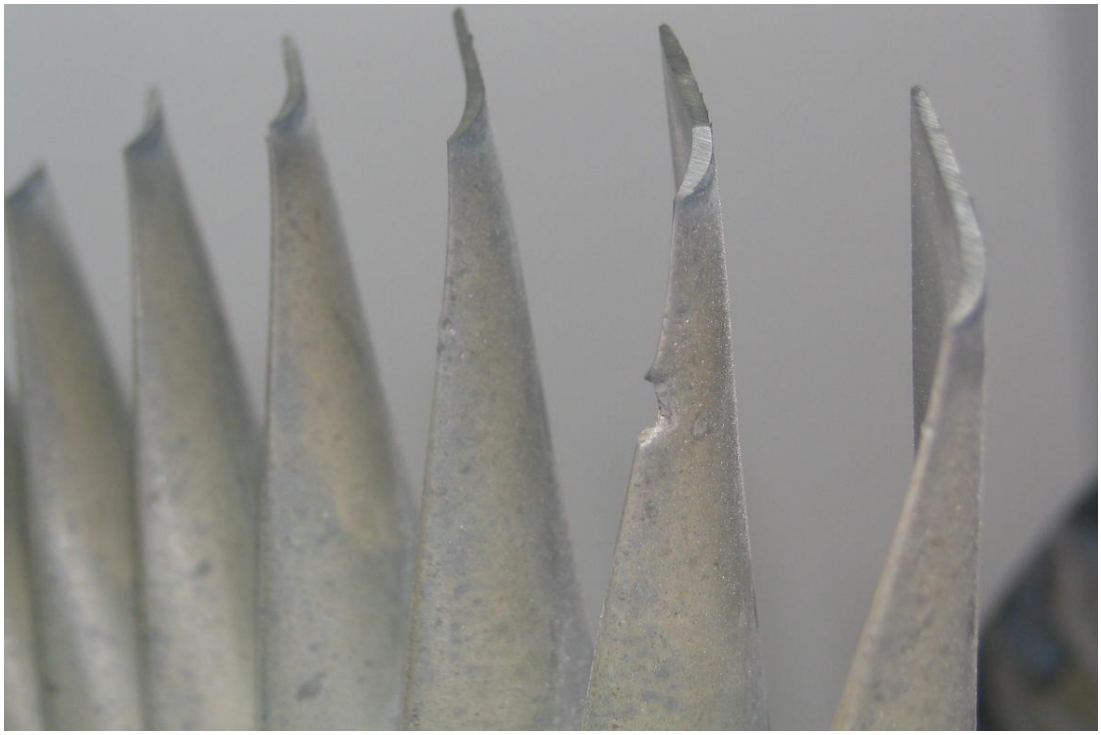

Figure 7G. Blade damage and coating material wear note tip of the blades- [Ref. 60]

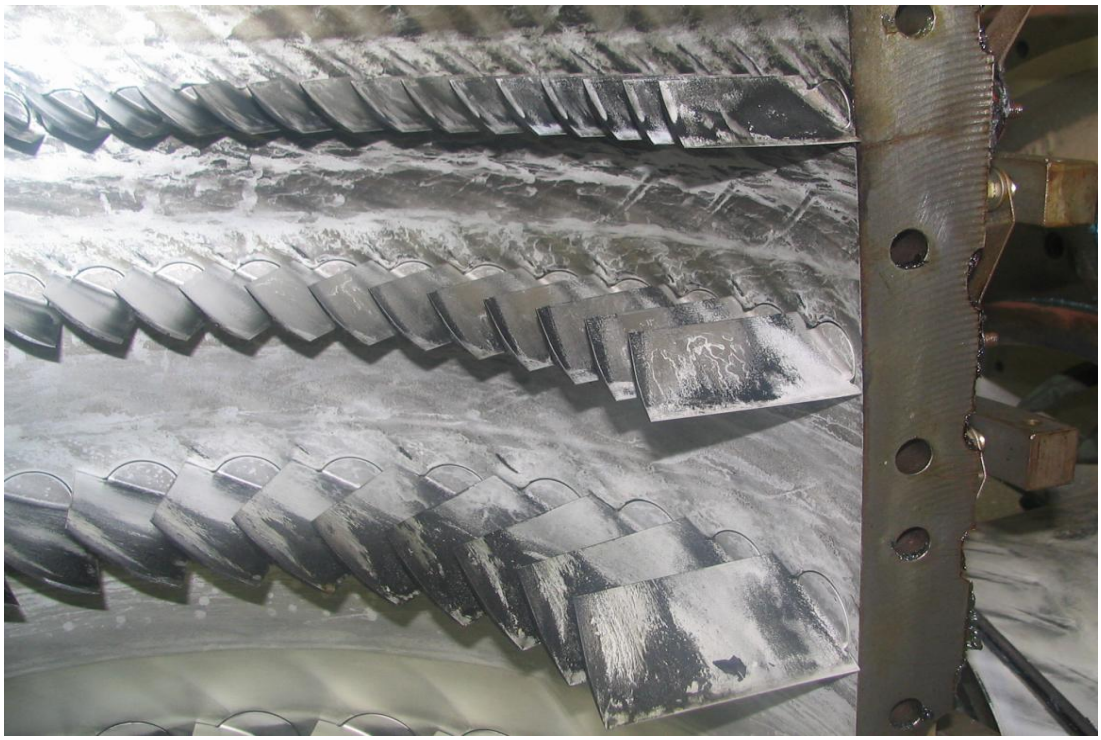

Figure 7H. Fouling deposition and blade damage [Ref. 60]

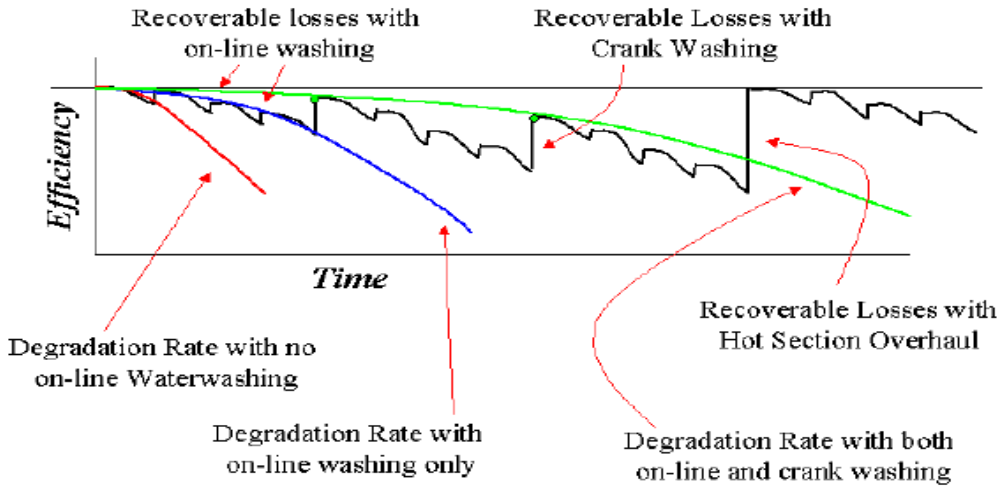

Figure 8. The profile of performance deterioration of a fouled compressor with and without treatment [Ref. 57]

The effect of material degradation on rotating equipment availability is phenomenal.

Around 70% of turbomachinery equipment failure is due to surface degradation out of which about 40% is due to wear and the balance is due to corrosion. For the axial compressors of gas turbines, solid particle erosion (SPE) and therefore the degradation of moving blades is the most commonly occurred fault [Refs 20, 21] due to air intake composition and the fall in the performance of air filters with time. For process gas centrifugal compressors the cause of degradation is erosion primarily due to presence of foreign particles such as burnt lube oil, seals oil leaks, mechanical impurities from water evaporation cooling systems (heat exchangers), salt and heavy hydrocarbons within the process gas. FOD and DOD result in the change in the flow paths through compressors and turbines. They also alter the surface finish. These effects can result in a reduction in both flow capacity and efficiency. The component failures within the process gas centrifugal compressors (based on a survey of 500 olefin plants [Ref 27]) is shown in Figure 9 where impeller problems tops the chart with 32% of the reported problems followed by fouling (28%), case leaks (14%) and seals (10%).

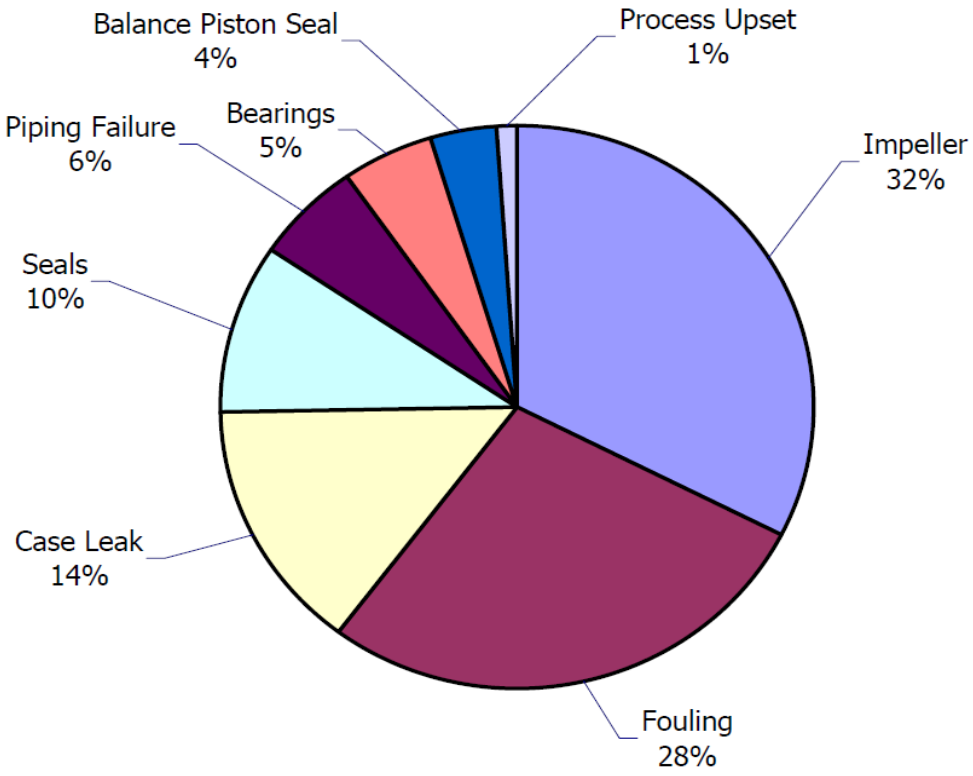

Figure 9. Centrifugal Compressor component failures (based on industry survey of 500 olefin plants between 1994 and 1999) [Ref 27]

A case study found that after 24000 hours of operation, 2-6% performance degradation would occur assuming no degraded parts are replaced and if replaced the expected performance degradation would be 1-1.5% [Ref 23]. Case studies carried out by others [Ref 24] have found fouling resulted in 5% reduction in throughput along with 2.5% reduction in efficiency and a 10% rise in shaft power demand. The effect of roughness (due to erosion) on measurable or dependent parameters is not uniform. Erosion effect on efficiency reduction is more pronounced than on pressure ratio; 2% versus 0.5% based on a case history [Ref 18] and on another axial type compressor engine it was found that 6 stages fouling caused 4.5% reduction in mass throughput, 4% reduction in pressure ratio a 2% reduction in efficiency [Ref 24].

It is due to the above significant effects of fouling on performance and therefore economics that since 1970s and 80s many researchers have attempted to model compressor fouling and its effects on performance.

In the late 80s, Aker and Saravanamuttoo [Ref 15] demonstrated that a linear or stage stacking fouling model gives an accurate representation of the fouling process up to approximately half way through the compressor. It is likely that

fouling is not a linear process for the entire compressor stages; it is most sever right after compressor washing, and thereafter it slows down and eventually it stabilizes [Ref 25]. For the linear part, the compressor fouling can be modeled as a "Linear Progressive Model" [Refs 15, 24, 26]. This means the 1st interval corresponds to the fouling of the 1st stage and the decrease in head and efficiency equals Δh and $\Delta \eta$; the 2nd stage causes further decrease in head and efficiency of the 1st stage by $2\Delta h$ and $2\Delta \eta$ and so on up to the 6th stage.

In mid 90s, based on degradation modeling aided by field data, Tarabrin et al [Ref 24] developed an index of compressor sensitivity due to fouling (ISF) that show strong dependency on tip diameter as follows:

$$ISF=10^{-6}.\ m.\ C_p.\ \Delta T_{stage}\ /((1-F^2_h).\ D^3_c))$$

Where,

ISF= Index of Compressor Sensitivity to Fouling
m= Compressor mass throughput, kg/sec
C_p=Specific Heat Capacity, J/kg. K
ΔT_{stage} =Average total temperature rise between each compressor stage, K
F_h =Hub to Tip ratio of 1st stage
D_c=Tip Diameter, meters

The above equation shows that a smaller axial type compressor engine is more susceptible to fouling than the larger one. High head stages of the compressor are more sensitive to fouling than the low head.

In 2000, Kurz and Brun [Ref 16] published their works on the changes in clearances and seal geometries due to degradation and changes in blade surfaces and aerodynamics due to erosion or fouling and have included a methodology to simulate the effects of gas turbine engine and driven equipment degradation and have proposed 'linear deviation factors' by comparing the test data to rotating equipment maps at various stages of degradation.

Based on analytical works in 2002, Jordal and Asadi [Ref 25] demonstrated how blade materials and compressor fouling rate affect the blade life time and based on thermodynamic approach they arrived at determining an optimum time for compressor washing intervals. It is stated that compressor fouling is most sever after compressor washing, thereafter it slows down and eventually stabilizes and present the degradation in terms of mass throughput as follows:

$$(m_{clean} - m_{deg})/ m_{clean} = A\ [1-\exp(Bt)]$$

Where,

m=mass throughput and suffices “clean” and “deg” refer to clean and degraded conditions respectively

A= The mass flow rate deterioration at which fouling stabilizes (typically set at 5% or 0.05)

B= A constant and it determines the rate of fouling. Three different rates of fouling were investigated. The results for a 4% reduction in mass throughput gives a value for B as follows:

B=3.22 x 10^{-3} at 500 hours of operation
B=1.61 x 10^{-3} at 1000 hours of operation
B=1.07 x 10^{-3} at 1500 hours of operation

The representation of degradation in the equation above is similar to the works carried out by Tarabrin [Ref 24]. The reduction in polytropic efficiency was taken to be proportional to the inlet mass throughput. Jordal [Ref 25] also studied the effect of blade material and working temperature on the life of the blade and this is shown on Figure 10 below showing a higher temperature rise for the blade of a compressor that has a higher degradation rate.

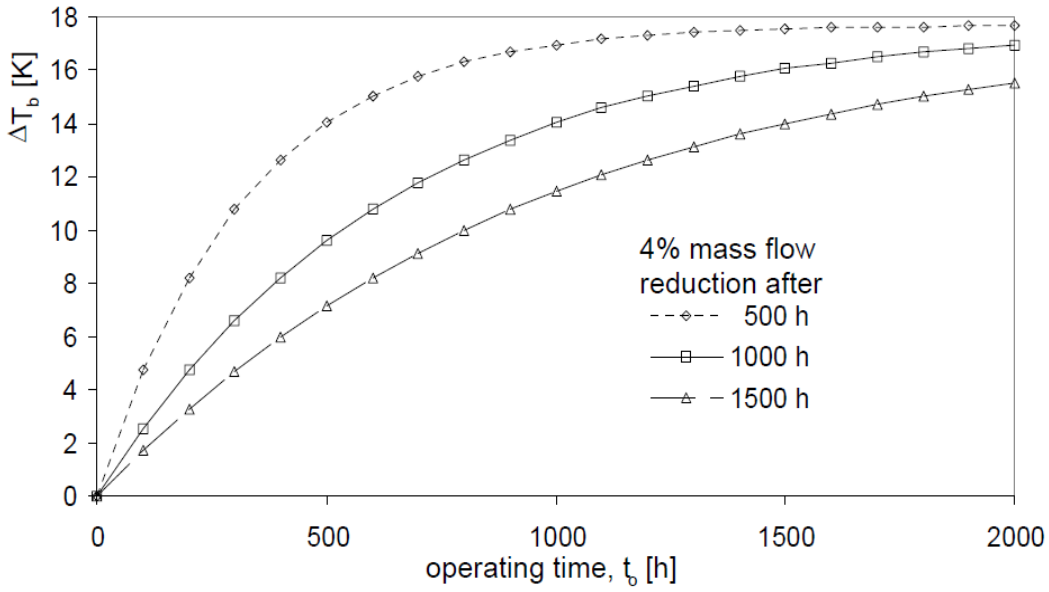

Figure 10. Increase in axial compressor engine model uniform blade temperature T_b as a function of operating hours for various degradation rates. No fouling at t_o=0 [Ref 25]

In same year as Jordal’s works above in 2002, Kubiak et al [Ref 21] modeled the effect of increased clearances, due to wear degradation, on power losses and it was found to be significant. An enlargement of compressor clearances

by 50% (measurements made during overhaul), diminished the power by about 5%.

More recently in 2009, Li [Ref 14] has developed a health status estimation method by defining compressor degradation as indices pertinent to flow capacity, pressure ratio and efficiency. Recognizing degradation causes a shift of the whole performance maps, the index of each the aforementioned independent parameter is the ratio of degraded value of the parameter to that of clean performance. Thus the current health of a compressor can be estimated at any time.

Also in recent times in 2010, Morini et al [Ref 35] has studied the effect of blade deterioration on performance maps, applying stage-by-stage simulations as well as applying scale factors that represented shift of compressor behaviour in deteriorated conditions. It was found that the flow rate decrease due to compressor fouling is proportional to, and varies linearly, with the number of stages affected reaffirming the result of earlier works on the degradation mechanism by Saravanamuttoo [Refs 15, 26] and Tarabrin [Ref 24] described earlier in this section. It was also found that scaled mapping gives a very accurate estimation with a RMS error less than 1% at areas close to design or test points.

Rotor blade erosion and geometry deterioration are strongly dependent on particle concentration and duration of ingestion. The patterns of erosion effects on blades depend on quantity of throughput relative to its design rate. Gheaiet has developed formulas giving approximate life time of blades [Ref 22] in the axial compressor due to sand ingestion which is a common problem due to filter inefficiency at the air intake.

Mechanical degradation of compressors parts has different symptoms. Seal's wearing out (clearance) is associated with sever rotor vibrations. The symptoms of blade degradation are not same as seals wearing out.

Degradation causes visible or measurable changes in performance such as reduction in pressure ratio, compressor efficiency and mass throughput. In all these cases, the initial effect is that the compressor discharge temperature goes up and it has to work harder to meet the set discharge pressure and mass throughput. This in turn will lead to increase in fuel or electric demand driving the compressor. To get an appreciation on the scale of economics involved here, for a single 40 MW gas turbine machine at a rated heat rate of 10,000 Btu/kW.hr at an average load level of 80% operating throughout the year, an increase of 1% in fuel at a cost of $8/MMBtu will lead to an extra cost of $200,000 per year [Ref. 19]. The ultimate effect of compressor degradation is significant deviation from acceptable performance specification and component failure. It is ironic at the same time, however, that compressor

failures have reduced in the past decade due to better technology and online health monitoring but the frequency of failures is still significant.

The degradation cannot be measured. However, the degraded performance produces deviations in measurable parameters such as discharge pressure and temperature, mass throughput etc. Gas Path Analysis (GPA) is a technique for analyzing deterioration effects of a compressor. GPA provides the means for assessing the independent (non-measurable) compressor parameter deviations by establishing a relationship between them and the dependent (measurable) parameters. Based on the changes from a new and clean status (base line) a compressor gas path diagnosis is issued. In the proceeding sections compressor diagnostics and techniques are discussed in detail.

As it will be seen in the later sections, compressor degradation causes the performance curves move downward and to the left due to polymer build up, dirt, corrosion, increased seal wear and greater restriction to process flow in general due to fouling. The efficiency is reduced because of increased frictional losses and/or increased internal recirculation (wear, rubbings, clearances, etc). As a result of compressor degradation, surge margins are reduced meaning the compressor will go into surge mode at higher flow rates than the rated OEM values for a clean compressor causing potentially extensive damage to the compressor. Thus lower surge margins are indicators of compressor fouling. References 8, 9, 15, 18, 34-38, 50 and 51 provide further in-depth theory and survey on compressor fouling, tip clearance and compressor performance deterioration and modeling.

In axial compressors performance deterioration results in increase in operating temperature which in turn may result in an increase in operating speed and higher firing temperature which results in accelerated creep life usage.

2.3.4 Recent advances in compressor design for optimum efficiency

In the preceding section it was realized that up to 70% of turbomachinery equipment failure is due to surface degradation and in case of centrifugal compressors in the process industry impeller problems due to rubs and erosion tops the chart of reported problems with well over 30% of reported failures followed by compressor fouling. Also in the preceding section, the effect of fouling and erosion/corrosion was emphasized on the performance by numbers that for a case, fouling had resulted in 5% reduction in throughput along with 2.5% reduction in efficiency and a 10% rise in shaft power demand.

It is for the above reasons that much research and development has been concentrated on minimizing rubs and minimizing possibility of foreign particle sedimentation on the compressor surfaces by the application of special

coatings and materials that have specific favourable properties such as low coefficient of expansion.

Certain and some finite controlled leakages must exist in a process gas centrifugal compressor (see Figure 6A) such that the compressed gas, which if released will be harmful to operators and environment, is in isolation and do not travel outside the casing into the ambient. Furthermore materials generally expand outwardly due to temperature increase or centrifugal forces. This means that some clearances must exist between the moving and stationery parts to allow for the mentioned physical changes. Too wide a gap, though, increases leakages and pressure losses leading to reduced compressor efficiency and lower throughput capacity.

Recent advances for improvements include use of superior materials and coatings in the various parts of the compressor that are:

1) Resistant to erosion/corrosion,
2) Able to withstand higher stresses without physical damage or deformation,
3) Limited coefficient of expansion of the casing and impellers

Other areas of advances include superior and abradable seals in the impeller eye and shaft seal areas.

The limited expansion of the casing is accomplished by a superior material so that their expansion is very finite due to temperature increase and therefore do not rub against the moving parts leading to tighter design operating clearances and minimal efficiency effects after a seal rub.

The application wear rings shroud the exposed surface of the shaft to the corrosive gas hence disallowing continuous contact between the process gas and the shaft in corrosive environments and fluids resulting in the shaft being far less prone to corrosion and instead the wear rings are easily replaced when required and these rings are special corrosion/erosion resistant materials.

Recent developments to further improve compressor efficiency include the full application of computational fluid dynamics (CFD) to ensure full, gentle and radiused gas flow paths control minimizing gas velocity changes and flow separation for the compressor stage as well as for the auxiliary flow paths such as the inlet and discharge nozzles and volute design which are all part of compressor rotor dynamics and aerodynamics design and analysis. Figure 11A gives an example of CFD modeling where the problem areas are identified in the original design (red spots on the impeller) and the new design where the flow is smooth and stresses are reduced.

Figure 7A shows the long term effect of coated and non-coated surfaces on dirt/polymer buildup in diffuser passage of a centrifugal compressor. The type

of material and coatings used are being updated regularly with superior properties and the clearances are reduced to absolute minimal to minimize losses and increase the compressor efficiency. Figure 11B shows the effect on compressor efficiency due to the coating used. A material composition applied by a specific manufacturer [Ref. 55] consists of three different layers and these are from inside to outside (the latter is in contact with the process gas):

- Chromate/phosphate coating with aluminum
- Polymeric coating
- Coating layer containing PTFE

Together these layers achieve good bonding, provide corrosion protection and achieve a very smooth surface of the rotor and prevent fouling from sticking to the rotor. Coating can be applied on rotor as well as on stationary parts. Maximum continuous operating temperature for the coating is approx. 250°C [Ref. 55].

The application of advanced tools for health monitoring, effective shift of maintenance strategy to predictive or conditioned based maintenance, innovative noise reduction for the health and accuracy of measuring devices, the application of “integrally geared” centrifugal compressors featuring multi-shaft arrangements with different speeds, new and extended software applications in aerodynamic, structural, rotordynamic and manufacturing are among the other recent advances in compressor design for optimum performance and power consumption.

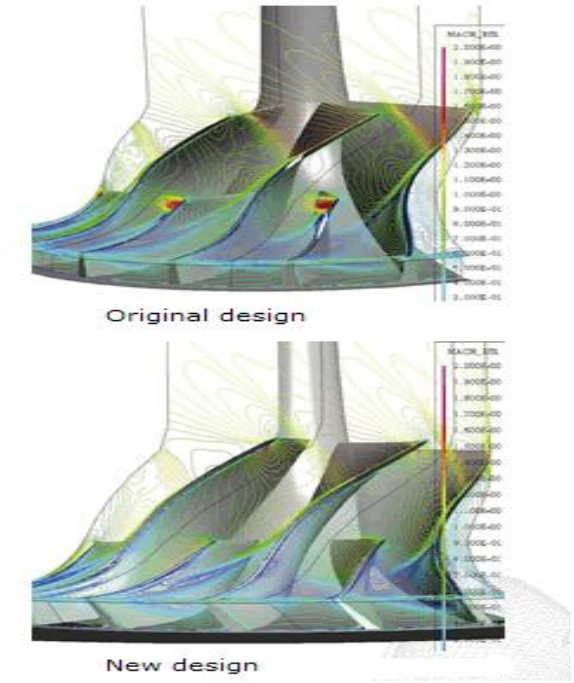

Figure 11A. Computational Fluid Dynamic (CFD) modeling of compressor's moving parts showing how stresses are reduced during design phase [Ref 54].

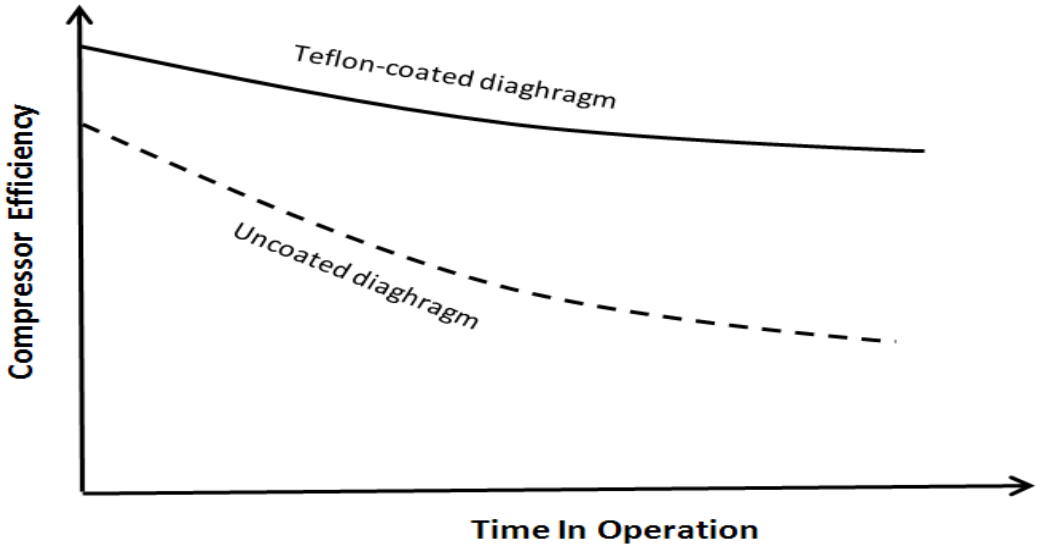

Figure 11B. Effect of coated and non-coated surfaces on dirt/polymer buildup in diffuser passage of a centrifugal compressor [Ref 28]

2.4 Performance Simulation and Analysis

The performance of a compressor is best modeled by simulation. In order to come up with the correct diagnostic results, the prediction of performance by the simulated model must be highly accurate so that any simulation errors are not comingled or confused with performance deterioration. Once an accurate model of the compressor is built then the model could be impregnated (stimuli) with a known fault and the resultant changes or the responses (fault signature) are analysed. These patterns compared with the real compressor but unknown fault will lead to fault finding or diagnostics. It is better to apply two different approaches for diagnostic determination.

Advanced simulation programmes are available for performance modeling purposes and the one chosen for this thesis is the application of HYSYS.

In HYSYS, the feed composition, pressure and temperature as well as two of the following four variables:

- Flow rate
- Duty
- Efficiency
- Outlet Pressure

Once the necessary information is provided, the appropriate speed is determined and the other two variables are calculated. If speed curves are available then the polytropic or isentropic heads and efficiencies for a range of flows and speeds are input from the user into HYSYS which, for a given speed and flowrate, calculates the outlet pressure. If the inlet and outlet measurable parameters such as flow, pressure and temperature are entered, then HYSYS calculates the actual compressor polytropic efficiency and speed. The input/output to and from this software and the thermodynamic equations used for the compressor model building and performance evaluation are laid out in Appendix B.

2.5 Diagnostic Methods for Compressors

2.5.1 Diagnostics by definition

The compressor diagnostics are the application of available methods to detect and quantify faults within the compressor. The compressor may be the axial type as an integral part of a gas turbine or a centrifugal type compressing gas in a process plant. The diagnostic technologies have shifted the maintenance from preventative type to reliability centred maintenance (RCM) based and in so doing they have increased the compressor availability. For example, reference to Figure 1, the detection and quantification of fault of a compressor (i.e., compressor health) at current time is diagnostics and prediction of behaviour in future and therefore the imminent maintenance/spare parts requirement is prognostics. The time at which maintenance action is taken depends on company tolerances and policies. In order to carry out the diagnostics, correctly selected performance data coming from the compressor must be monitored and analyzed by various available tools and methods including accurate simulation of the compressor under investigation by an advanced simulation module leading to true diagnostics and advice on the required maintenance. This cycle for an axial compressor in a gas turbine is shown on Figure 2 [Ref.33].

2.5.2 The available diagnostic methods

In order to keep high availability and reliability effective maintenance is essential meaning the asset holder must shift from preventative maintenance philosophy to RCM and this is essentially accomplished by compressor health monitoring and fault diagnostics.

The most common cause of degradation for both centrifugal and axial compressors is fouling (see section 2.3.3), tip clearance due to wear and erosion and labyrinth seal damage, body/shaft erosion and corrosion. These faults result in changes in thermodynamic performance evaluated fundamentally by efficiency and flow capacities which in turn produce changes in the measured or observable dependent parameters such as discharge pressure and temperature and rotational speed. The respective degree of change reflects degradation which can be used to detect and isolate the unhealthy subcomponent.

The relation between the performance deterioration and the resultant changes in the measured parameters, fault detection and isolation was first realized by Urban in the mid 1960s and since then up to now many sophisticated methods of diagnostic techniques has been developed and some techniques such as transient measurement techniques and expert systems are still under development.

The purpose of condition monitoring is to draw conclusions on the condition of the rotating equipment from the measured data in a cost effective manner. The diagnostic techniques broadly fall into two groups of Model based and Non-model based methods as shown on Figure 12 which are broadly applicable to compressors as well. There are many condition monitoring techniques (CMT) available but there is no single technique that can satisfy the requirement of fault detection for all the conditions and sub components of the compressor.

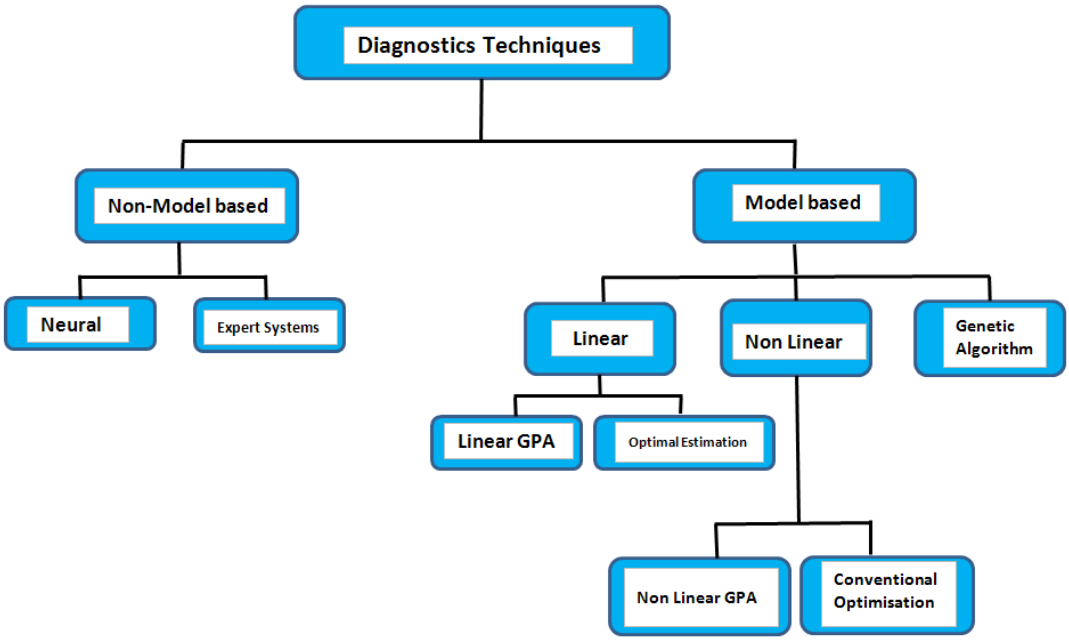

Figure 12. The structure of rotating equipment diagnostic techniques [Ref 37]

The following are the commonly used techniques for compressor diagnostics:

1) **Performance analysis based diagnostic techniques**:-

The GPA approach is mostly used in compressors. This is one of the most useful approaches which allows the Engineer to identify current operation points and position on performance map, if the compressor or compression train is a cause of bottleneck in the system, performance losses, power balance calculations, causes of vibration, limited production (hence bottleneck), temperature limitations and recycle operations. Understanding these points can help to determine an operational strategy or actions for maintenance to maximize production, reduce the number of machinery trips, extend life of machinery and plant.

Performance based diagnostics are discussed further after highlighting other available techniques.

2) **Oil system monitoring technique**:-

This technique is useful to identify temperatures which can show increased bearing load or worn components. Also sampling of oil is useful when there are known failures. These all are only typically manually monitored, with some temperature alarms usually in place.

3) Vibration monitoring techniques:-

Very useful coupled with performance analysis. DE and NDE radial vibration probes with high alarm and trip set-points. Axial displacement vibration probes to indicate worn components badly performing balance piston or even operating performance of the compressor. Probes are set with =/- alarm and trip set-points. Trends are typically manually monitored or analysed by performance and vibration analysis contracts. Usually clients contract out the vibration analysis (typically given so called “performance monitoring” title to the contracts, even though only the vibration is monitored), however, the complexities of performance analysis and understanding the link between performance and vibration is only possible by specialist companies.

4) **Engine usage monitoring techniques**:-

Many Oil and gas clients do not use sophisticated monitoring systems. The main observation is on the running hours to determine when to wash the engine and maintenance period, also monitored are; firing temperature (EGT or ECT), and filter inlet DP in case of axial compressors in gas turbines. Most operators do not understand the importance of monitoring engine compressor discharge temperature and pressures, or what these parameters tell them about the performance of the engine. Therefore typically these are not even instrumented.

5) **Visual condition monitoring techniques**:-

This is borescope inspection (although typically very limited) or physical examination of components when compressor bundle is pulled.

6) **Engine exit spread monitoring**:-

Useful for power balance checks between engine and compressor to determine the average EGT if not recorded. Useful mainly to engine performance assessment and component lifting/ maintenance schedules.

7) **Limited transient monitoring**:-

This is not carried out for performance monitoring, although some specialist companies use data (with some caution due to transient data and heat soakage effects) to look into start-up issues. Used for offline analysis and anti-surge and plant control assurance studies and training simulators.

8) **Acoustic monitoring**:-

Acoustic emission monitoring is carried out on critical parts that are prone to failure in certain types of compressors; for instance the reciprocating compressor valves. Here technology exists that records an acoustic emission (AE) and temperature fingerprint for the operation of each valve (baseline). Data is analyzed against the baselines to determine whether anomalies with the operation of the compressor are present. The system is able to detect changes in the timing and nature of valve opening & closing events and detect the presence of leakage when valves should be closed.

A source of statistics reported by Li [Ref 39] for breakdown of faults reveal 28% of detected faults are due to oil leakage, 24% is attributed to oil lubricated component problems, 14% due to engine performance problems and 10% due to component vibration problems. Goetz [Ref 40] provides an excellent statistical database for various types and components of turbomachinery.

The diagnostics based on performance analysis is one of the most effective tools where the analysis of gas path parameters provides information on the severity of degradation. Many of these techniques utilize state of the art technology. In this respect some of the available techniques are:

- Gas Path Analysis (GPA- linear/non-linear, Kalman Filter)
- Health Indices
- Artificial Neural Networks (ANN)
- Genetic Algorithms (GA)
- Pattern Matching
- Fuzzy Logic (part of Expert Systems)
- Transient Measurements

The methods listed above apply to both compressors and gas turbines. In the current research works, Health Indices will be concentrated upon, developed and applied to the site compressor in the later sections.

Gas Path Analysis or GPA was first introduced in 1967 by Urban [Ref 29] as a linear model based method. In 1990, Estamatis accounted for the non-linearity of gas turbine engine behaviour in his modeling using conventional optimization method. But this method may at stop at local minimum. This

limitation was overcome by the application of Genetic Algorithm first by Zedda and Singh in the late 90s. Further development of the non-linear method was done at Cranfield by Escher in 1995 utilizing Newton-Raphson technique and a computer code “PYTHIA” [Refs 49, 32]. Neural Networks (NN) were first introduced by Denny in 1965 and it has been widely used since mid 1980s. NN has the advantage that only engine experimental knowledge for the training of neural nets and once the NNs are trained computational time for diagnosis is very short. Application of “Expert Systems” for engine diagnostics was first developed in 1980s and this group of techniques is one of the best method and still under development which also applicable to compressors. More recent advances in rule-based fuzzy expert system were introduced after mid 90s such as those introduced by Fuster & Sui et al in 1997. The computational speed for expert systems is fast but, it is however, a complicated modeling approach.

A neural network is artificial intelligence based diagnostic method. It is a massively parallel distributed processor made up of simple processing units, which has a natural propensity for storing experimental knowledge and making it available for use. The most popularly used artificial neural network in gas turbine diagnostics is the Feed-Forward Back-Propagation Networks, a supervised network, where sensed information is propagated forward from input to output layers while calculated errors are propagated backward and used to adjust synaptic weights of neurons for better performance.

Artificial neural networks and diagnostics is based on similarities of the way neurons and brain work and the system allows apply the “experience” to isolate and quantify the fault. Artificial neural networks (ANNs) are a group of algorithms originated within the field of artificial intelligence. They are not programmed; they learn from experience. It can handle multidimensional nonlinear systems. The ANN must first be trained before becoming useful; Li and Arriagada give more details [Refs 39 and 42].

In Genetic Algorithm diagnostics, the idea of a fault diagnosis with genetic algorithm is similar to a recycle feed controller in a control loop. With an initial guess of engine component parameter vector, the engine model provides a predicted performance measurement vector. An optimization approach is applied to minimize an objective function meaning the predicted value by the model becomes very close to the actual measurement with a minimum set difference and once the set difference is reached, iteration is stopped. More details are given by Li [Ref 39].

Li and Singh [Refs 29, 31] provide further sources of information and further reading for the current available diagnostic techniques listed at the start of this section.

Broadly speaking all diagnostic techniques listed above and others rely on GPA [Ref 31]. The fundamental concept of gas path diagnostics is shown in Figure 13 and it illustrates the nature of the gas path diagnostic problem. The common features of all Gas Path Diagnostic Techniques are:

- **Objective Function** – This is a representation of the problem (minimization of objective function), easy to solve and take into account measurement noise and sensor bias. Figure 14 shows a high pressure compressor search space and the model. It is obtained by varying the deterioration or degradation in mass flow from –3.5% to +3.5% and the deterioration in efficiency from 0 to 3.5%. The values obtained are then compared with data generated by introducing a 2.75% efficiency deterioration in the high-pressure compressor. Each point on the surface plot is a potential solution and the best solution is the one having the lowest objective function.
- **Number of Operating Points** – A technique using a single operating point can result in a high degree of accuracy if the number of measurements is higher than the performance parameters. For the case of number of measurements being lower than the number of performance parameters, a more judicious choice of diagnostic technique is needed such as multiple operating point analysis technique (MOPA). Here the accuracy of diagnostics depends on the choice and number of data points [Ref 31].
- **Number of Measurements** - The choice of number and type of sensors is a critical issue which can greatly affect the final results as well as the computational burden of the diagnostic technique. A high number of sensors invariably makes the search space smoother and therefore reduces the computational burden. Refer to the two plots shown on Figure 15. The graph on the left shows the search space generated with 9 instruments and the graph on the right is for the same engine but with 16 instruments. The flatness of the plot around the minimum on the left graph implies that optimum would be difficult to be identified. Whereas for the same engine using 16 instruments referring to the graph on the right of Figure 15, it shows a distinct convergence to a global minimum which is easier to locate.
- **Quality of Measurements** – This is another important issue with diagnostics techniques related to the quality of the measurements or observability. Not all choices of measurements will allow the identification or observability of all the faults.
- **Search Algorithm** – The complexity of the search space characterized by several rather than one local minima favours the utilization of search methods other than classic optimization techniques. This include “random search” whereby controlling a set of parameters the random search is guided progressively towards a solution. However, Genetic

Algorithm (GA) often outperforms the referred method in many optimization problems.

The factors that give may result in erroneous diagnostics is measurement noise causing data scattering around the true value and in this instances data filtering and averaging are applied to reduce the errors and the diagnostic accuracy. Li [Ref 29] has identified good sources of referencing for measurement noise filtering via the application of auto associated neural network (AANN).

In GPA there are two methods available: linear and nonlinear and these are described later in more details. Since the behaviour of a compressor's component is generally non-linear, the application of linear method for diagnostics is limited although it has its own advantageous including providing a quick solution and fault isolation, quantification and multiple fault diagnostics. Both of the linear and non linear GPA apply optimization methods to deduce a fault and nonlinear GPA is combined with a conventional optimization method. But conventional optimization stop at a local minimum and genetic algorithm has overcome this disadvantage. Kalman filters and optimal estimation are applied to GPA in order to overcome its setbacks [Ref 31].

In the current compressor performance adaptation and diagnostic research at hand, linear and non-linear model based diagnostic is of particular interest which is described more fully in the next section.

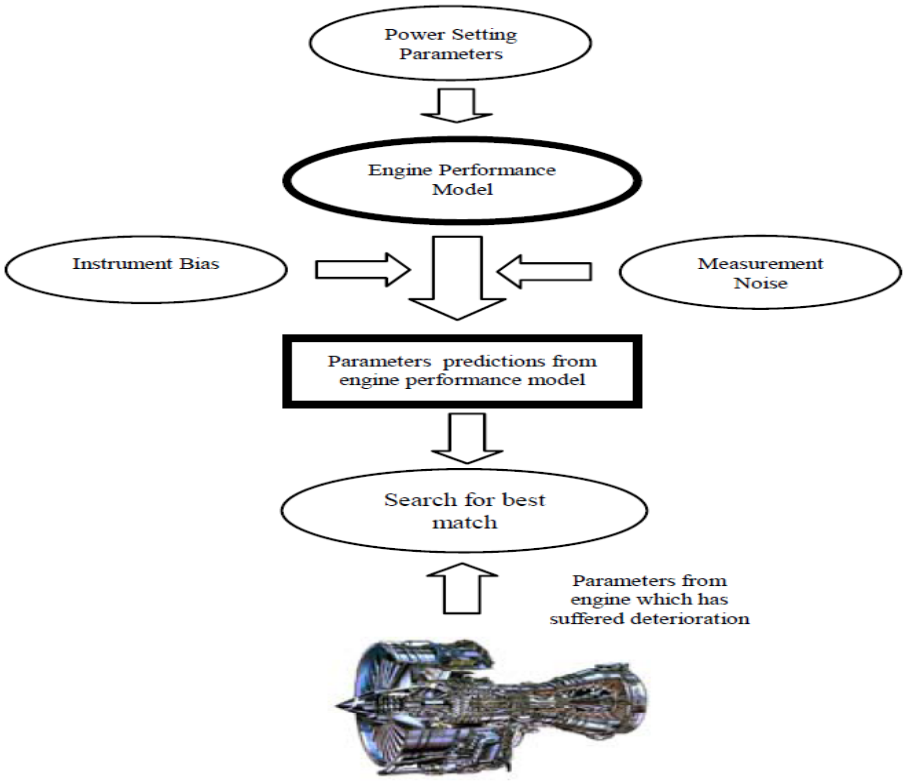

Figure 13. Fundamental concept of gas path diagnostics [Ref 31]

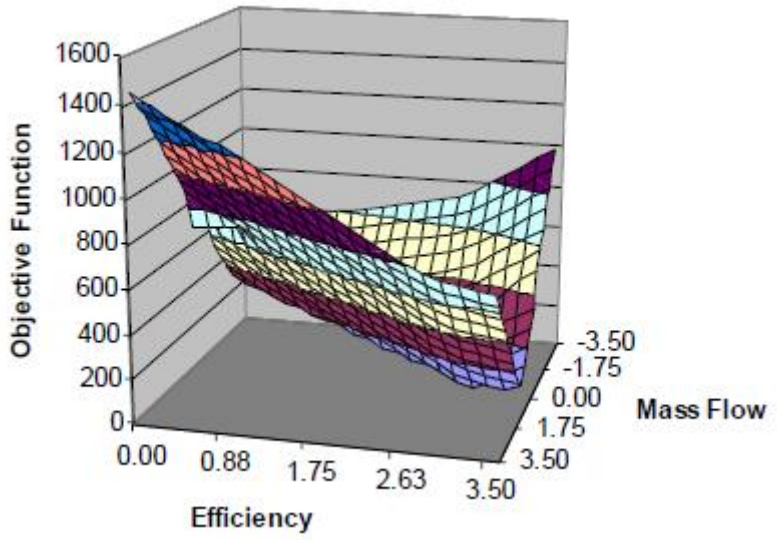

Figure 14. Search space for compressor [Ref 31]

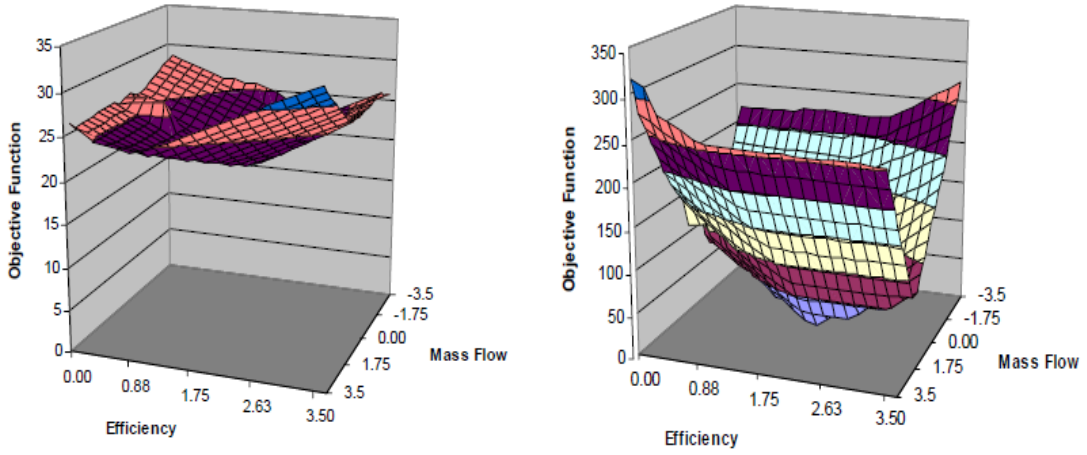

Figure 15. Effects of number of measurements on diagnostics. [Ref 31]

2.5.2.1 Linear and Non-Linear GPA Model Based Diagnostic Method

A linear and non-linear GPA approach is an effective tool for performance diagnostics, the principle of which has been utilized for the subject research. The principle base description and rules for linear and non-linear GPA are described below.

Reference to Figure 16, if at a certain operating point of the compressor a linear relationship is taken between the dependent or measurable parameter such as gas path pressures and temperatures, mass throughput etc., and the independent parameter such as pressure ratio and efficiency the following relation is valid:

$\vec{z} = H.\ \vec{x}$

Degradation can be recognized as the deviation in performance from that when the engine was new. At a given operating point and at certain time during operation a linear relationship between gas path measurement deviation vector $\Delta\vec{z}$ and engine component health parameter deviation vector $\Delta\vec{x}$ can be obtained from the engine performance model $\vec{z} = f(\vec{x})$ using a tailor series expansion [Ref 30]:

$\Delta\vec{z} = H.\ \Delta\vec{x}$

Where H = Influence Coefficient Matrix (ICM)

Therefore the engine performance degradation represented with $\Delta\vec{x}$ can be obtained with the following equation if the number of measurements is at least equal the number of health parameters:

$\Delta\vec{x} = H^{-1}.\ \Delta\vec{z}$

Where,

$\vec{x}$ = An independent variable such as pressure ratio, flow capacity or efficiency

$\vec{z}$ = A dependent variable. These are the measurable variables such as pressure, temperature or mass flow rate, and,

Δ denotes a change (deterioration or degradation) in vector parameter

H^{-1} = Fault Coefficient Matrix (FCM) or Diagnostic Matrix.

The above equation shows that by multiplying the measured changes in the dependent parameters by the FCM, the changes in the independent parameters can be found. This allows the cause of the deterioration to be determined. Linear GPA is suitable for small changes or degradations as changes at or near the operating point are linear.

The above is the linear GPA. Since performance normally deviates non-linearly with degradation, solution by linear method may lead to significant errors and a non-linear GPA is developed where the linear GPA is used iteratively in the following manner until a converged solution is obtained using Newton-Raphson method; see Figure 16A.

With an initial guessed parameter vector $\vec{x}'$, the compressor or engine model provides a predicted performance measurement vector $\vec{z}'$. An optimization approach is then applied to minimize an Objective Function (see Figures 14, 15 and 16A) minimizing the error by an iterative process. The iteration is carried out until the best predicted component parameter vector $\vec{x}'$ for real $\vec{x}$ is obtained. The error is defined as the difference between the real

measurement of vector $\vec{z}$ and the predicted measurement of vector $\vec{z}$ and it is normally a very small value (0.001-0.002).

The non linear method described above utilizes a computer code, PYTHIA, which was developed by Cranfield University [Ref 33] and it has the axial compressor module as a part of the gas turbine. Others have also produced optimization programmes for engine simulation adaptive modeling applying for instance Generalized Minimum Residual (GMR) method or Maximum Likelihood Estimate (MLE) method [Ref 29], which are also adaptable to compressors.

In order to make all differential GPA methods valid, the number of measured performance variables must be greater than or at least equal to the number of diagnostic parameter to be estimated.

The success of identifying a given fault set depends greatly on the set of monitored parameters. In other words, if the dependent variables do not relate to the sought-after fault, then either the diagnostic or the fault set is in error.

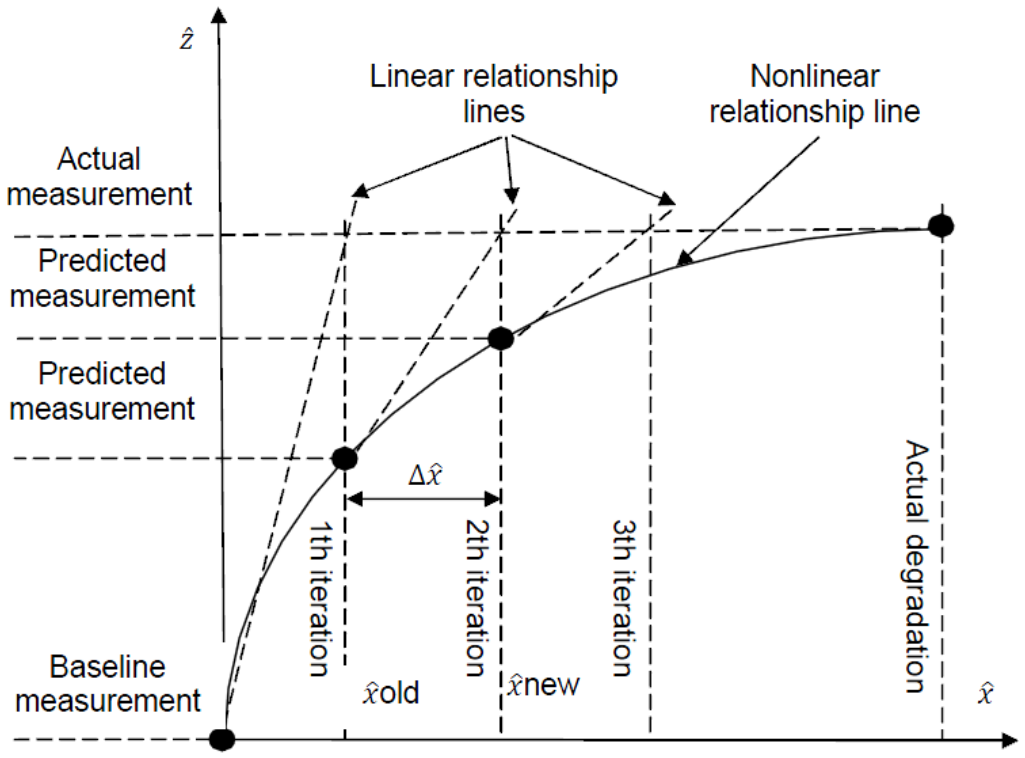

Figure 16A. Nonlinear Solution (by repetitive linear iterations) for compressor diagnostics [Ref. 49]

Taking into account the influence of ambient and operating conditions, sensor failure and compressor component degradation, an “integrated” GPA diagnostic system should be described. By applying Theta (θ) and Delta (δ) factors to the data (see later in Chapter 4), performance data comparison of clean and degraded compressor on the same environmental and inlet conditions are enabled so that environmental changes do not interfere with the degradation results and differences in actual and expected performance would be due to degradation and instrument errors only. Reference to the site compressor under research, all critical instruments are regularly calibrated, maintained and failed sensors are automatically reported to the control room. Only instrument noise is inevitable which due to the design and operational constraints and it is not considered to have significant effect on the diagnostic results as the instruments are regularly calibrated and have self diagnosing and reporting capabilities. Li [Ref 32] has provided an insight into measurement errors, in which, sources for further referencing has also been identified.

GPA provides the means for assessing the non-measurable or independent compressor parameter deviations by establishing a relationship between them and the measurable or dependent parameters. Based on the changes from a new and clean status which is the base line, a compressor gas path diagnosis is issued.

Based on the works by Marinai [Ref. 66], Kammunge [Ref. 63] has summarised the diagnostic methods as follows:

1) Linear GPA with ICM inversion are based on the relative changes in the health parameters are relatively small. The inadequacy of this assumption has led to the development of nonlinear methods

2) Multiple Fault Isolation (MFI) are suited for the analysis of slow deteriorating components, whereas Single Fault Isolation (SFI) implies a rapid trend shift, perhaps due to a single or multiple entity going skewed.

3) Estimation techniques require prior information and the solution can be dramatically affected by this choice.

4) Expert systems, ANNs and fuzzy logic systems are referred to as model-free systems. This feature has the advantage of data fusion capability but the limitation is that no model-based proof of robustness is possible.

Figure 16B shows the summary of diagnostic methods [Res. 66, 63] and Figure 16C is an illustrative summary of the diagnostic methods based on model complexity and computational speed [Refs 41, 58].

	Methodology										
Strategy	Linear GPA with ICM inversion	Non-linear GPA with ICM inversion	Linear Kalman filter	Linear WLS	Non-linear Kalman filter	Non-linear model based with GA	Artificial neural networks	Bayesian belief networks	Expert systems	Fuzzy Logic	Rough-Sets
Linear/non-linear model	Linear	Non-linear	Linear	Linear	Non-linear	Non-linear	Non-linear	Non-linear			
Small changes of health parameters	X		X	X							
Addresses Random noise			X	X	X	X	X	X	X		
Addresses Bias			X	X	X	X	X		X		
N Parameters, M Measurements	M>=N	M>=N	M<N	M<N	M<N	M<N	M<N	M<N	M<N		M<N
Singe/Multiple fault(s)	MFI	MFI	MFI	MFI	MFI	SFI/Limited MFI	SFI/Limited MFI	SFI/Limited MFI	SFI/Limited MFI		MFI
Smearing Vs concentration			Smearing	Smearing	Smearing	Concentration	Concentration	Concentration			
Difficulty and dependence on training/tuning			Prior knowledge	Prior knowledge	Prior knowledge	Number of string assignment	Long training and data selection	Effort in gathering info for setting-up			Need to generate rules
Artificial intelligence based						X	X	X	X	X	X
Computational burden						X		X			
Model free							X	X			X
Data-fusion capability							X	X			
"Black-box" (not observable)							X				X
Good accuracy in pre-defined ranges only						X	X	X			X
Expert knowledge capability								X	X	X	X
On-wing			X	X	X		X			X	

Figure 16B. Principle summary and comparison of gas path diagnostic methods [Refs. 66, 63]

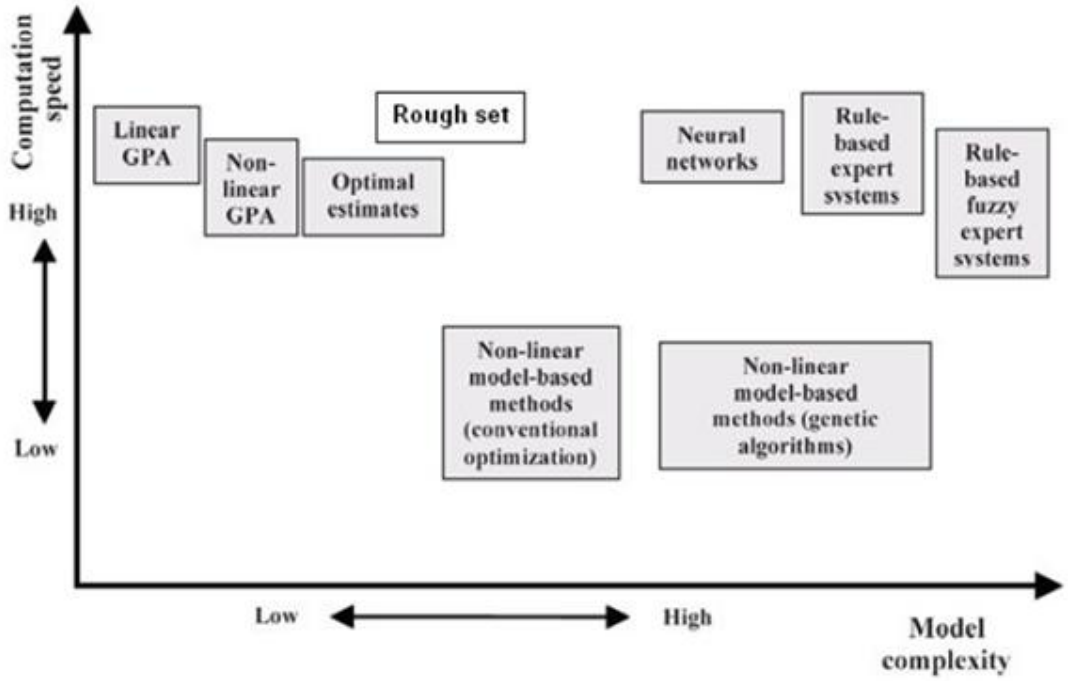

Figure 16C. Summary of diagnostic methods based on model complexity and computation speed [Refs 41, 58]

2.6 Continuous on-line monitoring for compressor health monitoring

As with most mechanical devices, the performance of a running compressor slowly deteriorates from its normal healthy condition. This degradation can be quantified by comparing the real runtime process parameters to those provided by compressor manufacturer (OEM data), the latter is a (decreasing) variable and a function of time before a major overhaul is carried out (see Figure 1 and Ref. 57).

Diagnostics of a running compressor is necessary to optimize the performance as well as optimizing the maintenance strategy saving in periodic shutdowns leading to less operational costs. Continuous performance monitoring of the compressor is the best available mean to provide real time performance data tracking degradation and ensuring remedial action is taken as forecasted in advance of the failure. Figure 17 shows how the online information can help decide the washing time for the compressor. The highpoints are the peak performances which depreciate with time. Notation “0” is an established base line. The negative troughs are the lowest performance that the operator will allow before washing is performed after which the performance is picked up again.

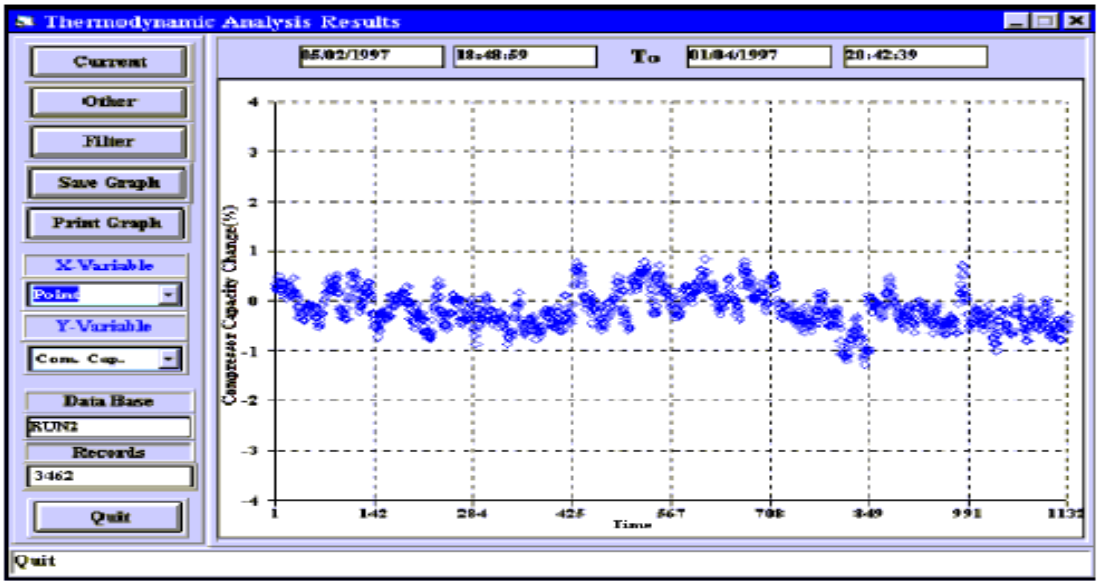

Figure 17. Online performance monitoring – thermodynamic analysis of compressor capacity index [Ref 11]

A program that incorporates the condition of a critical component (condition monitoring) rather than its operating time (time based or pre-scheduled maintenance) offers benefits to the economics of the plant because the equipment may still be healthy if the replacement is time based. The on-line performance monitoring (OPM) helps turbomachinery operators to know

instantly when something goes wrong or starting to go wrong. By definition rotating equipment condition monitoring is a management technique that uses the regular evaluation of actual operating conditions of the machinery to optimize the total machinery operation.

OPM benefits the plant operators by confirming if the equipment is performing as promised by the manufacturer. Maintenance scheduling, including cleaning and major overhaul such as a crack that may appear in the diffuser of the compressor, can be based on equipment condition. Current and historical data are invaluable when rerates are considered.

By informing the operator where the compressor is operating on its curve, online monitoring can help prevent mechanical problems such as avoiding impeller failures. Start ups and other transients such as trip will remain unknown unless OPM is implemented.

The main difference between gas turbine OPM and that of compressor is the medium going through the engine in the entire path: in gas turbine the medium is air and fuel or its products whereas in compressors the medium is normally a process gas whose properties such as density and specific heat ratio vary from plant to another [Refs. 43, 44, 45]. Therefore the gas path and the thermodynamic properties analysis in a compressor is a distinguished difference with gas turbine. As the correct diagnosis depends on the accuracy of the predicted or simulation model, then the properties or equations used to generate or predict the gas behaviour under an envelope of operating scenario must be accurate as well. In OPM systems compressor health is measured by comparing the current performance with manufacturer's data. Raw operating data such as discharge pressure or pressure ratio are not sufficient indicators of compressor performance as these parameters can change with inlet temperature and pressure. But head and efficiency are accurate indicators of compressor performance as they are not affected by process conditions. The BRW (Benedict, Webb & Rubin) EOS (Equation of State) is used to calculate the head and this EOS is a comprehensive equation that defines gas parameters accurately [Ref 47]. In HYSYS simulation program this option is available. Sandberg [Ref 48] provides an excellent insight into use of various EOS and the relative accuracies under various scenarios. Calculating compressor gas power (i.e., the energy transferred from the impeller blades to the gas) helps to confirm the input data are accurate. Any degradation in the interstage seals, corrosion or fouling will show up as a loss in efficiency and head but the work input stays the same.

Real-time software model that can be adapted to the site compressor is a tool to provide constant health monitoring system. This model may be built from OEM performance data, which is for the case at hand by the application of HYSYS advanced simulation software capable of precise mapping of the site

compressor online as it is performing. When OEM data is not available, the data necessary to build a normalized mathematical model through field-testing can be performed. This baseline performance data is then continuously compared to the actual compressor performance using real-time field data. Online performance monitoring can be regarded as one of the most powerful tools to continuously monitor the health of the compressor in real time and warn the operator in advance if the deviation of a performance indicator is more than expected so that the fault can be inspected and resolved.

As it will be described in the next section continuous on-line monitoring allows specific trends to be developed in real time for the compressor and these trends can be compared with a established base line where the operator can decide in advance the need for, and the nature of, the maintenance thus shifting the pre-scheduled maintenance policy to condition based maintenance. Further references on OPM can be found elsewhere [Refs. 1, 2, 4, 10-13, 19-20, 47 and 57].

The techniques and applications of online monitoring have been discussed in this chapter and the next chapter focuses on compressor performance adaptation.

2.6.1 Requirements for rotating equipment condition monitoring system

The following must be satisfied in order that a condition monitoring system can be used in compressor (or gas turbine) applications:

- Reliability
- Accuracy
- Robustness
- Computational Efficiency
- Hybrid Schemes
- Data Fusion
- Data Uncertainty
- Online Application
- Sensor Faults
- Multiple Component Fault/Sensor Fault
- Prognostics
- Maintenance Advice

Prognostics and the resultant maintenance advice are the “fruits” of online monitoring once the other referred factors are established for the rotating equipment.

2.6.2 Benefits of online monitoring

Real time performance data must be integrated with mechanical parameters including vibration data, bearing temperatures and oil condition so that operators can better select operating regimes and maintenance schedules. By going through the literatures, it is established that the key benefits of online monitoring system include:

- Faster troubleshooting minimizing downtime and loss of production
- The trending of machinery performance helping to isolate the operating points that may have caused machine's current condition
- Immediate evaluation of the effects of process changes
- Extended scheduled maintenance as knowing the machine performance along with vibration, thrust bearing temperature and oil condition enables this strategy. This effectively enhances the availability which is described in details in Section 2.6.2.1.
- Minimizing insurance premiums

For the current research at hand on compressor model adaptation and diagnostics, all the OEM and actual (site) performance curves are available (Appendix C). HYSYS is also available to simulate the real compressor for ANY inlet/outlet conditions or gas properties. Drawing from above, all the tools are available for compressor monitoring and diagnostics works to be carried out.

2.6.2.1 Effect of OLM on Reliability-Availability-Maintainability (RAM)

Online monitoring effectively increases the rotating equipment or plant's Reliability-Availability- Maintainability (RAM) due to advance warnings to the operator on the behaviour of the rotating equipment and the shift of maintenance philosophy from preventative mode to reliability centred maintenance.

It must be emphasized that on-line monitoring cannot pick up all types of faults of the centrifugal compressor or axial compressor in a gas turbine. There are essentially three types of failures to all failures: The "instantaneous failures" such as fatigue failure of compressor blades give no warning. No amount of monitoring will detect the onset of these types of failures. The" delayed time-dependant failures" are those for which there is no detectable change until at some point of its life deterioration occurs. The ability to detect early the start of deterioration is a challenge and hence requires a sophisticated system of Equipment Health Monitoring to identify it. The "pure time-dependant type of failure" is also a candidate for engine online health monitoring.

Since online monitoring of the rotating equipment enhances reliability and availability, it is prudent to highlight the definitions and importance of reliability and availability.

Reliability is defined as [Ref 39]:

Reliability = (1-(FOH/PH))*100%.

FOH= Total forced outage hours and PH=Period hours.

Reliability is a design feature and the rotating equipment can at best be restored to its design level. Reliability could be increased by stress margins used for critical speeds, blade and vane vibration frequencies and environmental conditions including fuel, air and oil specifications. Higher reliability causes higher costs but has an optimum point in the “costs versus reliability graph” and good maintenance techniques are required to keep it which increases with increase in reliability. Note reliability falls with time unless there is maintenance programme so there is a requirement to have knowledge of the engine condition at the operating time.

The largest contributor to forced outage rates are often the support systems such as control and fuel systems. The associated down-time can be managed to acceptable levels by design redundancies and spares. Refer to Figure 18 below for a comparison of contributions to outages by gas turbine components which include the axial compressor section.

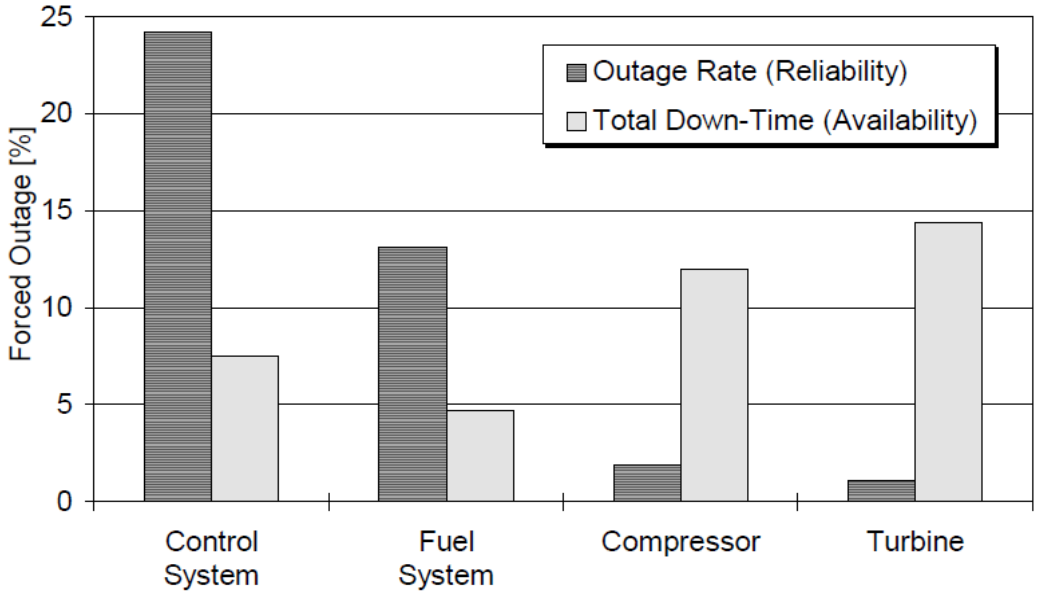

Figure 18. Contribution of gas turbine components to outages [7]

The major gas path components such as compressors and turbines have a high reliability. However, downtime could be large if outage is caused by these

components. Statistics show that gas path components contribute a lot to down time even though they exhibit high reliability.

Outage rate is related to reliability and total downtime is related to availability.

Availability may be defined as:

Availability= MTBF/ (MTBF + Downtime), MTBF depends on reliability

For the same downtime the availability increases with increasing MTBF and this is shown in Figure 19, i.e., the availability is inversely proportional to downtime. MTBF is influenced by reliability whereas downtime is influenced by factors such as equipment design is modular, instrumentation and diagnostic capability are adequate and access for inspection is good.

With reference to Figure 20, if down time associated with maintenance action is large, relatively poor availability will result. For example, if MTBM is 20,000 hrs and procurement of a part is 3 months, availability achieved is 90%. But if due to diagnostic techniques the parts could have been identified in advance and reduced the downtime to 7 days, then availability would be 99%. This offers a significant improvement in economics. Figure 21 shows the trend of how the overall availability is improved by having spares available [Ref. 39]. An economical analysis should be carried out to see the balance between extra expenditures in fixed costs and the gains in terms of higher availabilities.

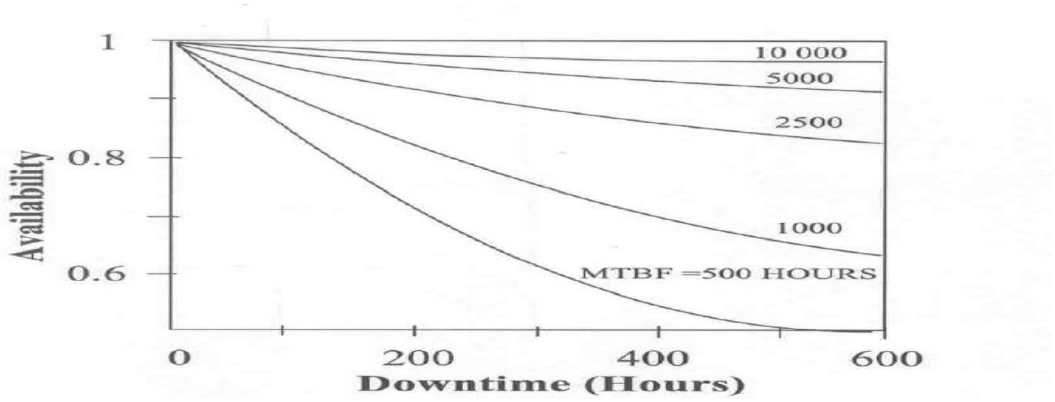

Figure 19. Relation between mean time between failure, downtime and availability [Ref. 39]

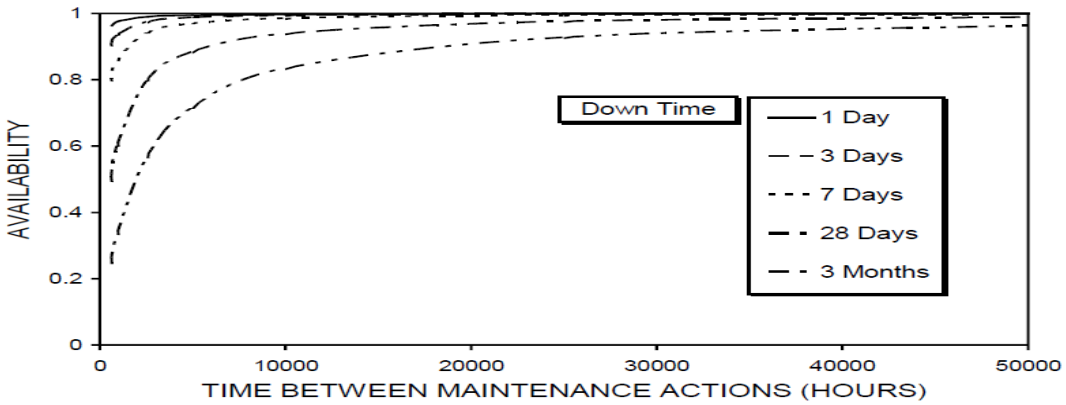

Figure 20. Relation between availability and downtime [Ref. 39]

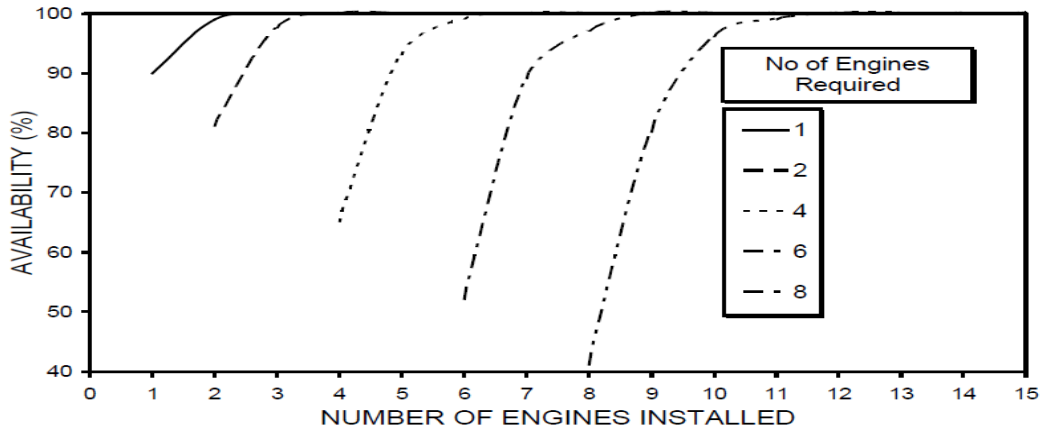

Figure 21. Plant availability taken at gas turbine availability of 90% [Ref. 39]

3. Compressor Degradation Modeling and Simulation

3.1. Introduction

As compressors continue to operate, there are deviations to gas path measurements such as rotational speed, discharge pressure and temperature and gas throughput. These variations may be due to varying ambient conditions and/or process gas properties and the degradation of compressor associated with prolonged operation time. The performance of the compressor may be represented by pressure ratio and efficiency and its health may be represented by the magnitude of deviation from the clean state in throughput and efficiency. As compressors degrade the whole of performance curves shift to a new position which is downward and generally to the left of the original performance map. The amount of shift is indication of severity of the degradation and thus based on this information the operator can decide the operation or maintenance period of the compressor.

During the compressor operation, the gas path measurements are obtained on regular basis and these are used to model the degraded performance of the compressor. With the effects of ambient conditions and gas property variations taken out, the fall in performance may be due to degradation alone taken that the measurement errors are within an acceptable band. Thus in the following works it is taken that all measurements are taken at same environmental condition and the gas properties do not change during the test period. It is also assumed that gas path sensors are in good health thus there is no measurement bias. Since some measurement noise is inevitable in the measurements which will impact the diagnostics they are discussed separately. However, the errors due to noise and bias are reducing with advancing technologies and state of the art compressor and layout designs for measurements.

The compressor characteristic maps are developed from the basic data. This model generates polytropic heads for a range of flows and speeds which are then fed into HYSYS advanced simulation programme to model the performance of the compressor in its initial or clean state. Degradation is then modeled and simulated by step reductions in mass throughput and efficiency and the effects on the measured parameters are then deduced. These measured parameters include speed, discharge temperature and power. Similar to the high quality of model built by HYSYS for clean or un-degraded compressors, representative models are also built for degraded compressors as the simulation programme is highly adaptable. There is no library of performance curves stored in HYSYS and therefore curves specific to the compressor of interest need to be generated using actual or simulated data. For an accurate and complete build up of the compressor model, in addition to thermodynamic principles, computational fluid dynamics (CFD) should be

considered taking into account the geometry and build the compressor model stage by stage.

The above works are divided into three sections:

1) **Compressor model generation**: Development of a representative model generation for a clean or un-degraded compressor utilizing thermodynamics principles. This has been done under the current Chapter. The effects of degradation on the whole characteristic maps have been calculated and demonstrated on the same maps to show the degradation effect on the entire performance map rather than at one point of operation. The un-degraded or clean compressor model is transferred to HYSYS for further analysis on degradation by simulation. The transfer of clean model into HYSYS and the works below have been described in Chapter 6.

2) **Compressor degradation simulation**: A progressive degradation with time has been assumed for an operating point and performance has been monitored by HYSYS simulations for a period of 1 year since the start of the clean compressor. As an operational constraint, the pressure ratio has been held constant throughout the test period. Two modes of degradation patterns have been assumed over the control year: linear and non-linear falls in mass throughput (0 – 5%) and efficiency (0 – 3%) simultaneously throughout the same period of 1 year. The simulated measurements have been taken as the 'actual' readings in compressor discharge temperature, gas power demand and speed. The estimation of degradation in throughput and efficiency has been estimated using scaling method applied over the measured parameters.

3) **Compressor diagnostics:** The fault signatures (relative measurement deviation compared with clean measurements) have been presented and the degradation have been estimated for both the linear and non-linear degradation path. Results are then analysed and discussed with conclusions.

3.2. Compressor health status estimation

The operating point on a degraded compressor map can be compared with the same point but on the un-degraded (clean) compressor map leading to estimation of degradation. This comparison necessitates the assumption that conditions of gas entry and environmental remain the same. In case these change, they need to be accounted for in the comparison.

The degradation of the compressor is represented by the shift of the characteristic curves on the maps and such shifts are represented by Degradation Indices. The solid lines on Figure 22 represent the un-degraded or clean compressor map and doted lines represent the degraded compressor map. Reference to the same figure, the degradation of a compressor may be described by the deviation of 3 degradation indices: pressure ratio, flow capacity and efficiency. The degree of shift of characteristic speed lines from when the compressor was new, may describe the health state of the compressor. Thus 3 independent degradation indices (scaling factors) can be devised to describe the health state of the compressor as shown below:

$SF_F = FC_{deg}/FC_{cl}$ Eq. 3-1

$SF_{PR}=PR_{deg}/PR_{deg}$ Eq. 3-2

$SF_{Eff}= \eta_{deg}/\eta_{cl}$ Eq. 3-3

On the basis of above, the closer the scaling factor is to unity (1), the healthier (clean) is the compressor. At the initial day of operation (t=0), compressor may be taken as un-degraded (clean) and all the scaling factors are 1 and degradation is 0. Later on in the time scale, the difference between these scaling factors and unity denotes the degradation.

In the proceeding works, the health of the simulated compressor at regular intervals after the initial operation are estimated and measurable and measurable output are deduced by simulation and the results are presented and discussed.

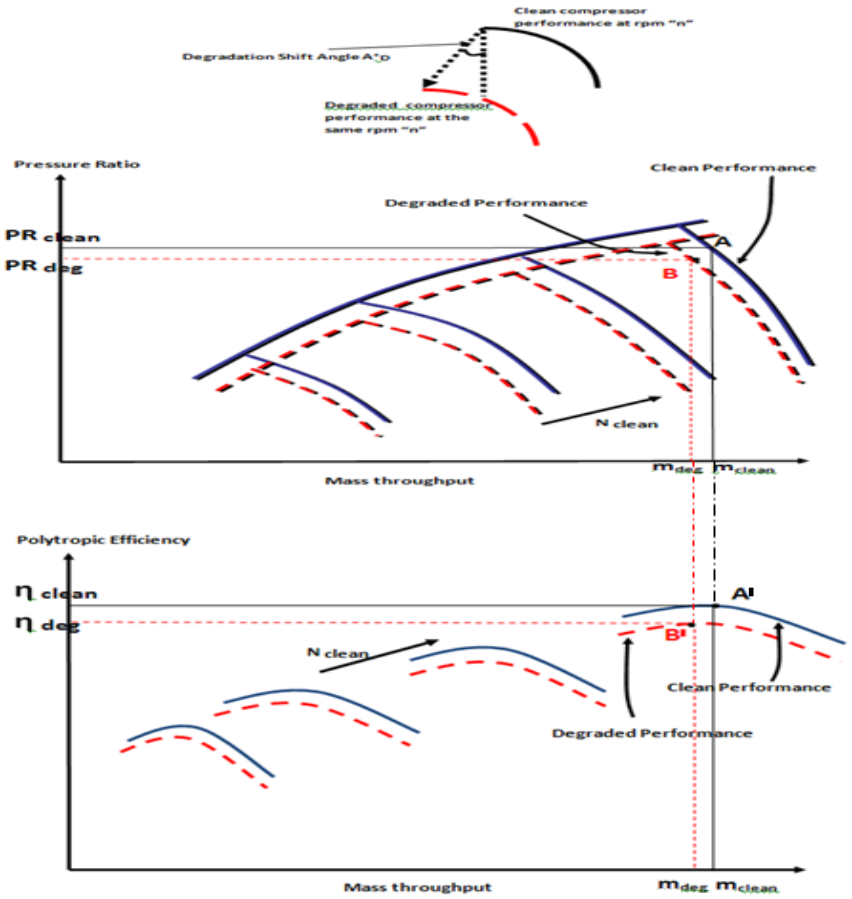

Figure 22. Clean and degraded compressor performance map

3.3. Data measurements, corrections and uncertainty

The selected instrumentation set for the analysis of the compressor model is described in Table 1.

No.	Symbol	Description
1	m (kg/hr)	Throughput on mass basis
2	T_1/T_2(K)	Compressor Temperature
3	P_1/P_2(bara)	Compressor Pressure
4	N (rpm)	Shaft Rotational Speed
		Note: Subscripts 1 & 2 denotes compressor inlet (suction) and outlet (discharge)

Table 1. Instrumentation set for compressor simulation

For the purpose of the proceeding works, it is assumed that all gas path sensors are in good health (no measurement bias). The compressor inlet gas properties and the environmental changes over the testing and sampling period are ignored and hence both clean and degraded compressor performance are measured at the same external conditions to make the data comparable otherwise corrections are necessary to adjust for gas property and environmental changes.

The deviation of the compressor gas path parameters indicates degraded compressor performance. The simulated samples of those parameters are collected and regarded as actual gas path measurements. Statistically, the larger the number of samples, the greater the certainty on the readings. In the gas fields the traditional practice has been to obtain compressor readings by daily monitoring for the purpose of performance evaluation and the trend is becoming more intense as operators become more aware of benefits of online monitoring. Nowadays rotating equipment purchased automatically has an associated online monitoring system.

Some measurement noise is inevitable in compressor measurements and has a negative impact on diagnostic results if the noise effect is not quantified. Therefore the intention should always be to introduce measurement errors in the gas path simulation works.

Error is the difference between true value and measured value. An associated interval that include the true measured value should be included in the analysis. The errors may be classified as two types of fixed and random. The random error between repeated measurements is called precision error and a standard deviation may be used as a tool to measure the precision error as follows:

$$s = \sqrt{\frac{1}{N-1}\sum_{i=1}^{N}(x_i - \overline{x})^2}$$ Eq. 3-4

Where,

S=Precision Error Index

x_i=Observed value of the sample items

$\overline{x}$= Mean value of the observations

N= Total no. of samples

Bias is the constant or systematic error. To obtain the bias, the “true” value is defined together with an associated limit.

Uncertainty may be centred about the measurement and defined as:

$U=+/- (B+t_{95}S)$ Eq. 3-5

Where,

B=Bias limit

S=Precision Error Index (obtained by the previous equation)

t_{95}=95th percentile point of the two –tailed student’s ‘t’ distribution and t=2 if sample size is greater than 30.

The maximum measurement noise for different gas path measurable parameters is based on the information provided by Dyson and Doel [Ref. 64], shown in the Table 2 below.

Measurement	Range	Typical Error
Pressure	3-45 psia 8-460 psia	±0.5 % ±0.5 % or 0.125 psia whichever is greater
Temperature	-65 – 290 °C 290 – 1000 °C 1000 – 1300 °C	± 3.3 °C $\pm \sqrt{2.5^2 + (0.0075 \cdot T)^2}$ $\pm \sqrt{3.5^2 + (0.0075 \cdot T)^2}$

Table 2. Maximum measurement noise [Ref. 64]

To reduce the negative impact of measurement noise on performance and diagnostic analysis, multiple gas path measurement samples are obtained in the simulation and a “rolling averaging” may applied to get an averaged measurement sample prior to processing of the measurements. Rolling averaging reduces noise for a measurement by taking a rolling average (RA), as expressed in the equation below, of its values in certain last period [Ref. 58]:

$$RA(z_k) = \frac{1}{I}(z_k + z_{k-1} + z_{k-2} + \cdots + z_{k-I+1})$$

Eq. 3-6

Where,
z_k is the value of a measurement at time *k*, *RA* is the rolling average of the measurement, *I* is the total number of measurement values that involved in the rolling average calculation process.

Alternatively, in an “exponential averaging” (*EA*) as expressed in equation (3-7) of a measurement is calculated by its current value and the average of the last ten values, where the current value is associated with a weight with 15% and the average with a weight with 85% [Ref. 58]:

$$EA(z_k) = \frac{1}{10}(z_{k-1} + \cdots + z_{k-10}) * 0.85 + z_k * 0.15$$

Eq. 3-7

As a result data averaging the scatter of sample data over the original data are appreciably reduced and the averaged sample values approach the true values.

3.4. A brief description of the simulation programme, HYSYS

The simulation programme HYSYS is industry proven and widely used throughout the oil & gas and energy industries for simulation of major equipment and compressor is one of them.

HYSYS does not have any pre-stored compressor performance maps. This programme utilizes the rigorous equations of state for property generation of hydrocarbon gas feeding the compressor as well as the thermodynamic and iterative laws and proportionality laws to give result and data necessary for compressor design and operation. HYSYS is a suitable programme for the generation of performance curves both for new and degraded compressors alike based on, and generated by, the input data of the user. Sufficient number of runs without the performance curves using site measured data can lead to building a complete map of actual compressor performance curves.

The input to the programme with and without the performance curves is given below in Table 3.

HYSYS is considered a simulation tool to simulate new and degraded compressors as well building the actual site compressor model for data analysis and operational optimization and as such it is used for the current works under research.

Without Curves	With Curves
1. Flow rate and inlet pressure are known. Then: A) Specify outlet pressure. And, B) Specify either Adiabatic or Polytropic efficiency. HYSYS calculates the required energy, outlet temperature, and other efficiency.	Flow rate and inlet pressure are known. Then: A) Specify operating speed. B)HYSYS uses curves to determine efficiency and head. HYSYS calculates outlet pressure, temperature, and applied duty.
2. Flow rate and inlet pressure are known. Then: A) Specify efficiency and duty. HYSYS calculates outlet pressure, temperature, and other efficiency.	Flow rate, inlet pressure, and efficiency are known. Then: A)HYSYS interpolates curves to determine operating speed and head. HYSYS calculates outlet pressure, temperature, and applied duty.

Table 3. Variables requiring input in HYSYS compressor calculations

3.5. Development of performance curves and performance degradation modeling

Reference is made to the compressors curves supplied by the vendors. These curves are obtained for the rated conditions based on the physical properties for the hydrocarbon gas. However, the curves supplied by OEM are not always available and the performance curves need to be developed by applying thermodynamic equations.

Spreadsheet is developed to calculate Pressure ratio, Discharge Pressure, Discharge Temperature and the Power requirement for the given volumetric flow rate through the compressor.

Following sets of Equations are used for determining discharge conditions for a given Compressor and inlet volumetric flow rate for any gas composition taken into consideration.

Isentropic Exponent K, is given by
Eq. 3-8:

$$k = \frac{C_p}{C_v}$$

Where,
k = Isentropic exponent
C_p = Specific Heat at Constant pressure (kJ/kg K)
C_v = Specific Heat at Constant volume (kJ/kg K)

It is known that
Eq. 3-9:

$$MC_p = MC_v + R$$

Where,
R = Universal Gas Constant 8.314 kJ/k-mole K
MC_p = Molar Specific Heat at constant pressure kJ/k-mole K
MC_v = Molar Specific Heat at constant volume kJ/k-mole K

Hence Rearranging Eq. 3-9 and substituting for C_v in Eq. 3-8, obtain:
Eq. 3-10:

$$k = \frac{MC_p}{MC_p - 8.314}$$

The Discharge Temperature of the Gas leaving the Compressor is calculated using following.

Eq. 3-11:

$$T_d = \left[(T_s + 273)\left(\frac{P_d}{P_s} \right)^{\frac{n-1}{n}} - 273 \right]$$

Where,
T_d = Discharge Temperature in degC
T_s = Suction Temperature (or T_1) in degC
P_d = Discharge Pressure (or T_2) in bar
P_s = Suction Pressure in bar
n = polytropic exponent

Polytropic Exponent is defined as
Eq. 3-12:

$$\frac{n}{n-1} = \left[\frac{k}{k-1} \right] \eta_p$$

Where,
k = Isentropic Exponent
η_p = Polytropic Efficiency

Polytropic Head is calculated using following
Eq. 3-13:

$$H_p = \frac{8314 \times Z_{avg} T_s}{MW\left(\frac{n-1}{n} \right)} \left[\left(\frac{P_d}{P_s} \right)^{\frac{n-1}{n}} - 1 \right]$$

Where,
H_p = Polytropic Head Nm/kg
Z_{avg} = Average Compressibility Factor
P_d = Discharge Pressure bara
P_s = Suction Pressure bara
MW = Molecular Weight of the Gas

T_s = Suction Temperature K

A generalized equation to determine the discharge conditions for a given compressor and inlet volumetric flow rate that results from a variation of all inlet condition at rated conditions developed for any given (constant) rotational speed is given below [Lapina: 1982]. Reference may be made to Table 6-1 where the basic data for both rated and site (new) conditions are available.

Eq. 3-14A:

$$\left(\frac{P_d}{P_s}\right)_N = \left[\left(\frac{Z_R}{Z_N}\right)\left(\frac{T_{sR}}{T_{sN}}\right)\left(\frac{MW_N}{MW_R}\right)\left(\frac{n-1}{n}\right)_N\left(\frac{n}{n-1}\right)_R\left(\left(\frac{P_d}{P_s}\right)_R - 1\right) + 1\right]^{\left(\frac{n}{n-1}\right)_N}$$

Where subscripts N and R denotes New (site) and Rated compressor respectively.

If the test gas is principally same as OEM, rearranging for pressure ratio calculation is found in
Eq. 3-14B:

$PR = [(H_p/a) + 1]^{(n/(n+1))}$

Where PR is the ratio of discharge to inlet Pressure

And a =

$$\frac{8314 \times Z_{avg} T_s}{MW\left(\frac{n-1}{n}\right)}$$

The Gas Power is calculated using following
Eq.3-15:

$$G_P = \frac{w \times H_p}{\eta_p \times 3.6 \times 10^6}$$

Where,
G_P = Gas Power kW
m = Gas Flow rate kg/h
η_p = Polytropic Efficiency
H_p = Polytropic Head Nm/kg

Inlet Volumetric Gas Flow through the Compressor is calculated using following
Eq. 3-16:

$$Q = \frac{w}{\rho}$$

Where,
Q = Volumetric Inlet Flowrate, m3/h
m = Mass Flow Rate, kg/h
ρ = Gas Density at suction conditions, kg/m3

And Gas Density is given by following
Eq. 3-17:

$$\rho = \frac{PM}{zRT}$$

Where,
ρ = Gas Density kg/m
P = Suction pressure bara
z = Compressibility Factor
R = Universal Gas Constant N m/mole K
T = Suction Temperature K
M = Gas Molecular weight

3.5.1. Affinity (Fan) Laws

The compressor maps including off design can be generated using the affinity laws (Fan laws or laws of proportionality). These relationships are accurate for ideal gas and medium pressures (as in the research case) and that these laws do not take into account the volume ratio effects. Natural gas follow closely follow the ideal gas laws unless the gas is very sour. For very high pressures, Fan laws should be used with caution.

Once the performance curve (polytropic head or H_p versus throughput) is developed for 100% speed applying the thermodynamic equations in the previous Section, affinity (proportionality or Fan) laws can be applied to estimate the H_p versus throughput for other speeds.

The basic Fan laws are [Ref 28]:
Eq. 3-18:

(a) $Q \propto N$

(b) $H_p \propto N^2$

(c) $PWR \propto N^3$

(d) $\text{Delta T} \propto N^2$

(e) $\ell n\left(\frac{Pd}{Ps}\right) \propto N^2$

Based on the above, the following is deduced.
Eq. 3-19:

Q/N=Constant1=K1 and Hp/N2=Constant2=K2,

And,

Eq.3-20:

$$N_{deg} = \sqrt{\left(\frac{Hp,deg}{Hp,clean}\right)} \times N_{clean}$$

Or
Eq. 3-21:

$$N_{rerate} = \sqrt{\left(\frac{Hp,rerate}{Hp,original}\right)} \times N_{original}$$

4. A Novel Compressor Performance Adaptation Technique

4.1 Use of dimensionless groups in compressor performance analysis [Ref. 56]

Dimensional analysis is very important in compressor performance as it is only necessary to plot 2 sets of curves in order to define the compressor performance completely. In this respect the importance of Dimensionless, Quasi-dimensionless, Referred and Scaling Parameter Groups in all aspects of rotating equipment performance can not be over emphasized. “Dimensionless” groups are the groups that contain all variables affecting component performance including linear scaling and fluid properties. This form is of interest if different working fluids are to be considered. “Quasi-dimensionless” groups are those having the specific gas constant, gamma and the physical diameter omitted. This suits the situation of a component design of linear scale, using a fluid of fixed properties such as molecular weight; i.e., only operational condition shall be considered. “Scaling parameters” groups are the dimensionless groups with only the working fluid properties omitted. This will allow assessment on performance effects of linear scaling an existing compressor or matching differentially scaled existing compressors. Referred (or corrected) groups are the groups that are directly proportional to Quasi-dimensionless groups. The difference is the substitution of theta (θ) for component inlet temperature and delta (δ) for component inlet pressure.

The compressor performance maps supplied by OEM such as pressure ratio or discharge pressure versus throughput are normally for a specific sets of compressor inlet temperature, pressure and gas physical properties such as gamma and molecular weight. An attempt to carry out full range of tests and make the full presentation of variations of these quantities would be an impossible task because of so many variables required to describe numerically compressor performance throughout the operational envelope. A large part of this complication is eased with applying the dimensional grouping through which the dimensionally related variables are combined so that the performance analysis becomes manageable. Thus the complete characteristics of any compressor can be defined by two sets of curves only. When compressing a specific gas for a machine of fixed size, there will be:

$$f\,(P_2/P_1,\ T_2/T_1,\ m\sqrt{(T_1)}/P_1,\ N/\sqrt{T_1}) = 0$$

Suffices 1 and 2 denote compressor entry and exit conditions. Each of terms within the function is either dimensionless or quasi-dimensionless. Plotting one group against the other for various fixed values of the third will characterise the performance of a compressor allowing ‘on the spot’ tracking of the compressor performance changes with variations in environmental

condition or scaling. The useful plots are pressure ratio P_2/P_1 or temperature ratio T_2/T_1 versus non-dimensional mass flow $m\sqrt{(T_1)}/P_1$ for a range of non-dimensional rotational speed $N/\sqrt{T_1}$.

In the proceeding works where site data has been applied to building the performance characteristics of the compressor, the concept of (θ) for component inlet temperature and delta (δ) for component inlet pressure have been applied as a tool to simplify the analytical aspect of this research without compromising the conclusions reached.

4.2 Performance Data Referring and Scaling

The OEM performance data for a compressor is for a specific set of predetermined ambient and gas inlet conditions and properties. At site, however, very often the compressor runs or it is tested at a set of gas inlet, speed and ambient conditions different from those of OEM and therefore the compressor performance can not be diagnosed based directly on OEM data. Hence to model the performance of the real compressor and see how it is performing based on OEM data, it is needed to:

1. Convert the OEM basis and performance curves to a referred site conditions and generate new performance curves. This is described in this section below.

2. Establish site compressor's referred performance at specific site or test flow rates and speeds. Speed curve interpolation for data between the curves and extrapolation for establishing the curves outside the tested range may be necessary, depending on the values of tested speeds and the corresponding flow rates. Scale factors are then applied by comparing the referred OEM curve and the site performance to shift the OEM speed curves and generate actual site compressor performance curves for a range of compressor speeds by successive iteration. The performance adaptation by successive iteration is novel and the technique has been detailed out in the Chapter 7 and Appendix D. Performance predictions based on scaling are very accurate close to the test or local point (say at design point or highest rotational speed) but the accuracy decreases as the operating point move away further and further from the locality. The latter is true if the scaling factor remains the same under all speeds of rotation. But how about if the scaling factor is given an opportunity to update itself (performance adaptation) as the operating point move from high speed to lower speed curves so that curve shifts are adjusted. Starting from the highest down to the lowest available test speeds, in each iteration one curve is fixed in position until all test points are completed and then there will be a family of performance curves on the map with the test points falling

exactly on the curves and this graph will be actual performance map of the compressor at a particular time.

The proceeding works in this section and Chapter 7 describe step-by-step the procedures for the accomplishment of the above objectives. All the measurement data are validated by regularly calibrated and self diagnosing instrument sets such that errors in measurements are diminishingly small and have no determinant effect on the purpose of performance mapping. The full details of application and sample calculation are in Appendix D.

All the OEM and site data must be converted to "referred data" of performance parameters such as Pressure Ratio (PR) and Efficiency versus mass flow so that the same environmental and gas inlet conditions applies and comparisons between the OEM and site data is made possible. By applying interpolation technique between referred OEM speed curves, a performance curve is generated for the speed that match the site referred speed and the scale factor is calculated which is the ratio of referred OEM performance and referred site performance at the particular site referred mass flow rate. The scale factor is then applied to the entire OEM referred speed curve such that the whole speed curve is shifted. The site performance curve is thus established for a particular referred speed and the procedure is repeated for other available lower referred speeds at site. In each iteration, the position of speed curves are updated and revised with one speed curve (the highest speed) getting fixed in position. This is repeated until all data points at various speeds are entered and all these points fall exactly on the characteristic maps. It is required to apply the scale factor in the manner described because unlike the OEM performance data being available for a wide range of flows, site performance data for a particular referred speed is normally available only for a particular mass flow or a "point" on the curve.

Plotting the performance curves on dimensionless or quasi-dimensionless axes is very useful as it is only necessary to plot 2 sets of curves in order to define the compressor performance completely. Scaling parameters Theta (θ) and Delta (δ) are used to refer the OEM and site data to a common datum, where,

$$\text{Theta } (\theta) = T_1 / T_{ref} \text{ (Dimensionless)} \quad (1)$$

$$\text{Delta } (\delta) = P_1 / P_{ref} \text{ (Dimensionless)} \quad (2)$$

The subscript "1" refers to compressor inlet conditions. T_{ref} and P_{ref} are arbitrary chosen values as a base temperature and base pressure upon which all the operating variables either from OEM or site are compared. It is normal to set reference values same as the most common site compressor inlet

conditions for temperature, pressure and the molecular weight controlling the mass flow.

The flowchart for the methodology of the performance scaling is shown in Chart 1.

The following are the equations used to refer the OEM and test data:

$$T_{referred} = T_n / \theta \quad (3)$$

$$P_{referred} = P_n / \delta \quad (4)$$

$$m_{referred} = W * \sqrt{(\theta)} / \delta \quad (5)$$

$$PW_{referred} = PW / (\delta * \sqrt{(\theta)}) \quad (6)$$

$$N_{referred} = N / \sqrt{(\theta)} \quad (7)$$

$$EEP_{referred} = EEP / 1 \quad (8)$$

Where, n=1, 2

In this work, subscript “1” refers to inlet of compressor and “2” refers to the compressor outlet. For an “n” set of site cases, there will be an “n” set of Thetas (θ) and Deltas (δ).

The OEM data is normally supplied on the basis of actual inlet volumetric flow rates. If the OEM/Site performance data are not available on mass basis, then volumetric flow need to be converted to mass flow using the following equation:

$$W=q.\rho=q.(P.M)/(z.R.T) \quad (9)$$

ρ , q, P, z and T are at compressor suction conditions. It is to be noted that referring the mass flow to a datum temperature and pressure (equations 3 & 4) assumes the molecular weight do not change. If the molecular weight change over years of operation, then correction must also be applied to molecular weight change. The simulation programme HYSYS adjusts the performance curves automatically with varying molecular weights by a push of a radio button by the user.

4.3 Generation of actual performance curves for the site compressor by successive iteration method

It was referred in the previous section that performance curves supplied by OEM applies to a fleet of compressors rather than the particular compressor supplied at site and therefore does not constitute the exact performance of the supplied compressor. Furthermore, the curves have limited application as they are for a specific set of inlet gas and environmental conditions. Hence it is needed to apply the proceedings as soon as the compressor is supplied and positioned at site for operation. The shift of performance due to degradation

applies to the whole family of curves from the highest RPM to the lowest RPM but the magnitude of this shift is not the same for all speeds. A way of minimizing error in shifting, is to carry out the testing for as wide a speed range as practically possible and shifting the curves by iteration. This novel method is fully described below and the accuracy of performance increase with the number of iteration. These steps are described below:

1. Determine and apply δ and θ to both OEM and site data as described in Chapter 4.2 and performed in appendix D so that performance is referred on the same inlet conditions for all cases. This enables performance comparison between OEM and site.

2. The referred speeds of OEM and Site must be the same. For this purpose, produce several speed lines between the referred OEM speed curves. Linear interpolation is valid for this purpose and confirmed as being practiced by industry [Ref 52].

3. For each of n site test data points and N speeds (all referred) , carry out the following **starting from the highest test speed**:

    3.1) Start by placing a base site case on the map shown as a star on PR_n speed line in Graph 1. Compare the site Pressure Ratio to OEM Pressure Ratio and deduce the scale factor (SF). Shift the original OEM curve "N_n" by applying the scale factor so that the site point falls exactly on the modified OEM curve. The parameter variable on y axis may not be only PR but also be any other parameter that map out the compressor characteristics depending on whether a suitable range of information has been supplied by OEM and there are readings taken at site or accurate simulation tools or mathematical tools to deduce the equivalent at site.

    3.2) Apply the same SF obtained in 3.1 above to all the Lower OEM referred speed curves (N_{n-1}, N_{n-2}, …) and shift the curves accordingly, as shown in Graph 1. The new modified OEM speed curve matching the site data is now fixed in position and will not move in the subsequent lower speed curves fitting.

4. Finally there will be a performance map that has a set of test data points falling exactly on the modified OEM speed curves. There are no limitations on the number of curves.

For the range of speed curves that no test data are available, the last set of shifted OEM speed curves shall be applied for performance evaluation.
Chart 2 defines the procedure for the generation of actual performance curves for the site compressor by successive iteration method.

Defining the above procedure mathematically, for an “n” number of test data, there will be an “n” number of speed curve shift for each iteration “i”. The higher the “n”, the more the shifting iteration and the more accurate is the prediction of performance, even outside of the tested speed ranges although the proposed method gives very accurate performance values for the tested speed range.

(I) For each measurable parameter and for the 1st shifting iteration (i=1) at the highest site speed:

$N_{ref,n=1}$

$$SF_{(n=1)} = [X_{Site} / X_{OEM}]_{n=1} \quad (10)$$

Where

$SF_{(n=1)}$ = Scale Factor for the 1st test point

X= variable (pressure ratio, dimensionless mass flow rate, polytropic efficiency, etc. at speed $N_{ref,n=1}$)

(II) Shift all the speed curves of N_{ref} and lower OEM speed curves by SF_1.

(III) The test point for $N_{ref,n=1}$ will fall exactly on the OEM modified speed curve. This point will remain FIXED in the following iterations.

(IV) Repeat (II) and (III) for lower speed successively.

(V) Finally:

$$SF_{(n=i)} = X_{Site,\ n} / X_{OEM,\ n} \quad (11)$$

Equation (11) shows that number of successive shifting iterations is equal to the number of test points at different speeds. For example, for three test data points at different speeds there will be 3 scale factors.

The developed method above shall be applied for the site compressor described in Chapter 6 and full sample calculation is laid out in Appendix D.

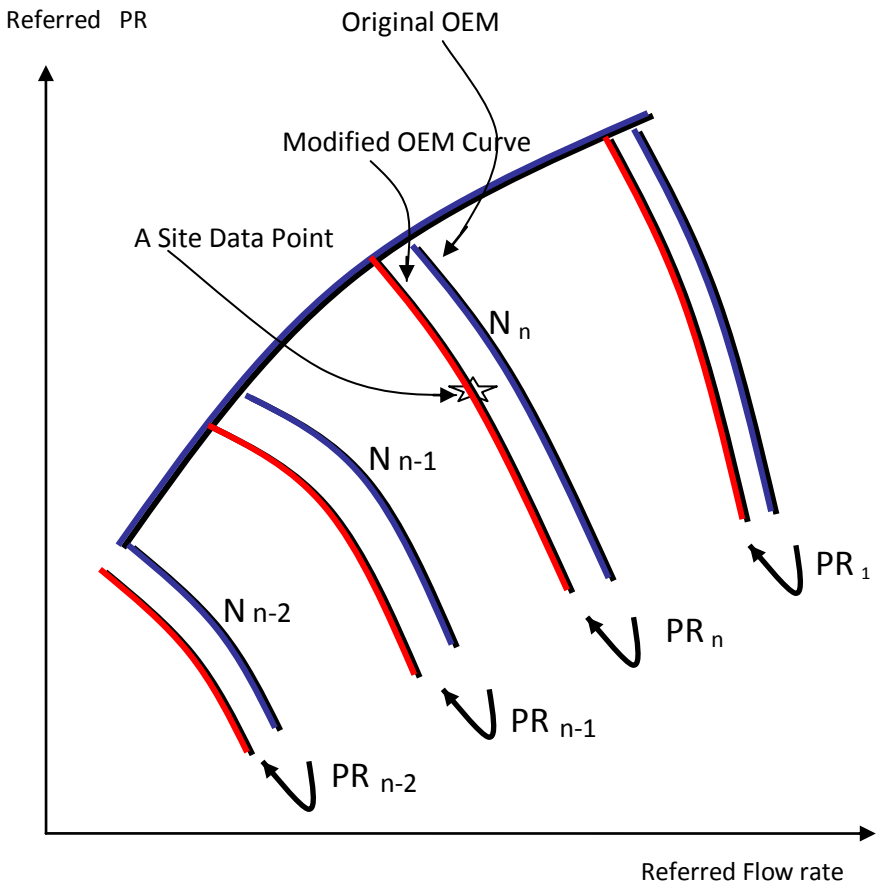

Graph 1. Performance scaling method matching the OEM and Site data

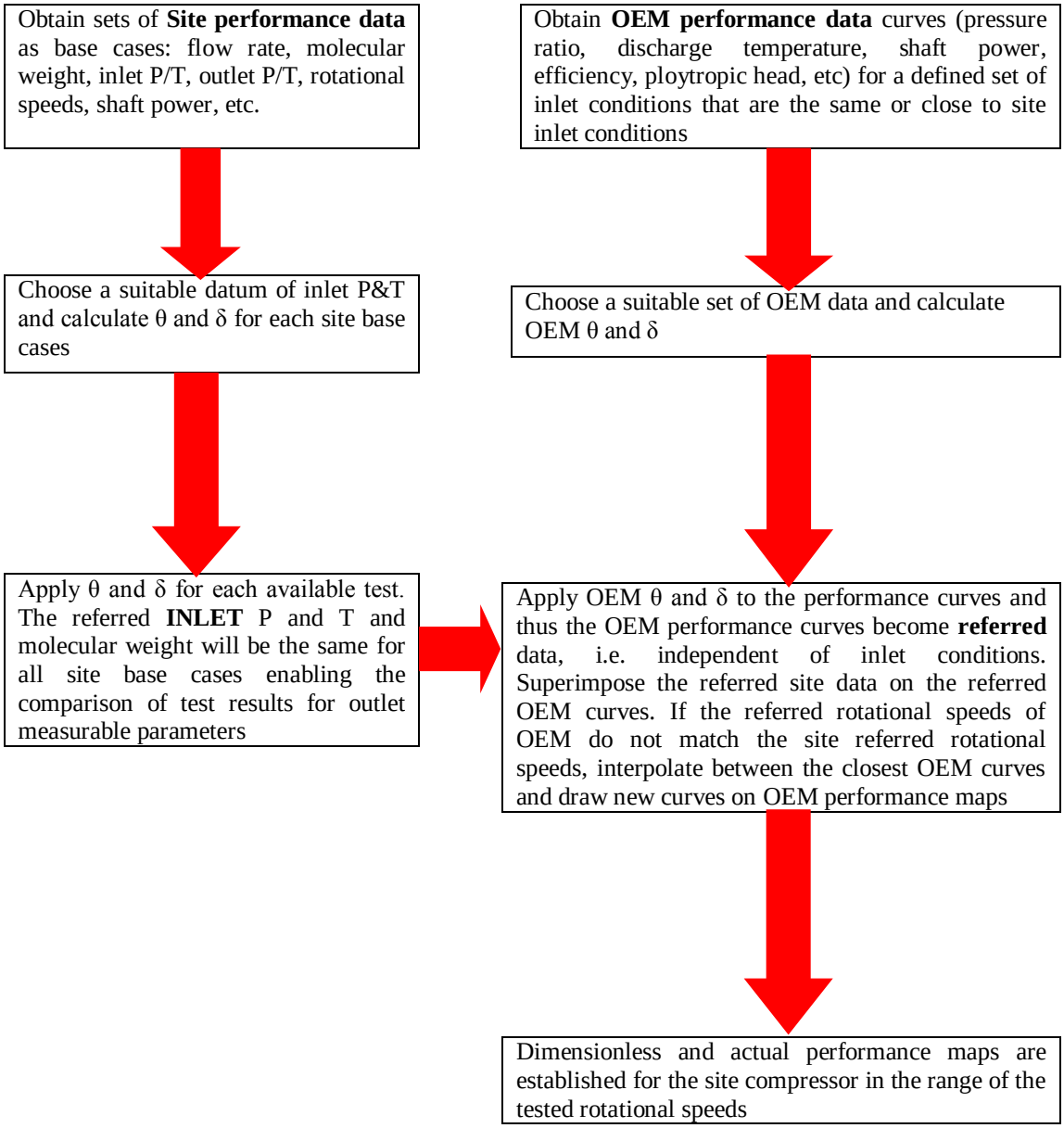

Chart 1. Flow Chart for establishing the actual site compressor performance by scaling

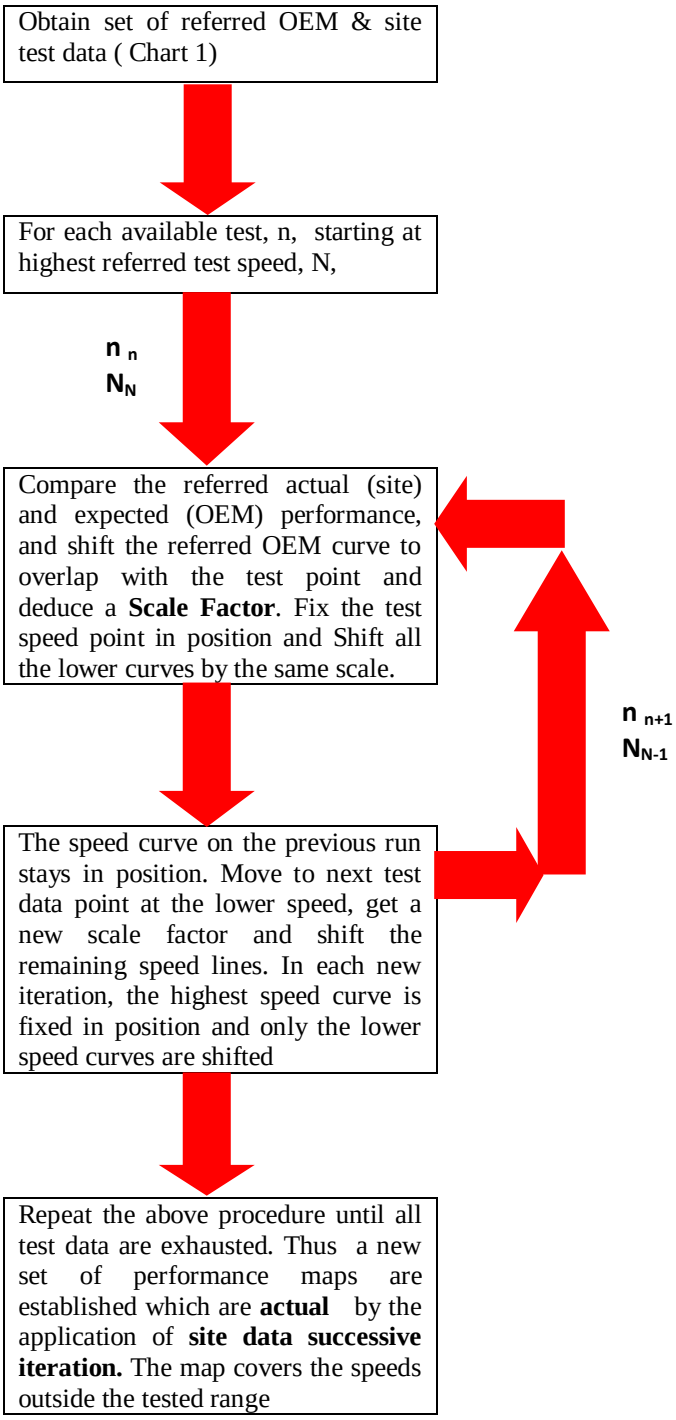

Chart 2. A novel flow chart for establishing the actual site compressor performance maps by successive iteration method

4.4 Trend analysis in compressor diagnostics

Accurate trend analysis on compressors can be very difficult as the operating point and even the gas analysis change although at a very slow paste. So how can the trend be evaluated. One method that has been used with good success is plotting the percentage change of a parameter (independent parameter in our case such as PR or Efficiency or mass throughput) to a known base line. It is important to establish the base line and in general predicted performance curve is used and this adjusted in accordance with the field data such as inlet conditions, speed and so on. For compressor efficiency the changes are plotted against timer as shown on Figure 23A [Ref. 28].

As referred in the earlier sections compressor degradation causes the performance curves move downward and to the left due to polymer build up, dirt, corrosion, increased seal wear and greater restriction to process flow in general due to fouling. The efficiency is reduced because of increased frictional losses and/or increased internal recirculation (wear, rubbings, clearances, etc).

The best trending data is when the data curves are densely populated with relevant changes in parameters. However, these data may not be available all of the time or continuously due to process restrictions or upsets. A way of overcoming this issue, is to request the manufacturer (OEM) upfront to analytically predict the relative effect of fouling. By plotting several degrees of fouling on a speed-compensated plot, it is easy to distinguish the trend of fouling. The degree of fouling is plotted versus time with reasonable confidence and prediction of timing for maintenance is simplified [Ref 28]. Figures 23A and 23B demonstrate the required plots for the expected trends in performance degradation by the OEM [Ref 28].

Trending the key performance parameters as continuously as possible with time has the advantage of observing the performance in real time. Given a time laps of sufficient period, the actual trends in performance against an expected trend appear and the operator can decide in advance the required actions such as inspection, cleaning, repair, part replacement or overhaul.

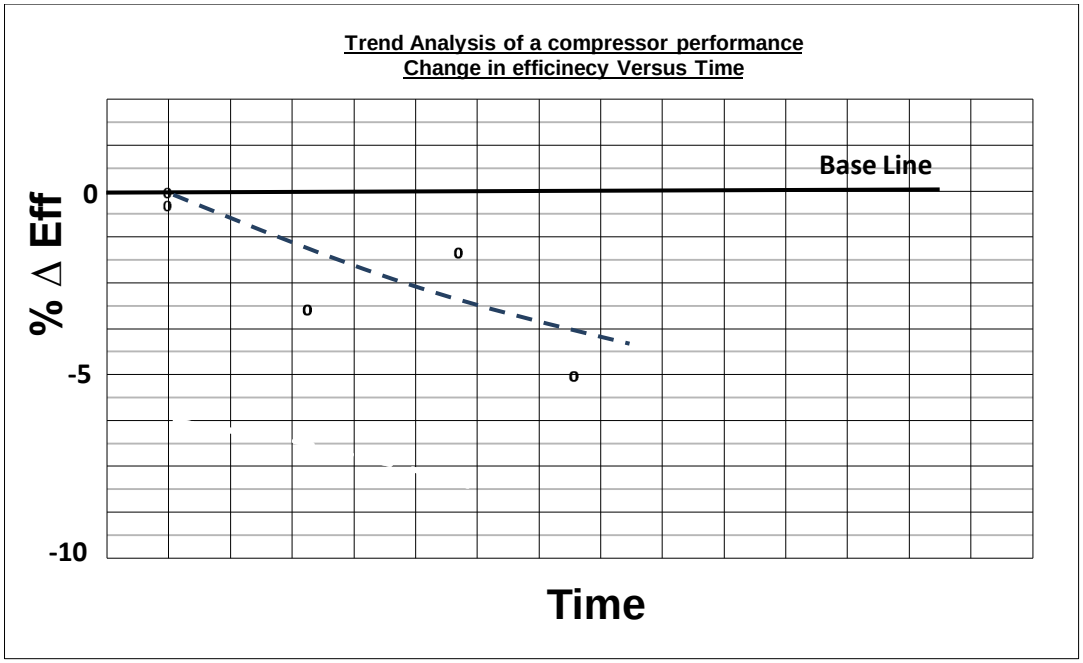

Figure 23A. Trend analysis of compressor performance: fall in efficiency with time against a base line [Ref. 28]

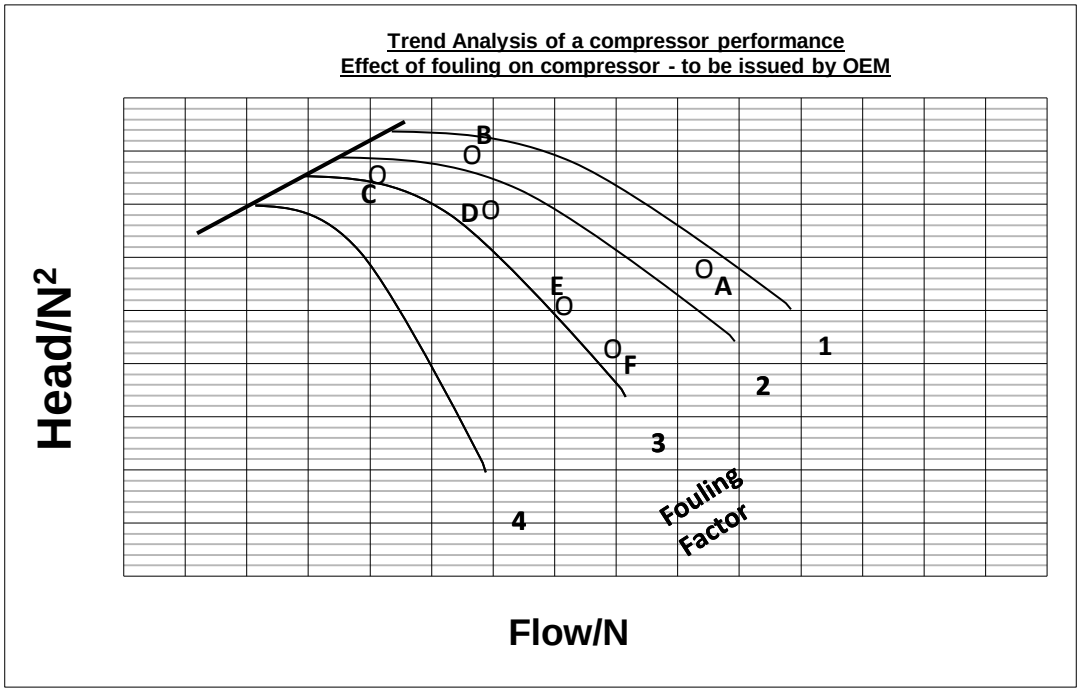

Figure 23B. Plot of performance data by OEM to map the expected degradation [Ref. 28]

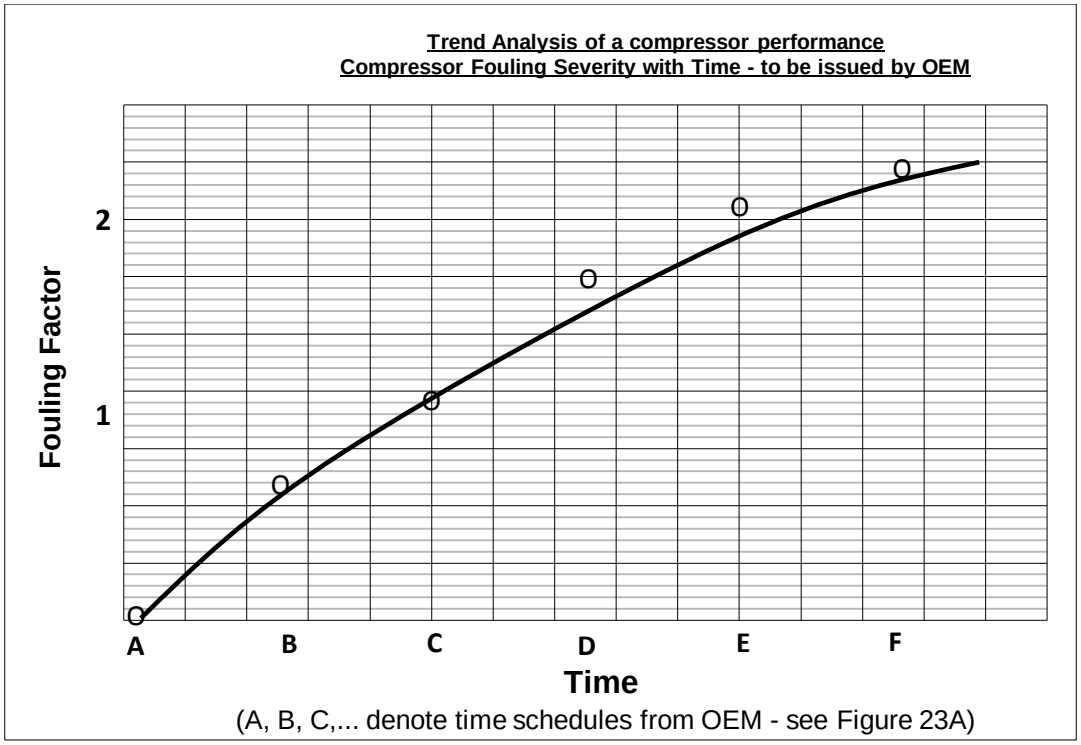

Figure 23C. Plot of performance data by OEM to develop fouling factor curve [Ref. 28]

5. Developed Methodology for Compressor Degradation Estimation

5.1 Compressor Degradation Estimation

As compressor degrade, the **whole** performance maps **shift**. Thus degradation is the shift of performance maps. The health parameters of a compressor can be described by establishing degradation scale factors. These health parameters are Pressure Ratio (PR), Polytropic Efficiency (η) and Mass Throughput (m) where these parameters are independent from each other and thus can fully define the characteristics of the compressor. Degradation scale factor or health parameter is the ratio of each of the referred independent variables (PR, η, m) under degraded condition relative to the performance at un-degraded or clean conditions of the same compressor.

The shift of the performance maps normally follows a diagonal shift to the bottom and to the left (i.e., south west), i.e., degradation is expected to result in not just a drop in PR (primarily as a result of wear in seals and increase in clearances between moving and stationery parts) or in mass throughput (mainly as a result of fouling and erosion/corrosion), but more realistically a combination of both. However, in this research in order to explore the extreme conditions, in addition to the realistic diagonal shift resulting from degradation, it is proposed to have an entirely vertical drop as well as having an entirely horizontal shift to the left as a separate case and gauge the differences in degradation prediction.

- For a vertical performance drop on the compressor performance map, degradation in PR is maximum and in m is zero,
- For a purely horizontal shift to the left on the compressor performance map, degradation in PR is zero and in m is maximum,
- The real drop is often diagonal. This results in a degradation estimate which is between the two extremes above. For an accurate prediction of diagonal drop it is proposed to use Fan laws as will be explained later as Fan laws are proven to be accurate especially for small changes measured over small periods of time. For determination of vertical drop and/or horizontal shift, it is proposed to directly measure and record the drop or shift on the map.

As operation time progresses, it is expected that degradation will also be propagating. In order to investigate the relationship between degradation and time, the health parameters or degradation indices at various times during compressor operation will be established. The performance curves generated by the novel method of successive iteration method described in Chapter 7 above to the site compressor will be utilized. The building of the actual

performance curves for the “clean” compressor ought to have been done at the start of its operation in 2004, but it was not carried out. Hence the operational data post 2004 that are available will be utilized to build the actual performance maps of the “clean” compressor (the “clean” performance is the first generated performance curves or base line performance) complemented by the advanced simulation programme HYSYS (see Appendix B). Once the “clean” or un-degraded compressor performance maps have been built, the available site performance data from mid 2006 onwards (Appendix C(I) and C(II)) shall be applied to obtain the compressor’s degraded health parameters (pressure ratio, polytropic efficiency and throughput). These health parameters will then be compared with the clean health parameters obtained as described earlier and establish the degradation scale factors at various time and record the trends on graphs.

The GPA Index for the above will be established as defined in Chapter 7, to gauge the accuracy of predicted values by simulation compared with actual site data. The closer the GPA Index is to 1, the more accurate the predictions. This will followed by a series of sensitivity analysis using the advanced simulation programme HYSYS to gauge how degradation affects the measurable parameters.

The followings give the details of the approach:

The shift in performance due to performance degradation may be represented as in Figures 24 and 25. Degradation causes a fall in performance and an erosion of surge margins, i.e., the shift of performance curves shall be downwards and to the left. Increase in clearance spaces is a natural phenomena and will cause the compressor performance curves move downward. Degradation due to fouling creates changes in its performance and later on it may change the blade shape if fouling is allowed to become severe. The latter statement is especially true for axial compressors. For centrifugal compressors fouling is mainly due to the build up of materials on the blades. These will cause the shift of performance curves to the left. On Figures 24 and 25, the solid line represents the performance of clean compressor and the dashed line may represent the performance of the degraded version of the same compressor.

By comparing the operating point on its characteristic map when the compressor is degraded (Point A on Figure 24A and A^{I} on 25) with the operating point on the same map for a clean (un-degraded) compressor (Point B on Figure 24A and B^{I} on Figure 24B) leads to the estimation of degradation. The assumption here is that the degraded performance map keeps almost the same shape as their original maps (i.e., linear approach) and this may be justified by the fact that often the geometries are not changed significantly

after they are degraded [Ref. 14]. It will be attempted to improve this assumption by the application of Fan laws as described in the proceeding works. Fan laws are the laws of relation between old and new measured parameters and are accurate, especially for small changes or frequent readings. Thus compressor degradation is represented by the shift of the characteristic curves on the respective maps and such shifts are represented by degradation or health indices. For a compressor the primary performance indicators are pressure ratios (PR) and efficiencies while the compressor health status represented by PR, efficiency and flow capacity indices [Ref 14]. These will determine the measure of performance shift and can describe the compressor degradation. Based on these definitions, the following relationship exists as shown earlier in Chapter 3:

$$SF_{fl} = m_{deg} / m_{clean} \quad (1)$$

$$SF_{PR} = PR_{deg} / PR_{clean} \quad (2)$$

$$SF_{eff} = \eta_{deg} / \eta_{clean} \quad (3)$$

Where,

SF=Scale Factor
m=mass throughput
PR=Pressure Ratio
η=Polytropic Efficiency
And subscripts fl, deg and c represent flow, degraded and clean compressor respectively.

Reference to Figure 24A, Point A is the starting position and refers to the conditions of an un-degraded or clean compressor performance at m_{clean} on the X-Axis and PR_{clean} on the Y-Axis and B refers to the referred corresponding points on X and Y axis but at degraded conditions, i.e., m_{deg} and PR_{deg} respectively. Point A may be obtained from OEM when the operator request the OEM to perform a full set of performance tests for a wide range of RPMs once the compressor arrives at site thus the actual performance curves specific to the supplied compressor are available. In case these are not done or data not available, at the earliest opportunity the operator needs to establish the actual performance curves of the compressor by performing performance tests for a wide range of RPMs on his own accord in the manner described under Chapter 4. These data then become the performance data for the “clean” compressor and the subsequent tests will be for the degraded compressor. All performance data are referred to the same datum by the application of Theta (θ) and Delta (δ) to eliminate the influence of environmental changes and gas inlet conditions on the compressor performance and thus the fall in measurement will be solely due to

degradation and not a combination of degradation and environmental changes. It is to be borne in mind that speed cannot be scaled thus point A and point B refer to the same referred speed.

Figure 24B is similarly explained as Figure 24A, Point A^I is the starting position and refers to the conditions of an un-degraded or clean compressor performance at m_{clean} on the X-Axis and η_{clean} on the Y-Axis and B^I refers to the referred corresponding points on X and Y axis but at degraded conditions, i.e., m_{deg} and η_{deg} respectively.

Degradation in compressor performance is normally associated with small changes in key performance indicators as the operator is not prepared to observe the fall in performance and profitability without taking proactive action. Thus Fan laws apply whenever necessary and are especially accurate for the small changes in the designated compressor under observation for degradation. These laws may be used to confidently estimate the degradation in mass throughput, as mass throughput (m) is related to q which is in turn proportional to compressor speed and pressure ratio as shown below:

$q \alpha N$, $Hp \alpha N^2$, $\ell n\, PR \alpha N^2$, $\Delta T \alpha N^2$, $PWR \alpha N^3$ (4) [Ref 28]

Alternatively, the clean performance curve (point A on Figure 24A) can be manually shifted until it hits the point on the degraded performance curve (point B on Figure 24A) since both the degraded mass throughput and PR are known. In this manner the degradation in throughput is indirectly evaluated.

The degradation indices described by equation 1 to 3 above are the ratios between the values of degraded (dotted lines) and original performance curves (solid lines). These indices are independent from each other. Reference to Figure 24A, the performance of a clean compressor at a particular throughput, speed and pressure ratio/efficiency is represented by point “A” on the map and after some time the corresponding degraded performance is shown by point “B”. It is to be noted that rotational speed can not be scaled in the same manner described by equations 1 to 3 in this section for a clean and degraded compressor. In other words, the analysis between clean and degraded compressor should based and compared for the same speed.

For the compressor under observation there are available measured compressor speeds, flowrates, pressure ratios, efficiencies and a host of other measureable parameters such as inlet/outlet temperatures and power consumption reported electronically to DCS (distributed control system room) as well as hand written from field instruments once every 4 hours. All the instruments are regularly calibrated with online self diagnosing (fault finding) capabilities. In order that the gas path measurements between clean and

degraded conditions are comparable the measurements shall be “referred” to a common datum by the application of theta (θ) and delta (δ) to all the parameters. In this manner the environmental and gas inlet variations on compressor performance degradation are taken out of the equation and errors due to instrumentation are minimized so that, overall, the changes in performance values are significantly due to compressor degradation only rather than true compressor degradation lumped with environmental changes and instrument noise and bias.

As it was stated earlier in this section the result of degradation is the shift of performance curves downward (due to increase in clearances as a result of rubbings between stationary and moving parts) and to the left (due to fouling). Reference to Figures 24 and 25, the shift angle $A°_D$ (a new terminology introduced here) is not the same for all compressors and the magnitude depends on the thermodynamic properties of the fluid going through the compressor as well as the compressor loading (partial or full) and the physical geometry of the compressor [Refs 16, 17].

The method of health estimation or measure of degradation presented above takes a “snap shot” of the compressor health situation, i.e., analyzing the data as and when deemed required.

The proposed procedure for an accurate estimation of compressor performance and health status is shown in Chart (3) and this has been carried out for the site compressor whose data are included in Appendix C.

Referring to Table C2A in Appendix C (I), base case 5 was chosen for the proposed health estimation because this base case happens to have the same referred speed as the “clean” compressor. This procedure is recommended for all future works of similar nature. In case the referred speed at test point for the degraded compressor is not the same as that of the same compressor at clean conditions, it is perfectly acceptable to interpolate between two referred speeds at clean conditions for speed matching. The validity of interpolation method is confirmed [Refs 52, 53].

5.2 Compressor health estimation and GPA Index

In order to express the confidence level in the prediction of degradation, a GPA Index shall be set up defined as:

$$\text{GPA index} = 1/(1+\varepsilon) \qquad (5)$$

Where ε is a measure of the difference between the measured and predicted deviations of compressor gas path measurements and it is mathematically expressed as:

$$\varepsilon = \frac{1}{N}\sum_{i=1}^{N}\left|\frac{\Delta z_{i,measured}}{z_{i,measured}} - \frac{\Delta z_{i,predicted}}{z_{i,predicted}}\right| \quad (6)$$

$\Delta Z_{i,\ measured}$ / $Z_{i,\ measured}$ and $\Delta Z_{i,\ predicted}$ / $Z_{i,\ predicted}$ are the measured and predicted deviations of measurement Z_i, respectively.

The GPA predicts the degradation of a predefined compressor fault case and this information shall be sent to the model compressor to produce a predicted measurement deviation. The comparison between the real measurement deviation and the predicted is ε and then GPA Index shall be calculated. If the pre-defined case is correct then GPA Index will be close to 1. Thus a GPA Index approaching 1 indicates a very accurate degradation prediction while a GPA Index close to 0 means the other way around. Figure 25 shows the calculation process for GPA Index.

5.3 Sensitivity Analysis

Compressor degradation does not have equal effect on measurable parameters variables. It is important to recognize which variables are sensitive and which ones are insensitive to degradation so that maintenance items and schedules are classified accordingly. Furthermore the nature of relation (linear or non linear) between degradation and compressor dependent variables is important to be established so that the future behaviour can be estimated by extrapolation. GPA Indexing shall be carried out for the diagnostic method developed above and a full range of sensitivity analysis shall be carried out for the site compressor. These sensitivity analyses for the site compressor are shown in Chapter 7, Section 7.

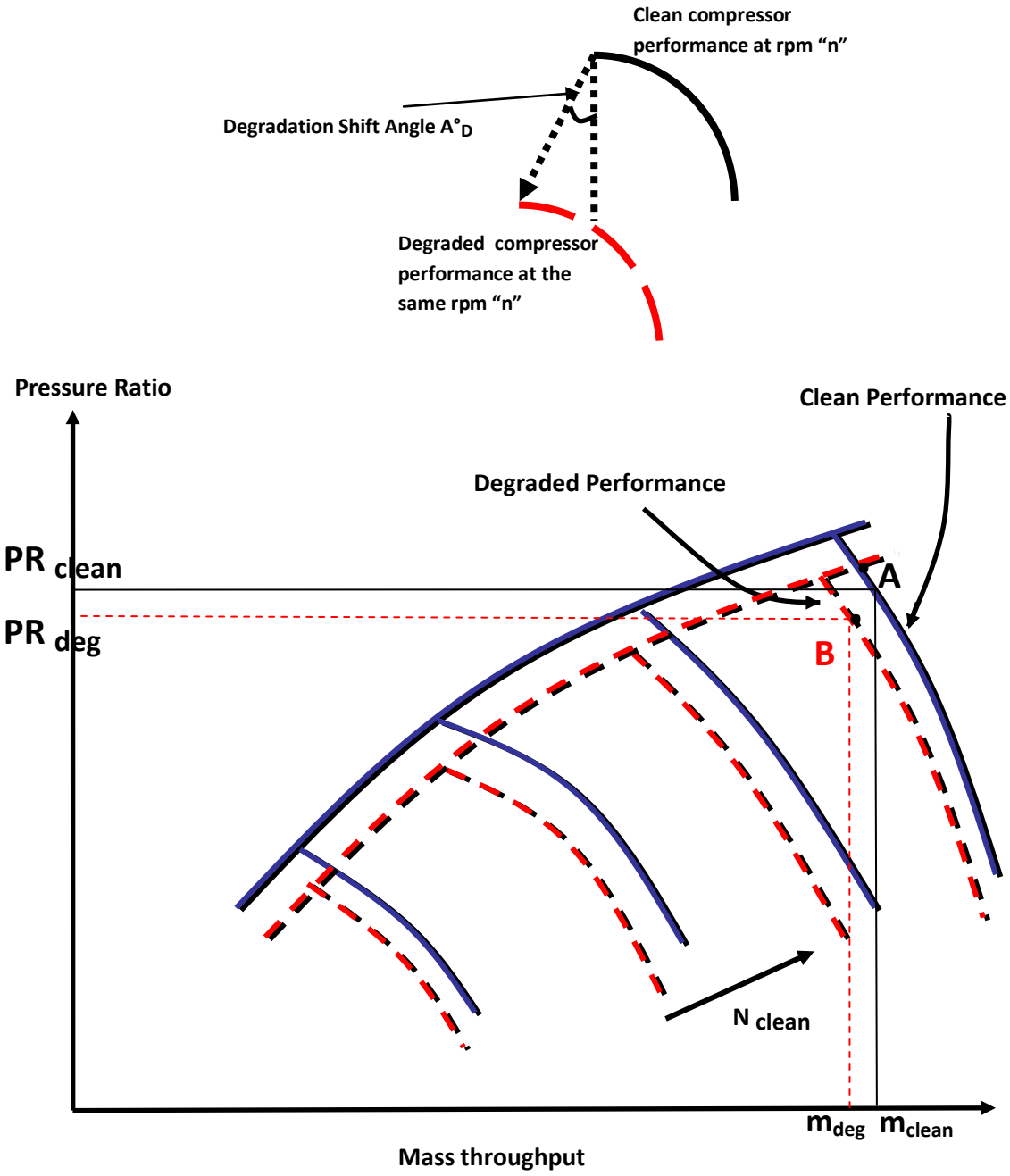

Figure 24A. The effect of compressor degradation on PR performance

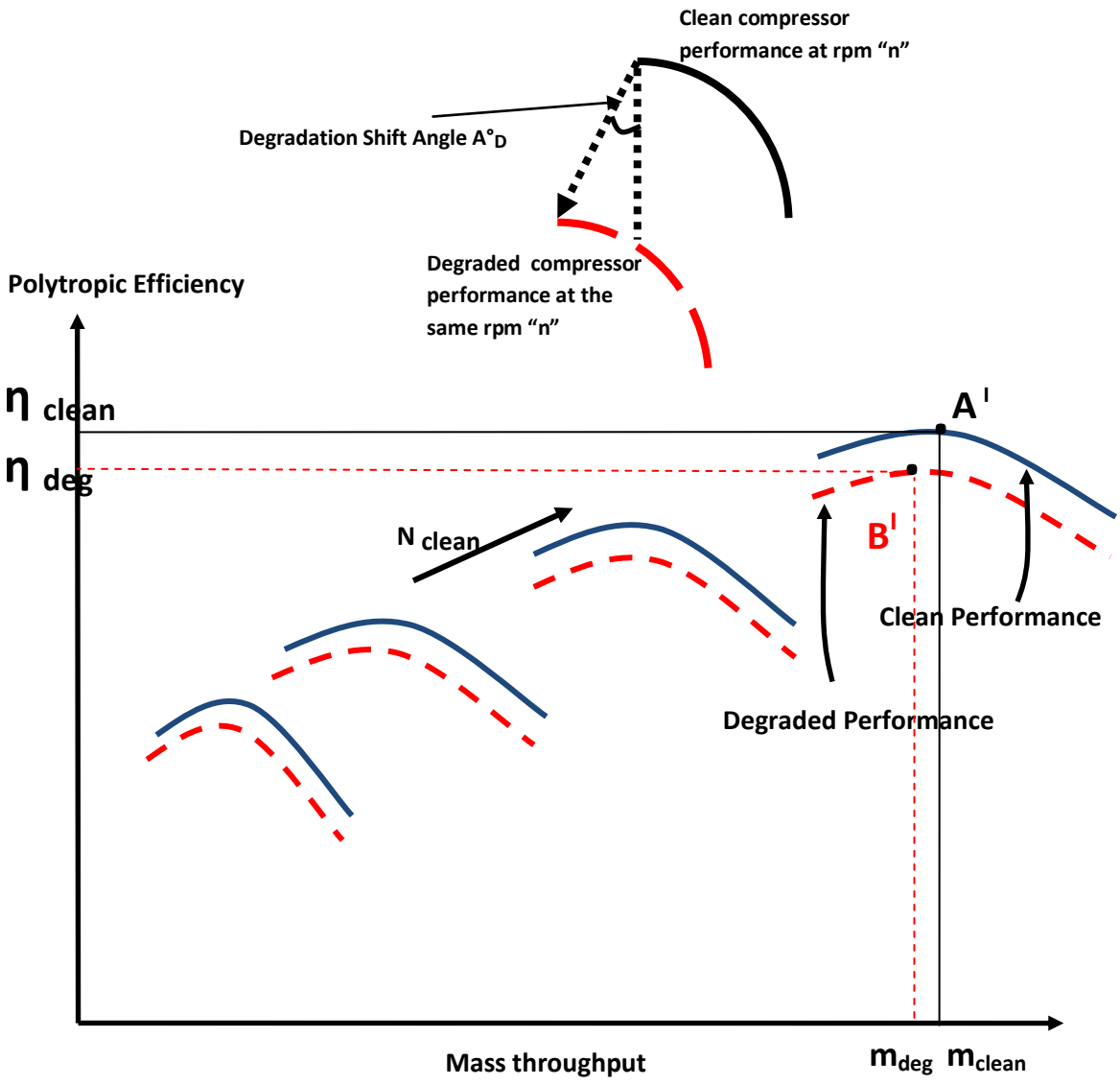

Figure 24B. The effect of compressor degradation on Compressor Efficiency

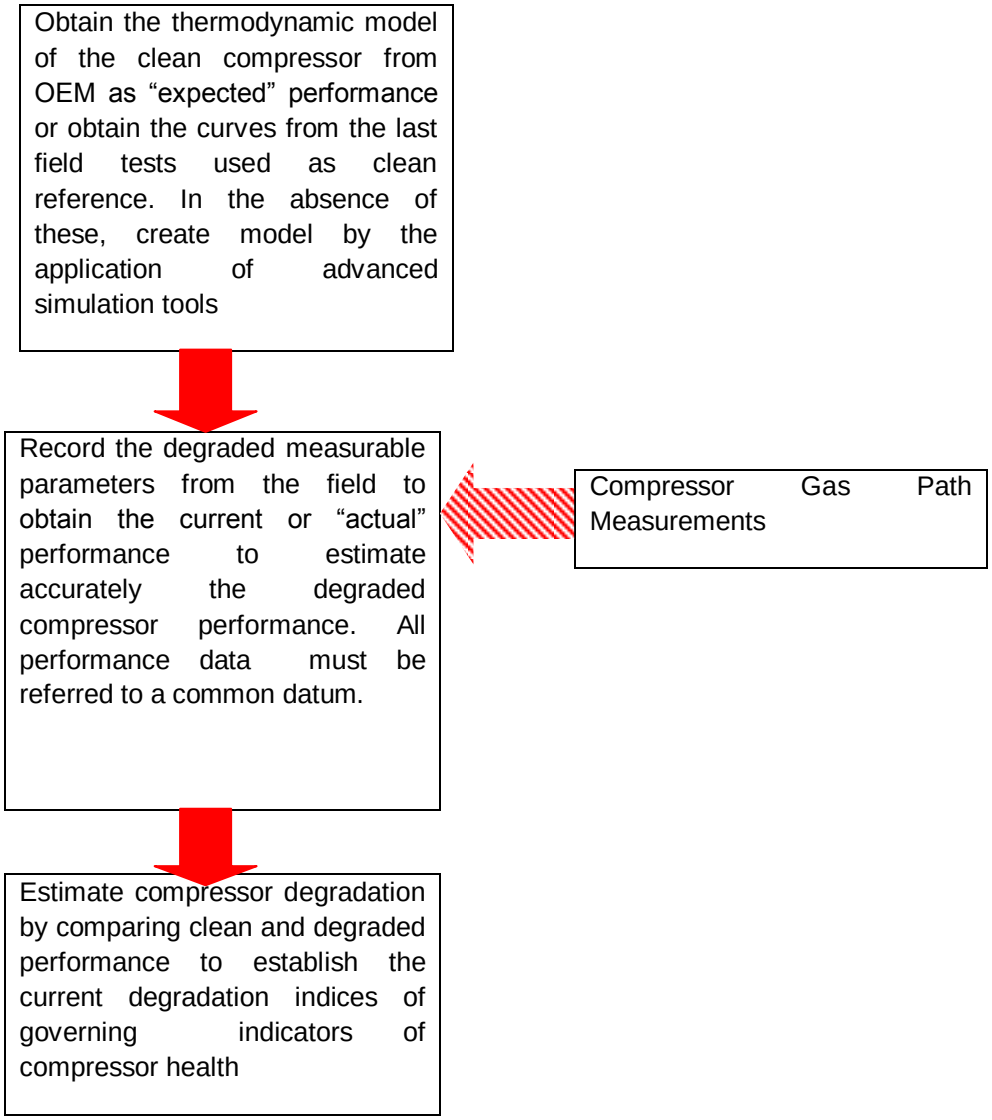

Chart 3. Procedure of Compressor Performance and Health Status

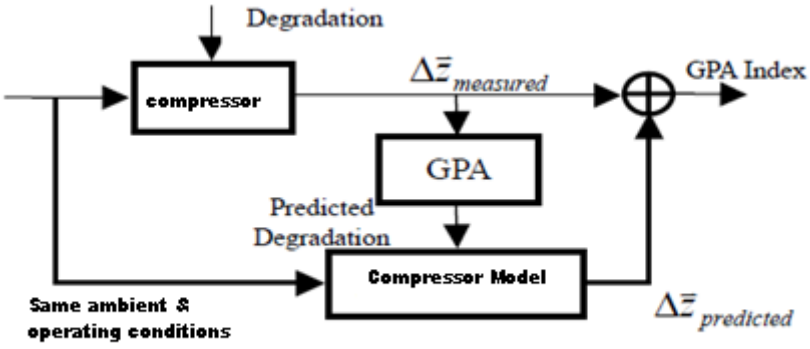

Figure 25. Calculation process for GPA Index

6. Application of compressor degradation modeling by simulation

To begin the work, a range of flows versus polytropic heads for 100% speed should be available. The sources of availability are OEM data for the same compressor and process gas properties. If the gas properties and the compressor under research are similar to a rated case from OEM at a given speed, equation 3-14A is used to calculate the pressure ratios. Alternatively, a range of polytropic heads (H_p) from equation 6 or a range of pressure ratios (PR) from equation 3-14B, at a given speed, are calculated which will subsequently be used to construct the compressor performance maps.

6.1 Generation of a compressor map for the clean (un-degraded) compressor

For the purpose of simulations, to generate a compressor map, two options are available:

1) Use any compressor map to start the works which is the current practice at the department of Engineering of Cranfield, or,

2) Generate a representative site compressor map.

It is obvious that the latter is superior as it enables the user to generate specific and representative performance curves tailor suited for any compressor and therefore the method has a much wider and useful application. In order to generate a representative site compressor map one of the following may be carried out:

A) Search for a single rated (OEM) supplied speed curve that resembles the site compressor gas and inlet conditions. This is shown in Table 4. Apply Equation 3-14A in Chapter 3 to generate modified or new pressure ratios for the given (100%) speed. Fan Laws as described under Chapter 3, Section 3.5.1 are then used to obtain the polytropic heads and throughputs for other speeds and this is followed by applying the rest of the equations in Chapter 3 to obtain the other performance parameters such as H_p, discharge temperature and power.

B) For a defined inlet conditions and series of assumed throughputs and pressure ratios (PR), use Eq. 3-13 to calculate the polytropic heads. Alternatively assume Polytropic head for each flow and use equation 3-14B to calculate pressure ratios. Apply affinity (Fan) Laws in Chapter 3, Section 3.5.1 to obtain the polytropic heads and throughputs for other speeds. This is followed by applying the rest

of the equations shown in Chapter 3 to obtain the measurable parameters such as discharge temperature and power.

In this work, the polytropic head for a range of flows at 100% speed is calculated using the equation (3-14A) modifying the OEM (rated) compressor and gas data to site (new) gas data. Reference to Table 4, it will be noted that polytropic efficiency is taken as a constant value. In real terms polytropic efficiency varies with flow rate. However, with superior design capabilities of the OEM, compressors hold a fairly constant and high value for a wide range of flowrates and deviate from the peak only at extremely low or extremely high flowrates which under the normal circumstances, operator does not operate in these regions.

3) The volumetric flowrate & polytropic head values are transferred into the spreadsheet specifically developed for generation of performance curves for other speeds based on proportionality (Fan) laws as described in Chapter 3, Section 3.5.1 and thus the flows and heads for other speeds are deduced. It will be noted that for each lower speeds, the performance curve is shifted to the left of the curve and the flow range is reduced. This is shown in Table 5.

4) For each set of Hp versus volumetric throughputs at defined speeds obtained above, equations (3-11), (3-14A), (3-15) and (3-16) are used to calculate discharge temperature, pressure ratio, power and mass throughput and these are shown in Table 6. These are graphically shown on Figures 26A –26E for the clean or un-degraded compressor.

Gas Properties	Site Conditions	Rated Conditions (OEM)
	Site Hydrocarbon	A Hydrocarbon
Mol. Weight	24.60	24.88
Suction Pressure	10.7	10.06
Intake Temperature K	315.3	303.85
Compressibility	0.95	0.96
C_p/C_v	1.20	1.236
Poly. Eff.(at rated flow)	0.85	0.85
n/(n-1)	5.10	4.45
k/(k-1)	6.00	5.24

Volumetric Flow Rate m^3/h	Pressure Ratio (Rated) P_d/P_s
10000	3.83
11000	3.79
12000	3.72
13000	3.62
14000	3.49
15000	3.31
15500	3.18
16000	3.04
16500	2.87
17000	2.70

Table 4. Available gas properties and basic rated performance data for a compressor

Manufacturers Data	
105%	10029
Flow	Head
[Act_m3/hr]	[kJ/kg]
Base Curve	9500
Flow	Head
[Act_m3/hr]	[kJ/kg]
10000	152.8
11000	151.4
12000	149.0
13000	145.4
14000	140.7
15000	133.9
15500	128.8
16000	123.1
16500	116.0
17000	108.5
94.737%	9000
Flow	Head
[Act_m3/hr]	[kJ/kg]
84.211%	8550
Flow	Head
[Act_m3/hr]	[kJ/kg]
73.684%	7600
Flow	Head
[Act_m3/hr]	[kJ/kg]
68.421%	6334
Flow	Head
[Act_m3/hr]	[kJ/kg]

	Fan Laws	
	105%	9975
	Flow	Head
	[Act_m3/hr]	[kJ/kg]
	10500	168.46
	11550	166.92
	12600	164.27
	13650	160.30
	14700	155.12
	15750	147.62
	16275	142.00
	16800	135.72
	17325	127.89
	17850	119.62
	Base Curve	9500
	Flow	Head
	[Act_m3/hr]	[kJ/kg]
1	10000	152.8
2	11000	151.4
3	12000	149.0
4	13000	145.4
5	14000	140.7
6	15000	133.9
7	15500	128.8
8	16000	123.1
9	16500	116.0
10	17000	108.5
	94.737%	9000
	Flow	Head
	[Act_m3/hr]	[kJ/kg]
1	9474	137.14
2	10421	135.88
3	11368	133.73
4	12316	130.50
5	13263	126.28
6	14211	120.18
7	14684	115.60
8	15158	110.48
9	15632	104.11
10	16105	97.38
	84.211%	8000
	Flow	Head
	[Act_m3/hr]	[kJ/kg]
	8421	108.36
	9263	107.36
	10105	105.66
	10947	103.11
	11789	99.78
	12632	94.95
	13053	91.34
	13474	87.30
	13895	82.26
	14316	76.94
	73.684%	7000
	Flow	Head
	[Act_m3/hr]	[kJ/kg]
	7368	82.96
	8105	82.20
	8842	80.90
	9579	78.94
	10316	76.39
	11053	72.70
	11421	69.93
	11789	66.84
	12158	62.98
	12526	58.91
	68.421%	6500
	Flow	Head
	[Act_m3/hr]	[kJ/kg]
	6842	71.53
	7526	70.88
	8211	69.75
	8895	68.07
	9579	65.87
	10263	62.68
	10605	60.30
	10947	57.63
	11289	54.30
	11632	50.79

Compressor Speeds	
Speed [%]	[rpm]
105	9975
100	9500
94.74	9000
84.21	8000
73.68	7000
68.42	6500

	Fan law Constants	
	K1	K2
1	1.05	0.000002
2	1.16	0.000002
3	1.26	0.000002
4	1.37	0.000002
5	1.47	0.000002
6	1.58	0.000001
7	1.63	0.000001
8	1.68	0.000001
9	1.74	0.000001
10	1.79	0.000001

	K1	K2
1	Q1/N1	H1/(N1^2)
2	Q2/N1	H2/(N1^2)
3	Q3/N1	H3/(N1^2)
4	Q4/N1	H4/(N1^2)
5	Q5/N1	H5/(N1^2)
6	Q6/N1	H6/(N1^2)
7	Q7/N1	H7/(N1^2)
8	Q8/N1	H8/(N1^2)
9	Q9/N1	H9/(N1^2)
10	Q10/N1	H10/(N1^2)

Surge Line - Fan Laws		Surge Line - Manufacturer's Data	
Flow	Head	Flow	Head
[Act_m3/hr]	[kJ/kg]	[Act_m3/hr]	[kJ/kg]
6842	71.53	0	0.00
7368	82.96	0	0.00
8421	108.36	0	0.00
9474	137.14	0	0.00
10000	152.80	10000	152.80
10500	168.46	0	0.00
Stone Wall Line - Fan Laws		Stone Wall Line - Manufacturer's Data	
Flow	Head	Flow	Head
[Act_m3/hr]	[kJ/kg]	[Act_m3/hr]	[kJ/kg]
11632	50.79	0	0.00
12526	58.91	0	0.00
14316	76.94	0	0.00
16105	97.38	0	0.00
17000	108.50	17000	108.50
17850	119.62	0	0.00

Notes:
1. Enter Only Manufacturer's Data
2. Enter only 100% Speed for Under Compressor Speed Column
3. Enter cells which have background colour as
4. The tool calculates the performance curves using Fan Laws based on the 100% Speed curve (i.e., Base Curve)

N2 (9000 rpm)

	Flow	Head
	[Act_m3/hr]	[kJ/kg]
1	K1,1 x N2	K2,1 x (N2^2)
2	K1,2 x N2	K2,2 x (N2^2)
3	K1,3 x N2	K2,3 x (N2^2)
4	K1,4 x N2	K2,4 x (N2^2)
5	K1,5 x N2	K2,5 x (N2^2)
6	K1,6 x N2	K2,6 x (N2^2)
7	K1,7 x N2	K2,7 x (N2^2)
8	K1,8 x N2	K2,8 x (N2^2)
9	K1,9 x N2	K2,9 x (N2^2)
10	K1,10 x N2	K2,10 x (N2^2)

Table 5. Generation of speed curves based on Affinity (proportionality or Fan) Laws

9500 rpm, Vol flow & Hp supplied, rest calculated by thermodynamic equations

Volumetric Flow Rate	Polytropic Head	Pressure Ratio	Discharge Pressure	Mass Flow	Discharge Temperature	Power
m^3/h	KJ/Kg	Pd/Ps	bara	kg/h	°C	KW
10000	152.8	3.75	40.14	105697	135.6	5277
11000	151.4	3.71	39.72	116266	134.8	5753
12000	149.0	3.64	38.98	126836	133.3	6174
13000	145.4	3.54	37.93	137406	131.1	6529
14000	140.7	3.42	36.56	147975	128.2	6802
15000	133.9	3.24	34.67	158545	124.1	6936
15500	128.8	3.11	33.31	163830	120.9	6895
16000	123.1	2.98	31.85	169115	117.5	6804
16500	116.0	2.81	30.07	174399	113.1	6609
17000	108.5	2.64	28.30	179684	108.5	6369

9000 rpm, values calculated by Fan laws and thermodynamic equations

Volumetric Flow Rate	Polytropic Head	Pressure Ratio	Discharge Pressure	Mass Flow	Discharge Temperature	Power
m^3/h	KJ/Kg	Pd/Ps	bara	kg/h	°C	KW
9474	137.1	3.325	35.57	100134	126.1	4488
10421	135.9	3.292	35.23	110147	125.3	4891
11368	133.7	3.237	34.64	120160	124.0	5251
12316	130.5	3.156	33.77	130174	122.0	5551
13263	126.3	3.052	32.66	140187	119.4	5785
14211	120.2	2.907	31.11	150201	115.7	5899
14684	115.6	2.802	29.98	155207	112.9	5863
15158	110.5	2.688	28.77	160214	109.8	5785
15632	104.1	2.552	27.31	165221	105.9	5621
16105	97.4	2.414	25.83	170227	101.8	5417

8000 rpm, values calculated by Fan laws and thermodynamic equations

Volumetric Flow Rate	Polytropic Head	Pressure Ratio	Discharge Pressure	Mass Flow	Discharge Temperature	Power
m^3/h	KJ/Kg	Pd/Ps	bara	kg/h	°C	KW
8421	108.4	2.642	28.27	89008	108.5	3152
9263	107.4	2.621	28.04	97908	107.9	3435
10105	105.7	2.585	27.66	106809	106.8	3688
10947	103.1	2.531	27.08	115710	105.3	3899
11789	99.8	2.462	26.35	124611	103.2	4063
12632	95.0	2.366	25.31	133512	100.3	4143
13053	91.3	2.295	24.56	137962	98.1	4118
13474	87.3	2.218	23.74	142412	95.6	4063
13895	82.3	2.125	22.74	146863	92.5	3948
14316	76.9	2.031	21.73	151313	89.3	3805

7000 rpm, values calculated by Fan laws and thermodynamic equations

Volumetric Flow Rate	Polytropic Head	Pressure Ratio	Discharge Pressure	Mass Flow	Discharge Temperature	Power
m^3/h	KJ/Kg	Pd/Ps	bara	kg/h	°C	KW
7368	83.0	2.138	22.88	77882	93.0	2111
8105	82.2	2.124	22.73	85670	92.5	2301
8842	80.9	2.101	22.48	93458	91.7	2471
9579	78.9	2.066	22.11	101246	90.5	2612
10316	76.4	2.021	21.63	109034	89.0	2722
11053	72.7	1.958	20.95	116823	86.7	2775
11421	69.9	1.911	20.45	120717	85.0	2759
11789	66.8	1.860	19.91	124611	83.1	2722
12158	63.0	1.799	19.25	128505	80.8	2645
12526	58.9	1.735	18.57	132399	78.3	2549

6500 rpm, values calculated by Fan laws and thermodynamic equations

Volumetric Flow Rate	Polytropic Head	Pressure Ratio	Discharge Pressure	Mass Flow	Discharge Temperature	Power
m^3/h	KJ/Kg	Pd/Ps	bara	kg/h	°C	KW
6842	71.5	1.938	20.74	72319	86.0	1691
7526	70.9	1.927	20.62	79551	85.6	1843
8211	69.8	1.908	20.42	86783	84.9	1978
8895	68.1	1.881	20.12	94014	83.9	2091
9579	65.9	1.845	19.74	101246	82.5	2179
10263	62.7	1.794	19.20	108478	80.6	2222
10605	60.3	1.757	18.79	112094	79.1	2209
10947	57.6	1.715	18.36	115710	77.5	2179
11289	54.3	1.665	17.82	119326	75.5	2118
11632	50.8	1.614	17.27	122942	73.3	2041

Table 6. Calculation of un-degraded compressor variables for all speeds

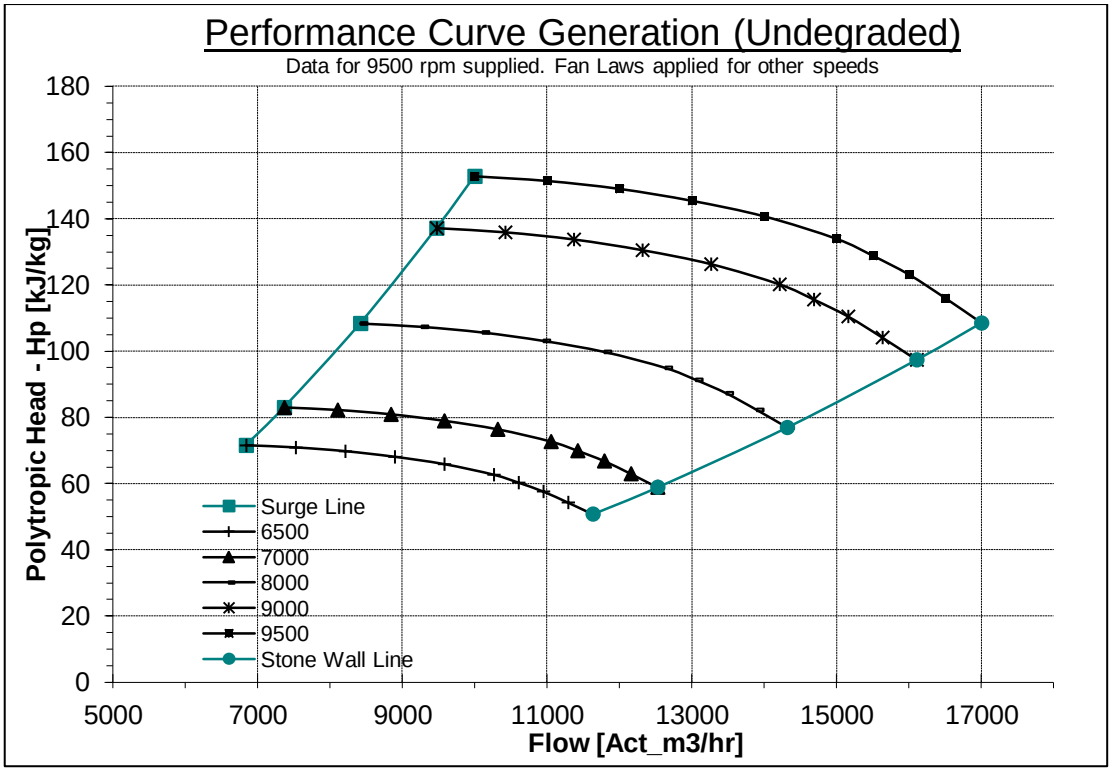

Figure 26A. Compressor performance generation, polytropic head versus volume flow

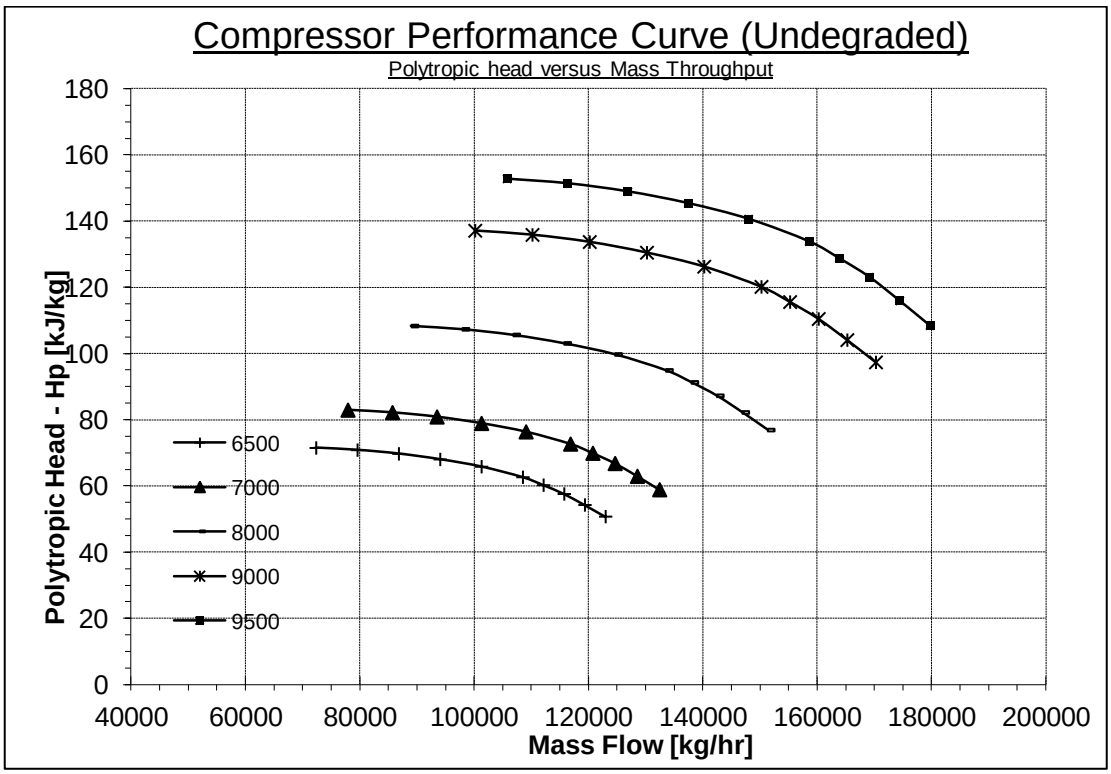

Figure 26B. Compressor performance generation, Polytropic head versus mass flow

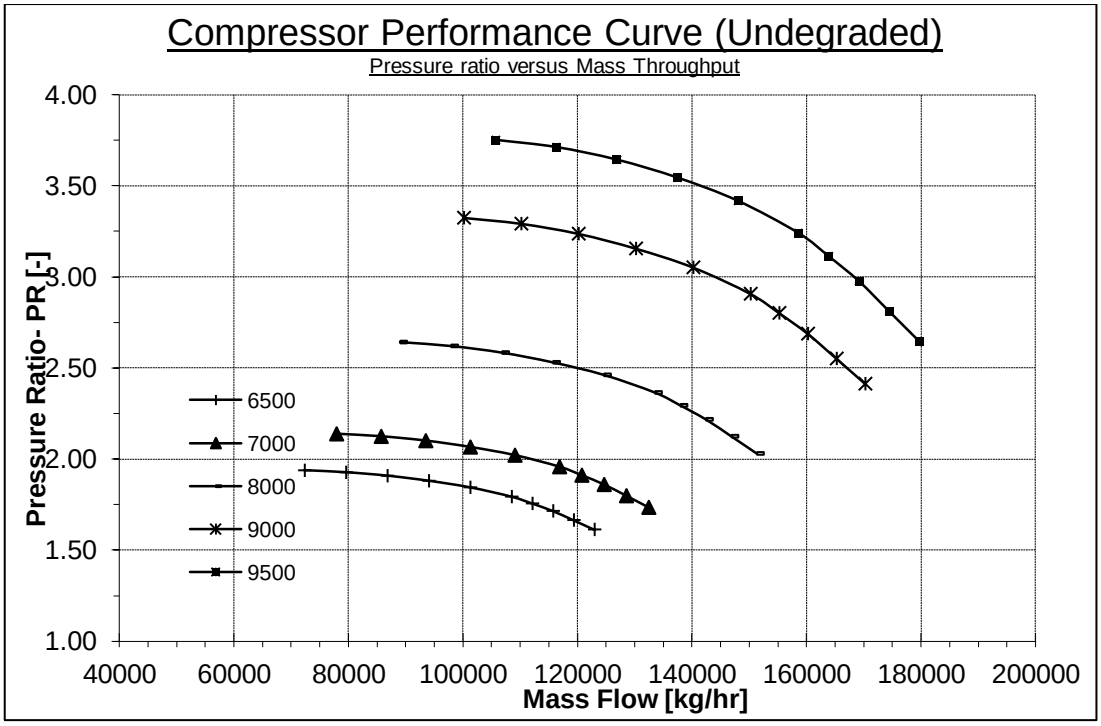

Figure 26C. Compressor performance generation, Pressure ratio versus mass flow

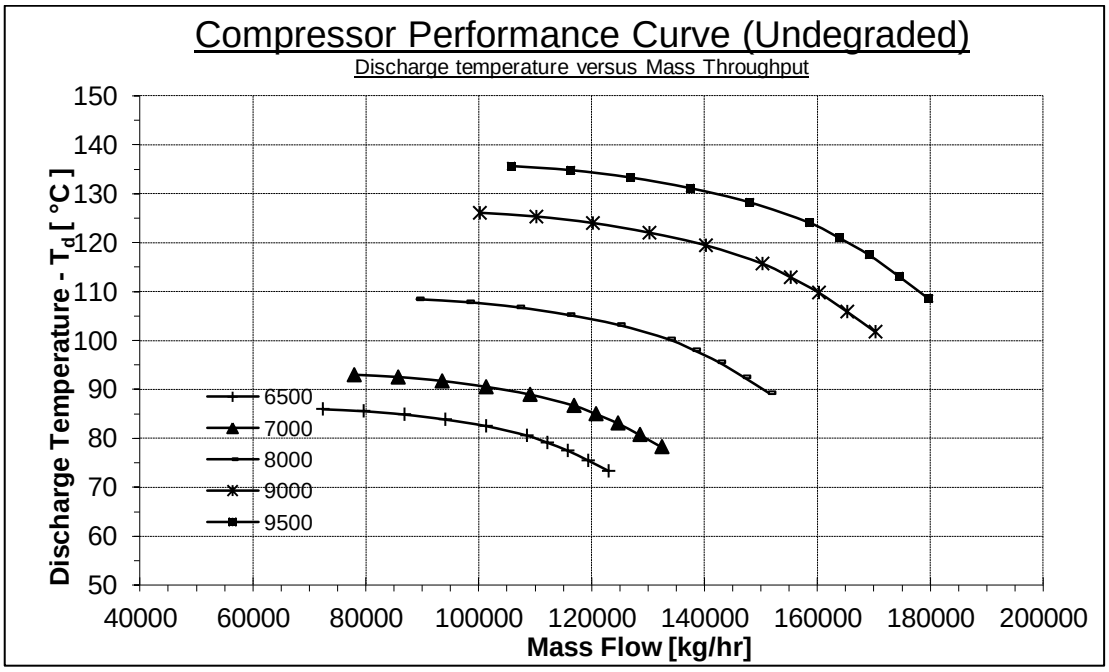

Figure 26D. Compressor performance generation, Discharge temp versus mass flow

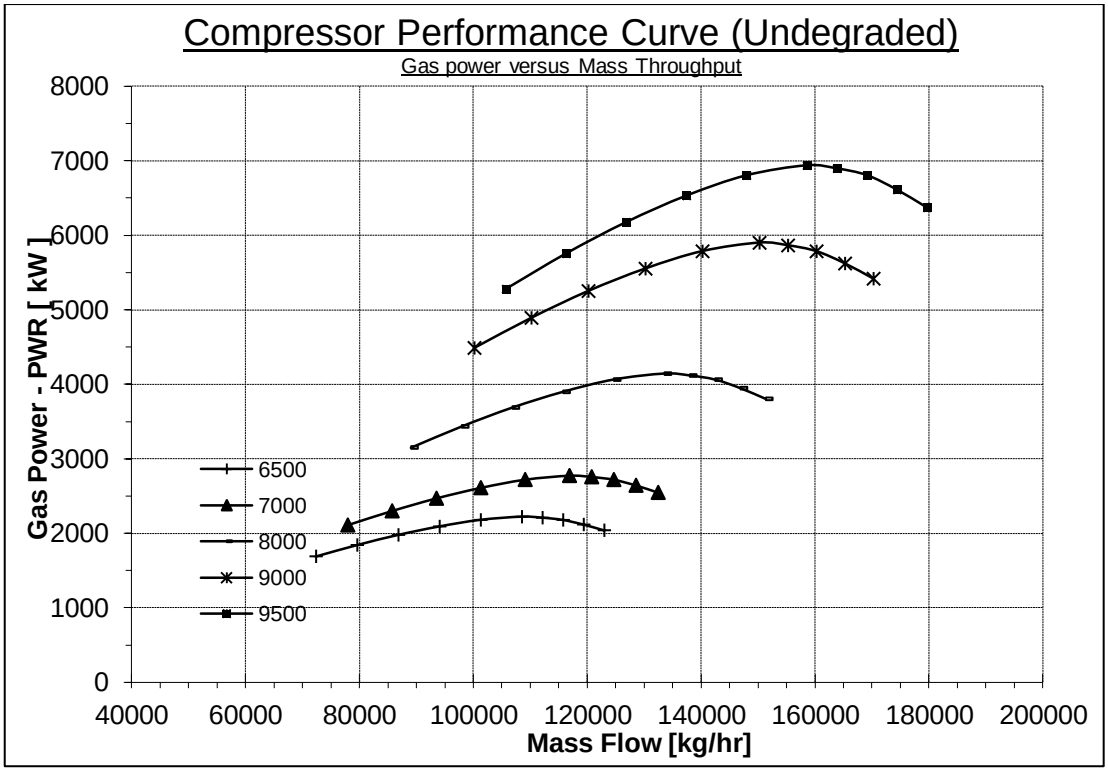

Figure 26E. Compressor performance generation, Gas power versus mass flow

6.2 Generation of a compressor map for the degraded compressor

When a compressor degrades, the performance curves shift down and generally to the left. These shifts translate into a reduction in dependent parameters including pressure ratio (for a fixed inlet pressure), efficiency and throughput. Thus if the clean un-degraded compressor is giving a pressure ratio of 3.75 at a flow of 10,000 m3/hr and 9500 rpm (Table 6), under degraded conditions it will give a PR smaller than 3.75 at the same rpm. Thus in order to keep the PR the same as un-degraded, the compressor has to increase the speed beyond 9500 rpm (rerate) demanding more power from the driving turbine. The increase in rpm may be beyond the design margin of the compressor (normally capped at 5% above maximum continuous speed) or that the availability of excess power supply may be the limiting factor. An a-priori data analysis is required so that allowable ranges or tolerable regions of compressor degradation are mapped out in advance of the project implementation by the operators and thus the frequency of maintenance is predicted.

The performance curves for the clean compressor were developed in the previous section. In this section, the curves for degraded compressor shall be developed and the rerates shall be determined.

The criteria chosen for evaluation of degradation are:

A) 5.0% Deg in PR, No Deg in η, No Deg in m
B) 5.0% Deg in PR, 2.5% Deg in η, No Deg in m
C) 5.0% Deg in PR, 2.5% Deg in η, 5.0% Deg in m
D) 10.0% Deg in PR, 5.0% Deg in η, 10.0% Deg in m

Table 7 shows the performance parameter values for all the above cases and the rerates required at 100% speed. Affinity laws (Equations 3-18 to 3-21) are used to calculate the polytropic head & rotational speeds under degraded conditions as well as for the rerating. Table 8 shows the calculated polytropic heads for other speeds. Referring to Table 7, for a 10% degradation in PR, the compressor curve at 100% speed falls from 9500 rpm (clean or un-degraded compressor) to an equivalent of 9290 rpm. Thus for this degraded compressor to give the original discharge pressure, it has to run at the speed of 9715 rpm under degraded condition to give the equivalent of 9500 rpm of a clean or un-degraded compressor and as a result the power demand by compressor increases and as a result if this surge in power demand is combined with high ambient temperatures and/or efficiency degradation, the operator may face operational limitations or even face the inability to deliver the gas as per the specification. It shall be noted from the same Table 7 that for this compressor the design limit in terms of maximum allowable continuous speed is reached well before 10% degradation in PR. The power requirement is also a sensitive function of state of the compressor which if left unattended, the demand increase in supplied power may be the limiting factor for allowed level of compressor fouling.

Figures 27, 28 and 29 show the remarkable effect of degradation on compressor performance. The effect of degradation on gas power demand has also a very profound effect even for small degradation levels and this is shown on Figures 30A and 30B.

100% Speed									Re-rate			
Clean Volume Flow Rate m3/h	Clean Pressur Ratio Pd/Ps	Clean Discharg Pressure bara	Deg Discharg Pressure bara	Deg Press Raio	Deg Hp kJ/kg	Ndeg	Ndeg/Ncl	Tdis °C	Speed rpm	% inc rpm	Hp kJ/kg	PWR
						Degrdation Case A						
								(no chng)				
10000	3.75	40.14	38.1	3.56	146.09	9290	0.9778	135.6	9715	2.266	159.78	5519
11000	3.71	39.72	37.7	3.53	144.72	9288	0.9777	134.8	9717	2.282	158.39	6018
12000	3.64	38.98	37.0	3.46	142.30	9285	0.9774	133.3	9720	2.312	155.92	6463
13000	3.54	37.93	36.0	3.37	138.77	9281	0.9770	131.1	9724	2.358	152.33	6840
14000	3.42	36.56	34.7	3.25	134.08	9275	0.9764	128.2	9730	2.422	147.55	7135
15000	3.24	34.67	32.9	3.08	127.36	9266	0.9754	124.1	9740	2.522	140.70	7290
15500	3.11	33.31	31.6	2.96	122.32	9259	0.9746	120.9	9747	2.605	135.57	7258
16000	2.98	31.85	30.3	2.83	116.71	9250	0.9737	117.5	9757	2.705	129.86	7177
16500	2.81	30.07	28.6	2.67	109.63	9237	0.9723	113.1	9770	2.845	122.65	6990
17000	2.64	28.30	26.9	2.51	102.22	9222	0.9708	108.5	9786	3.013	115.10	6759
						Degrdation Case B						
						9290	0.9778	135.6	9715	2.266	159.78	5686
						9288	0.9777	134.8	9717	2.282	158.39	6200
						9285	0.9774	133.3	9720	2.312	155.92	6659
						9281	0.9770	131.1	9724	2.358	152.33	7048
						9275	0.9764	128.2	9730	2.422	147.55	7352
						9266	0.9754	124.1	9740	2.522	140.70	7511
						9259	0.9746	120.9	9747	2.605	135.57	7478
						9250	0.9737	117.5	9757	2.705	129.86	7394
						9237	0.9723	113.1	9770	2.845	122.65	7202
						9222	0.9708	108.5	9786	3.013	115.10	6964
						Degrdation Case C						
						9290	0.9778	135.6	9715	2.266	159.78	5402
						9288	0.9777	134.8	9717	2.282	158.39	5890
						9285	0.9774	133.3	9720	2.312	155.92	6326
						9281	0.9770	131.1	9724	2.358	152.33	6695
						9275	0.9764	128.2	9730	2.422	147.55	6984
						9266	0.9754	124.1	9740	2.522	140.70	7135
						9259	0.9746	120.9	9747	2.605	135.57	7104
						9250	0.9737	117.5	9757	2.705	129.86	7025
						9237	0.9723	113.1	9770	2.845	122.65	6842
						9222	0.9708	108.5	9786	3.013	115.10	6615
						Degrdation Case D						
			36.1	3.38	139.10	9065	0.9542	127.2	9956	4.80	167.81	5543
			35.7	3.34	137.75	9062	0.9538	126.4	9960	4.84	166.40	6046
			35.1	3.28	135.35	9056	0.9532	125.0	9966	4.90	163.92	6497
			34.1	3.19	131.87	9047	0.9523	122.8	9975	5.00	160.31	6884
			32.9	3.08	127.22	9035	0.9511	120.0	**9989**	**5.15**	155.51	7191
			31.2	2.92	120.57	9016	0.9490	115.9	**10010**	**5.37**	148.62	7364
			30.0	2.80	115.59	9000	0.9474	112.9	**10027**	**5.55**	143.47	7345
			28.7	2.68	110.04	8981	0.9454	109.5	**10049**	**5.77**	137.74	7279
			27.1	2.53	103.03	8955	0.9426	105.2	**10078**	**6.09**	130.51	7113
			25.5	2.38	95.69	8923	0.9393	100.7	**10114**	**6.47**	122.95	6904
									DESIGN LIMIT EXCEEDED			

Degrdation	
Case A	PR=5%, Eff=0, m=0
Case B	PR=5%, Eff=2.5%, m=0
Case C	PR=5%, Eff=2.5%, m=5%
Case D	PR=10%, Eff=5%, m=10%

Table7. Degradation modeling of a compressor at 100% speed (Table 8 for other speeds)

Degradation		Rerate		Degradation		Rerate	
0% m, 5% PR, Eff:0%				10% m,10%PR, 5 eff%			
(Figures 2 & 3)		(Figure 3)		(Figure 2 & 4)		(Figure 4)	
Base Curve	**9500**	**Base Curve**	**9500**	**Base Curve**	**9500**	**Base Curve**	**9500**
Flow	**Head**	**Flow**	**Head**	**Flow**	**Head**	**Flow**	**Head**
[Act_m3/hr	**[kJ/kg]**	**Act_m3/hr**	**[kJ/kg]**	**Act_m3/hr**	**[kJ/kg]**	**Act_m3/hr**	**[kJ/kg]**
10000	146.10	10000	159.78	9000	139.10	9000	167.81
11000	144.70	11000	158.39	9900	137.75	9900	166.40
12000	142.30	12000	155.92	10800	135.35	10800	163.92
13000	138.80	13000	152.33	11700	131.87	11700	160.31
14000	134.10	14000	147.55	12600	127.22	12600	155.51
15000	127.40	15000	140.70	13500	120.57	13500	148.62
15500	122.30	15500	135.57	13950	115.59	13950	143.47
16000	116.70	16000	129.86	14400	110.04	14400	137.74
16500	109.60	16500	122.65	14850	103.03	14850	130.51
17000	105.20	17000	115.10	15300	95.69	15300	122.95
94.7%	**9000**	**94.7%**	**9000**	**94.7%**	**9000**	**94.7%**	**9000**
Flow	**Head**	**Flow**	**Head**	**Flow**	**Head**	**Flow**	**Head**
[Act_m3/hr	**[kJ/kg]**	**Act_m3/hr**	**[kJ/kg]**	**Act_m3/hr**	**[kJ/kg]**	**Act_m3/hr**	**[kJ/kg]**
9474	131.13	9474	143.41	8526	124.84	8526	150.61
10421	129.87	10421	142.16	9379	123.63	9379	149.35
11368	127.72	11368	139.94	10232	121.48	10232	147.12
12316	124.57	12316	136.72	11084	118.35	11084	143.88
13263	120.36	13263	132.43	11937	114.18	11937	139.57
14211	114.34	14211	126.28	12789	108.21	12789	133.39
14684	109.77	14684	121.68	13216	103.74	13216	128.76
15158	104.74	15158	116.55	13642	98.76	13642	123.62
15632	98.37	15632	110.08	14068	92.47	14068	117.13
16105	91.02	16105	103.30	14495	85.89	14495	110.35
84.2%	**8000**	**84.2%**	**8000**	**84.2%**	**8000**	**84.2%**	**8000**
Flow	**Head**	**Flow**	**Head**	**Flow**	**Head**	**Flow**	**Head**
[Act_m3/hr	**[kJ/kg]**	**Act_m3/hr**	**[kJ/kg]**	**Act_m3/hr**	**[kJ/kg]**	**Act_m3/hr**	**[kJ/kg]**
8421	103.61	8421	113.31	7579	98.64	7579	119.00
9263	102.61	9263	112.32	8337	97.68	8337	118.00
10105	100.91	10105	110.57	9095	95.98	9095	116.24
10947	98.43	10947	108.03	9853	93.51	9853	113.69
11789	95.10	11789	104.64	10611	90.22	10611	110.28
12632	90.34	12632	99.78	11368	85.50	11368	105.39
13053	86.73	13053	96.14	11747	81.97	11747	101.74
13474	82.76	13474	92.09	12126	78.03	12126	97.68
13895	77.72	13895	86.98	12505	73.06	12505	92.55
14316	72.08	14316	81.62	12884	67.86	12884	87.19
73.7%	**7000**	**73.7%**	**7000**	**73.7%**	**7000**	**73.7%**	**7000**
Flow	**Head**	**Flow**	**Head**	**Flow**	**Head**	**Flow**	**Head**
[Act_m3/hr	**[kJ/kg]**	**Act_m3/hr**	**[kJ/kg]**	**Act_m3/hr**	**[kJ/kg]**	**Act_m3/hr**	**[kJ/kg]**
7368	79.32	7368	86.75	6632	75.52	6632	91.11
8105	78.56	8105	86.00	7295	74.79	7295	90.35
8842	77.26	8842	84.66	7958	73.49	7958	89.00
9579	75.36	9579	82.71	8621	71.60	8621	87.04
10316	72.81	10316	80.11	9284	69.07	9284	84.43
11053	69.17	11053	76.39	9947	65.46	9947	80.69
11421	66.40	11421	73.61	10279	62.76	10279	77.89
11789	63.36	11789	70.51	10611	59.74	10611	74.78
12158	59.51	12158	66.59	10942	55.94	10942	70.86
12526	55.19	12526	62.49	11274	51.96	11274	66.75
68.4%	**6500**	**68.4%**	**6500**	**68.4%**	**6500**	**68.4%**	**6500**
Flow	**Head**	**Flow**	**Head**	**Flow**	**Head**	**Flow**	**Head**
[Act_m3/hr	**[kJ/kg]**	**Act_m3/hr**	**[kJ/kg]**	**Act_m3/hr**	**[kJ/kg]**	**Act_m3/hr**	**[kJ/kg]**
6842	68.40	6842	74.80	6158	65.12	6158	78.56
7526	67.74	7526	74.15	6774	64.49	6774	77.90
8211	66.62	8211	72.99	7389	63.36	7389	76.74
8895	64.98	8895	71.31	8005	61.73	8005	75.05
9579	62.78	9579	69.08	8621	59.56	8621	72.80
10263	59.64	10263	65.87	9237	56.44	9237	69.58
10605	57.25	10605	63.47	9545	54.11	9545	67.16
10947	54.63	10947	60.79	9853	51.51	9853	64.48
11289	51.31	11289	57.42	10161	48.23	10161	61.10
11632	47.59	11632	53.88	10468	44.80	10468	57.56

Table 8. Generation of degraded performance curves using affinity laws

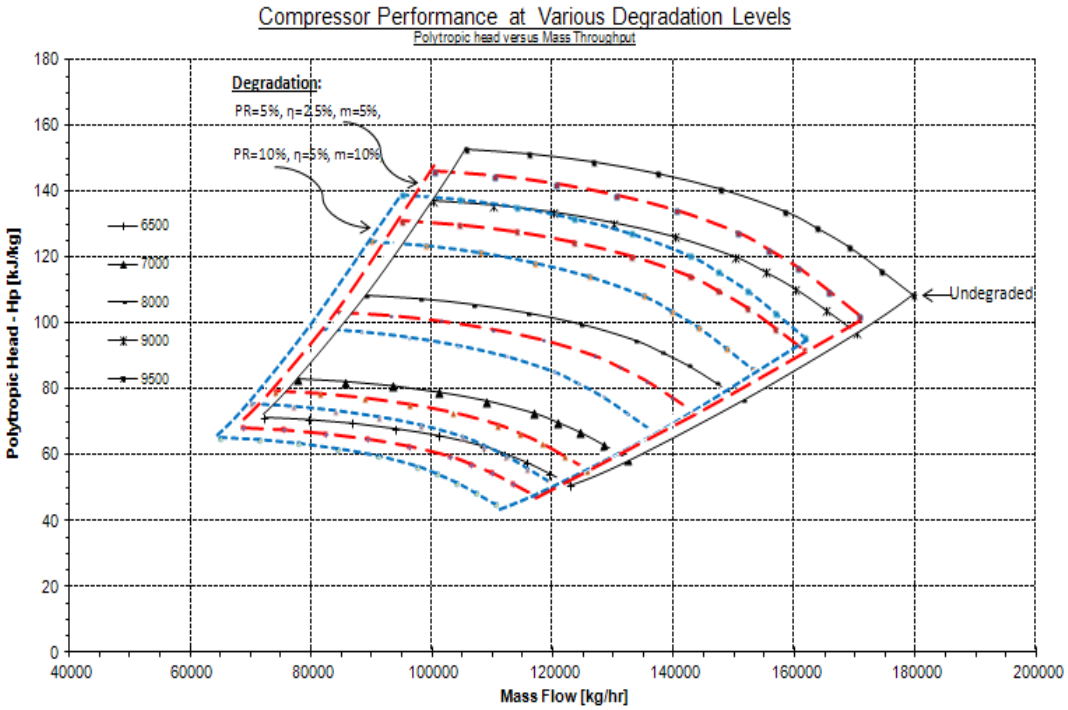

Figure 27. Compressor performance at various degradation levels (values from Table 7)

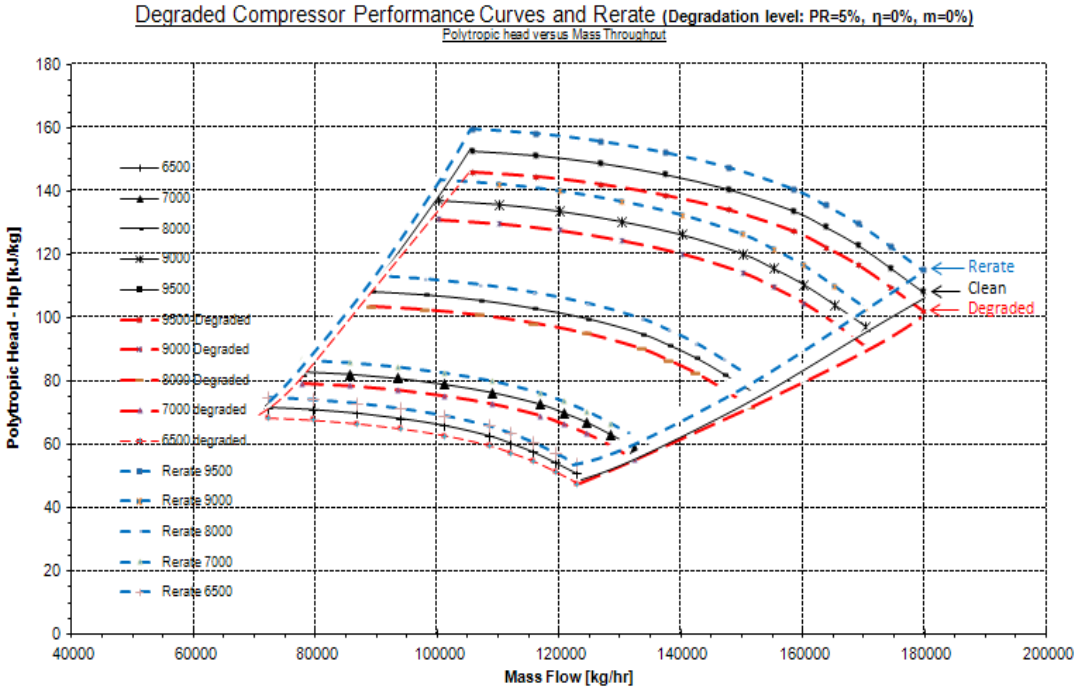

Figure 28. Performance prediction for degraded compressor and the required rerate

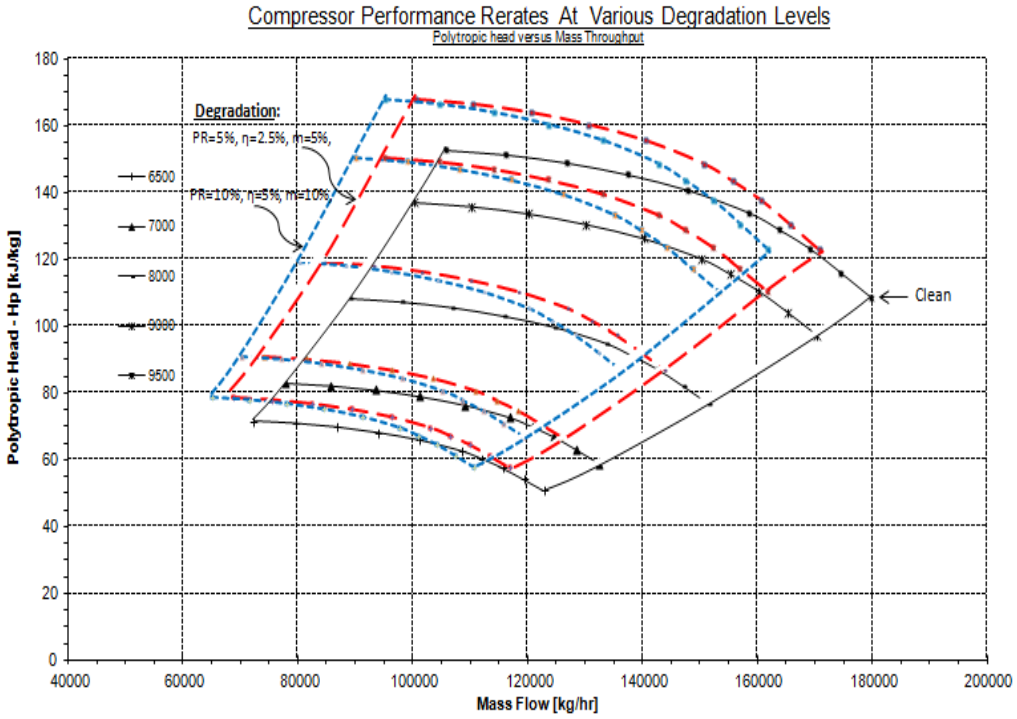

Figure 29. Compressor performance rerates for various degradation levels
(Table 7 for values)

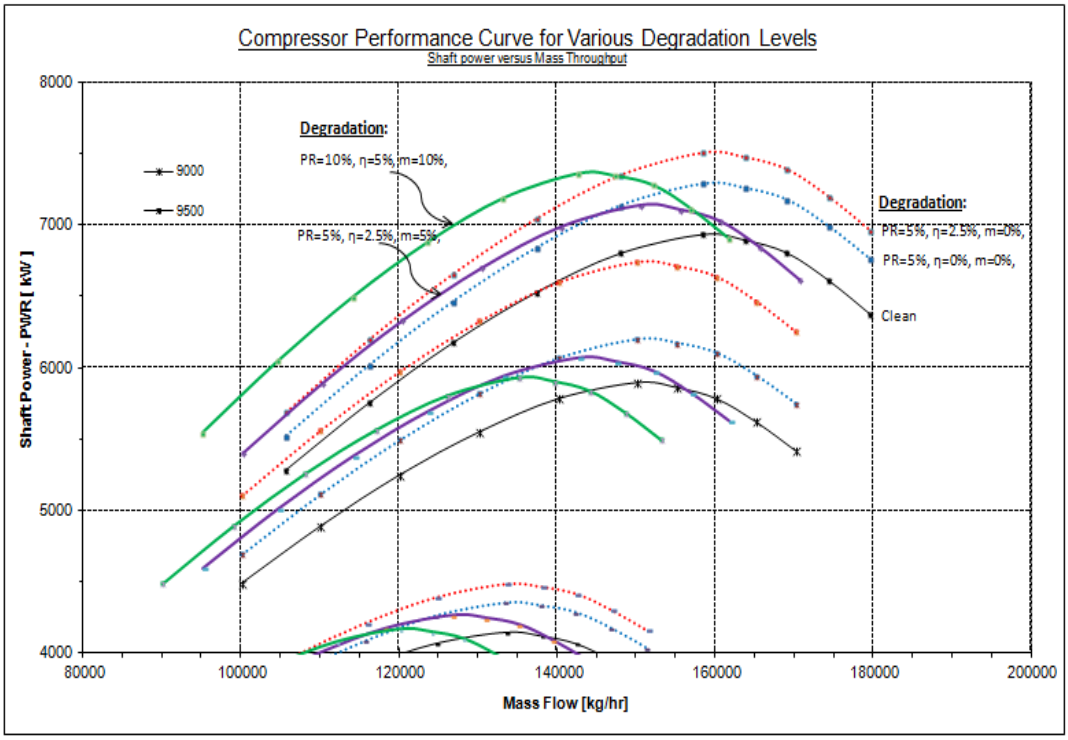

Figure 30A. The variations in gas power demand due to degradation (high speeds)

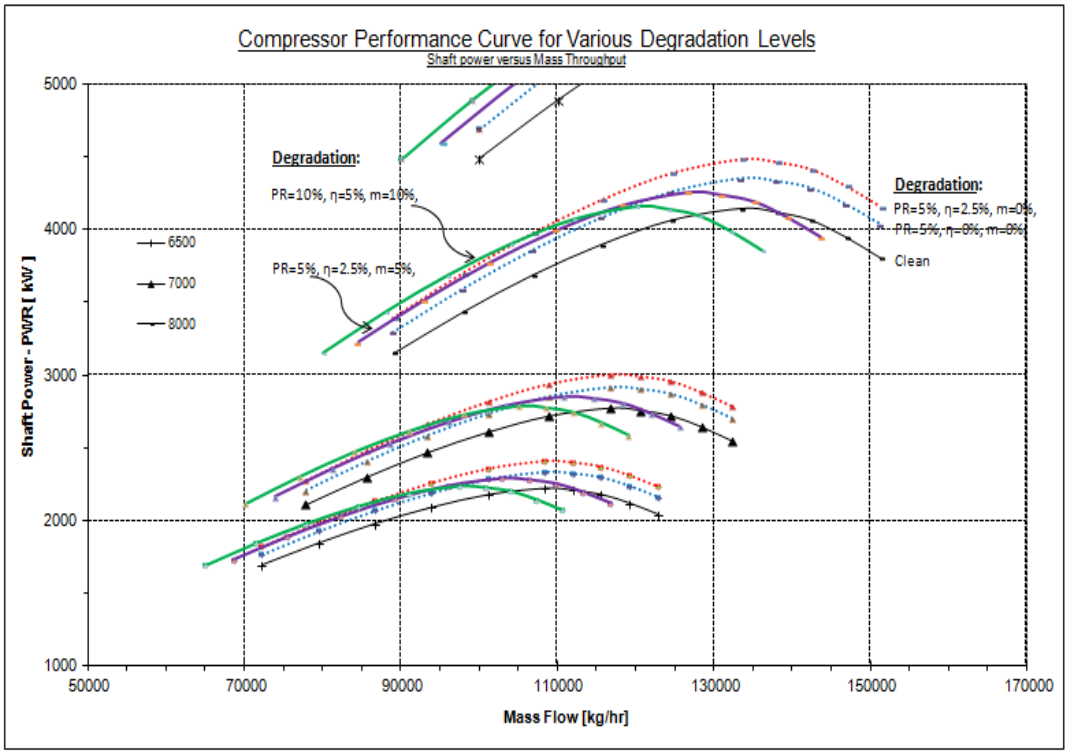

Figure 30B. The variations in gas power demand due to degradation (low speeds)

6.3 Degradation Simulation Test Case

The clean or un-degraded compressor map generated in the previous Section was fed into HYSYS in terms of polytropic heads and volumetric flows (Figure 26A). For the purpose of this work a single operating point at 100% speed is used at a predetermined (assumed) rate of degradation in flowrate and efficiency respectively with time. The head curves for the clean compressor as entered into HYSYS are shown in Figure 31. The single operating point is shown on the same Figure.

For the analysis of degradation at various speeds, HYSYS also requires the corresponding polytropic efficiencies if multiple efficiency points are to be used in the degradation analysis. By observing many compressor performance curves using advanced design tools, it is noted that the efficiency remains more or less constant, regardless of speed, except for extremely low or extremely high flowrates, in the range of which the operator is unlikely to operate to order to avoid surge or stonewall. The efficiency curves are thus generated unless actual efficiency curves are determined under compressor testing conditions. The efficiency curves for the clean compressor as entered into HYSYS are shown in Figure 32.

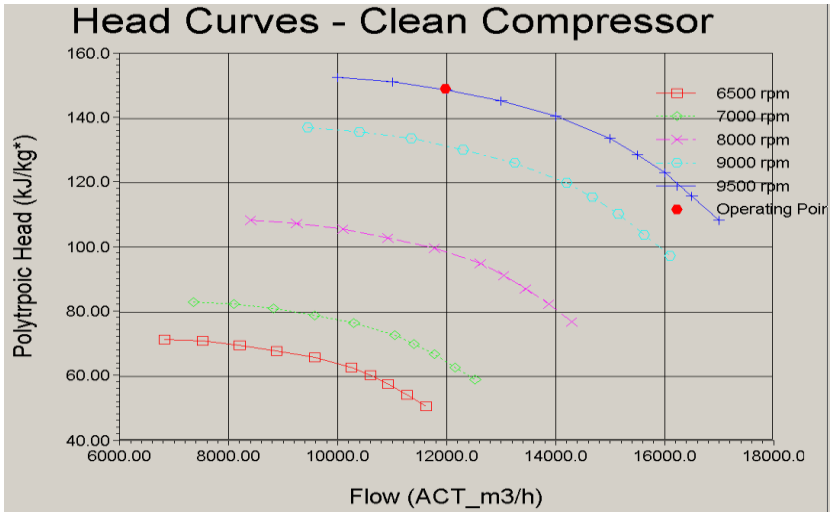

Figure 31. Polytropic Head versus Flow for clean compressor in HYSYS

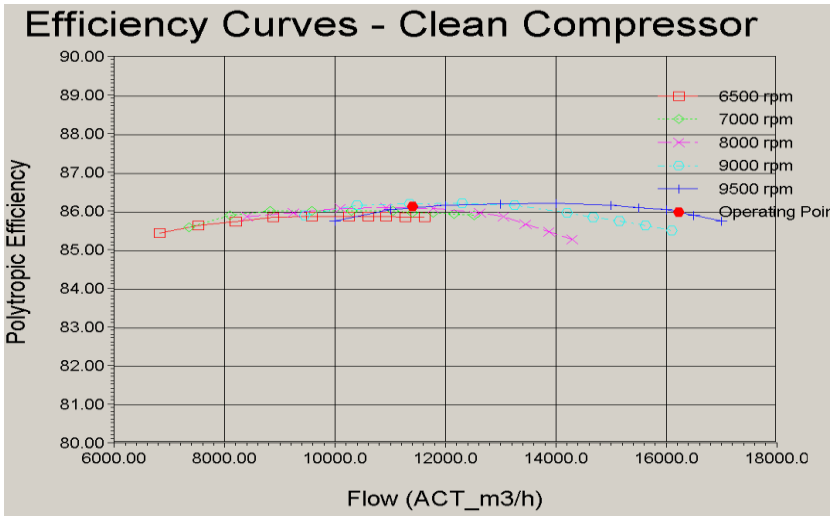

Figure 32. Polytropic Efficiency versus Flow for clean compressor in HYSYS

Once the clean compressor commences operation, the performance start to degrade and the degradation manifests itself in terms of measurable output following a characteristic trend. The rate of degradation with time may be linear or non linear. In order to investigate the effect of degradation mechanism on measurable compressor parameters, both linear and non linear degradation patterns were assumed over time.

1) A linear degradation pattern is assumed over a period of one year from a known compressor operation. Total no. of samples is 12, i.e., one taken per month. It is taken that flow capacity degrades (reduces) 5% and efficiency falls 3% over the year. This is graphically and numerically shown below in Figure 33 and Table 10A.
2) A non-linear pattern is assumed with time over the same period of 1 year from a known compressor operation. Total no. of samples is 12, i.e., one taken per month. It is taken that flow capacity degrades (reduces) 5% and efficiency falls 3% over the year. This is graphically and numerically shown below in Figure 33 and Table 10B.

The compressor inlet conditions of the throughput gas for which the HYSYS simulations were carried out is described in Table 9. Keeping the Pressure Ratio constant as an operational constraint, HYSYS was run at each degraded point as shown on Figure 33 to obtain and record the degraded discharge temperature (T_2), power (G_p) and rotation speed (N). As the compressor inlet pressure remains unaltered, constant pressure ratio implies the discharge pressure is constant.

The numerical results are tabulated in Tables 10A and 10B for linear and non-linear degradation respectively. From statistical point of view a larger number of samples would have been advantageous so that the robustness of analysis is increased using data averaging shown under Chapter 3, Section 3. From

practical point of view, however, the frequency of compressor measurements is only once in while, although there is a growing trend to increase the performance checking periods to access the compressor performance in real time. Hence 12 samples have been identified over the 1 year test period and all are used for HYSYS analysis and a larger number of samples would not have changed the trend, observations or results.

The graphical results are shown on Figure 34. Reference to this Figure, it is seen that at time 0 the compressor is taken as un-degraded or clean and at 6 month after initial operation, there is remarkable difference between the performances at this time and these differences are tabulated on Table 11. The dotted lines on Figure 34 shows the health of the compressor after 6 months of operation based on degradation indices (SF_{FC} and SF_{Eff}) discussed in Chapter 3, Section 2 earlier. It is seen from Figure 34 that at 6 months period, a 0.9% variation in power demand, corresponds to 1.5% degradation in efficiency for a linear degradation pattern. In general, it can be seen that linear degradation pattern produce nearly linear changes in measurable compressor parameters. Likewise for non-linear degradation pattern, there will be a non-linear pattern in measurable compressor parameters. Describing the current health condition by degradation indices is clearly a powerful tool which should be used for future applications as well.

Figure 35 shows the differences in measurable and non measurable compressor parameters after 6 months of operation for both linear and non linear degradation patterns taken from HYSYS. Although the final mass and efficiency degradation at the end of 1 year period are taken as the same for both linear and non-linear, it is evident that for in-between periods, each pattern of degradation induces different effects on measurable parameters.

In real field life, most degradation mechanisms are likely to be non linear and therefore more frequent operational data gathering and analysis for predictive maintenance is necessary.

6.4 Application of Scale Factors for diagnostics

Upon performance degradation, the performance curves shift to a new location on the performance maps. If an operating point on the clean performance curve can be considered, upon degradation, in the extreme sense it can be shifted in two distinctive ways until it lies on the degraded performance curve: pure vertical or pure horizontal shifting. For the map of power versus mass throughput, the horizontal shift considers no degradation (increase) in power demand and assumes the total degradation is due to the mass throughput component only. Like wise, for a pure vertical shift, until the operating point on the clean and original curve hits the degraded curve, the entire mass degradation component is taken out and it is taken that the

degradation is due to efficiency drop only. This practice is useful because it gives an estimate of the maximum shift in compressor health indicators such as mass and efficiency indices. The operator can simply take compressor measurements and estimate the current health of the compressor relative to when it was new by indirectly evaluating the drop in mass throughput and efficiency as the health indicators.

In this study, the measurements are the discharge temperature, power and speed and the compressor health indicators are mass throughput and efficiency health indices. Reference to Figure 34, the operator may take the direct measurements of discharge temperature, power and shaft speed and apply them to estimate the drop in throughput, pressure ratio and efficiency relative to when it was new which are the health indicators of the compressor.

Also in this study it is taken that:

(1) The rise in discharge temperature is primarily due to drop in polytropic efficiency, i.e., there is a relationship between the dependent (measured) parameter (temperature) rise and the independent parameter (polytropic efficiency).Or,
(2) The rise in compressor power demand is primarily due to drop in polytropic efficiency, i.e., there is a relationship between the dependent (measured) parameter (power demand) rise and the independent parameter (polytropic efficiency).

Both the above points are manifested in the pure vertical shift of the performance curve, i.e., the horizontal component (mass throughput) taken completely out. For the case of power, reference to Eq. 3-15 in Chapter 3, the power demand is directly proportional to mass and inversely proportional to polytropic efficiency. For a vertical shift, mass change due to degradation is zero and thus for constant polytropic head, the power demand rise will be due to drop in polytropic efficiency only. From Chapter 3, Section 2 earlier it was stated that:

$SF_F = FC_{deg}/FC_{cl}$
$SF_{PR}=PR_{deg}/PR_{deg}$
$SF_{Eff}= \eta_{deg}/\eta_{cl}$

In this study PR is taken as constant as an operational constraint. This leaves scaling flow and efficiency as health indicators of the compressor. Scaling the flow is straight forward since it explicitly appears on the X axis of performance curves. The drop in polytropic efficiency may be taken as a scale of discharge temperatures of degraded compressor after six months of operation over the new or clean compressor at time zero. This is the vertical component on Figures 36 and 37 and the numerical and graphical results are shown on Table 12 and Figure 40.

The drop in polytropic efficiency may also be taken as a scale of power demand of degraded compressor after six months of operation over the new or clean compressor at time zero. This is the vertical component on Figures 38 and 39 and the numerical and graphical results are shown on Table 13 Figure 41.

On comparing Figure 41 with Figure 40, it can be clearly seen that error in prediction of mass and efficiency drops are greatly reduced when power measurements are take as the basis for health indication rather than temperature increase.

Another important measurement which may lead to estimation of mass and efficiency drops as health indicators is the measurement of rotation speed variation. However, as far as speed is concerned, reference to Equations 3-18 (a) to (e), increase in speed requirement is a lump function of several variables which will need further investigations.

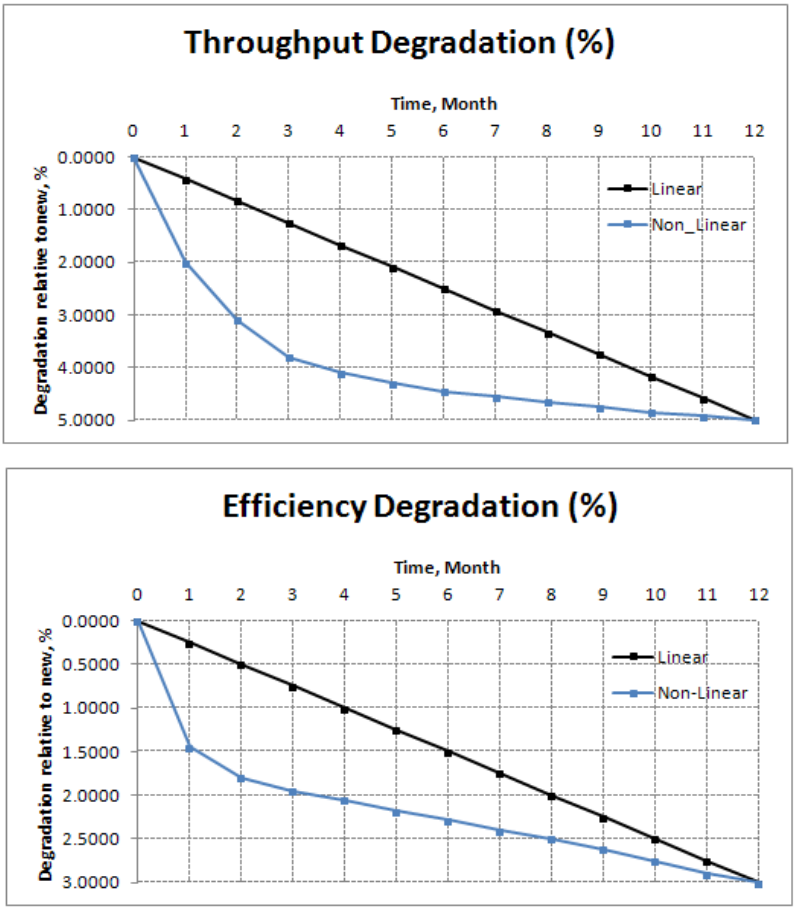

Figure 33. The throughput and efficiency degradation trend assumed over a year

Gas Properties	Gas Conditions
Mol. Weight	24.60
Suction Pressure (Bara)	10.7
Intake Temperature K	315.3
Flow (kg/hr)	125,625
Flow (MMscfd)	102.4

Table 9. Compressor inlet condition in HYSYS for degradation investigation

Compressor input for simulation							compressor simualtion output					% speed change Relative to New	% T dis change Relative to New	%PWR change Relative to New	%PR change Relative to New	
SampleTime	m deg %	SFc, fc	ṁ	η deg %	SFc,Ef	η	PR	P_2	T_2	Power	Speed					Remarks
per month	(%)	(-)	(kg/hr)	(%)	(-)	(%)	-	(bara)	(°C)	(kW)	(rpm)	-	-	-	(Constant)	
0	0.0000	1.0000	125.628	0.0000	1.0000	86.1400	3.61	38.63	136.2	6031	9500	0.000	0.000	0.000	0.000	Clean Compressor, PR constant
1	0.4167	0.9958	125.105	0.2500	0.9975	85.9247	3.61	38.63	136.4	6024	9496	0.039	0.147	0.116	0.000	
2	0.8333	0.9917	124.581	0.5000	0.9950	85.7093	3.61	38.63	136.6	6016	9492	0.083	0.294	0.249	0.000	
3	1.2500	0.9875	124.058	0.7500	0.9925	85.4940	3.61	38.63	136.9	6009	9488	0.121	0.514	0.365	0.000	
4	1.6667	0.9833	123.534	1.0000	0.9900	85.2786	3.61	38.63	137.1	6000	9484	0.171	0.661	0.514	0.000	
5	2.0833	0.9792	123.011	1.2500	0.9875	85.0633	3.61	38.63	137.3	5992	9480	0.215	0.808	0.647	0.000	
6	2.5000	0.9750	122.487	1.5000	0.9850	84.8479	3.61	38.63	137.5	5983	9475	0.264	0.954	0.796	0.000	
7	2.9167	0.9708	121.964	1.7500	0.9825	84.6326	3.61	38.63	137.7	5975	9471	0.308	1.101	0.929	0.000	
8	3.3333	0.9667	121.441	2.0000	0.9800	84.4172	3.61	38.63	137.9	5967	9467	0.352	1.248	1.061	0.000	
9	3.7500	0.9625	120.917	2.2500	0.9775	84.2019	3.61	38.63	138.2	5959	9462	0.396	1.468	1.194	0.000	
10	4.1667	0.9583	120.394	2.5000	0.9750	83.9865	3.61	38.63	138.4	5950	9458	0.445	1.615	1.343	0.000	
11	4.5833	0.9542	119.870	2.7500	0.9725	83.7712	3.61	38.63	138.6	5941	9453	0.494	1.762	1.492	0.000	
12	5.0000	0.9500	119.347	3.0000	0.9700	83.5558	3.61	38.63	138.8	5933	9449	0.538	1.909	1.625	0.000	End of control period

Table 10A. HYSYS input and output for linear degradation

Compressor input for simulation							compressor simualtion output					% speed change Relative to New	% T dis change Relative to New	%PWR change Relative to New	%PR change Relative to New	
SampleTime	m deg %	SFc, fc	ṁ	η deg %	SFc,Ef	η	PR	P_2	T_2	Power	Speed					Remarks
per month	%	(-)	(kg/hr)	(%)	(-)	(%)	-	(bara)	(°C)	(kW)	(rpm)	-	-	-	(Constant)	
0	0.0000	1.0000	125.628	0.0000	1.0000	86.1400	3.61	38.63	136.2	6031	9500	0.000	0.000	0.000	0.000	Clean Compressor
1	2.0000	0.9800	123.116	1.4500	0.9855	84.8910	3.61	38.63	137.5	6011	9490	0.110	0.954	0.332	0.000	
2	3.1000	0.9690	121.734	1.8000	0.9820	84.5895	3.61	38.63	137.8	5968	9467	0.347	1.175	1.045	0.000	
3	3.8000	0.9620	120.854	1.9500	0.9805	84.4603	3.61	38.63	137.9	5935	9450	0.527	1.248	1.592	0.000	
4	4.1000	0.9590	120.477	2.0500	0.9795	84.3741	3.61	38.63	138.0	5923	9444	0.593	1.322	1.791	0.000	
5	4.3000	0.9570	120.226	2.1800	0.9782	84.2621	3.61	38.63	138.1	5920	9442	0.609	1.395	1.840	0.000	
6	4.4500	0.9555	120.038	2.2800	0.9772	84.1760	3.61	38.63	138.2	5917	9441	0.626	1.468	1.890	0.000	
7	4.5500	0.9545	119.912	2.4000	0.9760	84.0726	3.61	38.63	138.3	5919	9442	0.615	1.542	1.857	0.000	
8	4.6600	0.9534	119.774	2.5000	0.9750	83.9865	3.61	38.63	138.4	5919	9442	0.615	1.615	1.857	0.000	
9	4.7500	0.9525	119.661	2.6200	0.9738	83.8831	3.61	38.63	138.5	5922	9443	0.598	1.689	1.807	0.000	
10	4.8500	0.9515	119.535	2.7500	0.9725	83.7712	3.61	38.63	138.6	5925	9445	0.582	1.762	1.758	0.000	
11	4.9200	0.9508	119.447	2.9000	0.9710	83.6419	3.61	38.63	138.7	5931	9448	0.549	1.836	1.658	0.000	
12	5.0000	0.9500	119.347	3.0000	0.9700	83.5558	3.61	38.63	138.8	5933	9449	0.538	1.909	1.625	0.000	End of control period

Table 10B. HYSYS input and output for non-linear degradation

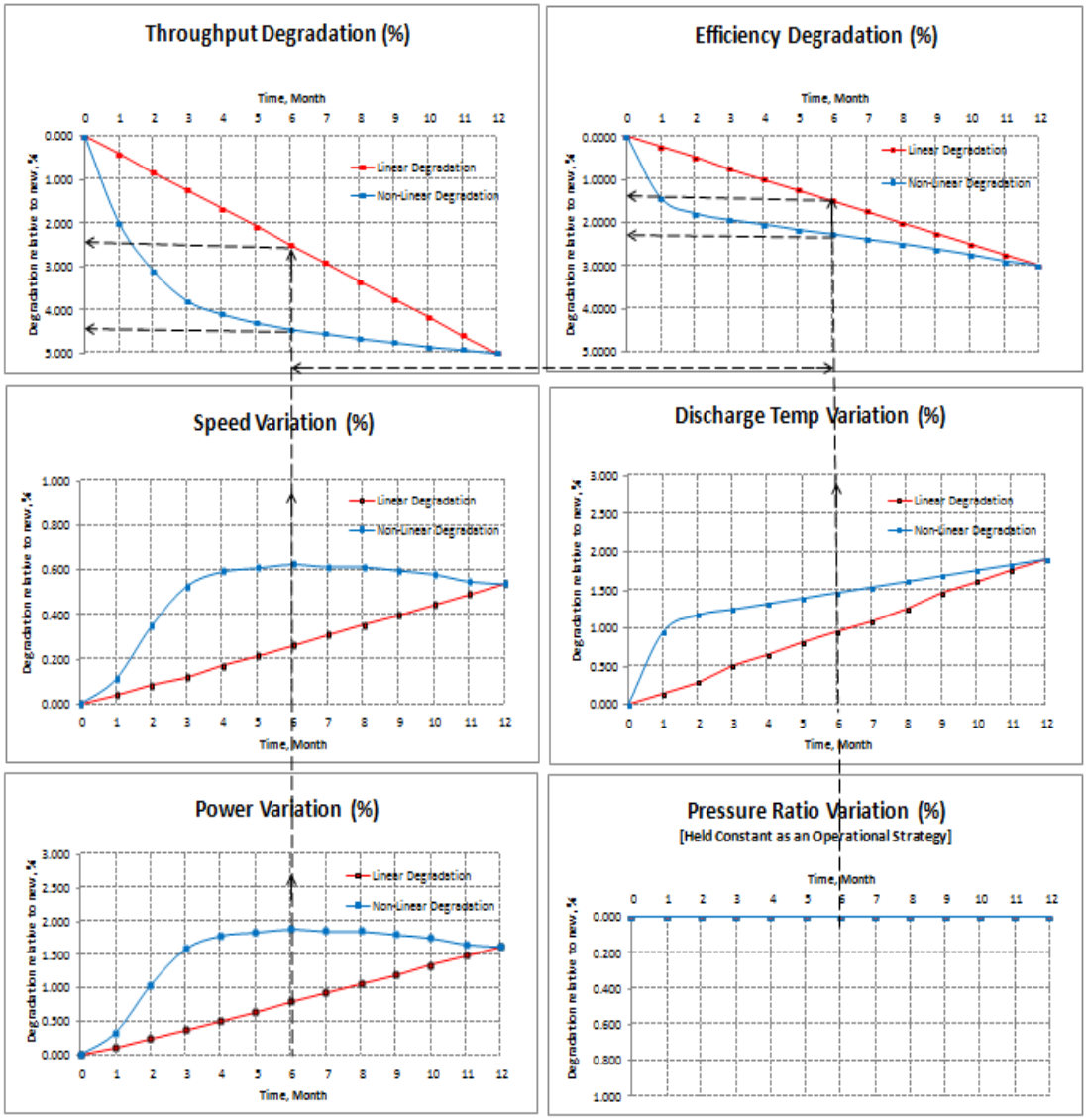

Figure 34. HYSYS input and output for linear and non-linear degradation

Parameter	Unit	Clean (time 0)	Compressor degraded "actual" measurements			
			Linear	Relative to clean	Non-Linear	Relative to clean
m	Kg/hr	125,628	122,487	-2.5%	120,226	-4.5%
η_p	-	86.1	84.8	-1.5%	84.2	-2.3%
T_2	C	136.2	137.5	+1.0%	138.2	+1.5%
N	rpm	9500	9475	+0.3%	9441	+0.6%
G_p	kW	6031	9583	+0.8%	5917	+1.9%

Table 11. HYSYS output taken as 'measurements' six month after initial operation

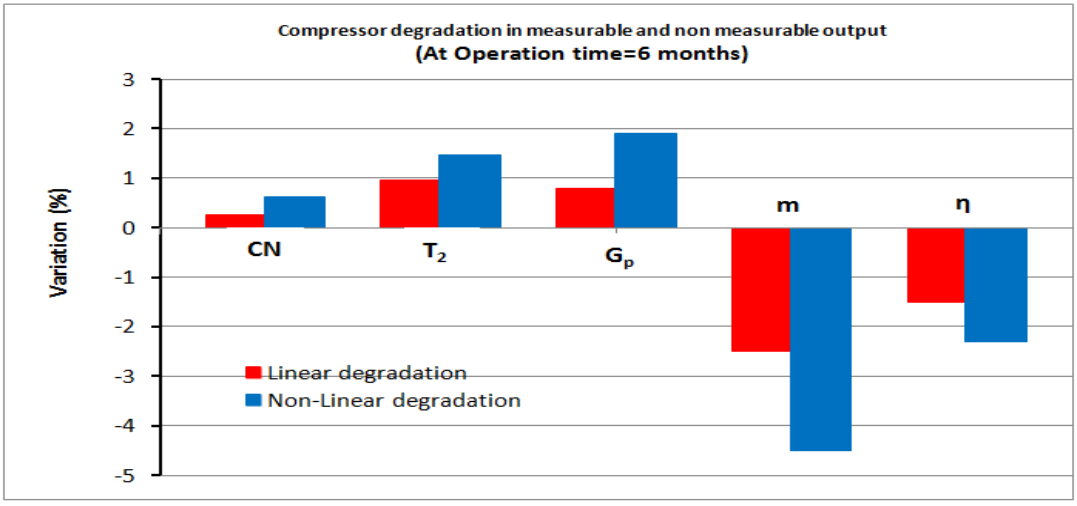

Figure 35. Comparison of 'actual' measurements for linear and non-linear degradation

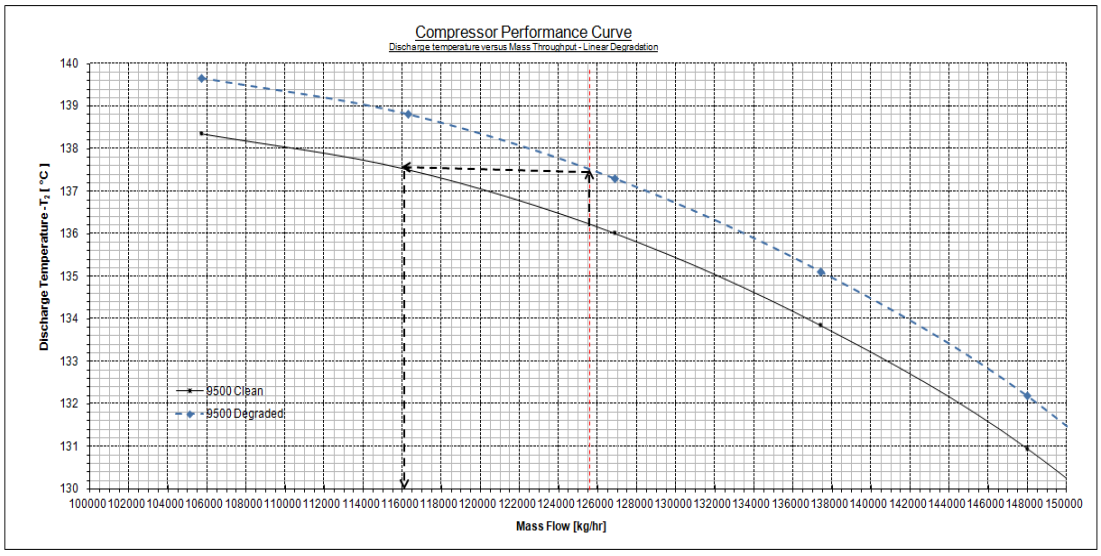

Figure 36. Performance curve (T_2 vertical/Horizontal) shift - linear degradation case

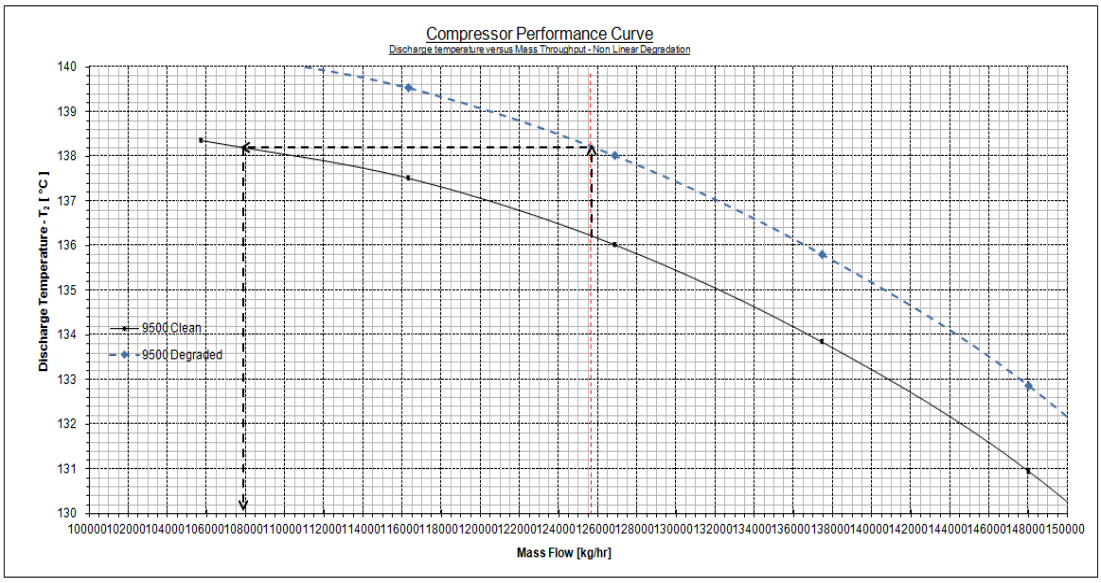

Figure 37. Performance curve (T_2 vertical/Horizontal) shift – Nonlinear degradation case

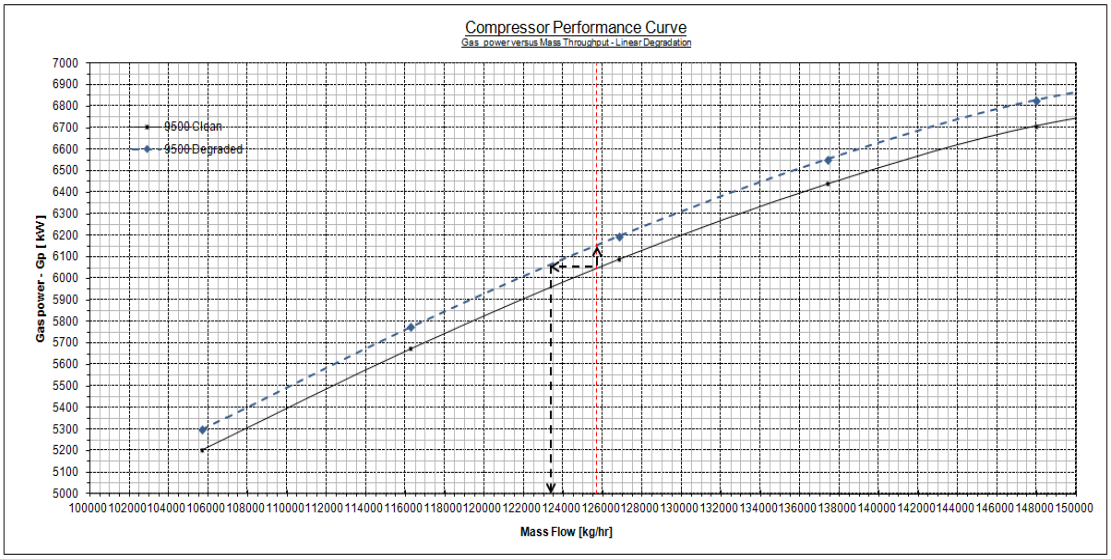

Figure 38. Performance curve (G_p vertical/Horizontal) shift - linear degradation case

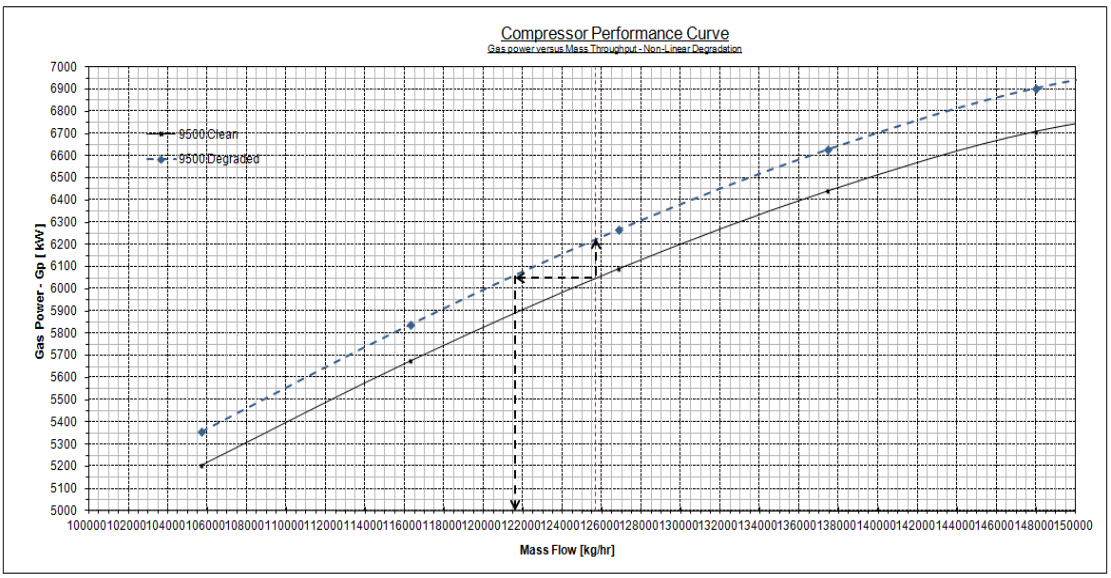

Figure 39. Performance curve (G_p vertical/Horizontal) shift - Nonlinear degradation case

Degradation	Parameter	Predicted	Actual	Unit	Remarks
Linear	m_{deg}	116,050	122,487	kg/hr	From horizontal shift on Figure 36
	m_{clean}	125,628	125,628	kg/hr	Mass flow at time 0 or clean compressor
	m_{deg}	-7.62	-2.50	%	
	$T_{2, deg}$	137.5		°C	From vertical shift on Figure 36
	$T_{2, clean}$	136.2		°C	
	$SF_{,Eff\text{-}deg}$	-0.954	-1.500	%	Discharge temp rise taken as efficiency drop (Table 11)
Non-Linear	m_{deg}	107,950	120,226	kg/hr	From horizontal shift on Figure 37
	m_{clean}	125,628	125,628	kg/hr	
	m_{deg}	-14.07	-4.50	%	Predicted thorughput degradation is maximum
	$T_{2, deg}$	138.2		°C	From vertical shift on Figure 37
	$T_{2, clean}$	136.2		°C	
	$SF_{,Eff\text{-}deg}$	-1.468	-2.300	%	Discharge temp rise taken as efficiency drop (Table 11)

Table 12. Predicted (by scaling) and Actual degradations using discharge temp. rise

Degradation	Parameter	Predicted	Actual	Unit	Remarks
Linear	m_{deg}	123,400	122,487	kg/hr	From horizontal shift on Figure 38
	m_{clean}	125,628	125,628	kg/hr	Mass flow at time 0 or clean compressor
	m_{deg}	-1.773	-2.50	%	
	$G_{p, deg}$	5983		kW	From vertical shift on Figure 38
	$G_{p, clean}$	6031		kW	
	$SF_{,Eff\text{-}deg}$	0.796	-1.500	%	Power demand rise taken as efficiency drop (Table 11)
Non-Linear	m_{deg}	121550	120,226	kg/hr	From horizontal shift on Figure 39
	m_{clean}	125,628	125,628	kg/hr	
	m_{deg}	-3.246	-4.50	%	
	$G_{p, deg}$	5917		kW	From vertical shift on Figure 39
	$G_{p, clean}$	6031		kW	
	$SF_{,Eff\text{-}deg}$	-1.890	-2.300	%	Power demand rise taken as efficiency drop (Table 11)

Table 13. Predicted (by scaling) and Actual degradations using power demand rise

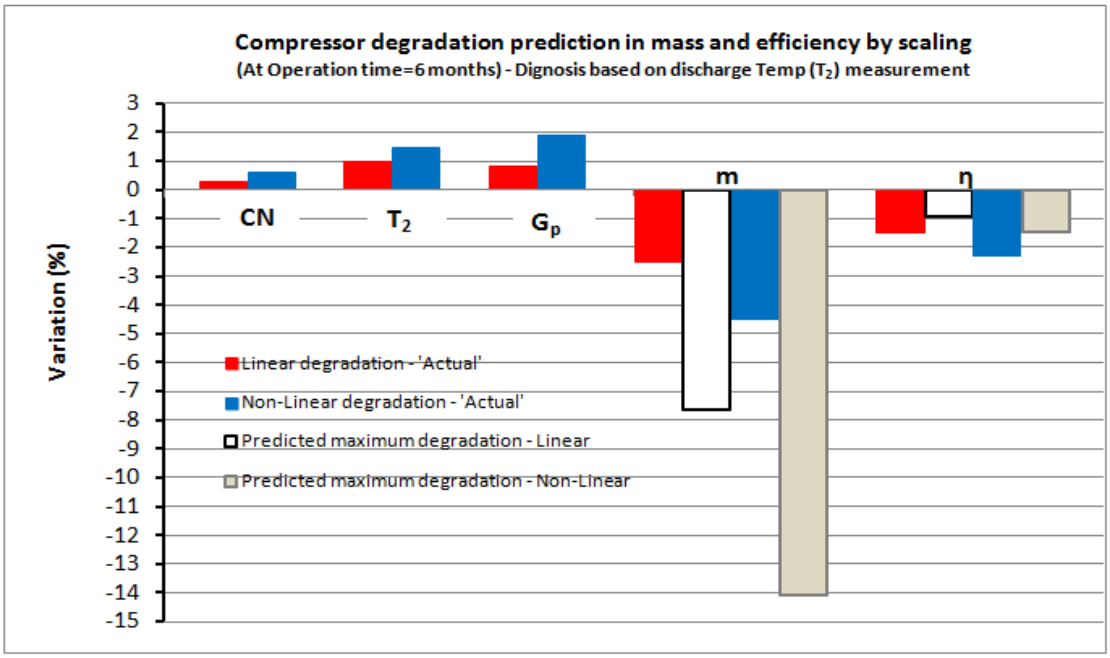

Figure 40. Compressor diagnostics based on discharge temperature measurements (Figures from Table 12)

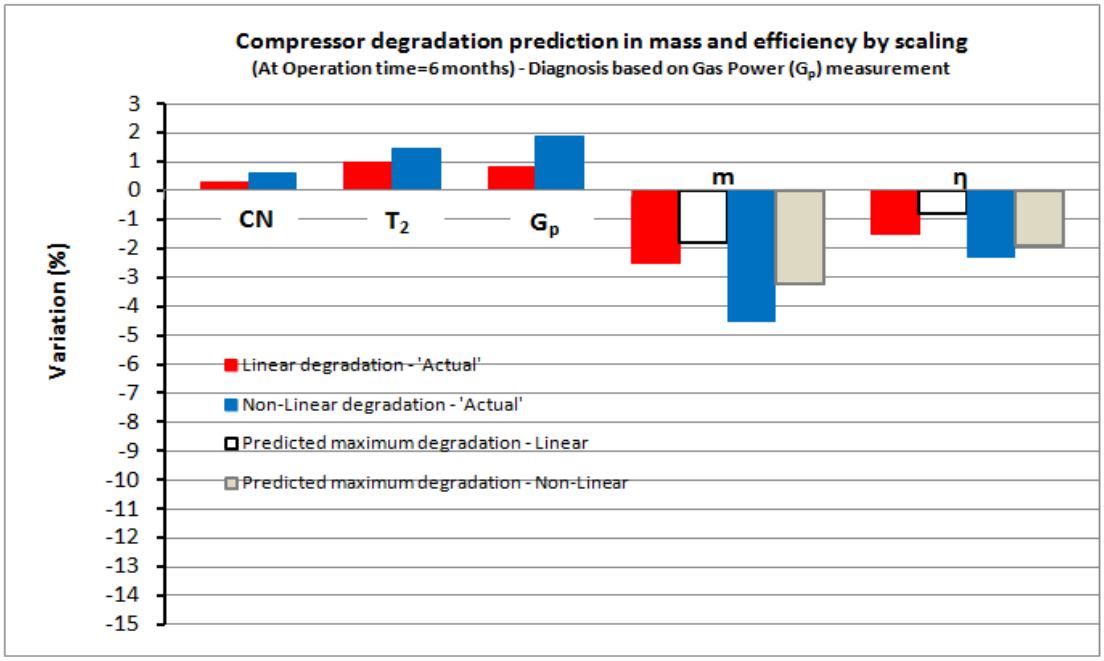

Figure 41. Compressor Diagnostics based on power measurements (Figures from Table 13)

7 Novel Scaling Method and Diagnostics Applied to Site Compressor

7.1 About Site Compressor and Instrumentation

The overview of plant is shown in Figure 42. The wet process gas form various wellhead sources get conditioned through separators and knockout drums, get compressed through 3 stages of compression so that the discharge pressure is sufficiently high enough to be transferred through pipelines to a stripping plant. The site compressor under observation is the 3rd stage compressor (14K-5201) and its position within the plant is as shown in Figure 42. A typical input/output of the compressor from the DCS (distributed control system) in the control room is demonstrated in Figure 43. The compressor model is MCL525 (Nuovo Pignone) and is powered by Solar Turbines, Mars 100 model. The compressors were put into commission in 2004 and since that time up to now there has been no compressor overhaul.

For the compressor under observation there are available measured compressor speeds, flow rates, pressure ratios, efficiencies and a host of other measureable parameters such as inlet/outlet temperatures and power consumption reported electronically to DCS as well as hand written from field instruments once every 4 hours. All the instruments are regularly calibrated with online self diagnosing (fault finding) capabilities. Although measurement noise is inevitable but its interference with sensor accuracy is minimized diminishing the reading errors.

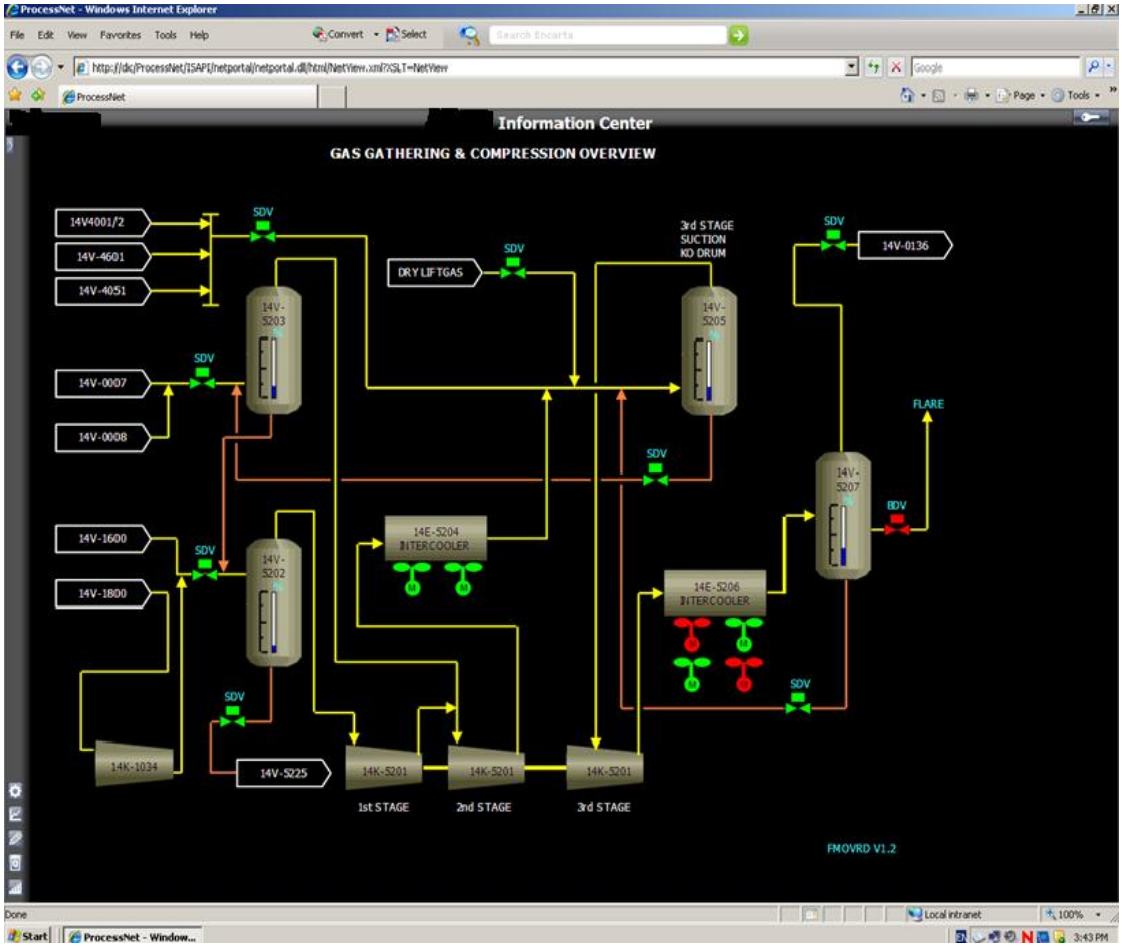

Figure 42. The gas gathering and compression overview showing the position of 3rd stage compressor within the plant

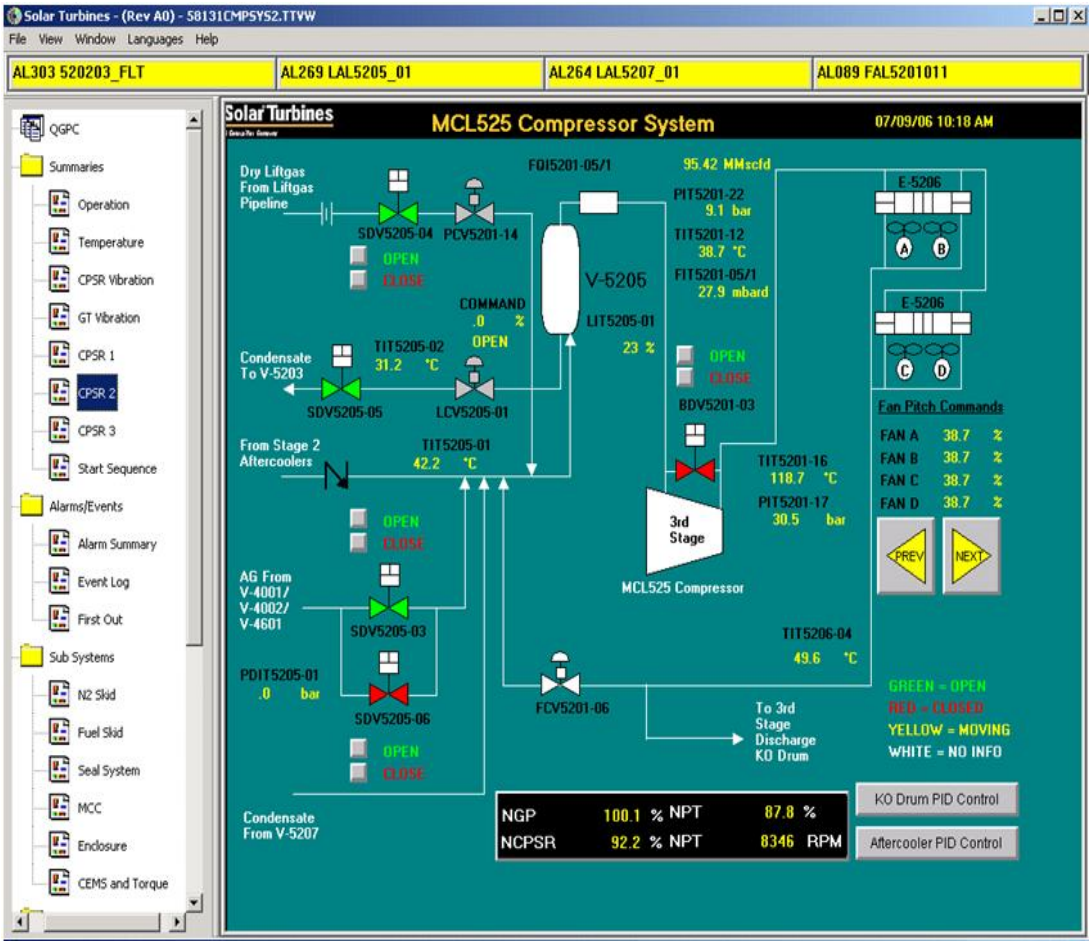

Figure 43. A snapshot of the DCS (distributed control centre) room showing the typical input and output to and from the 3rd stage compressor

7.2 Performance Adaptation by Successive Iteration

In Chapter 4 it was stated that the compressor should ideally be tested at site by OEM as early as it is moved to site and for as wide a speed range as possible in order to establish the actual site compressor performance. This performance mapping also represents the performance of a clean or un-degraded compressor. If this actual performance mapping is not done at the start of the operational life, then it should be done as early as possible. With the latter scenario, the issue here is that production has already started and the operator is already committed to deliver the process gas under predefined conditions to the downstream facilities or end users, hence testing the compressor under a wide range of speeds is difficult while on-line.

For the site, the compressor was not tested at full range of speeds at the beginning of its life to map the actual performance of the clean compressor. The earliest set of available operational data (early 2006) at various speeds (see Appendix D) were identified and treated through referring followed by successive iteration method in accordance with Chart 2 in Chapter 4 to deduce accurate performance maps of the compressor and this is shown in Graph 2. Appendix D contains the full sample calculations. Graphs 2 and 3 show the build up of performance information in pressure ratio and polytropic efficiency versus mass throughput.

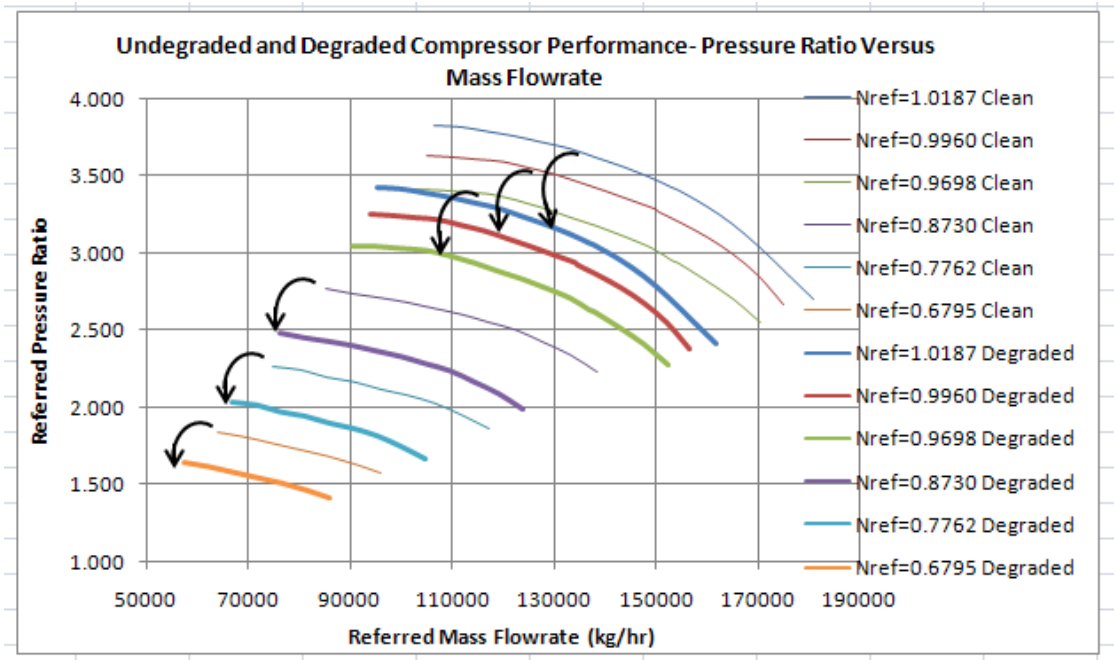

Graph 2. Performance Adaptation by Successive Iteration for Pressure Ratio (In accordance with Chart 2 and operational data and treatment in Appendix D)

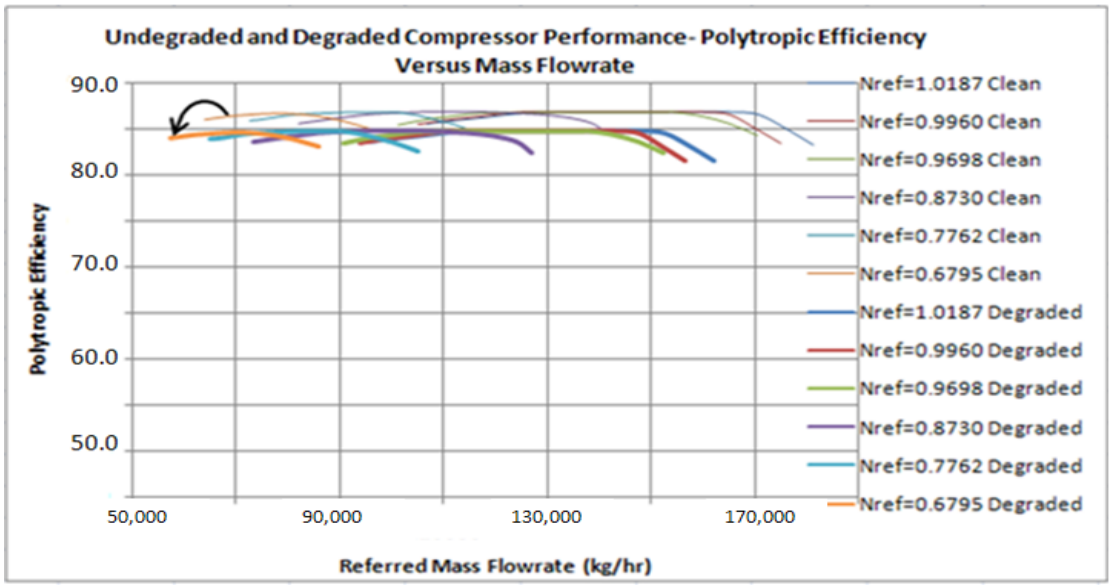

Graph 3. Performance Adaptation by Successive Iteration for Polytropic Efficiency (In accordance with Chart 2 and operational data and treatment in Appendix D)

Tables 14-19 show the expected (OEM) values and actual (site) values for compressor performance (pressure ratio, efficiency and discharge temperature). Graphs 4-66 demonstrate the errors before and after the adaptation technique for pressure ratio, efficiency and discharge temperature respectively. The analysis may be repeated for any required variable.

Referring to Graph 7, it shows the overlap of referred performance curves for varied and extreme ambient conditions (Source data taken from OEM, Table D15 in Appendix D) showing that generation of performance curves on **referred** basis are independent of varied ambient conditions demonstrating the wider application of dimensionless numbers in performance analysis. For un-referred data, performance maps do not overlap.

To summarize all the above, the site compressor data at various RPMs (Ref. Appendix D) were used in successive iteration method to generate accurate performance data (performance adaptation) in accordance with Chart 2 in Chapter 4. These adapted data were used as input block data into the simulation programme HYSYS which utilized and completed these data for the generation of polytropic heads and completion of accurate performance models. Figure 44 shows the model in HYSYS and Graphs 8 and 9 demonstrate the actual and “clean” performance curves for the site compressor in terms of polytropic head and efficiency.

Mass Flow, ref(kg/hr)	N_{ref}	OEM (-)	Site (-)	Scale Factor
150,400	0.996	3.27	2.93	0.896
140,499	0.942	2.468	2.76	1.118
122,227	0.928	2.68	2.99	1.116

Table 14. Generated Pressure Ratio Scale Factors (Appendix D for Calculation Details)

Mass Flow, ref(kg/hr)	N_{ref}	PR Site	PR_{OEM} Before Adaptation	PR_{OEM} After Adaptation	Error Before Adaptation	Error After Adaptation
150,400	0.996	3.27	2.93	3.27	-11.6%	0%
140,499	0.942	2.47	2.76	2.47	+5.8%	0%
122,227	0.928	2.68	2.99	2.68	+10.4%	0%

Table 15. Pressure Ratios Before and After Adaptation (Appendix D for Calculation Details)

Mass Flow, ref(kg/hr)	N_{ref}	OEM (%)	Site (%)	Scale Factor
150,400	0.996	84.5	86.5	1.024
140,499	0.942	84.8	87.5	1.032
122,227	0.928	86.4	86.8	1.005

Table 16. Generated Polytropic Efficiency Scale Factors (Appendix D for Calculation Details)

Mass Flow, ref(kg/hr)	N_{ref}	EFFP Site	$EFFP_{OEM}$ Before Adaptation	$EFFP_{OEM}$ After Adaptation	Error Before Adaptation	Error After Adaptation
150,400	0.996	86.5	84.5	86.5	-2.4%	0%
140,499	0.942	87.5	84.8	87.5	-3.2%	0%
122,227	0.928	86.5	86.4	86.5	-0.1%	0%

Table 17. Polytropic Efficiencies Before and After Adaptation (Appendix D for Calc. Details)

Mass Flow, ref(kg/hr)	N_{ref}	OEM (-)	Site (-)	Scale Factor
150,400	0.996	401.0	398.2	0.993
140,499	0.942	395.0	394.6	0.999
122,227	0.928	402.2	401.9	0.999

Table 18. Generated Discharge Temp. Scale Factors (Appendix D for Calculation Details)

Mass Flow, ref(kg/hr)	N_{ref}	T_{out} Site(K)	$T_{out\ OEM}$ Before Adaptation	$T_{out\ OEM}$ After Adaptation	Error Before Adaptation	Error After Adaptation
150,400	0.996	398.2	401.0	398.2	+0.251%	0%
140,499	0.942	394.6	395.0	394.6	+0.253%	0%
122,227	0.928	401.9	402.2	401.9	+0.249%	0%

Table 19. Discharge Temp Before and After Adaptation (Appendix D for Calculation Details)

The OEM supplied data for the prediction of performance is for a fleet of compressors and not the specific compressor supplied at site and it is expected that there will be differences due to manufacturing tolerances. Furthermore, the OEM supplied performance curves are based on a specific and defined set of compressor inlet and gas conditions. As soon as the actual

site conditions differ from these conditions, as they often do, direct use of OEM supplied curves become impractical for diagnostic purposes where accurate performance prediction is required. Thus a common datum or reference data must be established by the application of θ and δ such that the performance can be predicted for any inlet conditions. Also a unique iterative performance adaptation method must be devised in order to reduce the performance prediction errors. The preceding works carried out have demonstrated a successful implementation of both of these methods.

The advantages of the proposed method are that it is accurate in the prediction of compressor performance for the tested range and it can accurately predict the performance outside the tested range of speeds because of successive application of scale factors to improve the prediction of performance curves for lower speeds. The more number of test data, the more the scale factors and the accuracy of performance prediction is increased.

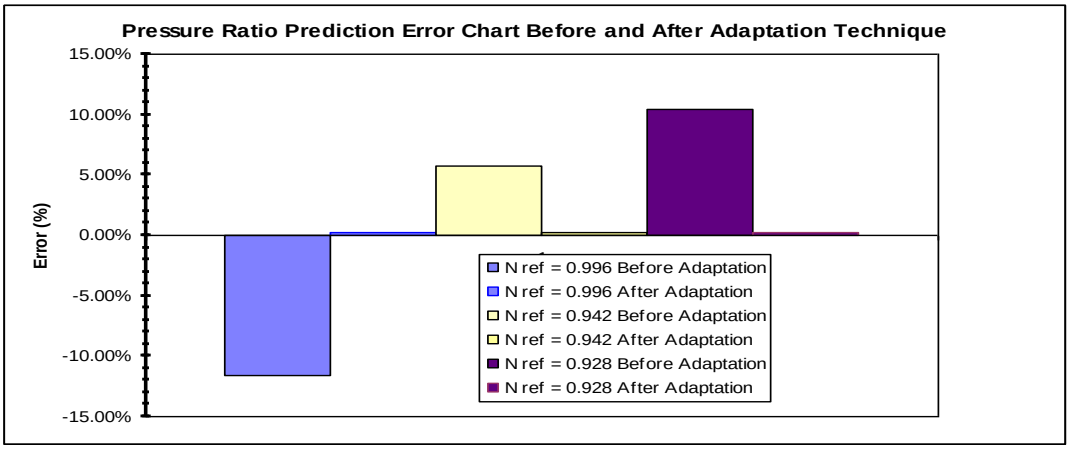

Graph 4. Pressure Ratio prediction error for three speed curves before and after adaptation technique

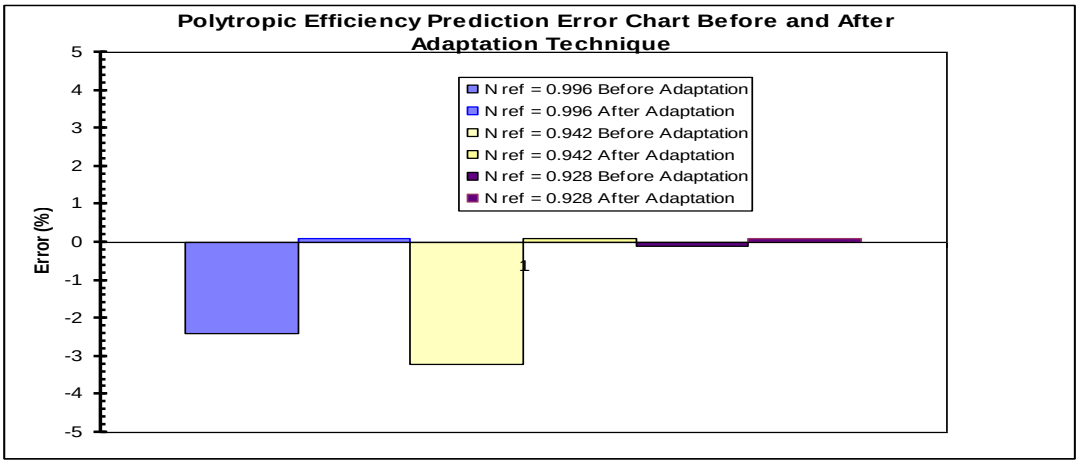

Graph 5. Polytropic Efficiency prediction error for three speed curves before and after adaptation technique

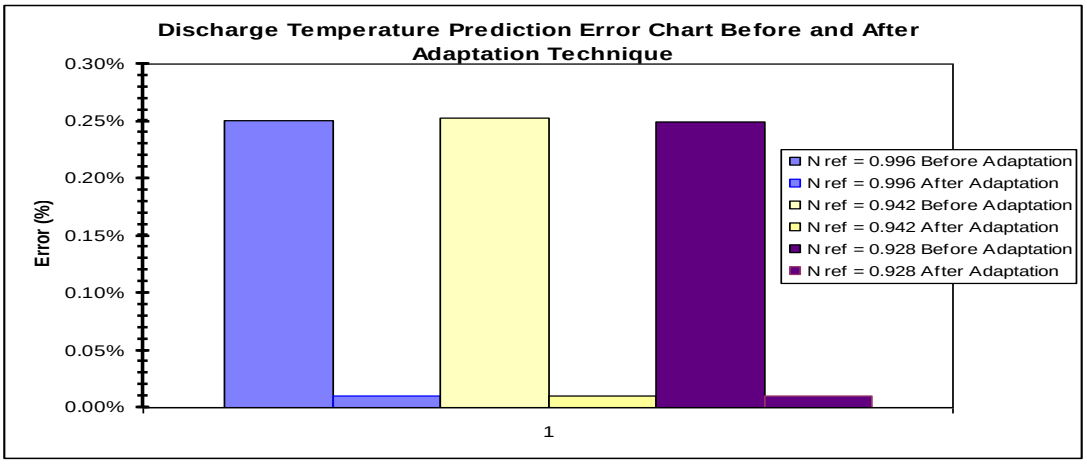

Graph 6. Discharge Temperature prediction error for three speed curves before and after adaptation technique

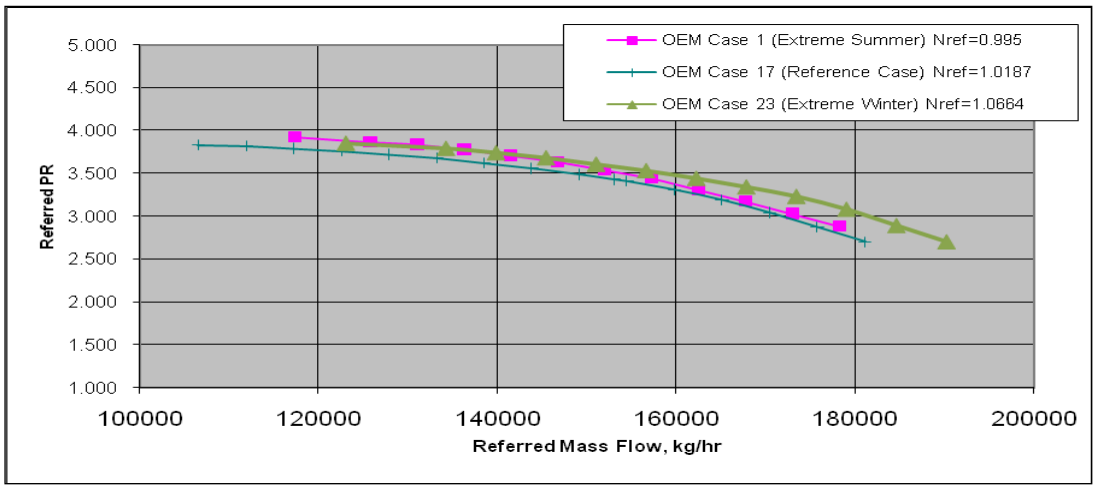

Graph 7. Referred values obtained from extreme summer and extreme winter OEM data superimposed on data derived for OEM reference case (reference Appendix D, Table D15)

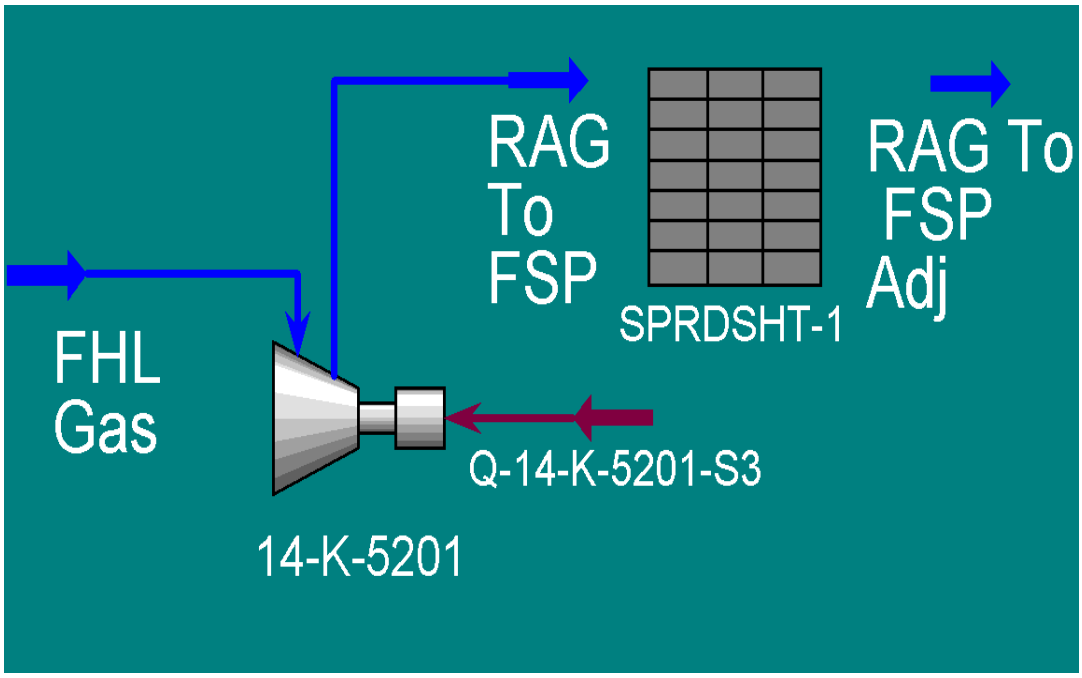

Figure 44. Site compressor simulation model in HYSYS

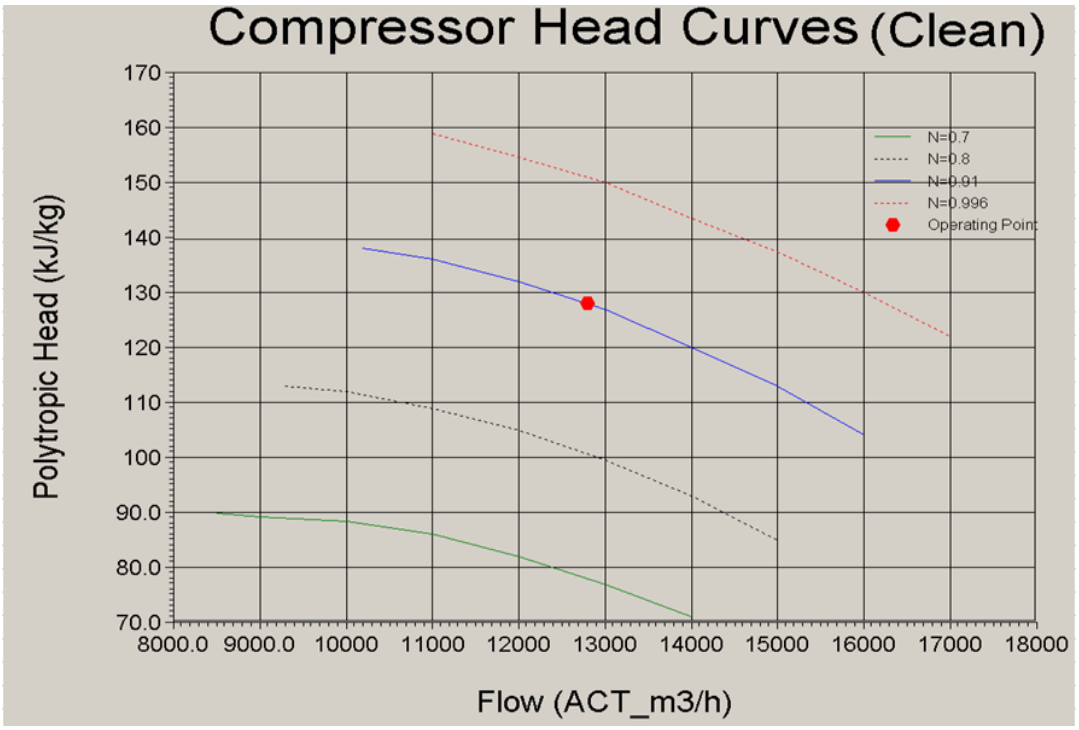

Graph 8. HYSYS performance output of polytropic head versus flow for site compressor (data input source was the performance data from the final performance map by successive iteration method (Ref, Graphs 7&8))

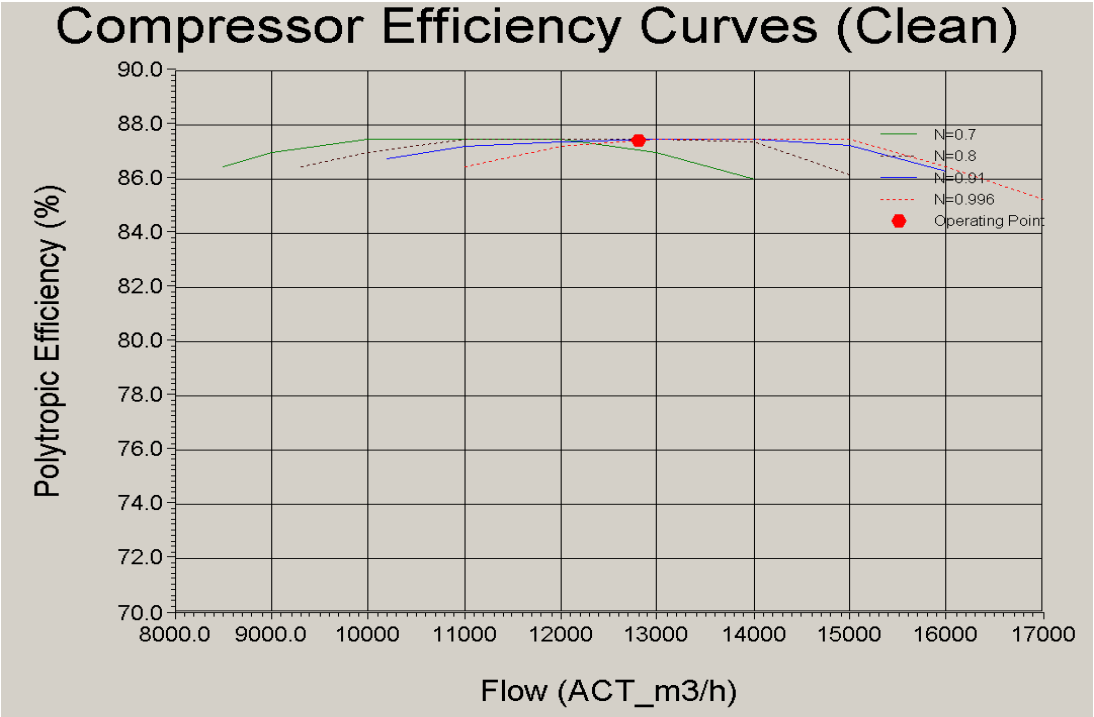

Graph 9. HYSYS performance output of polytropic efficiency versus flow for site compressor (data input source was the performance data from the final performance map by successive iteration method (Ref, Graphs 7&8))

7.3 Application of Health Estimation Methodology

It was stated in previous section that the adapted performance data generated by the innovative successive iteration method were used as input block data into the simulation programme HYSYS which complemented and utilized these data for the generation of polytropic heads and building of accurate performance models of the “clean” compressor. Figure 44 shows the model in HYSYS and Graphs 8 and 9 demonstrate the actual and “clean” performance curves for the site compressor.

It was also stated in Chapter 4 that compressor degradation is represented by the shift of the characteristic curves on the respective maps and such shifts are represented by degradation or health indices. For a compressor the primary performance indicators are pressure ratios (PR) and efficiencies while the compressor health status represented by PR, efficiency and flow capacity indices [Ref 14]. These will determine the measure of performance shift and can describe the compressor degradation. Based on these definitions, it was deduced in Chapter 4 that:

$$SF_{fl} = m_{deg} / m_{clean} \quad (1)$$

$$SF_{PR} = PR_{deg} / PR_{clean} \quad (2)$$

$$SF_{eff} = \eta_{deg} / \eta_{clean} \quad (3)$$

Where,

SF=Scale Factor
m=mass throughput
PR=Pressure Ratio
η=Polytropic Efficiency
And subscripts fl, deg and c represent flow, degraded and clean compressor respectively.

The application of compressor health estimation methodology shall be made in two steps.

In step 1, in order to separate out apparent degradation in performance from actual degradation due to environmental changes, the latter effects on performance are eliminated by the application of θ and δ.

In step 2 suitable test data will be selected to obtain the degradation index and applied to the whole map to map out the degraded performance expectation. Instrumentation errors are considered as minimal here with negligible effect on the reading accuracy as all key instruments are regularly calibrated and these instruments have self-diagnosing and fault reporting capabilities.

Step 1: Tables C1A and C1B (Appendix C(I)) refer to the new site base cases taken in 2009 and 2010 to analyze and diagnose the status and health of the compressor. Reference to Chapter 4, correction parameters (θ and δ) are used to refer the OEM and site data to a common datum such that,

Theta (θ) = T_1/ T_{ref} (Dimensionless) (4)

Delta (δ) = P_1/ P_{ref} (Dimensionless) (5)

The subscript "1" refers to compressor inlet conditions. T_{ref} and P_{ref} are arbitrary chosen values as a base temperature and base pressure upon which all the operating variables either from OEM or site are compared. It is normal to set reference values same as the most common site compressor inlet conditions for temperature, pressure and the molecular weight controlling the mass flow. For an "n" set of site cases, there will be an "n" set of Thetas (θ) and Deltas (δ).

The following are the equations used to refer the OEM and test data:

$T_{referred} = Tn / \theta$ (6)

$P_{referred} = Pn / \delta$ (7)

$m_{referred} = m * \sqrt{(\theta)} / \delta$ (8)

$PWR_{referred} = PWR/ (\delta * \sqrt{(\theta)})$ (9)

$N_{referred} = N/\sqrt{(\theta)}$ (10)

$\eta_{P,\ referred} = \eta_P / 1$ (11)

$PWR \alpha\ m\ Hp / \eta_P$ (12)

Fan laws apply, especially accurate for the small changes in our designated compressor degradation:

$Q \alpha N$, $Hp \alpha N^2$, $\ell n\ PR \alpha N^2$, $\Delta T \alpha N^2$, $PWR \alpha N^3$ (13) [Ref 28]

Where Q is the volumetric flowrate and hence mass flowrate is also proportional to speed, for the same inlet gas and environmental gas conditions. Referring to equation (8) if there is a change in molecular weight over time, then this change must be compensated when the mass flow rate is referred. HYSYS does this automatically by clicking the available radio button on the compressor input data tab.

Tables C2A and C2B (Appendix C(I)) demonstrate converting the data in Tables C1A and C1B (Appendix C(I)) to referred values by the application of

Theta (θ) and Delta (δ) through choosing T_{ref} and P_{ref} as 315.3 K and 1070 kPaa respectively with a base line molecular weight of 24.6. These values are the most common inlet conditions of the compressor.

STEP 2: Referring to Base Case 5 of Table C2A in Appendix C(I) which are the referred site measured parameters in August 2009 and referring to the compressor actual performance map deduced for 2Q 2006 (solid lines of Graphs 15 and 16, obtained by performance adaptation described in the previous section),

Using Equation (2) above:

$SF_{PR} = PR_{deg} / PR_{clean}$

PR_{deg}= 2.82 (Base Case 5 of Table C2A, Appendix C(I))

PR_{clean}= 3.10 (The earliest treated performance data presently available for the compressor back in 2Q 2006 and these were used for performance adaptation model by successive iteration method and these are shown on graphs 13, 14, 15 and 16)

Therefore the scaling factor using Equation 2 above for pressure ratio is:

$\underline{SF_{PR} = 2.82 / 3.1 = 0.9097}$ (14)

In order to fix a point on the performance map, at least 2 points are needed. We have obtained The degraded Pressure Ratio has been obtained, how about degraded mass throughput?. The degradation in mass flow rate cannot be directly measured but it is recalled that fan laws apply and are accurate especially for small changes of parameters. Using relationships equation (13) above:

$\ell n\ PR \alpha N^2$ or $PR \alpha \exp(N)^2$

and $Q \alpha N$

This implies: $PR_1 / PR_2 = \exp(N_1)^2 / \exp(N_2)^2$

$3.10 / 2.82 = \exp 0.85^2 / \exp (N_2)^2$

Therefore $\underline{N_2 = 0.793}$

The above shows that, had the compressor has stayed clean, it should have achieved the PR of 2.82 with a referred speed of 0.793. But with reference to Base case 5 of Table C2A in Appendix C(I), the compressor under observation was actually achieving the stated PR of 2.82 with the higher referred speed of N_{ref}=0.88. The increase in speed requirement, and therefore the increase in power draw by compressor is due to degradation.

Since Q α N, deterioration in throughput is equivalent to increase in speed to achieve the target PR, i.e.

$SF_{fl} = m_{deg} / m_c$ (Equation 1 above)

$SF_{fl} \equiv N_{deg}/N_{clean} = 0.793 / 0.88 = 0.9011$ (15)

Now the two points that fix the shift on the performance map of PR versus mass throughput are known and the whole map is shifted as follows using scale values obtained in (14) and (15) above respectively:

Pressure Ratio degradation (vertically downward on the performance map) by (1-0.9097) x 100% = 9.03%

Throughput degradation (horizontally leftward on the performance map) by (1-0.9011) x 100% = 9.89%

Thus the mass throughput and PR has deteriorated about the same amount and by 9-10% each.

As it was referred earlier in Chapter 4.1, as an alternative to the use of Fan laws described above, the curve of test point A (clean performance) on Graph 10 below can manually be shifted until it hits point B (degraded performance) and in this manner the degradation mass throughput is implicitly solved.

The degradation indices for Pressure Ratio and flow are now obtained as shown above (0.9097 for SF_{PR} and 0.9011 for SF_{fl}) and the performance maps can be shifted accordingly. This is shown in Graph 10 below. Reference to Figures 24 and 25, it is found that the shift angle is around 45° as the degradation in both directions (down and left) are almost the same. It is expected that the shift angle increases with the time interval of analysis. The smaller the time gap between analysis, the smaller the shift angle and the more accurate the analysis as the shift trend will be built up on regular intervals.

Similar as in PR calculations, but for polytropic efficiency:

$SF_{eff} = \eta_{deg} / \eta_{clean}$ (Equation 3 above)

η_{clean} = 87.0% (“Clean” compressor, from 2Q 2006 records)

η_{deg} = 84.1% (“Degraded” compressor, from August 2009 records, Appendix C(III)-Table C2A)

Therefore, the scale factor for efficiency is

$SF_{eff} = 84.1/87.0 = 0.9670$

Thus the degradation in polytropic efficiency is (1-0.967) x 100% = 3.3%

The degradation of mass throughput for efficiency curves is expected to be the same as for pressure ratio because the same compressor applies. Refer to Graph 11 below for the shifted efficiency curve of the site compressor.

The methodology and application above is an improvement to the works already carried out by others [Ref 14], where the degradation in PR is assumed to be same as that for throughput. In this work, these degradations have been estimated by the application of affinity (Fan) laws.

It is to be noted that the compressor degradation under investigation is less pronounced in efficiency (3.3%) than in pressure ratio (9.0%) and in mass throughput (9.9%). The degradation has had more effect on pressure ratio and mass throughput. The effect on both pressure ratio and mass throughput are about the same. An important realization here is that the downward shift combined with shifting to the left results in **narrower surge margins** built in design. If surge margins are exceeded, the compressor may be damaged in a short time. There are strict controls to avoid surge by mounting an Anti-Surge Valve between the discharge and inlet to the compressor. However, the operator must realize that compressor degradation results in surge settings change, therefore the operator should be in a position the change the valve settings in accordance with the compressor operation, online.

Reference to Graph 10 below, as it was described earlier in this section, to evaluate the search space or extreme solution for entirely vertical drop or an entirely horizontal shift of the performance curve to the left, the performance curve on which point “A” is situated is dropped vertically downward until it his point B. Thus it is noted from Graph 10 that in the case of entirely vertical drop a PR of 2.63 is achieved (a scale factor of 0.85) or 15.0% degradation and similarly in the case of purely horizontal shift to the left, an m of 107,000 kg/hr is obtained (a scale factor of 0.823) or 17.7% degradation.

Thus in a vertical map fall, degradation in m=0 & degradation in PR=15.0%.
In a horizontal shift left, degradation in m=17.7% & degradation in PR=0.0%.

Therefore the search space for degradation in PR is anywhere between 0 to 15% and degradation in mass throughput is anywhere between 0 to 17.7%.
As shown above, using real site data and applying proportionality (Fan) laws a diagonal shift is experienced with degradation in m=9.9% and degradation in PR=9.0%.

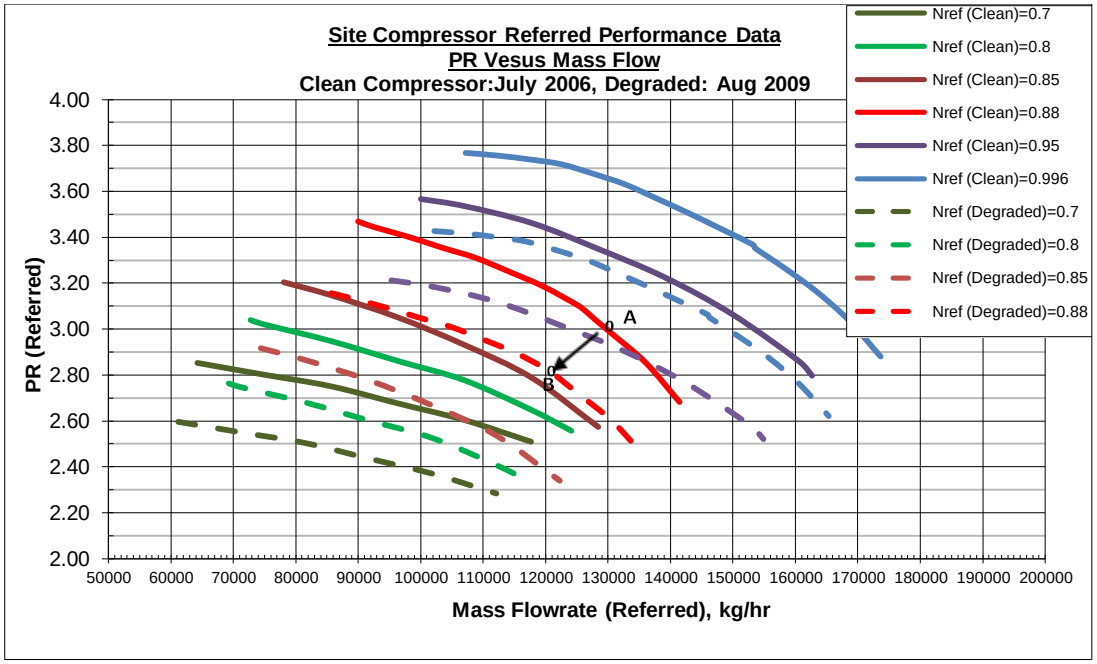

Graph 10. Site compressor characteristic map modification (PR shift) due to degradation

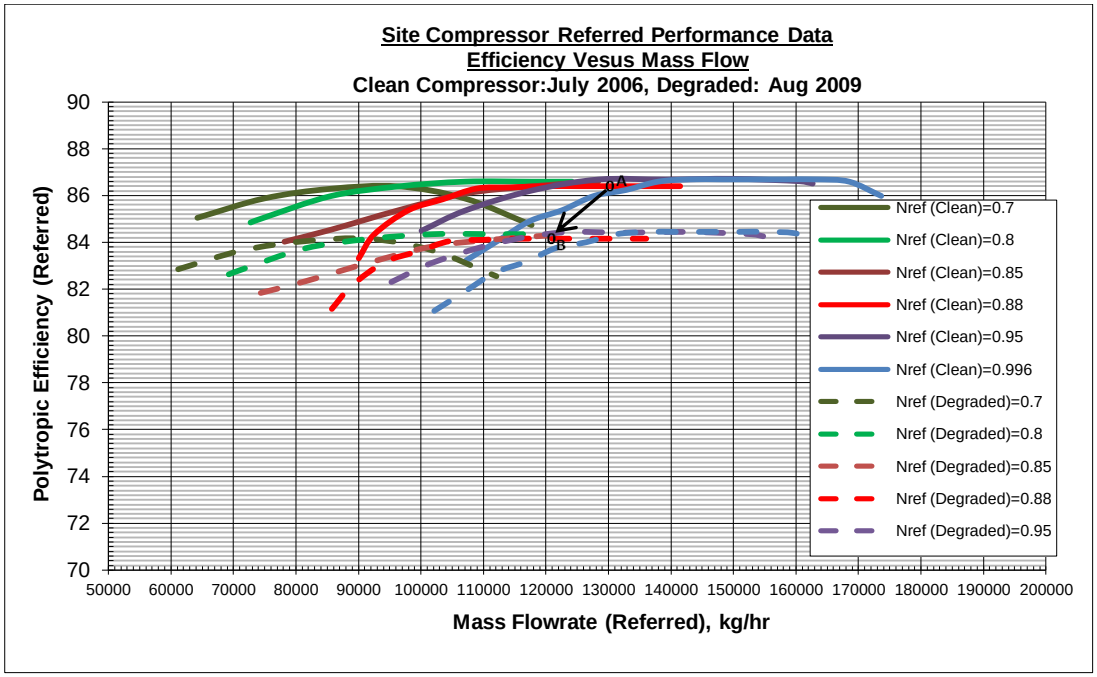

Graph 11. Site compressor characteristic map modification (Efficiency shift) due to degradation

7.4 GPA Index Calculations

It was stated in Chapter 5, Section 2 that evaluation of GPA Index for a particular diagnostic application is a powerful indicator of estimation success. It was stated that a GPA Index approaching 1 indicates a very accurate degradation prediction while a GPA Index close to 0 means the other way around.

Using the formulas shown in Chapter 5 as follows:

GPA index = 1/(1+ε)

Where ε is a measure of the difference between the measured and predicted deviations of compressor gas path measurements and it is mathematically expressed as:

$$\varepsilon = \frac{1}{N}\sum_{i=1}^{N}\left|\frac{\Delta z_{i,measured}}{z_{i,measured}} - \frac{\Delta z_{i,predicted}}{z_{i,predicted}}\right|$$

$\Delta Z_{i,\ measured}$ / $Z_{i,\ measured}$ and $\Delta Z_{i,\ predicted}$ / $Z_{i,\ predicted}$ are the measured and predicted deviations of measurement Z_i, respectively.

Applying the above equations to the site compressor data in Appendix C(I), ε which is a measure of the difference between the measured and predicted deviations of compressor gas path measurements and GPA Index are calculated for each case.

Table 20 shows the GPA Indices for the site compressor based on the developed performance adaptation methodology. Since they are very close 1, the methodology is considered to be accurate. In fact, the application of GPA Indices has proven very effective in compressor diagnostics with an average indices figure of 1.03 and variance of 0.003 over the last 4 years period.

Time: July-Aug 09 (Appendix C(I))

		Pressure Ratio				
Case	N_{ref}	Predicted	Measured	ε	GPA Index	Remark
1	0.85	2.43	2.71	-0.1033	1.1152	
2	0.87	2.80	2.76	0.0145	0.9857	
3	0.88	2.69	2.70	-0.0037	1.0037	
4	0.84	2.40	2.78	-0.1367	1.1583	
5	0.88	2.82	2.82	0.0000	1.0000	(Design Case)

Time: Apr-10 (Appendix C(I))

		Pressure Ratio				
Case	N_{ref}	Predicted	Measured	ε	GPA Index	
1	0.90	2.83	3.01	-0.0598	1.0636	
2	0.90	2.80	3.05	-0.0820	1.0893	
3	0.88	3.00	3.00	0.0000	1.0000	(Design Case)
4	0.91	3.02	3.21	-0.0592	1.0629	
5	0.91	3.02	3.20	-0.0563	1.0596	
6	0.90	2.83	3.02	-0.0629	1.0671	

Time: Apr-10 (Appendix C(I))

		Efficiency				
Case	N_{ref}	Predicted	Measured	ε	GPA Index	
1	0.84	84.0	82.0	0.0244	0.9762	
2	0.87	84.2	82.0	0.0268	0.9739	
3	0.88	83.9	81.8	0.0257	0.9750	
4	0.84	84.0	85.8	-0.0210	1.0214	
5	0.88	84.1	84.1	0.0000	1.0000	(Design Case)

Table 20. GPA Indices for the site compressor based on the developed performance adaptation methodology

7.5 Establishment of Degradation Indices for the Site Compressor and Data Trending

As stated in Sections 4.1, the Degradation Indices for Pressure Ratio and Polytropic Efficiency are:

$SF_{PR}=PR_{deg} / PR_{clean}$, and,

$SF_{eff} = \eta_{deg} / \eta_{clean}$

Applying the above to the site compressor data (Appendix C(II)), the degradation indices are calculated for both pressure ratio and polytropic efficiency through time. Table 21 is thus obtained and the respective trends for pressure ratio and efficiency are plotted on Graph 12 and Graph 13.

		Pressure Ratios			Polytropic Efficiency		
Compressor Case*	Date	Clean	Dirty	SF (PR)	Clean	Dirty	SF (EFF)
1	13/06/2006	3.26	3.26	1.0000	87.50	87.50	1.0000
8	07/09/2006	3.16	2.91	0.9209	87.30	87.00	0.9966
20	06/07/2009	3.42	2.90	0.8480	87.04	85.00	0.9766
29	06/04/2010	3.67	2.86	0.7793	87.12	81.00	0.9298
33	24/08/2010	3.62	2.72	0.7514	86.96	80.00	0.9200

Table 21. Establishments of degradation indices for the site compressor (*refer to Appendix C(II) for site data source)

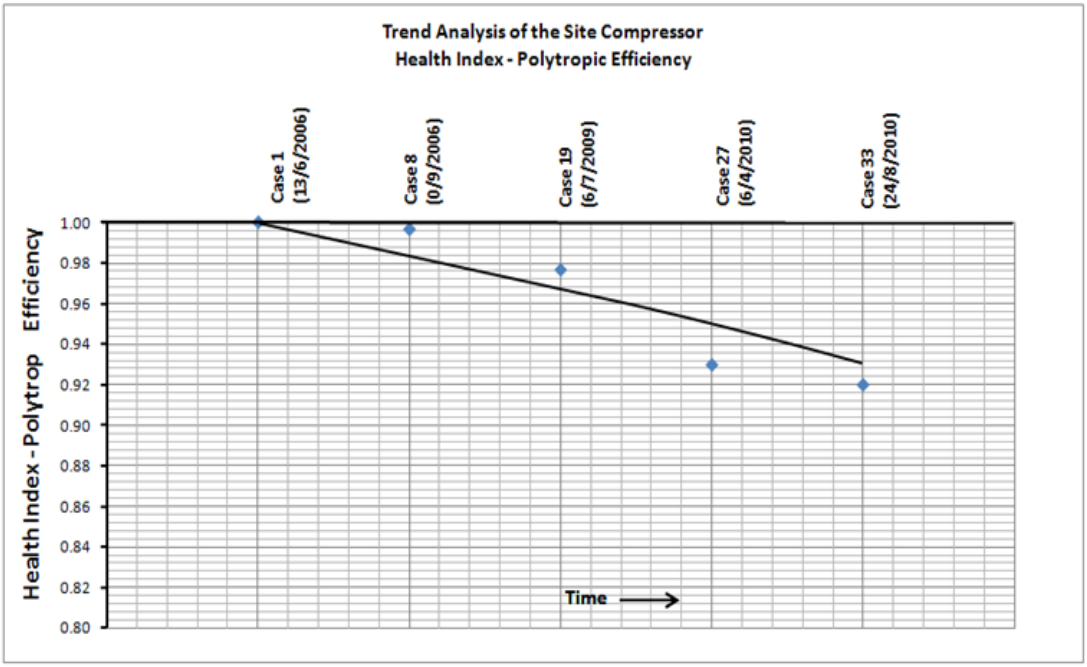

Graph 12. Derived PR degradation index versus time for the site compressor

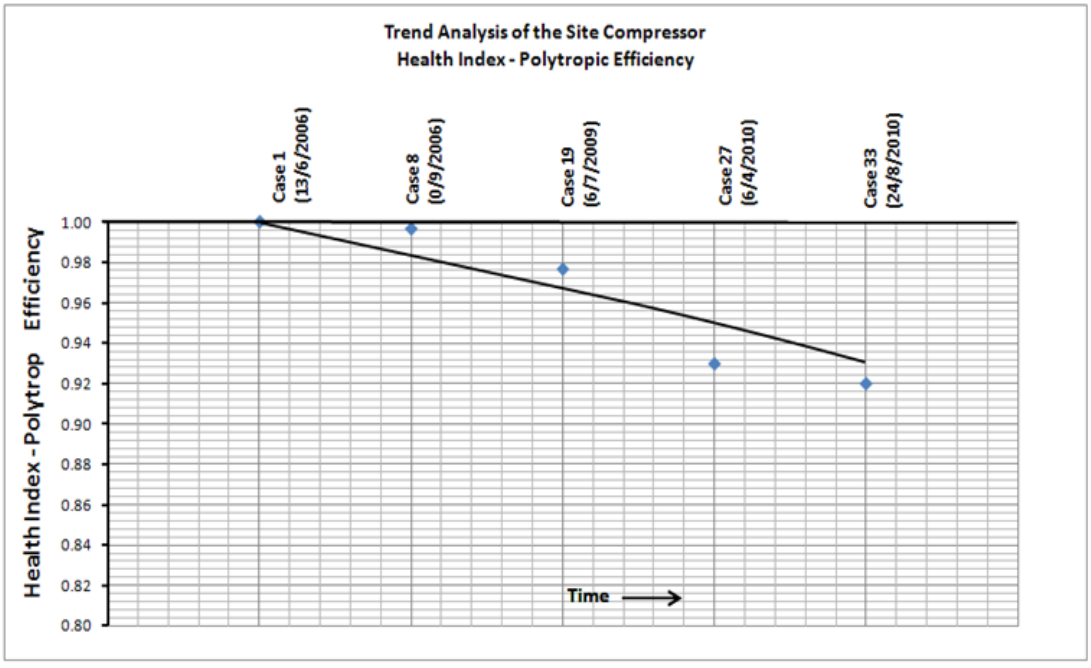

Graph 13. Derived efficiency degradation index versus time for the site compressor

7.6 Health trend generation for the site compressor

Due to the performance deterioration of compressor, the “expected” performance value is not a constant and changes with time. It would not be correct to assume a constant base line for establishing the compressor’s health status. It would thus be necessary to set a trend for the expected deterioration in performance, either from OEM before moving the compressor to site as described in Chapter 4, Section 4 or from performance observations at site over time. For the site compressor under investigation, OEM was not requested to produce the expected trend. However, the fall in efficiency over time has been established [Ref. Appendix C(I, II)] for the compressor and this is shown on Graph 14. Taken the expected trend in efficiency profile follows as shown on the referred Graph, then it is established that the expected efficiency trend is a polynomial fit and the equation is shown on Graph 15, with “Y axis” representing the expected efficiency and “X axis” representing operational time. On these bases, the equation may be used for diagnostic or prognostic purposes. Depending on how the compressor is performing, the actual trend could be having a smaller slope, meaning the compressor is doing better than expected or the slope could be steeper than the established curve fit meaning the compressor condition is deteriorating faster than expected (see Graph 15). In either case, the maintenance schedule or partial/full overhaul can be adjusted to suit the actual condition of compressor. Only by on-line monitoring or frequent evaluation of health indices could establish the compressor performance trend.

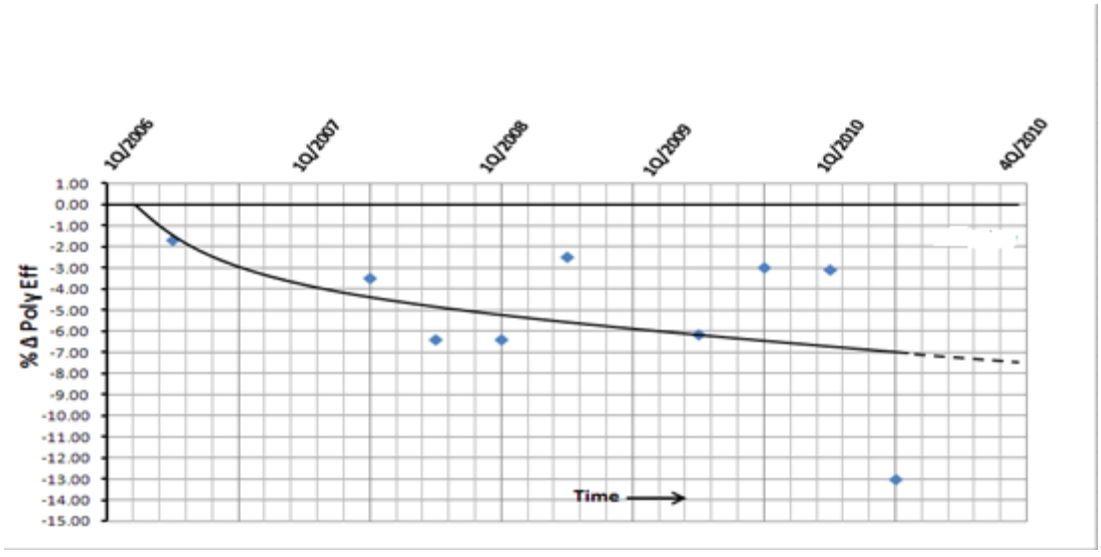

Graph 14. Trend Analysis of the Site Compressor: Degradation in Efficiency versus Time

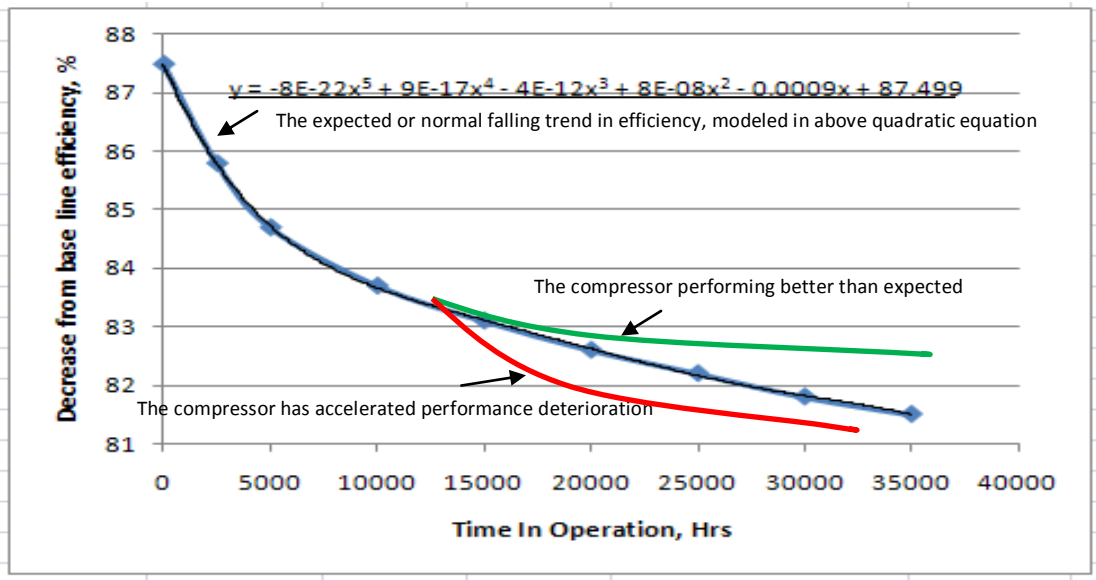

Graph 15. Site compressor efficiency degradation modeling to indicate the expected fall in performance

7.7 Sensitivity Analysis

It was referred in Chapter 5, Section 3 that compressor degradation does not have equal effect on measurable parameters variables. It is important to recognize which variables are sensitive and which ones are insensitive to degradation so that maintenance items and schedules are classified accordingly. Furthermore the nature of relation (linear or non linear) between degradation and compressor dependent variables is critical to be established so that the future behaviour can be estimated by extrapolation.

Using the advanced simulation programme HYSYS, Graphs 16-22 were obtained to show the effect of degradation, neglecting geometrical changes as a result of degradation, on measurable parameters. The analysis of these graphs show that the trend effect of increasing degradation levels in compressors on measurable parameters is fairly linear and that variations in performance as a result of degradation is not independent of the compressor speed meaning degradation do not have the same effect on performance parameters at high speeds compared at low speeds. It shall be noted that the graphical sensitivity analysis shown on Graphs 16-22 are based on thermodynamic changes only and do not consider any geometrical, or shape changes. For a detailed analysis, in addition to thermodynamic considerations, CFDs should also be engaged in modeling the detailed and accurate geometries of the compressor.

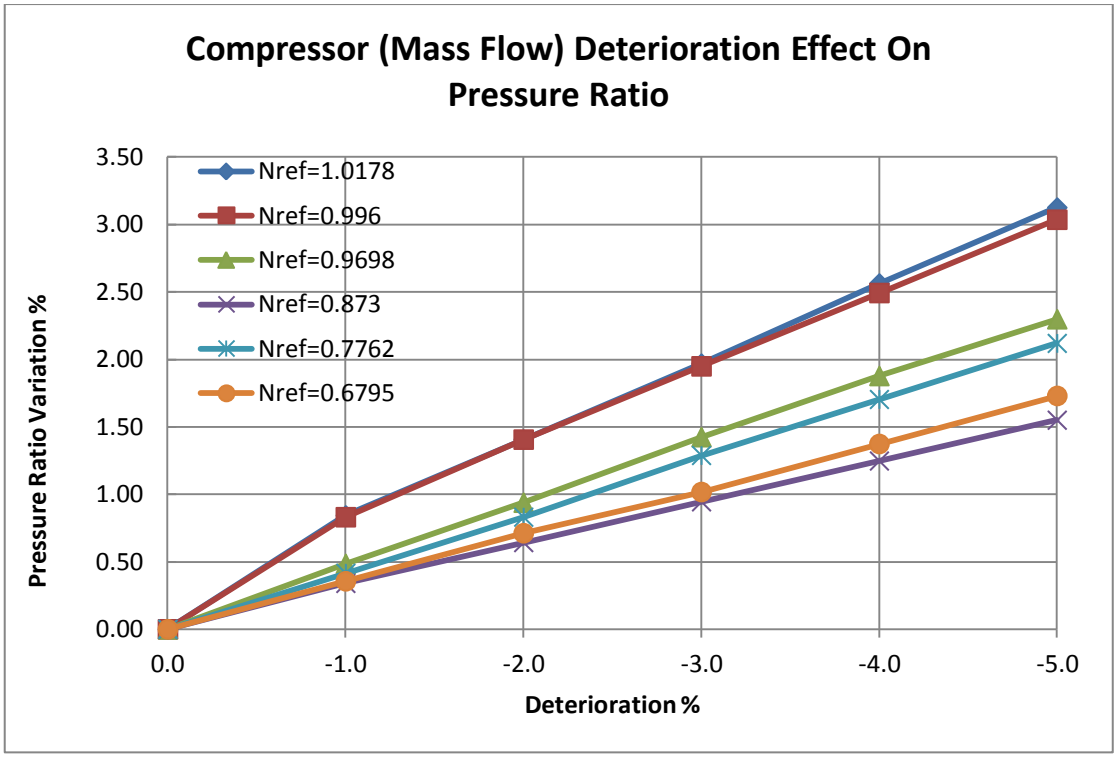

Graph 16. Compressor (Mass Flow) Deterioration Effect on Pressure Ratio

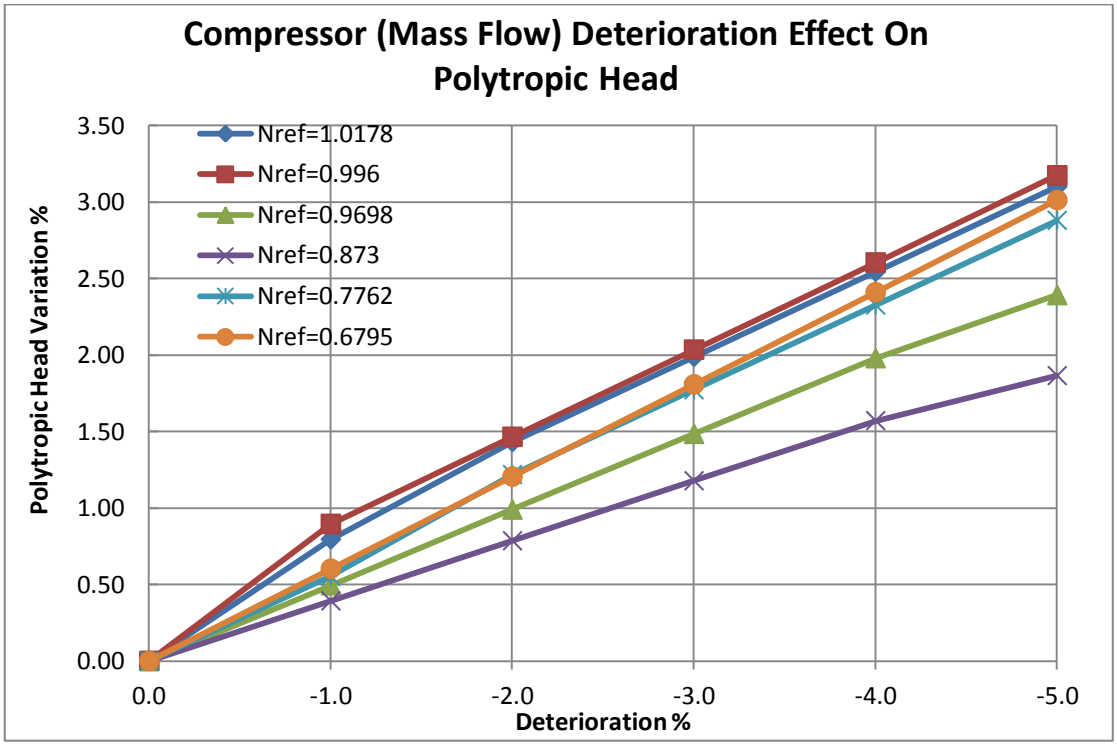

Graph 17. Compressor (Mass Flow) Deterioration Effect on Polytropic Head (Hp)

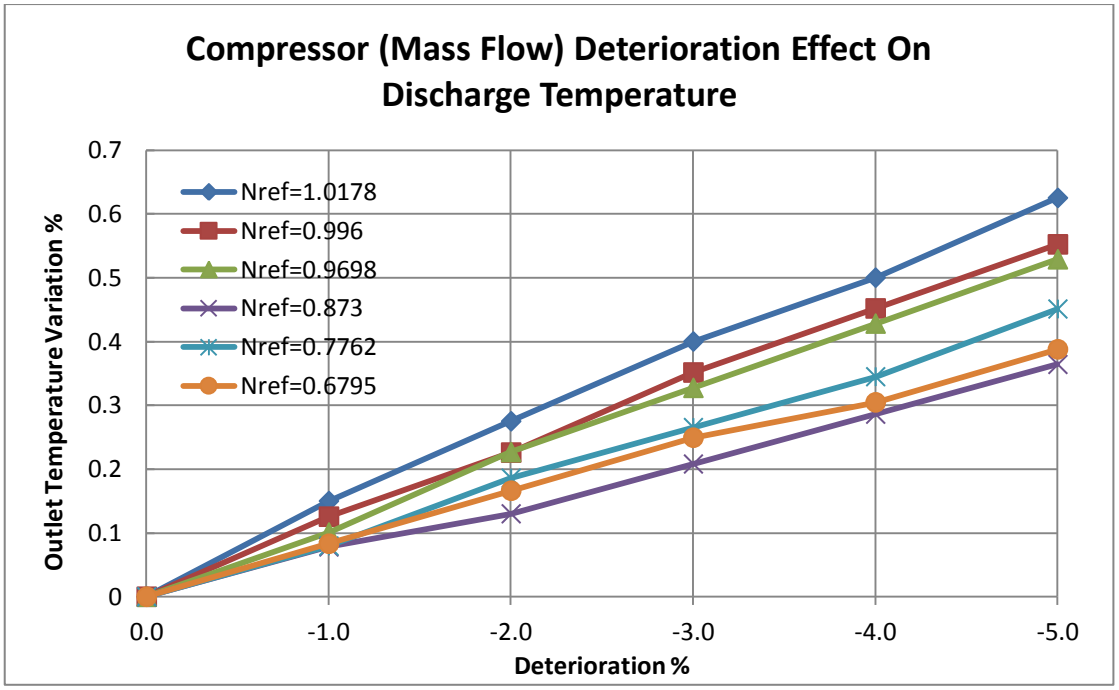

Graph 18. Compressor (Mass Flow) Deterioration Effect on compressor outlet temperature

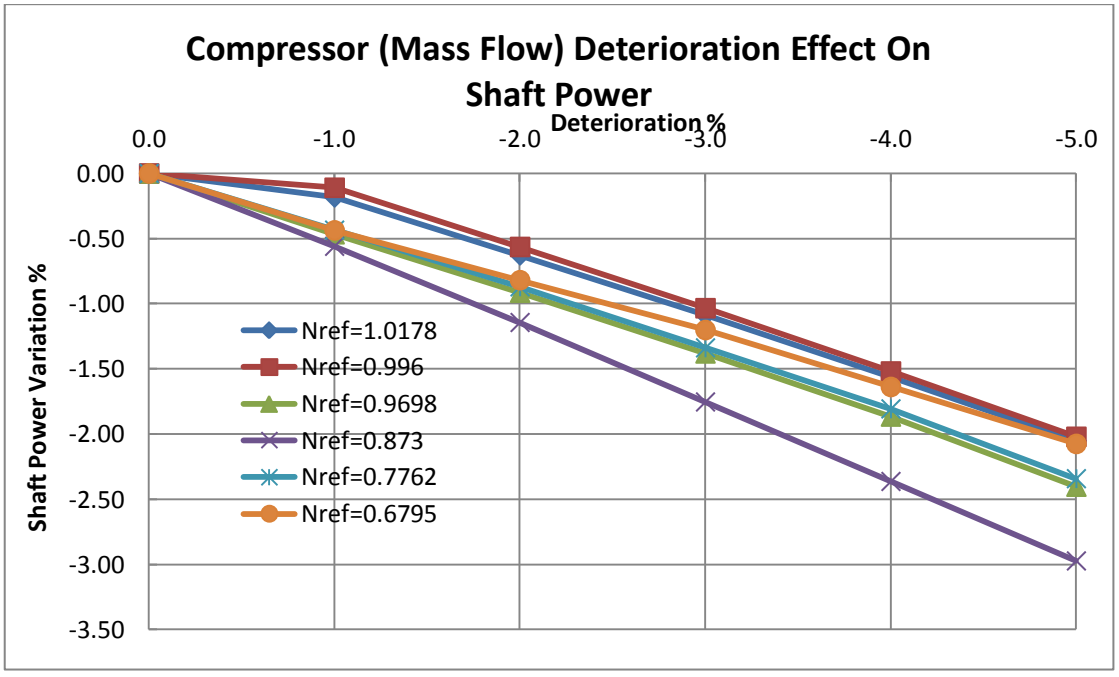

Graph 19. Compressor (Mass Flow) Deterioration Effect on compressor power

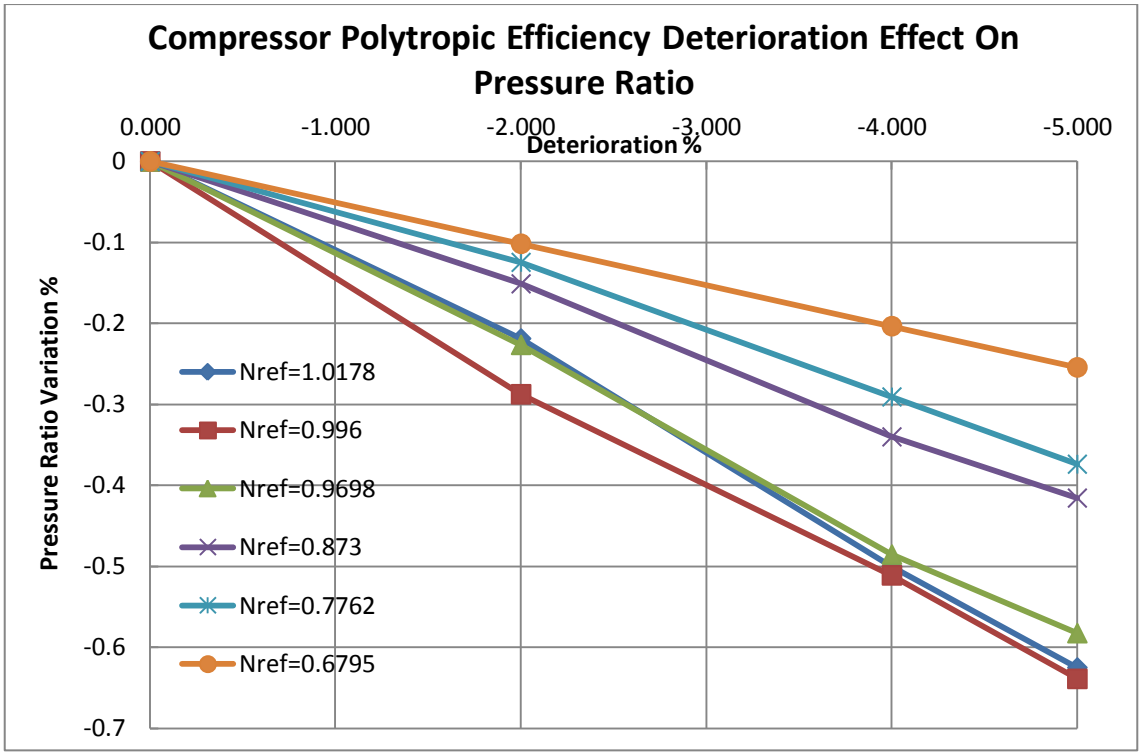

Graph 20. Compressor (efficiency) Deterioration Effect on compressor pressure ratio

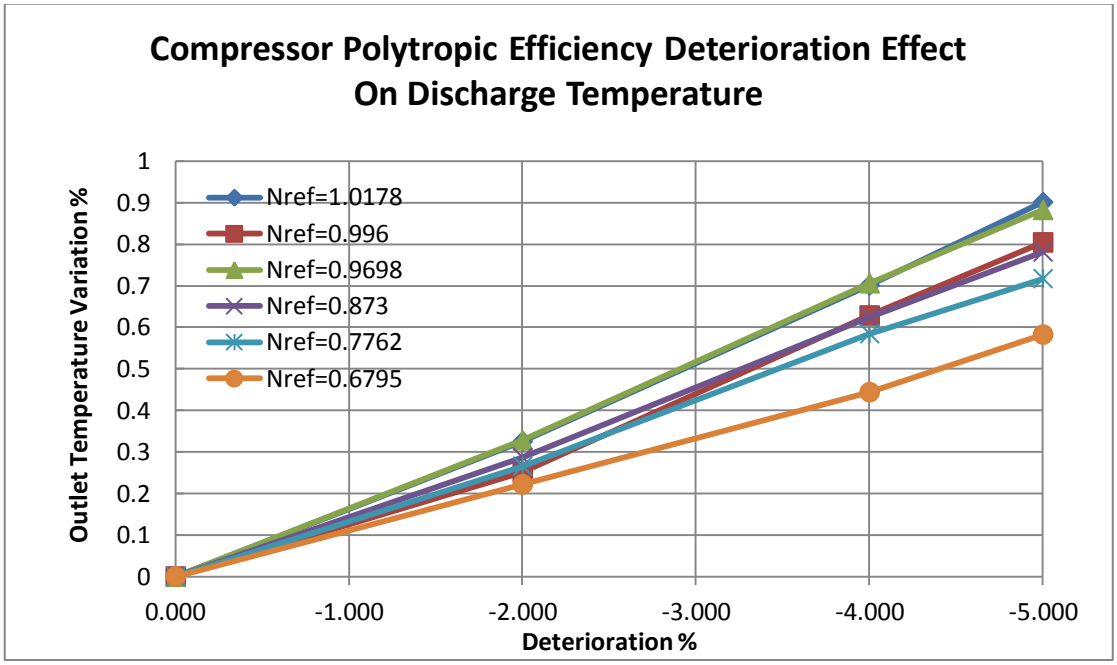

Graph 21. Compressor (efficiency) Deterioration Effect on compressor outlet temperature

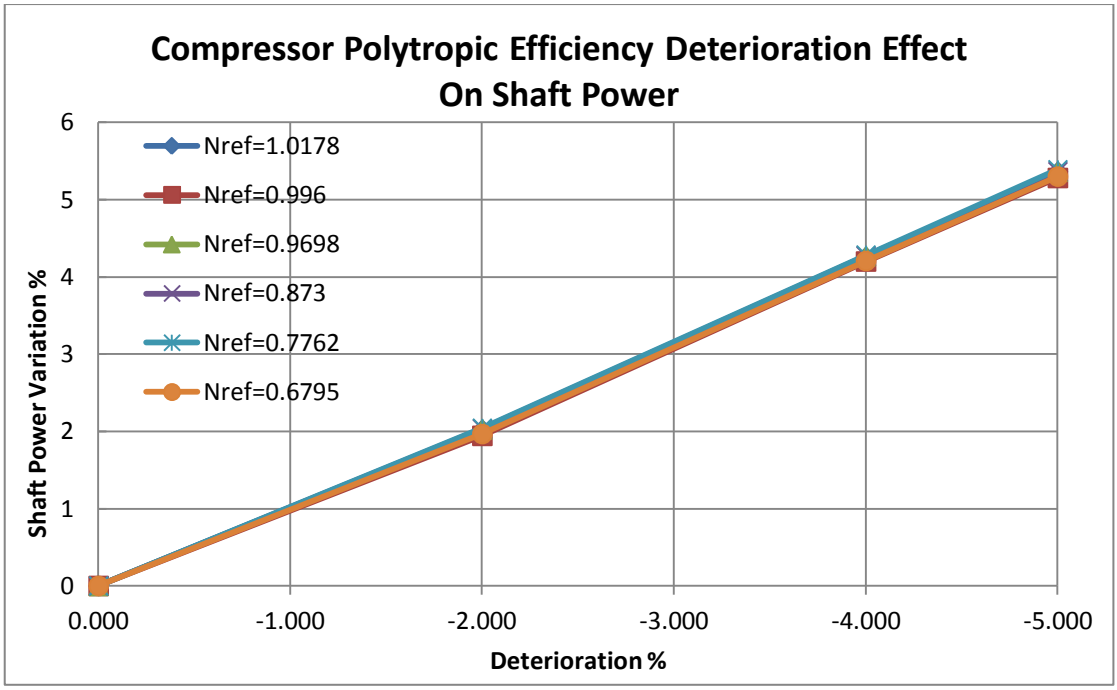

Graph 22. Compressor (efficiency) Deterioration Effect on compressor power

8. Discussion

8.1 Use of HYSYS for Compressor Applications and Limitations

HYSYS is an advanced simulation tool for the thermodynamic modeling of compressors. It has the capability of mimicking the actual compressor at site with extremely high accuracy. All the programme needs is in essence the inlet and outlet measurable parameters of the compressor and with the user intervention the programme builds the performance curves. For rotational speeds between the tested regions, the programme uses interpolation techniques which are also used and practiced in the industry. HYSYS carries out accurate interpolation between two curves. However, the accuracy of extrapolation, over the maximum speed curve or extrapolation lower than the minimum speed, could not be independently verified. Therefore it should always be ensured that the value of simulated speed is within the range of input maximum and minimum speed curve data. HYSYS also has transient analysis capabilities but it is more geared towards dynamic issue such as compressor surge, anti-surge control valve design, determining stonewall region and the settle out pressures in case of compressor trip. The user can model a degraded compressor on HYSYS in much the same way as modeling a new compressor. Once a model is set, a whole range of sensitivity analysis could be run by HYSYS given independent variables such as mass throughput, pressure ratio or efficiency decrease with time. Overall, HYSYS is a recommended simulation package for thermodynamic performance analysis of centrifugal compressors.

8.2 Degradation Modeling by Simulation and Health Estimation by Scaling

When compressors degrade, the performance behaviour change and the compressor characteristic curves fall downwards and generally to the left, reducing the deliverability, efficiency and increasing the performance uncertainty and reducing the operational area. Thus in order to know the factors limiting the operational flexibility and power demand, a a-priori knowledge is required on how degradation of various key parameters (PR, m and η) at various levels affect the compressor performance and these works was carried out under this research.

A representative performance map for a clean compressor has been developed from basic gas and operational data by applying the equations of thermodynamics and affinity laws. For an accurate performance mapping, CFD analysis is required to complement the thermodynamic simulation to precisely model the stage by stage physical geometries of the compressor.

The degraded compressor maps for various scenarios of degradation and rerates were superimposed on the same map to define the operational limits of the compressor. HYSYS was utilized to analyze the trends in measurable and non measurable parameters, over a period of 1 year, following a linear and nonlinear degradation patterns.

By simulation, it is found that linear degradation produce nearly linear changes in measurable output and non-linear degradation produce non-linear changes in measurable output.

The compressor degradation indices have been applied to examine the health of compressor over the time. In this thesis, it is demonstrated that estimation of degradation in health indicators (throughput and efficiency drops) by scaling the measurable parameters is a useful tool. The operator can simply take compressor measurements and estimate the current health of the compressor relative to when it was new by indirectly evaluating the drop in mass throughput and efficiency as the health indicators.

It was found that power demand variation produced the least errors in predicting the compressor health as a diagnostic tool. Using the speed measurement as a diagnostic tool, require further works and analysis since there are several factors that can affect speed.

In this study, the measurements are the discharge temperature, power and speed and the compressor health indicators are mass throughput and efficiency health indices.

The diagnostic method developed above need further refinement and research for minimization of errors between predicted and actual degradation levels.

8.3 Performance Adaptation by Successive Iteration Method and Data Trending

For operational companies to confirm acceptance, the compressor must be tested at full range of speeds and flowrates as soon as it is moved to site and operated to establish the real performance maps. At this time the performance can be scaled from OEM performance curves. The compressor under investigation was moved to site and started operations in 2004 but at the time, these tests were not done. This is one of the lessons learnt, which clearly indicate that the degradation of compressor does shift the performance map but the scale of shift or shift factor is not constant for all speeds. The proposed method of performance adaptation by successive iteration is based on the fact that scaling method work best at the or around the local test point but the accuracy is affected when moving further away from the locality if the same scale is applied. The successive iteration method gives an opportunity for the

new scale factor, obtained from site performance data, at each speed to be applied to performance map. In each iteration, the previous curve is fixed in position with the test point falling exactly on the curve until all curves are fixed in position. The wider the test point range, the better. Graphs 4-6 show the errors before and after the adaptation technique and it is evident that the technique is useful for accurate mapping of the performance curves. The performance maps should be built on referred conditions so that the environmental and inlet gas condition changes do not influence the curves and this was shown and proved on Graph 7 with the referred performance maps overlapping for extreme summer and winter conditions. The full data and calculation details are reflected in Appendix D.

The expected performance of compressor is not constant with time due to deterioration and the performance will decrease with time, i.e., the base line is not horizontal and falls with time unless and until a total overhaul is carried out. Comparing the actual performance with a constant expected value will lead to a wrong diagnosis. It is highly useful, if not critical, that at the time of compressor construction the OEM is requested to give a prediction in performance trend so that the actual compressor performance is evaluated against the expected performance for diagnostic or prognostic purposes any time during operation by online monitoring. The predicted OEM trend may be updated and revised with monitoring the compressor under observation. Reference to Graph 15, once the expected performance trend is established, the operator can compare the actual performance versus expected deterioration trend and decide in advance for remedial actions such as partial or full maintenance. This will provide an excellent opportunity for improving the availability of compressor and reduction of the operational cost which are critical part of process plant and operational strategy respectively.

8.4 Health Index and Diagnostics

Tables C1A and C1B in Appendix C (I) show the actual site data for August 2009 and several months later in April 2010. Tables C2A and C2B in Appendix C (I) show the derived quasi-dimensionless measured figures. After plotting these figures on the graphs, it was observed that the differences are too minute to report due to the relatively short time of between data capturing. Hence the compressor data of August 2009 were superimposed on July 2006 normalized performance curves.

The proposed method of developing health indices for independent parameters of PR, efficiency and mass throughput, based on performance indices developed from comparison of degraded and clean performance at a test point followed by the map , have been applied to the site compressor and these are shown on Graphs 14 and 15. The graphs clearly show compressor degradation over the 3 years period.

The health parameters that determine the current health status or degradation in a compressor are the three independent parameters of pressure ratio, efficiency and throughput capacity. Referring to the results obtained in Section 7.3 for the compressor under observation, the degradation in efficiency is less pronounced than in PR and mass throughput.

The fall in performance as reported by instruments and data readings at critical locations of the compressor is not just due to true degradation but a combination of true degradation, environmental effects and reading errors. Thus to obtain the true degradation the environmental impact should be taken out and reading errors otherwise environmental effects on performance and/or reading errors may be wrongly diagnosed as part of compressor degradation. Reading errors and noise and bias cannot be totally eliminated in practice but it is minimized by regular instrumentation calibration with self-diagnosing capabilities. Due to the continuous performance changes, data averaging cannot also be applied by an individual researcher (the author). To overcome these limitations, first of all the original compressor characteristic maps must be highly accurate, performance data should be referred to a common datum so that changes are relative to a common condition making all cases comparable & independent of environmental or gas inlet condition changes and the most valid set of site data should be utilized as analysis by performance adaptation is a “snap shot” of the compressor performance.

Generation of GPA indices to establish confidence, credibility and accuracy of applied health evaluation is an effective tool. Reference to Table 20 in Section 7.4 and analyzing the GPA Indices being mostly close to 1, the results show a very accurate estimation of actual compressor data especially at the tested speeds. A statistical analysis of GPA indices in Table 20 (Section 7.4) show an average GPA Index of 1.03 and a variance of 0.003 over the last 4 years of operation. This is an indication of accuracy and applicability of the compressor health indexing by the scaling.

Rotational speeds cannot be scaled in the same manner as setting up scale factors for the independent parameters of such as throughput, pressure ratio and efficiency. It must be emphasized here that it is normally expected that the compressor is run continuously at the design or continuous speed during the steady state period which constitute by far the majority of the plant life. Nevertheless the non-linearity for much lower speeds can be viewed as a shortfall in applying scale factor to the whole map which is a linear process. To overcome this situation the performance adaptation method must be applied at regular intervals updating the predicted performance curves. The intensity of interval depends on the cleanliness of the process gas and the environmental condition. Coherently, the non linear trend that will appear in the derived scale factors or health indices with time can be used for diagnostic and prognostic purposes.

It is also prudent to test the compressor at the whole envelope of rotational speeds so that the degraded compressor performance can be modeled as completely as possible. The gas path analysis method whether linear or non linear require '*a priori*' information on compressor performance which can be established by testing the compressor at site at various speeds as earlier on as possible. With the degraded compressor, the same pressure ratio as the clean compressor can be achieved but only at a higher RPM and this requires higher absorbed power which is also an indication of lower compressor efficiencies under the degraded conditions.

Due to the criticality of the operation, all main instruments at compressor site are, and shall be, regularly calibrated for accuracy and maintained. The instrumentation at site has self-diagnostic capability so that the operator at the control room (DCS) is notified of any failed instrument. Therefore the instrument readings taken from site are very accurate. Some measurement noise is expected to interfere with the transmitted or recorded readings, although these interferences are not anticipated to have detrimental effect for diagnostic purposes taking note of the site's superior design in terms of low noise interference, accuracy of parameter measurements and operational conditions. It may also be further noted that the noise effect is particularly applicable to gas turbines rather than process gas compressors because the measurements for compressor are taken "at source" (rotor) because of heavy structure whereas in gas turbines the readings are normally are taken on the casing.

For the site compressor under research, the degradation in efficiency is less pronounced (3.3%) than degradation in PR (9.0%) and in mass throughput (9.9%). In extreme cases (a vertical drop of performance map) the PR degradation is 15.0% and for a horizontal shift, mass throughput capacity is degraded by 17.7%.

Right from the start of compressor design OEM should be requested to deliver expected fouling factors for the supplied compressor by the operator providing the OEM with the anticipated process gas data during the project's life cycle, the environmental data and any other data OEM may request to build the expected fouling factors. This means during the design stage, the operator should request OEM to provide Graph 15 and this will be monitored during actual compressor operation. In addition to providing Graph 15, or alternatively, OEM may be requested to produce H_p/N^2 versus Q/N for several fouling factors expected during the compressor life as shown on Figure 23B in Chapter 4, Section 4.4. The aforementioned measures will lead toward valid compressor diagnostics. For the site compressor under investigation which started operating in 2004, Graph 15 nor Figure 23B were requested prior to hand over. The Graph 15 has been produced under this research by the

Author. This is another lesson learnt to be implemented for future compressor designs.

The various levels of degradation have different levels of effect on compressor performance and some compressor performance parameters are more sensitive toward degradation than other parameters. Carrying out these analyses is important because the operator can get a knowledge in advance which parameters of the compressor are affected the most by degradation and which parameters are least affected. In this manner the operator can plan ahead the expected changes in compressor delivery and change the production strategy accordingly. These are numerically demonstrated in Graphs 16-22 inclusive. To make the discussion clear, an example may be set as follows: reference to Figure 35, it is seen that for this particular compressor, medium degradation does not have any significant effect on discharge temperature, so the site operator does not need to be concerned with remarkable increase in cooling water requirement in the heat exchanger downstream of the compressor in case his compressor degrades. On the other hand however, for this compressor, the same amount of deterioration has a significant effect on power consumption which also shows the efficiency shows a marked deterioration. This finding is in line with most of the papers published on compressor performance deterioration modeling [Refs.14, 15, 16, 18]. Then the operator needs to be worried about power limits or availability for his deteriorated compressor. In fact, carrying out this exercise will inform him in advance to what degree of deterioration the plant can tolerate before power limitation apply and this could set the tolerance limit for compressor deterioration before an appropriate action is taken and an economical analysis based on unit cost of power may be beneficial. The Graphs 16-22 also show the degradation effect (due to fouling) is fairly linear on measurable parameters . These graphs also show that the variations in performance as a result of degradation is not independent of the compressor speed meaning degradation does not have the same effect on performance parameters at high speeds compared to low speeds. It shall be noted that the graphical sensitivity analysis shown on Graphs 16-22 are based on thermodynamic changes only and do not consider any geometrical change.

Graphs 12 and 13 demonstrate the derived health indices versus time for the site compressor from Table 21. It is noted that PR degradation is fairly substantial compared to efficiency degradation.

It is found that in terms of PR degradation, the site compressor is likely to be in the region of 9.0% and that for the mass throughput is 9.9% using Fan laws as fully explained in Chapter 7, Section 3. The shift angle of performance curve is about 45°. In addition, to obtain a search space for the possible range of degradation, purely vertical drop and purely horizontal shift of performance curve were also taken. In extreme cases (a vertical drop of performance map)

the PR degradation is 15.0% and for a horizontal shift, mass throughput capacity is degraded by 17.7%.

8.5 Major Contributions of This Thesis

- The application of thermodynamics and proportionality laws for the build up of a representative performance map for centrifugal compressors(Chapter 6)

- Development of a novel performance adaptation method mapping out the actual performance of centrifugal compressor under new and degraded conditions using site data (Chapter 7)

- Establishment of scaling factors being not uniform for all speeds. Thus as a result of degradation, the performance curves shift but the shift of each speed line is unique (Chapter 7)

- Calculation of flow capacity index due to degradation, rather than assuming it is equal to pressure ratio degradation (Chapter 7, Section 3)

- Publication of three relevant papers at international oil and gas conferences on compressor performance adaptation, diagnostics and the need for online performance monitoring of the rotating equipment (Appendix A)

8.6 Scope for Future Work

- Based on the success of the established method of performance adaptation and diagnostics presented in this thesis applied to the site compressor, followed by publication of three relevant papers between 2008 and 2012 (See Appendix A) discussing the methods of performance adaptation, performance monitoring and diagnostics, it is recommended that Cranfield offers an opportunity to the Author as a post doctoral work to carry out further research by writing a computer programme that is capable of adapting and establishing the actual performance of compressors freshly moved to site and is capable of performance monitoring on continuous basis and performance data trending online for diagnostics and prognostic purposes. The referred compressor shall not be confined to process centrifugal compressor types but also expanded into the axial type compressors (i.e., gas turbine axial compressor or axial process compressor).

9. Conclusions

The conclusions of this thesis are listed below:

- The performance maps supplied by OEM at early stages of project development are not accurate and have limited application as they are for a fleet of compressors and not for the specific compressor supplied for specific site related project. Moreover, these maps are for a defined gas inlet and environmental conditions. Hence, compressors must be tested at a full range of speeds and flow rates as soon as it is moved to site from the OEM shop and this will constitute the performance of the "clean" or "un-degraded" compressor. The results of errors in performance prediction before and after the adaptation technique by successive iteration developed in this thesis show that, once the model is set up, it could be applied to OEM and test data for an accurate performance prediction. The performance adaptation by successive iteration stems from the fact that curve correction factor is not the same for all speeds and this method allows for the scale variation for each speed.
- While on continuous operation, compressor starts to degrade via various mechanisms including wear and flow leak in seals and erosion/corrosion and fouling causing a shift in performance maps and these shifts must be investigated through establishing degradation indices for major independent parameters of pressure ratio, polytropic efficiency and mass throughput at regular intervals in the manner shown in this thesis. The actual performance can also be monitored in real time by continuous monitoring and data trending will lead to valid compressor diagnostics.
- Compressor health estimation method has been successfully developed and applied to the site compressor diagnostics (Chart 3). The established GPA Index for the applied method (Index as 1.03 and 0.003 as variance) over 4 years of operation indicate the approach taken for the health estimation is accurate. The three independent parameters that determine the health of the compressor are pressure ratio, efficiency and mass throughput capacity.
- The expected performance of the compressor is not constant during compressor operation but it is a variable depending on the environmental and gas inlet conditions, component ware out such as seals rubbing, as well as the expected health of the compressor since last major overhaul. That is, the base line for comparing the actual performance to the expected performance is time dependent and has a specific trend. Comparing the actual performance to a constant value will lead to a wrong diagnostic. Performance data trending for referred efficiency has been carried out for the site compressor and the trend

was found to be a polynomial fit. If this is taken as the normal expected trend in efficiency then monitoring the actual performance vis-a-vis the expected performance will lead to diagnostic and prognostic analysis and establishment of maintenance strategies for the compressor.

- Degradation of compressor results in a shift of performance curves to the bottom and to the left of the performance map (shift angle, $A°_D$). The amount of shift indicates the degree of degradation. For the compressor under research, the degradation in efficiency is less pronounced (3.3%) than degradation in PR (9.0%) and in mass throughput (9.9%). The degradation in pressure ratio and mass throughput are more or less the same. In order to find the degradation search space, in the extreme case, the degradation is 0-15.0% in PR (assuming purely a vertical drop of performance curve due to degradation) and a degradation of 0-17.7% in mass throughput (assuming purely a horizontal shift of performance curve due to degradation).
- In this work it is demonstrated that by the application of proportionality (Fan) laws, it is possible to identify the degradation in throughput, by relating the degradation in mass throughput with the increase in compressor rotational speed requirement as a result of degradation. The previous works by others have assumed degradation in PR and throughput are the same. In this work it is found that degradation in throughput is in the same order of magnitude as in PR by taking site measurements.
- The downward shift combined with shifting to the left due to the compressor degradation results in narrower surge margins built in design by the OEM. If surge margins are exceeded, the compressor may be damaged at start up. There are strict controls to avoid surge by mounting an Anti-Surge Valve between the discharge and inlet to the compressor. However, the operator must realize that compressor degradation results in changes in surge settings, therefore the operator should be in a position to change the valve settings in accordance with the compressor operational parameter requirements (i.e., PR and m) on-line.
- Based on supplied data to OEM on variations and quality of process gas flow properties and environmental conditions, OEM should be requested to produce the expected fouling factor curves for the supplied compressor in the manner described in this thesis and thereafter the compressor should be monitored accordingly.
- For measurable performance readings, faulty instruments, smearing effects, noise and bias should be avoided. For this site compressor the instruments are regularly calibrated, maintained and have self-diagnosing capability although some instrument noise cannot be

avoided. Furthermore, the noise effect on instrument error is less in process gas compressors than in gas turbines as the instrument readings are taken “at source” in compressors whereas in gas turbines reading are taken on the casing.

- The rate of degradation buildup varies with time. With reference to the sensitivity analysis cases ran by simulation in this thesis on the site compressor, the effect of degradation on performance parameters is not independent of compressor rotational speeds. This means that the shifting of performance curves as a result of degradation is not the same for all speeds.
- Application of degradation scale factors is an accurate description of degraded performance particularly at the tested points. It is also quick and robust. The accuracy somewhat reduces moving well away from the test point(s). This apparent limitation is not viewed critical, as the operators are expected to run the compressor at maximum speed continuously for most of the plant life. To overcome this limitation is to have the compressor performance tested at regular intervals and with updated degradation indices at each interval.
- HYSYS is a suitable simulation tool to complement the performance adaptation and simulate the real performance of compressors accurately. This is important for performance based diagnostic techniques as errors or uncertainties in performance prediction could be wrongly confused with degradation.
- Rotating equipment diagnostic is a powerful application to examine the health of the compressor and to predict which and when a component requires servicing. By fault reporting, data logging and trending one shall be able to link the type of degradation and the likely location of fault. This is currently being done by the major compressor /turbine manufacturers. It is recommended that all compressor packages should include the technology of on-line performance monitoring as a part of the package to a purposeful level capable of carrying out several diagnostic techniques complete with statistical analysis in order to have confidence in the results as critical operational and maintenance decisions shall be based on the diagnostic results. This has been echoed in the conference papers presented by the Author.
- Degradation simulations show that that linear degradation produce nearly linear changes in measurable output and non-linear degradation produce non-linear changes in measurable output. In this thesis, it is demonstrated that estimation of degradation in health indicators (throughput and efficiency drops) by scaling the measurable parameters is a useful tool. However, the diagnostic method developed using simulated measurements and applying scale factors to estimate the degraded health parameters of simulated compressor require

further considerations and refinement to reduce the differences between the predicted and simulated values.

References

1. Henderson J., Rainey D.E., “A comprehensive monitoring program integrating all data sources on a single platform at Nucor Hickman”, Azima/DLI, USA, 2007
2. White, D. C., “Increased refinery productivity through online performance monitoring”, Emerson Process Management, presented at NPRA computer conference- Dallas, Oct 2001.
3. ABB, “Gas Turbine – Gas Path Diagnostics”, Optimax Operations Product, A Review, 2009
4. “Special report-instrumentation and analytics”, ABB, 2009
5. Wagner J. R., George T. J., “An advanced diagnostic and prognostic system for gas turbine generator sets with experimental validation”, SCIES Project, Clemson University, 2003
6. Brooksbank B., Thiagarajah M., “Advanced tools for improving the profitability of pipeline operations” Honeywell
7. Singh R., “Managing gas turbine availability, performance and life usage via advanced diagnostics”, School of Mechanical Engineering, Cranfield University, UK, 2001
8. Loboda I., Amescua I. K. T., “Compressor fouling identification on gas turbine field data”, UDC 621.43.004.62, National polytechnic institute, Mexico, 2008
9. Mattern D., Jaw L., “Experimental results of an active tip clearance control system for a centrifugal compressor”, Intl Gas Turbine Congress and Exposition, 1997
10. Dynalco Controls, “Condition monitoring providing predictive maintenance”, Tx-USA, 2001
11. Mathioudakis K., Stamatis A., “Computer models for education on performance monitoring and diagnostics of gas turbines”, Intl Journal of Mech Eng Education, Vol 30 No. 3, 2001
12. Latcovich J., “Condition monitoring and its effects on the insurance of new advanced gas turbines”, Turbine power systems conference and condition monitoring workshop, Galvestone-Tx, Feb 25-27 2002, USA
13. McKee R., “Continuous compressor monitoring: leveraging current technology for optimal benefits”, GMRC Conference, Denvor-USA, Oct 1998
14. Li. Y. I., “Gas Turbine Performance and Health Status Estimation Using Adaptive Gas Path Analysis”, GT2009-59168, Proceedings of ASME Turbo Expo 2009-Power for Land, Sea and Air, Orlando, Florida, USA, June 8-12, 2009,
15. Aker, G. F., Saravanamuttoo, H.I.H., “Predicting Gas Turbine Performance Degradation Due to Compressor Fouling Using Computer Simulation Techniques”, J of Engineering for Gas Turbines and Power, Vol. 111, Apr 1989

16. Kurz R., Brun K., “Degradation in Gas Turbine systems”, 2000-GT-345, ASME, presented at Intl. GT & Aeroengine Congress in Munich, May 8-11, 2000
17. Dr. Akhtar S., Gibbs F., by correspondents, GASMAN consultants, UK, 2009
18. Hamed A., “Modeling of Compressor Performance Deterioration Due to Erosion”, Intl. J. of Rotating Machinery, Vol. 4, 1998, pp 243-248
19. J. Petek, “Performance Monitoring for Gas Turbines”, GE Energy, Vol. 25-No.1, 2005
20. Crissman J., Gobert J., “Reducing Rotating Equipment Downtime”, Journal of PTQ, 3rd Q 2006, pp 145-151
21. Kubiak J. S., “The diagnosis of turbine component degradation – case histories”, Applied Thermal Engineering 22 (2002), pp 1955-1963
22. Gheaiet A., “Prediction of an axial turbomachine performance degradation due to sand ingestion”, Proc. IMechE Vol. 219 Part A: J. Power and Energy, 2005, pp 273-287
23. Brooks F.J., “GE Gas Turbine Performance Characteristics”, GE Power Systems publications, 2000, pp 1-16
24. Tarabrin, A. P., Schaurovsky, V. A. I. and Stalder, J. P., "An analysis of Axial Compressor Fouling and a Cleaning Method of Their Blading", Proceedings of ASME TURBOEXPO 1996, Paper No. 96-GT-363, 1996
25. Jordal K., et al, “Variations in gas turbine blade life and cost due to compressor fouling – A thermo-economical approach”, Intl. J. of Thermodynamics, Vol. 5, (No 1), March 200, pp 37-47
26. Sedigh, F., Saravanamuttoo H.I.H., “A proposed method for assessing the susceptibility of axial compressor to fouling”, ASME Paper No. 90-GT-348, 1990
27. Taylor B., “RBI Centrifugal Compressors” presentation, API Spring Refining meeting, Dresser-Rand, Denvor-USA, 2009
28. Gresh T., “Compressor Performance - aerodynamics for the user”, 2nd edition, 2001, pp 22-80
29. Li. Y. G., “Performance analysis based gas turbine diagnostics: a review”, Proceedings of IMechE, Part A: J of Power and Energy, Vol 216, No. 5 (Sep 2002), pp 363-377
30. Li. Y. G., Nilkitsaranont. P., “Gas turbine performance prognostic for condition-based maintenance”, Applied Energy 86 (2009), pp 2152-2161
31. Singh., R., “Advances and opportunities in gas path diagnostics”, American Institute of Aeronautics and Astronautics Inc, ISABE, 2003
32. Li, Y.G., Singh, R., "An advanced gas turbine gas path diagnostic system - PYTHIA", ISABE-2005-1284.ISABE, Munich, Germany; Sep 2005
33. Li, Y. G., “Gas turbine diagnostic research at Cranfield University”, Nov 2003

34. Naeem, M., Singh. R., “Implications of engine deterioration for creep life”, Applied Energy 60, 1998, pp 183-223
35. Morini. M., Pinelli. M., “Influence of blade deterioration on compressor and turbine performance”, J. of Engineering for Gas Turbines and Power, Vol 132, Mar 2010
36. Dresser Rand data, 2009/2010
37. Arebi., A.W.A., ”The benefit of compressor cleaning on power output for oil and gas field applications”, MSc thesis, SoE-Cranfield University, 2005
38. Benjalool. A. A., “Evaluation of performance deterioration on gas turbines due to compressor fouling”, MSc, SoE-Cranfield University, 2006
39. Li, I.Y., “Gas Turbine Diagnostics”, Lecture materials, School of Engineering, Cranfield University
40. Goetz, W., Alexander, G., “Reliability improvement through the use of plant operating data and the ORAP (Operational Reliability Analysis Programme) database”, TUV energy services – UK
41. Flexware Incorporation, By Correspondence, May 2009
42. Arriagada. J., et al, IGTC2003Tokyo TS-001, “Fault diagnosis system for an industrial gas turbine by means of neural networks, Nov 2003, pp 1-6
43. Colby,G. M., Hydraulic shop performance testing of centrifugal compressors”, Proceedings of the 34th turbomachinery symposium, 2005, pp 147-154
44. Kurz, R., “Site performance test evaluation for gas turbine and electric driven compressors”, Proceedings of the 34th turbomachinery symposium, 2005, pp 53-60
45. ASME PTC-10, 1997, “Performance test code on compressors and exhausters”, American Society of Mechanical Engineers, New York
46. Hoveland., G., Antoine, M., ”Economic optimization of gas turbine compressor washing”, AUPEC, Sep 2004
47. Maria, B. D., Tangen, R., Gresh, T., “Online Performance Monitoring”, Turbomachinery Inc (TMI), Nov-Dec 2005
48. Sandberg M. R., “Equation of state influences on compressor performance determination”, Proceedings of the 34th turbomachinery symposium, 2005, pp 121-130
49. Escher., P. C., “PYTHIA: An object-oriented gas turbine gas path analysis computer programme for general application”, PhD thesis, SoE-Cranfield University-UK, 1995
50. Ishida. M., Senoo. M., “The pressure losses due to the tip clearance of centrifugal blowers”, ASME, New York, 1980
51. Lakshminarayana. B., “Methods of predicting the tip clearance effects in axial flow turbomachinery”, J. of Basic Engineering, ASME, NY, 1970
52. Siemens by correspondence, June 2008

53. HYSYS manuals, 2007
54. Joubert, H., “Turbomachinery design used intensive CFD”, ICAS 2000 Congress
55. Dongen, Van, Thomassen Compression Systems BV, 1st Middle East Turbomachinery Symposium (METS), Doha, 12th-14th Feb 2011
56. Walsh, P.P., Fletcher, P., “Gas Turbine Performance”, 1998, pp 143-158
57. Byington, C. S., “Prognostic Enhancements to Gas Turbine Diagnostic Systems”, , IEEE Aerospace Conference Proceedings, 6-2815 - 6-2824 vol.6, 2002
58. Wang L., “Rough set based gas turbine fault isolation study”, PhD thesis, SoE-Cranfield University-UK, 2010
59. Miller, H., “Benefiting from efficiency improvements to gas compression-The cost effectiveness of technology”, Dresser Rand Publication, 2002
60. Zohrabian A., Offshore department, Qatar Petroleum, 2010
61. Li I.Y., Pilidis P., Newby. M. A., “An adaptation approach for gas turbine design point performance simulation”, GT2005-68140, Nevada-USA, 2005
62. Stahley J.S., “Design, operation and maintenance considerations for improved dry gas seals reliability in Centrifugal Compressors”, Dresser Rand Publication, 2003
63. Kamunge D., “A non-linear weighted least square gas turbine diagnostic approach and multifuel performance simulation”, PhD thesis, SoE-Cranfield University-UK, 2011
64. Dyson R.J.E. and Doel D. L., “CF-80 Condition Monitoring-The engine manufacturing’s involvement in data acquisition and analysis”. AIAA-84-1412, 1987
65. Lapina R. P., “Estimating Centrifugal Compressor Performance”, Vol. 1, ISBN 0-87201-101-1, Gulf Publishing, 1982
66. Marinai L., Probert D. and Singh R., 2004, "Prospects for aero gas-turbine diagnostics: a review", Journal of Applied Energy, vol. 79, issue. 1, pp. 109-126,
67. Wilson D.G., Korakianitis T., “The design of high efficiency turbomachinery and gas turbines”, 2nd Ed., Prentice Hall, 1998

Appendix A

Published Papers by the Author during Research Thesis

(1) Paper Title: **Performance Modeling of Degraded Compressors and Fault Diagnostics**
Presented at: The International Production and Operation Conference and Exhibition, May 15th 2012, organised by SPE, Doha, SPE Paper 154136

(2) Paper Title: **Compressor Degradation, Performance Adaptation and Fault Diagnostics**
Presented at: Middle East Offshore, October 13th, 2010, Doha, Produced by PennWell and Sponsored by Oil & Gas Journal, Qatar Petroleum, Shell and other majors.

(3) Paper Title: **Compressor Performance Adaptation for Gas Path Analysis and Diagnostics**
Presented at: The 13th International Conference on Applied Mechanics and Mechanical Engineering (AMME), 27-29th May, 2008, Cairo

Appendix B

Compressor and Expander Calculations in HYSYS

B1. Interactive page in HYSYS for Compressor Data Input

The parameters for compressor design may be entered by an interactive process. The initial compressor page looks like the figure below. Single or multiple performance curves could be built into the model by pressing on “Rating” (see Figure B1). In case of multiple performance curves, a series of heads are entered for a set of flowrates and RPMs and the corresponding efficiencies for a single molecular weight or a series of different molecular weights using appropriate radio buttons. Either adiabatic or polytropic efficiency could be entered for calculations. The efficiency type must be the same for all input curves.

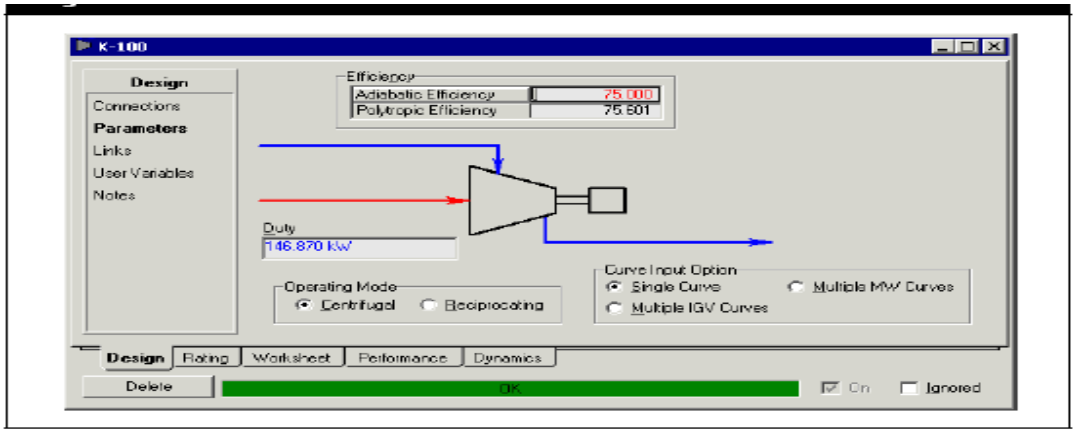

Figure B1. Input page in HYSYS for design and worksheet

The “Curves Page” in HYSYS is embedded below in Figure B2. This is the page that allows the user to enter the performance curves.

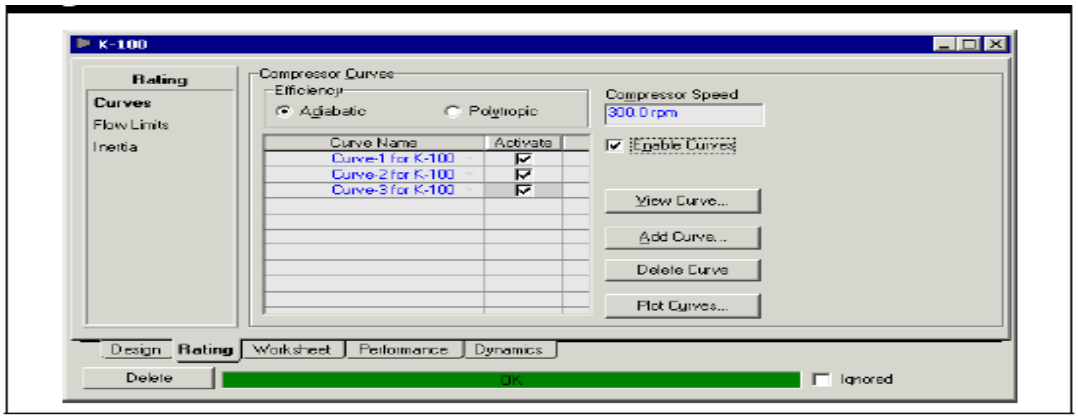

Figure B2. Input page in HYSYS for entering the available performance curves

By clicking on each curve name, the following interactive page appears for which data are entered:

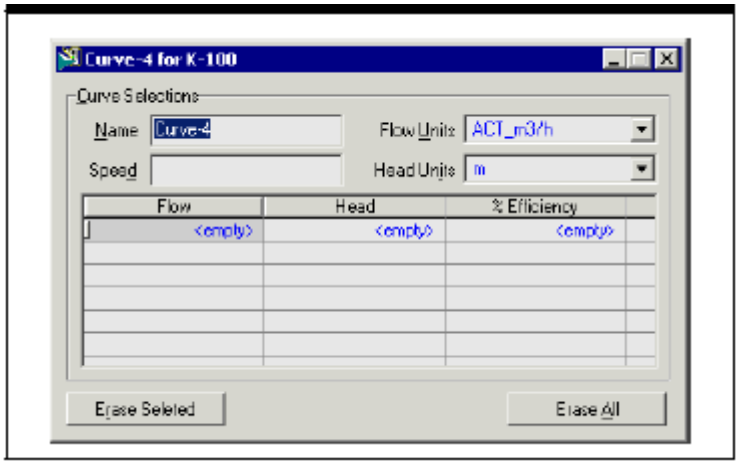

By pressing the Curve property view the following data may be entered as shown on Table B1:

Curve Data	Description
Name	Name of the curve.
Speed	The rotational speed of the Centrifugal Compressor or Expander. This is optional if you specify only one curve. HYSYS can interpolate values for the efficiency and head of the Centrifugal Compressor or Expander for speeds that are not plotted.
Flow Units/Head Units	Units for the flow and head.
Flow/Head/% Efficiency	One row of data is equivalent to one point on the curve. For better results, you should enter data for at least three (or more) points on the curve.

Table B1. Input requirement for the generation of speed curves

By disabling its “Activate” box, a specific curve can be removed from the calculations. Once a curve or curves have been created the relevant buttons are enabled to View or Delete or Plot the curves. If multiple curves have been installed, an operating speed has been specified, and none of the multiple curves' speed equals the operating speed, then all of the curves will be used within the calculation. For example, if curves for two speeds (l000/min and 2000/min) are provided, and an operating speed of l500/min is specified, HYSYS interpolates between the two curves to obtain the solution. Also an inlet pressure and one of the following variables should be provided: flow rate, duty, outlet pressure, or efficiency, as explained above. HYSYS can calculate the appropriate speed based on the input. In this case, it is needed to provide the feed composition, pressure, and temperature as well as two of the following four variables:

- Flow rate
- Duty

- Efficiency
- Outlet Pressure

Once the necessary information is provided, the appropriate speed is determined, and the other two variables are then calculated.

B2. Centrifugal Compressor Calculations in HYSYS

The Centrifugal Compressor operation is used to increase the pressure of an inlet gas stream with relative high capacities and low compression ratios. Depending on the information specified, the Centrifugal Compressor calculates either a stream property (pressure or temperature) or compression efficiency.

The Centrifugal Compressor operation takes into account the compressibility of the liquid, thus performing a more rigorous calculation.

There are several methods for the Centrifugal Compressor or Expander to solve, depending on what information has been specified, and whether or not you are using the compressor's characteristic curves. In general, the solution is a function of flow, pressure change, applied energy, and efficiency. The Centrifugal Compressor or Expander provides a great deal of flexibility with respect to what you can specify and what it then calculates. You must ensure that you do not enable too many of the solution options or inconsistencies may result.

The operating characteristic curves of a compressor is usually expressed as a set of polytropic head and efficiency curves made by manufacturers.

- Some of the features in the dynamic Centrifugal Compressor operations include:
- Dynamic modeling of friction loss and inertia in the Centrifugal Compressor.
- Dynamic modeling which supports shutdown and startup behaviour.
- Multiple head and efficiency curves.
- Modeling of Stonewall and Surge conditions of the Centrifugal Compressor.
- A dedicated surge controller which features quick opening capabilities.
- Handling of phase changes that may occur in the unit operation.
- Linking capabilities with other rotational equipment operating at the same speed with one total power.

B3. Compressor Solution Methods With and without Performance Curves

When the compressor is at design stage, the performance curves are not normally available. In this instance the compressor performance is estimated without the curves by fixing specific design parameters. However, when an existing compressor(s) is being analyzed for performance evaluation or data

matching, the performance curves are normally available from the manufacturer. It is to be noted that these performance curves are the expected values supplied by the manufacturer in the beginning and these do not necessarily represent the true or current performance of the compressor(s) as predicted by the manufacturer. This is when data matching becomes critical in the modeling so that effect of variables on the performance of the compressor could be reliably analyzed.

The table below (Table B2) represents the variables that need fixing for the analysis to begin with or without performance curves being available:

Without Curves	With Curves
3. Flow rate and inlet pressure are known. Then: A) Specify outlet pressure. And, B) Specify either Adiabatic or Polytropic efficiency. HYSYS calculates the required energy, outlet temperature, and other efficiency.	Flow rate and inlet pressure are known. Then: B) Specify operating speed. B)HYSYS uses curves to determine efficiency and head. HYSYS calculates outlet pressure, temperature, and applied duty.
4. Flow rate and inlet pressure are known. Then: A) Specify efficiency and duty. HYSYS calculates outlet pressure, temperature, and other efficiency.	Flow rate, inlet pressure, and efficiency are known. Then: A)HYSYS interpolates curves to determine operating speed and head. HYSYS calculates outlet pressure, temperature, and applied duty.

Table B2. Variables requiring values in HYSYS compressor calculations

B4. HYSYS Simulation Theory at Steady State

For a Centrifugal Compressor, the isentropic efficiency is given as the ratio of the isentropic (ideal) power required for compression to the actual power required:

$$\text{Isentropic Efficiency (\%)} = \frac{\text{Power Required}_{\text{Isentropic}}}{\text{Power Required}_{\text{Actual}}} \times 100\%$$

And

$$\text{Polytropic Efficiency (\%)} = \frac{\text{Power Required}_{\text{Polytropic}}}{\text{Power Required}_{\text{Actual}}} \times 100\%$$

For an adiabatic Centrifugal Compressor, HYSYS calculates the centrifugal compression rigorously by following the isentropic line from the inlet to outlet pressure. Using the enthalpy at that point, as well as the specified efficiency, HYSYS then determines the actual outlet enthalpy. From this value and the outlet pressure, the outlet temperature is determined.

For a polytropic Centrifugal Compressor or Expander, the path of the fluid is neither adiabatic nor isothermal. For a 100% efficient process, there is only the condition of mechanical reversibility. For an irreversible process, the polytropic efficiency is less than 100%. For compression, the work determined for the mechanically reversible process is divided by an efficiency to give the actual work.

Notice that all intensive quantities are determined thermodynamically, using the specified Property Package. In general, the work for a mechanically reversible process can be determined from:

$$W = \int V dP$$

Where:

W= Work
V= Volume
dP= Pressure Difference

As with any unit operation, the calculated information depends on the information which is specified by the user. In the case where the inlet and outlet pressures and temperatures of the gas are known, the ideal (isentropic) power of the Operation is calculated using one of the above equations. The actual power is equivalent to the heat flow (enthalpy) difference between the inlet and outlet streams.

For the Centrifugal Compressor:

$$\text{Power Required}_{\text{actual}} = \text{Heat Flow}_{\text{outlet}} - \text{Heat Flow}_{\text{inlet}}$$

where the efficiency of the Centrifugal Compressor is then determined as the ratio of the isentropic power to the actual power required for compression.

In the case where the inlet pressure, the outlet pressure, the inlet temperature and the efficiency are known, the isentropic power is once again calculated using the appropriate equation. The actual power required by the Centrifugal Compressor (enthalpy difference between the inlet and outlet streams) is calculated by dividing the ideal power by the compressor efficiency. The outlet temperature is then rigorously determined from the outlet enthalpy of the gas using the enthalpy expression derived from the property method being used. For an isentropic compression (100% efficiency), the outlet temperature of the gas is always lower than the outlet temperature for a real compression or expansion.

An essential concept associated with the Centrifugal Compressor (and Expander) operations is the isentropic and polytropic power. The calculation of these parameters and other quantities are taken from "Compressors and Exhausters - Power Test Codes" from the American Society of Mechanical Engineers.

The isentropic or polytropic power, W, can be calculated from:

$$W=F_1(M)\ (n/(n-1))CF\ (P_1/\rho_1)\ x\ [\ (P_2/P_1)^{((n-1)/n))}-1)\ ]$$

where:

n = volume exponent
CF = correction factor
P_1 =pressure of the inlet stream
P_2 = pressure of the exit stream
ρ_1 = density of the inlet stream
F_1 =molar flow rate of the inlet stream
M = molecular weight of the gas

Isentropic power is calculated by defining the volume exponent as:

$$n= \ell n\ (P_2/P_1)/(\ell n(\rho'_2/\ \rho_1))$$

Where:

ρ'_2 = density of the exit stream corresponding to the inlet entropy

Polytropic power is calculated by defining the volume exponent as:

$$n= \ell n\ (P_2/P_1)/(\ell n(\rho_2/\ \rho_1))$$

Where:
ρ_2 = density of the exit stream

The correction factor is calculated as:

$$CF = [h'_2 - h_1] / [(n/(n-1)) \times (P_2/ \rho'_2) - (P_1/ \rho'_2)]$$

Where:
$h'2$ = enthalpy of the exit stream corresponding to the inlet entropy
$h1$ = enthalpy of the inlet stream

An isentropic flash is performed to calculate the values of h'_2 and ρ'_2.

HYSYS calculates the compression rigorously by following the isentropic line from the inlet to the exit pressure. The path of a polytropic process is neither adiabatic nor isothermal. The only condition is that the polytropic process is reversible.

B5. Equation used in HYSYS

If the compressor (icon) is selected, the compressor equations are used. If the expander (icon) is selected, the expander equations are used.

GLOSSARY

Ideal	:	Isentropic (100% Efficiency)
Actual	:	Given efficiency
H	:	Mass Enthalpy
Out	:	Product Stream (discharge)
In	:	Feed Stream (suction)
P	:	Pressure
M	:	Molecular Weight
Z	:	Compressibility Factor
ρ	:	Mass Density
f	:	Polytropic Head Factor
n	:	Polytropic Exponent
k	:	Isentropic Exponent

B5.1 COMPRESSOR – Efficiencies

The Adiabatic and Polytropic Efficiencies are included in the compressor calculations. An isentropic flash (P_{in} and $Entropy_{in}$) is performed internally to obtain the ideal (isentropic) properties.

$$AdiabaticEff = \frac{Work\,\mathrm{Re}quired_{(ideal)}}{Work\,\mathrm{Re}quired_{(actual)}} = \frac{(H_{out} - H_{in})_{ideal}}{(H_{out} - H_{in})_{actual}} \qquad (1)$$

$$Polytropic\,Eff = \frac{\left[\left(\frac{P_{out}}{P_{in}}\right)^{\left(\frac{n-1}{n}\right)} - 1\right] \times \left[\left(\frac{n}{(n-1)}\right) \times \left(\frac{k-1}{k}\right)\right]}{\left[\left(\frac{P_{out}}{P_{in}}\right)^{\left(\frac{k-1}{k}\right)} - 1\right]} \times AdiabaticEff \qquad (2)$$

$$n = \frac{\log\left(P_{out}/P_{in}\right)}{\log\left(\rho_{out,actual}/\rho_{in}\right)} \qquad (3) \text{ and} \qquad k = \frac{\log\left(P_{out}/P_{in}\right)}{\log\left(\rho_{out,ideal}/\rho_{in}\right)} \qquad (4)$$

B5.2 COMPRESSOR – Heads

The Adiabatic and Polytropic Heads are performed after the compressor calculations are completed, only when the "Results" page of the compressor is selected. The Work Required (actual) is the compressor energy stream (heat flow).

$$AdiabaticHead = \left[\frac{Work\,\mathrm{Required}_{(actual)}}{MassFlowRate}\right] \times AdiabaticEff \times \frac{1}{(g/g_c)} \qquad (5)$$

The Polytropic Head is now calculated based on the ASME method ("The Polytropic Analysis of Centrifugal Compressors", Journal of Engineering for Power, J.M. Schultz, January 1962, p. 69-82).

$$Polytropic\,Head = f \times \left(\frac{n}{n-1}\right) \times \left[\left(\frac{P_{out}}{\rho_{out,actual}}\right) - \left(\frac{P_{in}}{\rho_{in}}\right)\right] \times \frac{1}{(g/g_c)} \qquad (6)$$

$$f = \frac{H_{out,ideal} - H_{in}}{\left(\frac{k}{k-1}\right) \times \left[\left(\frac{P_{out}}{\rho_{out,ideal}}\right) - \left(\frac{P_{in}}{\rho_{in}}\right)\right]} \qquad (7)$$

$$n = \frac{\log\left(P_{out}/P_{in}\right)}{\log\left(\rho_{out,actual}/\rho_{in}\right)}$$

As in equation (3) above, and,

$$k = \frac{\log\left(P_{out}/P_{in}\right)}{\log\left(\rho_{out,ideal}/\rho_{in}\right)}$$

As in equation (4) above

B5.3 EXPANDER - Efficiencies

The Adiabatic and Polytropic Efficiencies are parts of the expander calculations. An isentropic flash (P_{in} and $Entropy_{in}$) is performed to obtain the ideal (isentropic) properties. The flash is done internally on the expander fluid, and the results are not stored.

$$AdiabaticEff = \frac{Work\,Produced_{(actual)}}{Work\,Produced_{(ideal)}} = \frac{(H_{out} - H_{in})_{actual}}{(H_{out} - H_{in})_{ideal}} \tag{8}$$

$$PolytropicEff = \frac{\left[\left(\frac{P_{out}}{P_{in}}\right)^{\left(\frac{k-1}{k}\right)} - 1\right]}{\left[\left(\frac{P_{out}}{P_{in}}\right)^{\left(\frac{n-1}{n}\right)} - 1\right] \times \left[\left(\frac{n}{(n-1)}\right) \times \left(\frac{k-1}{k}\right)\right]} \times AdiabaticEff \tag{9}$$

$$n = \frac{\log\left(P_{out} / P_{in}\right)}{\log\left(\rho_{out,actual} / \rho_{in}\right)}$$

As in equation (3) above, and,

$$k = \frac{\log\left(P_{out} / P_{in}\right)}{\log\left(\rho_{out,ideal} / \rho_{in}\right)}$$

As in equation (4) above

B5.4 EXPANDER - Heads

The Adiabatic and Polytropic Heads are performed after the expander calculations are completed, only when the “Results” page of the expander is selected. The Work Produced (actual) is the expander energy stream (heat flow).

$$AdiabaticHead = \left[\frac{Work\,Produced_{(actual)}}{MassFlowRate}\right] \times \frac{1}{AdiabaticEff} \times \frac{1}{(g/g_c)} \tag{10}$$

$$PolytropicHead = -f \times \left(\frac{n}{n-1}\right) \times \left[\left(\frac{P_{out}}{\rho_{out,actual}}\right) - \left(\frac{P_{in}}{\rho_{in}}\right)\right] \times \frac{1}{(g/g_c)} \tag{11}$$

$$f = \frac{H_{out,ideal} - H_{in}}{\left(\frac{k}{k-1}\right) \times \left[\left(\frac{P_{out}}{\rho_{out,ideal}}\right) - \left(\frac{P_{in}}{\rho_{in}}\right)\right]}$$

As in equation (7) above

$$n = \frac{\log\left(P_{out}/P_{in}\right)}{\log\left(\rho_{out,actual}/\rho_{in}\right)}$$ As in equation (3) above

$$k = \frac{\log\left(P_{out}/P_{in}\right)}{\log\left(\rho_{out,ideal}/\rho_{in}\right)}$$ As in equation (4) above

B5.5 APPLICATION IN SI UNITS

H : Mass Enthalpy (kJ/kg)
P : Pressure (kPa)
ρ : Mass Density (kg/m3)

Equation (5):

$$AdiabaticHead(m) = \left[\frac{Work\,Required_{(actual)}}{MassFlowRate}\right] \times AdiabaticEff \times 1000\left(N \cdot m/kJ\right) \times \frac{1}{9.8066\left(N/kg\right)}$$

Equation (6):

$$PolytropicHead(m) = f \times \left(\frac{n}{n-1}\right) \times \left[\left(\frac{P_{out}}{\rho_{out,actual}}\right) - \left(\frac{P_{in}}{\rho_{in}}\right)\right] \times 1000\left(\frac{N/m^2}{kPa}\right) \times \frac{1}{9.8066\left(N/kg\right)}$$

Equation (7):

$$f = \frac{\left(H_{out,ideal} - H_{in}\right) \times 1000\left(N \cdot m/kJ\right)}{\left(\frac{k}{k-1}\right) \times \left[\left(\frac{P_{out}}{\rho_{out,ideal}}\right) - \left(\frac{P_{in}}{\rho_{in}}\right)\right] \times 1000\left(\frac{N/m^2}{kPa}\right)}$$

Equation (10):

$$AdiabaticHead(m) = \left[\frac{Work\,Produced_{(actual)}}{MassFlowRate}\right] \times \frac{1}{AdiabaticEff} \times 1000\left(N \cdot m/kJ\right) \times \frac{1}{9.8066\left(N/kg\right)}$$

Equation (11):

$$PolytropicHead(m) = -f \times \left(\frac{n}{n-1}\right) \times \left[\left(\frac{P_{out}}{\rho_{out,actual}}\right) - \left(\frac{P_{in}}{\rho_{in}}\right)\right] \times 1000\left(\frac{N/m^2}{kPa}\right) \times \frac{1}{9.8066\left(N/kg\right)}$$

B5.6 APPLICATION IN FIELD UNITS

H : Mass Enthalpy (Btu/lb)

P : Pressure (psia = lbf/in2)

ρ : Mass Density (lb/ft3)

Equation (5):

$$AdiabaticHead(ft) = \left[\frac{Work\,\mathrm{Re}quired_{(actual)}}{MassFlowRate}\right] \times AdiabaticEff \times 778.1692\left(ft \cdot lb_f / Btu\right) \times \frac{1}{1\left(lb_f / lb\right)}$$

Equation (6):

$$PolytropicHead(ft) = f \times \left(\frac{n}{n-1}\right) \times \left[\left(\frac{P_{out}}{\rho_{out,actual}}\right) - \left(\frac{P_{in}}{\rho_{in}}\right)\right] \times \left(12in/ft\right)^2 \times \frac{1}{1\left(lb_f / lb\right)}$$

Equation (7):

$$f = \frac{\left(H_{out,ideal} - H_{in}\right) \times 778.1692\left(ft \cdot lb_f / Btu\right)}{\left(\frac{k}{k-1}\right) \times \left[\left(\frac{P_{out}}{\rho_{out,ideal}}\right) - \left(\frac{P_{in}}{\rho_{in}}\right)\right] \times \left(12in/ft\right)^2}$$

Equation (10):

$$AdiabaticHead(ft) = \left[\frac{Work\,\mathrm{Pr}oduced_{(actual)}}{MassFlowRate}\right] \times \frac{1}{AdiabaticEff} \times 778.1692\left(ft \cdot lb_f / Btu\right) \times \frac{1}{1\left(lb_f / lb\right)}$$

Equation (11):

$$PolytropicHead(ft) = -f \times \left(\frac{n}{n-1}\right) \times \left[\left(\frac{P_{out}}{\rho_{out,actual}}\right) - \left(\frac{P_{in}}{\rho_{in}}\right)\right] \times \left(12in/ft\right)^2 \times \frac{1}{1\left(lb_f / lb\right)}$$

B5.7 Compressor Discharge Temperature Calculation

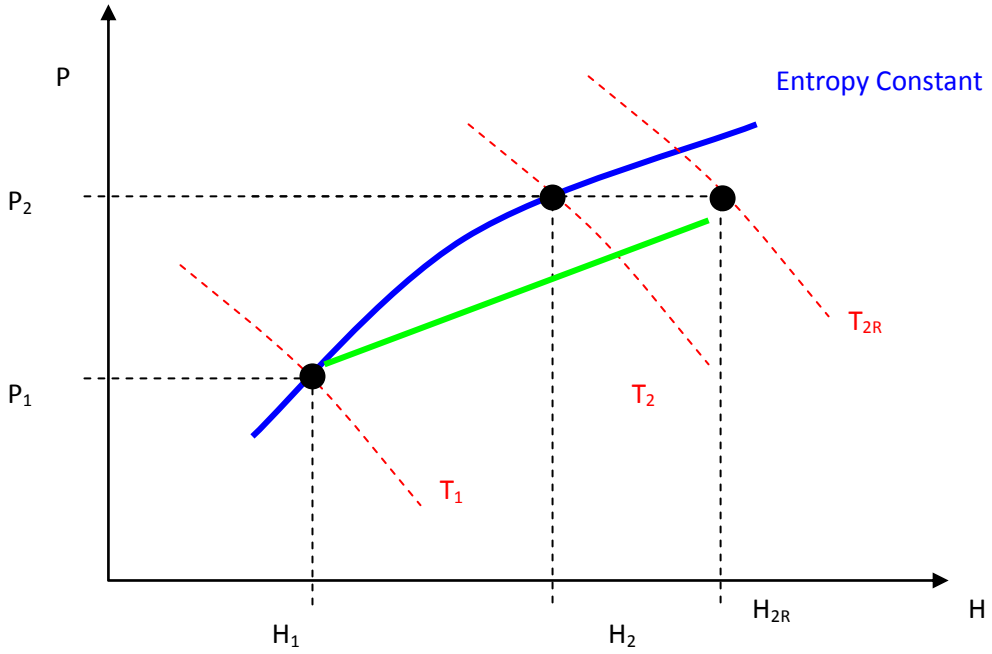

The above plot (Pressure Enthalpy) can be used to explain how HYSYS calculate outlet temperature:

Ideal Path (blue curve) : the gas is compressed from P_1(Inlet Pressure) to P_2 (Discharge Pressure) following the constant entropy curve.

1) At point 1 conditions are T_1(Inlet Temperature) and P_1 are known+ composition and flow. HYSYS flash the stream and calculate enthalpy H_1 and Entropy S_1.

2) At point 2 the gas is compressed to P_2 and S_2 is known from S_1-S_2=0 and the entropy (S(T,P)) is a function of T and P. T_2 (Discharge temperature) is calculate using an iterative procedure.

When the calculation of T_2 are converged H_2 and other properties at point 2 are also calculated. Point 2 now is defined.

3) Ideal Work: $W_{ideal} = H_2 - H_1$

4) To take the real path the efficiency (η) is introduced:

The real work = H_{2R}- H1 = W_{ideal}/η (R denotes real)

From this relation = $H_{2R} = H_1 + (W_{ideal}/\eta)$

In this point H_{2R} and P_2 are known and only T_{2R} is unknown. By iterative procedure HYSYS calculates T_{2R}, after which all other properties are calculated.

Method used to interpolate compressor/expander curves in HYSYS

General description of compressor curve interpolation

In the HYSYS compressor operation, a cubic spline method is used for the interpolation of the speed curves themselves and for the interpolation between speed curves. Here is an outline of the procedure:

When multiple curves of different speed are provided (for example three curves for 9000 rpm, 11000 rpm and 13000 rpm), given the flow F, the first step is to calculate the Head and Efficiency for the given flow (for each of the three curves) using a Cubic Spline Method (see below). When the three pairs of data available (9000 rpm, HeadFor9000; 11000 rpm, HeadFor11000; and 13000 rpm, HeadFor13000), the next step is to find out the head for a specified speed for the speed specified (10000 rpm for example) using the Cubic Spline Method again. The same procedure is used to find out the Efficiency.

If you input multiple curves into the compressor and then run the compressor at a speed below the lowest curve (i.e. lowest speed), the method used in HYSYS includes a limited functionality of extrapolation when the point lies outside of the data. Note that extrapolation is generally not accurate enough depending on the degree of curve non-linearity.

Description of the cubic spline interpolation

The cubic polynomials are used to approximate the curve between each pair of data points. The cubic spline uses a third-degree polynomial. Suppose there is a sets of data (t0,y0) .. (tn, yn) known:

x:	t0	t1	.....	tn
y:	y0	y1	....	yn

The ti's are the knots and are assumed to be arranged in ascending order.
The cubic spline function S that is used to construct consists of n cubic polynomial pieces:

S(x) = S0(x) t0 <= x <= t1
= S1(x) t1 <= x <= t2
.....
= Sn-1(x) tn-1 <= x <= tn

The interpolation conditions are:

S(ti) = yi (0 <= i <= n)

The other two conditions are:

S"(t0) = S"(tn) = 0

The function S can be determined as

$$S(x) \quad \frac{z_{i\ 1}}{6h_i}(x \quad t_i)^3 \quad \frac{z_i}{6h_i}(t_{i\ 1} \quad x)^3 \quad (\frac{y_{i\ 1}}{h_i} \quad \frac{h_i}{6}z_{i\ 1})(x \quad t_i) \quad (\frac{y_i}{h_i} \quad \frac{h_i}{6}z_i)(t_{i\ 1} \quad x)$$

where h1 = ti+1- t1

When the values z0, z1, .. zn have been determined, the spline function S(x) is obtained from equations of the above form for S0(x), S1(x), .., Sn-1(x).

The values z0, z1, .. zn can be obtained by solving a tridiagonal system of equations:
$z0 = 0$
$h_{i-1}z_{i-1} + u_i z_i + h_i z_{i+1} = v_i \quad (1 <= i <= n-1)$
$zn = 0$

where $v_i = 6(b_i - b_{i-1})$
$b_i = (1/h_i)(y_{i+1} - y_i)$

Appendix C

Site Compressor data

(I) Site base cases for health estimation
(II) Site compressor untreated data log since 2006
(III) Typical Performance Curves supplied by OEM

(I) Site base cases for health estimation

Parameter	Base Case 1	Base Case 2	Base Case 3	Base Case 4	Base Case 5	Unit
Inlet T	322.06	318.95	320.15	323.15	313.15	K
Inlet P	1076	1057	1086	1050	1040	kPaa
Mol. Wt.	26.1	26.1	26.1	26.1	26.1	Kg/kmol
Outlet T	395.33	393.15	393.15	395.15	388.15	K
Outlet P	3102	3100	3120	3100	3120	kPaa
Flow rate	125,020	125,460	135,390	123,400	126,320	kg/hr
Shaft Power	N/A	5,596	6,042	5080	5430.4	kW
Poly Efficiency	82.0	82.0	81.8	85.8	84.1	%
Rot Speed	0.88	0.891	0.9	0.871	0.89	-
Time	14:00	16:00	16:00	16:00	8:00	_
Test Date	24/08/2009	06/07/2009	29/07/2009	23/08/2009	24/08/2009	-

Table C1A. Site compressor 5 base case data for analysis and diagnostics – August 2009

Referred Parameter	Base Case 1	Base Case 2	Base Case 3	Base Case 4	Base Case 5	Unit
θ	1.02144	1.01158	1.01538	1.02490	0.99318	-
δ	1.00561	0.98785	1.01495	0.98131	0.97196	-
Inlet T	315.3					K
Inlet P	1070					kPaa
Mol. Wt.	24.6					Kg/kmol
Outlet T	372.98	374.54	373.13	371.55	376.62	K
Outlet P	2900.20	2950.43	2890.17	2970.10	3018.00	kPaa
Pressure Ratio	2.71	2.76	2.70	2.78	2.82	-
Flow rate	118,984	120,960	127,288	120,554	122,650	kg/hr
Shaft Power	N/A	5198	5452	4720	5174	kW
Poly Efficiency	82.0	82.0	81.8	85.8	84.1	%
Rot Speed	0.85	0.87	0.88	0.84	0.88	-
Date	24/08/2009	06/07/2009	29/07/2009	23/08/2009	24/08/2009	24/08/2009

Table C2A. The referred parameter values for the site compressor performance analysis and diagnostics –August 2009

Parameter	Base Case 1	Base Case 2	Base Case 3	Base Case 4	Base Case 5	Base Case 6	Unit
Inlet T	308.15	310.15	321.15	314.15	309.15	303.15	K
Inlet P	1044	1034	1054	1008	9910	1024	kPaa
Mol. Wt.	26.2	26.2	26.2	26.2	26.2	26.2	Kg/kmol
Outlet T	384.15	386.15	396.15	391.15	387.15	379.15	K
Outlet P	3146	3151	3150	3232	3173	3096	kPaa
Flow rate	129,630	129,478	123,045	128,877	126,418	129,584	kg/hr
Turbine Power	6,639	6,561	6,515	6,906	6,827	6573	kW
Shaft Power	5,997	5,926	5,885	6,238	6,166	5,937	kW
Poly Efficiency	82.0	82.0	81.8	85.8	84.1	83.8	%
Rot Speed	0.89	0.89	0.89	0.91	0.9	0.88	-
Time	08:00	12:00	16:00	20:00	00:00	04:00	-
Test Date	06/04/2010	06/04/2010	06/04/2010	06/04/2010	06/04/2010	06/04/2010	-

Table C1B. Site compressor 5 base case data for analysis and diagnostics – April 2010

Referred Parameter	Base Case 1	Base Case 2	Base Case 3	Base Case 4	Base Case 5	Base Case 6	Unit
θ	0.97732	0.98367	1.01855	0.99635	0.98049	0.96147	-
δ	0.97570	0.96636	0.98505	0.94206	0.92617	0.95701	-
Inlet T	315.3						K
Inlet P	1070						kPaa
Mol. Wt.	24.6						Kg/kmol
Outlet T	393.06	392.56	388.93	392.58	394.85	394.35	K
Outlet P	3224	3261	3198	3431	3430	3235	kPaa
Pressure Ratio	3.01	3.05	2.99	3.21	3.2	3.02	-
Flow rate	123,322	124,772	118,367	128,215	122,546	124,663	kg/hr
Shaft Power	6,217	6,183	5,920	6,634	6720	6,327	kW
Poly Efficiency	82.0	82.0	81.8	85.8	84.1	83.8	%
Rot Speed	0.90	0.90	0.88	0.91	0.91	0.90	-
Test Date	06/04/2010	06/04/2010	06/04/2010	06/04/2010	06/04/2010	06/04/2010	-

Table C2B. The referred parameter values for the site compressor performance analysis and diagnostics –April 2010

(II) Site compressor untreated data log since 2006

Test Date	13/6/06	13/6/06	13/6/06	14/6/06	14/6/06	14/6/06	14/6/06	7/9/06	1/8/08	1/8/08	Unit
Case	1	2	3	4	5	6	7	8	9	10	
Test Time	08:00	16:00	00:00	08:00	16:00	20:00	00:00	10:19	08:00	12:00	
Inlet T	38.2	39.1	32.0	36.6	41.0	32.4	31.5	38.7	36.0	47.0	C
Inlet P	10.10	10.90	10.20	10.40	10.30	9.75	10.52	10.10	11.00	11.40	Bara
Mol. Wt.	24.6	24.6	24.6	24.6	24.6	24.6	24.6	24.6	25.6	25.6	Kg/kmol
Outlet T	119.0	118.0	114.0	116.8	118.5	118.5	111.0	118.7	115.0	121.0	C
Outlet P	33	32.2	29.9	31.85	30.9	30.25	32	31.5	32	32	Bara
Flow rate	128,000	131,943	130,212	126,000	136,603	146,545	133,991	117,056	127,320	125,237	kg/hr
Poly Head	124.6	129.6	129.1	125.4	124.5	126.6	122.2	124.8	114.0	113.4	kJ/kg
Shaft Power	5,297	5,301	5,440	5,160	5,440	6,520	5,367	4,805	5,114	4,954	kW
Poly Efficiency	87.5	91.4	87.6	86.7	80.6	80.6	86.5	87.0	80.8	84.3	%
Rot Speed	0.91	-	0.92	0.9	0.9	0.93	0.9	0.922	0.89	-	-
Remark								DCS Screen Shot			-

Test Date	1/8/08	1/8/08	1/8/08	1/8/08	6/7/09	6/7/09	6/7/09	6/7/09	6/7/09	23/8/09	Unit
Case	11	12	13	14	15	16	17	18	19	20	
Test Time	16:00	20:00	00:00	04:00	12:00	16:00	20:00	00:00	04:00	08:00	
Inlet T	43.0	38.0	36.0	34.0	48.0	45.8	42.6	38.0	35.0	31.0	C
Inlet P	11.15	12.00	11.11	10.89	11.53	11.57	11.40	11.18	11.21	11.45	Bara
Mol. Wt.	25.6	25.6	25.6	25.6	26.1	26.1	26.1	26.1	26.1	26.1	Kg/kmol
Outlet T	120.0	117.0	116.0	116.0	122.0	120.0	117.0	117.0	114.0	119.0	C
Outlet P	32.76	32.20	32.40	31.89	31.90	32.00	32.40	32.60	32.00	31.98	Bara
Flow rate	125,382	123,412	123,633	123,040	131,131	135,410	127,160	143,604	127,597	123,439	kg/hr
Poly Head	117.3	105.8	114.4	114.5	109.2	108.4	110.1	111.9	108.4	109.3	kJ/kg
Shaft Power	4,937	5,022	5,030	5,155	4,995	5,148	4,792	5,756	4,995	5,638	kW
Poly Efficiency	84.4	74.0	80.0	77.5	81.2	80.8	82.8	79.1	85.0	68.0	%
Rot Speed	-	-	-	-	-	0.891	0.921	0.93	0.9	0.88	-
Remark											-

Test Date	23/8/09	23/8/09	23/8/09	23/8/09	23/8/09	6/4/10	6/4/10	6/4/10	6/4/10	6/4/10	Unit
Case	21	22	23	24	25	26	27	28	29	30	
Test Time	12:00	16:00	20:00	00:00	04:00	08:00	12:00	16:00	20:00	00:00	
Inlet T	31.4	31.0	31.0	31.3	31.2	35.0	37.0	48.0	41.0	36.0	C

Inlet P	11.56	11.50	11.28	11.44	11.28	11.44	11.34	11.54	11.08	10.91	Bara
Mol. Wt.	26.1	26.1	26.1	26.1	26.1	26.1	26.1	26.1	26.1	26.1	Kg/kmol
Outlet T	122.0	122.0	116.0	115.0	113.0	111.0	113.0	123.0	118.0	114.0	C
Outlet P	32.38	32.00	32.00	32.38	32.21	32.46	32.51	32.5	33.32	32.73	Bara
Flow rate	123,191	123,410	124,400	123,999	121,858	129,630	129,478	123,045	128,877	126,418	kg/hr
Poly Head	66.0	65.1	71.6	72.5	75.3	107.3	109.1	111.2	115.9	113.9	kJ/kg
Shaft Power	5,832	5,762	5,319	5,207	5,066	4,930	4,940	4,747	5,005	4,944	kW
Poly Efficiency	66.0	65.1	71.6	72.5	75.3	79.9	81.0	81.7	84.5	82.5	%
Rot Speed	0.88	0.871	0.891	0.89	0.89	0.89	0.89	0.89	0.91	0.9	-
Remark											-

Test Date	6/4/10	24/8/10	24/8/10								Unit
Case	31	32	33								
Test Time	04:00	08:00	14:00								
Inlet T	30.0	40.0	48.9								C
Inlet P	11.24	11.40	11.76								Bara
Mol. Wt.	26.1	26.1	26.1								Kg/kmol
Outlet T	106.0	115.0	122.2								C
Outlet P	31.96	32.20	32.02								Bara
Flow rate	129,584	126,320	125,020								kg/hr
Poly Head	110.5	108.6	107.6								kJ/kg
Shaft Power	5,123	4,787	4,722								kW
Poly Efficiency	85.1	81.2	80.0								%
Rot Speed	0.88	0.89	0.89								-
Remark			DCS Screen Shot								-

(III) Typical Performance Curves supplied by OEM

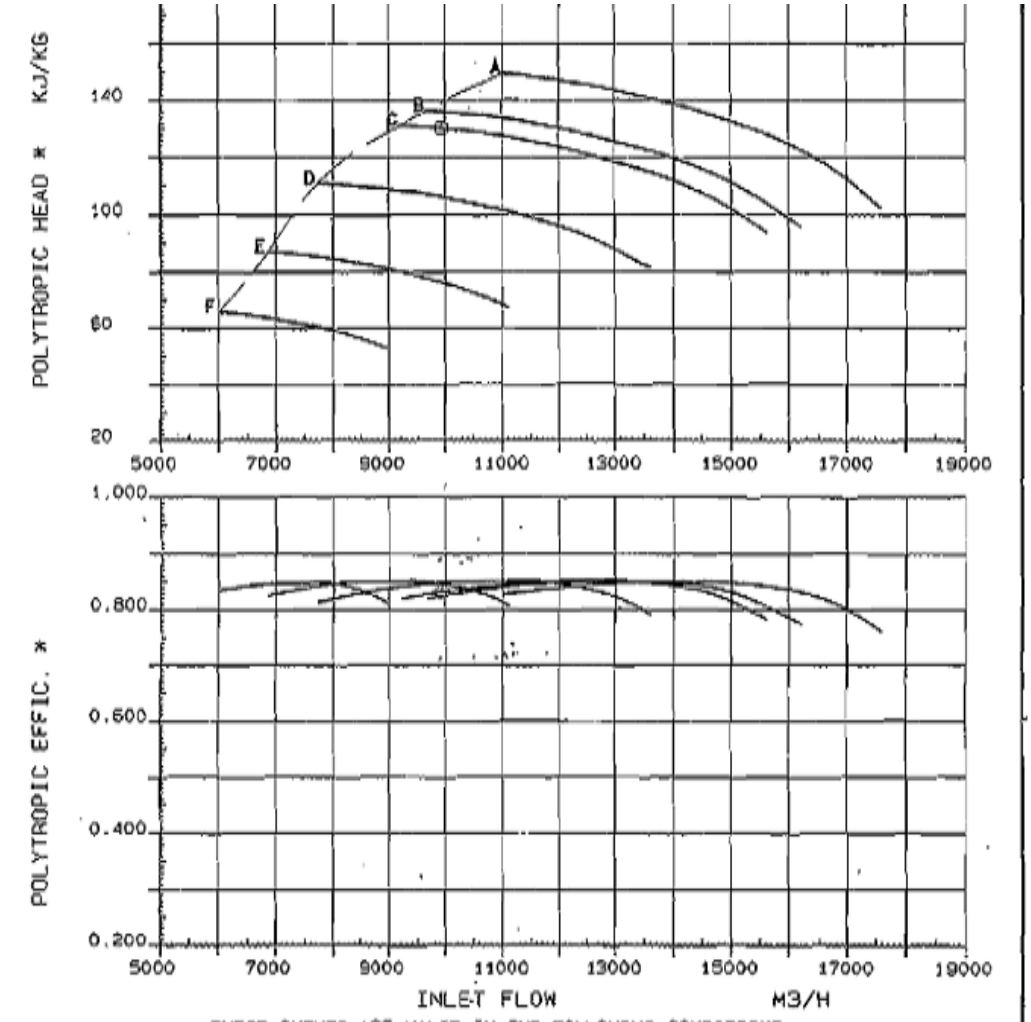

THESE CURVES ARE VALID IN THE FOLLOWING CONDITIONS

		RPM	
GAS HANDLED	RAG	A=9500	D=8142
MOLECULAR WEIGHT	24.59	B=9048	E=7238
INTAKE PRESSURE	9.43 BARA	C=8870	F=6333
INTAKE TEMPERATURE	5.1 DEG-C		
COMPRESS. AT SUCTION	0.952		
RATIO OF SPEC. HEATS	1.251		

* FLANGE TO FLANGE

JOB 1101641

Nuovo Pignone
FIRENZE

V.	DESCRIZIONE - DESCRIPTION	PREP'D	CONT-CHK'D	APP-APPR'D	DATA-DATE
1	Revised sheet				

N. SOS 98730 /4

TITOLO - TITLE QGPC
PREDICTED PERFORMANCE CURVES FOR CENTRIFUGAL COMPRESSORS

LINGUA-LANG. A

PAGINA-SHEET 46/47

SOSTITUISCE IL-REPLACES

SOSTITUITO DA-REPLACED BY

Appendix D

Performance Adaptation by Successive Iteration – Calculation Details

Performance Adaptation by Successive Iteration

D.1 Site and OEM Compressor Data

Three (3) site base case data at various compressor speeds (2Q 2006) and a wide range of OEM data are available for analysis in the proceeding works. The site data are shown in Table D1 below. A sample of the OEM performance curves for the site compressor closely matching the site conditions are shown in Figures D1 and D2 and full range of OEM data available for the compressor life cycle is shown in Table D15.

The site and OEM data will be treated as described in Chapter 4 for referring and de-dimensioning in accordance with Chart 1 in Chapter 4. These data will then be applied to deduce actual site performance using successive iteration method in accordance with Chart 2 in Chapter 4.

Site data for method application

The compressor data at site for 3 bases cases ranging from N=0.996 to N=0.900 are listed in Table D1 and these will be used in the analysis.

Table D1. Site compressor data for 3 base cases

Parameter	Base Case 1	Base Case 2	Base Case 3	Unit
Flow rate	150,400	145,000	126,000	kg/hr
	14370	13190	11220	Act m3/hr
Mol. Wt	24.6	24.6	24.6	kg/kmol
Inlet Press	1070	1090	1070	kPaa
Inlet Temp	42.1/315.3	34/307.2	23.5/296.7	Cº / Kº
Outlet Press	3130	3010	3200	kPaa
Outlet Temp	125/398.2	111.3/384.5	105/378.2	Cº / Kº
Rot Speed	0.996	0.93	0.900	-

OEM data for analysis

The unique advantage in this study is that there is a very wide range of OEM supplied data available for utilization and analysis. The OEM performance curves for various rotational speeds together with the associated inlet gas properties and compressor inlet conditions are listed in Table D15 at the end of this Appendix. Referring to this table, OEM Case Reference no. (17) is

ideally chosen for analysis as it closely resembles the site conditions. Figures D1-D2 show the performance curves for this case as supplied by OEM and Tables D2A-D7A list the numerical values of these curves.

The OEM curves are generated for a fleet of compressors rather than the specific compressor at site. However, these predicted curves are expected to have a fairly accurate (although not exact) representation of expected performance as the compressor is shop tested and commissioned under observed conditions under the ASME PTC10 tolerance requirements.

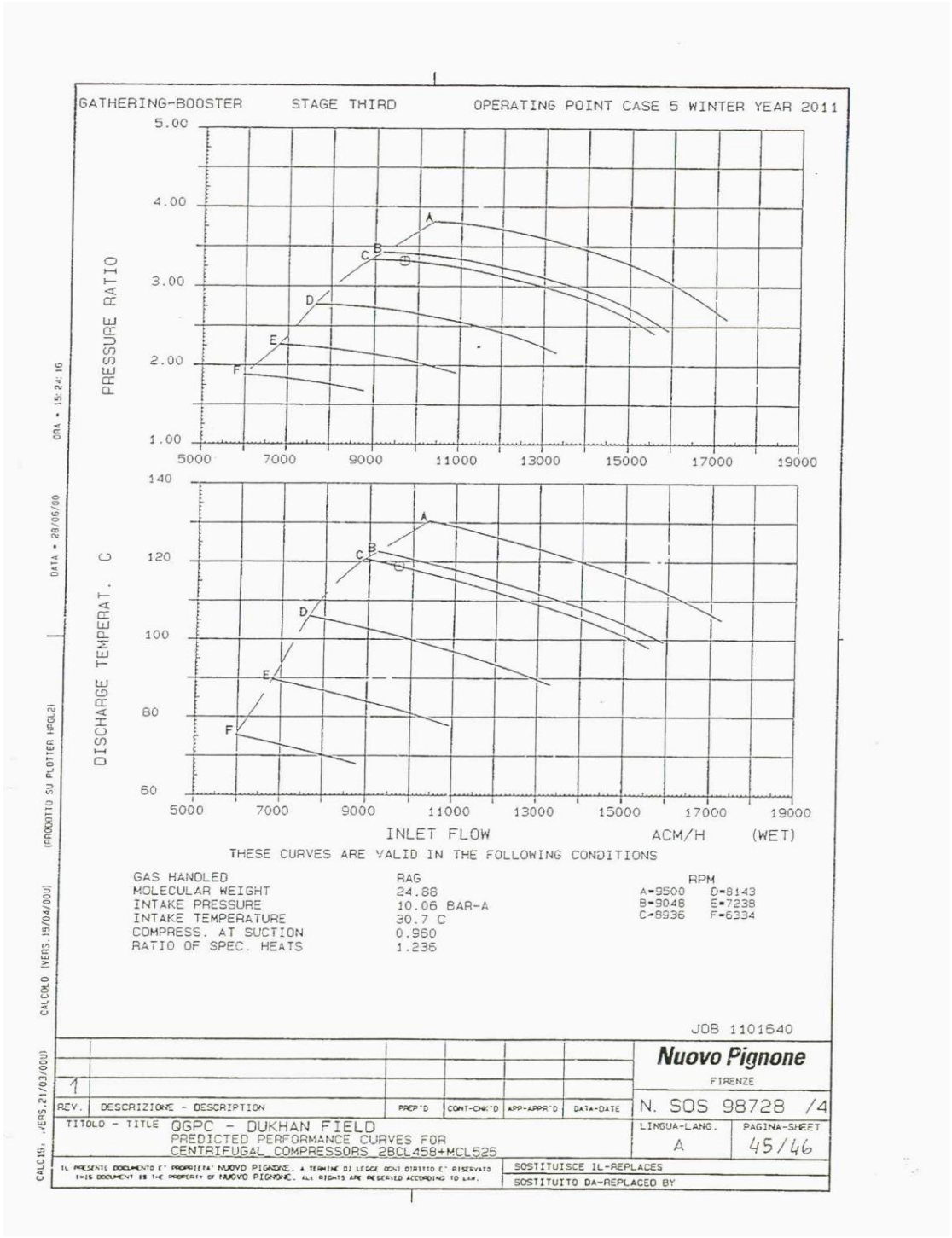

Figure D1. Pressure Ratio and Discharge Temperature versus Compressor Inlet Flow as supplied by OEM

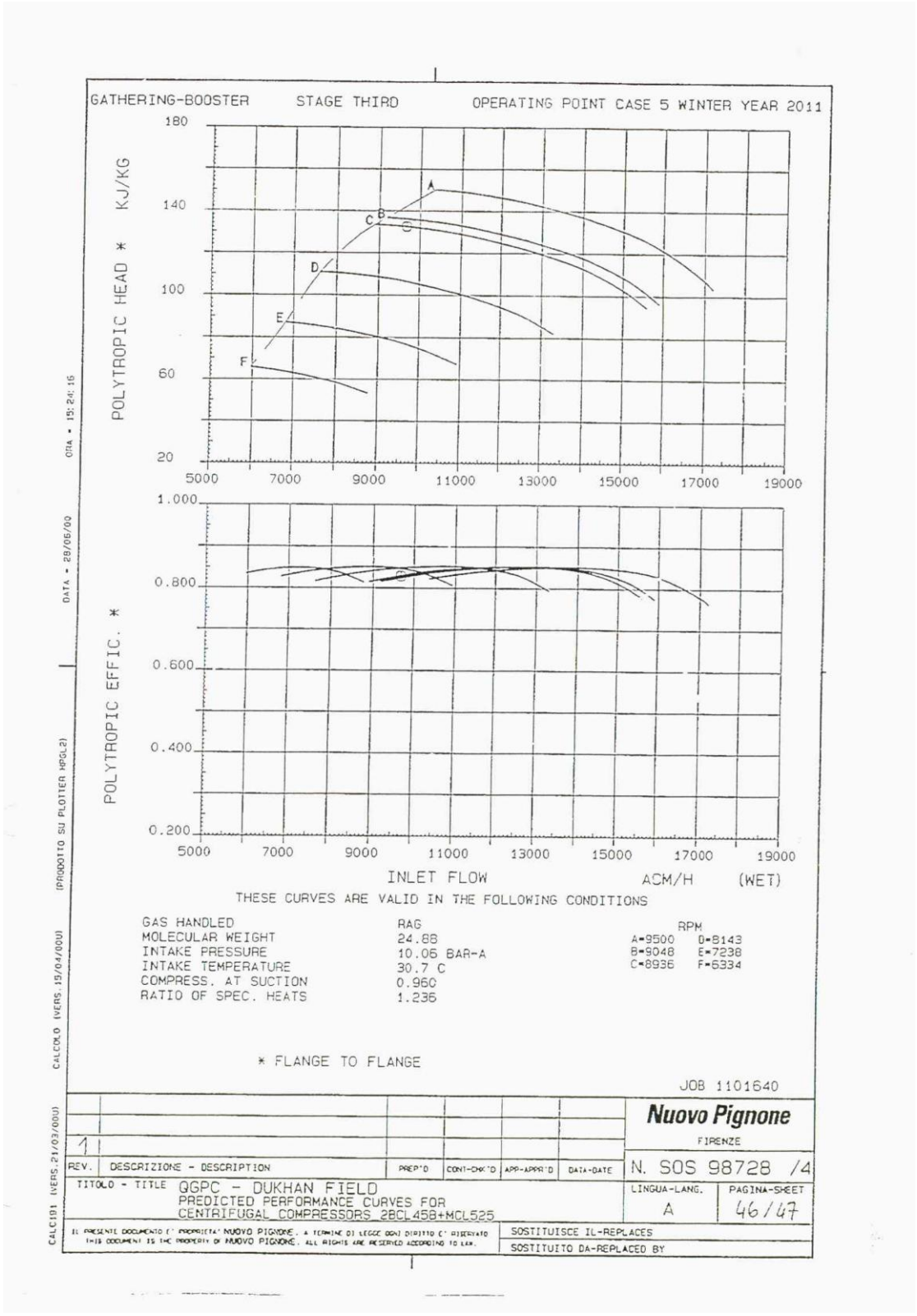

Figure D2. Polytropic Head and Efficiency versus Compressor Inlet Flow as supplied by OEM

Vol. Flow Rate m^3/h	Press. Ratio PR	Disch. Pressure bara	Disch. Temp °C	Mass Flow kg/h	Polytrop Head kJ/kg	Polytrop Efficiency %	Comp Shaft Power kW
10000	3.830	38.5	132.0	103207	152.0	82.0	5400
10500	3.820	38.4	130.4	108367	151.2	82.7	5575
11000	3.790	38.1	128.9	113527	150.0	83.3	5742
11500	3.760	37.8	127.4	118688	148.5	84.0	5915
12000	3.720	37.4	126.1	123848	146.7	84.5	6075
12500	3.675	37.0	124.5	129008	144.5	84.5	6235
13000	3.623	36.4	123.0	134169	142.3	84.5	6390
13500	3.560	35.8	121.5	139329	140.2	84.5	6505
14000	3.490	35.1	120.0	144489	137.6	84.5	6590
14370	3.430	34.5	118.5	148308	135.3	84.5	6640
14500	3.410	34.3	118.0	149650	134.5	84.5	6660
15000	3.310	33.3	116.0	154810	131.0	84.5	6720
15500	3.190	32.1	114.0	159970	127.3	84.5	6770
16000	3.040	30.6	111.8	165131	122.0	84.0	6795
16500	2.870	28.9	109.0	170291	115.0	81.0	6815
17000	2.700	27.2	106.0	175451	107.0	77.5	6810

Table D2A. Rated Process Conditions Direct From OEM for N=1 (9500 RPM)

Vol. Flow Rate m^3/h	Press. Ratio PR	Disch. Pressure bara	Disch. Temp °C	Mass Flow kg/h	Polytrop Head kJ/kg	Polytrop Efficiency %	Comp Shaft Power kW
9200					137.0	80.3	4520
9500	3.410	34.3	121.8	98046	135.0	81.7	4630
10000	3.407	34.3	120.4	103207	133.0	82.9	4780
10500	3.393	34.1	119.0	108367	131.4	83.7	4920

11000	3.380	34.0	117.5	113527	129.9	84.3	5055
11500	3.320	33.4	116.1	118688	129.2	84.4	5160
12000	3.281	33.0	114.7	123848	128.2	84.4	5260
12500	3.228	32.5	113.2	129008	126.4	84.5	5350
13000	3.171	31.9	111.6	134169	124.3	84.5	5435
13500	3.104	31.2	109.9	139329	121.5	84.5	5495
14000	3.030	30.5	108.1	144489	120.3	84.5	5560
14370	2.950	29.7	106.8	148308	118.1	84.5	5595
14500	2.930	29.5	106.4	149650	114.1	84.5	5610
15000	2.820	28.4	104.2	154810	109.7	83.6	5655
15500	2.700	27.2	102.0	159970	104.3	82.0	5685
16000	2.550	25.7	99.5	165131	97.1	79.5	5700
16500	2.385	24.0		170291			

Table D3A. Rated Process Conditions Direct From OEM for N=0.952 (9048 RPM)

Vol. Flow Rate m^3/h	Press. Ratio PR	Disch. Pressure bara	Disch. Temp °C	Mass Flow kg/h	Polytrop Head kJ/kg	Polytrop Efficiency %	Comp Shaft Power kW
9000	3.345	33.7	120.2	92886	134.0	80.5	4310
9500	3.323	33.4	118.8	98046	132.5	81.8	4440
10000	3.300	33.2	117.5	103207	131.0	83.0	4580
10500	3.273	32.9	116.0	108367	129.4	83.7	4740
11000	3.245	32.6	114.8	113527	127.9	84.4	4880
11220	3.220	32.4	114.1	115798	127.0	84.4	4930
11500	3.195	32.1	113.3	118688	126.0	84.4	5000
12000	3.145	31.6	112.0	123848	124.2	84.5	5100
12500	3.073	30.9	110.5	129008	122.1	84.5	5200
13000	3.000	30.2	109.0	134169	119.3	84.5	5290
13190	2.980	30.0	108.2	136130	118.0	84.5	5310

13500	2.917	29.3	107.0	139329	115.8	84.5	5350
14000	2.830	28.5	105.0	144489	111.8	84.5	5400
14500	2.705	27.2	102.8	149650	107.4	83.7	5450
15000	2.580	26.0	100.5	154810	102.0	82.6	5485
15500	2.420	24.3	97.8	159970	94.8	80.4	5500
16000	2.260	22.7	95.0	165131		78.0	5500

Table D4A. Rated Process Conditions Direct From OEM for N=0.941 (8936 RPM)

Vol. Flow Rate m^3/h	Press. Ratio PR	Disch. Pressure bara	Disch. Temp °C	Mass Flow kg/h	Polytrop Head kJ/kg	Polytrop Efficiency %	Comp Shaft Power kW
7700			106.0	79469	110.6	82.0	3038
8000	2.770	27.9	105.0	82565	110.5	82.5	3115
8500	2.736	27.5	103.6	87726	109.6	83.3	3250
9000	2.710	27.3	102.5	92886	108.8	84.0	3385
9500	2.680	27.0	101.2	98046	106.8	84.3	3500
10000	2.640	26.6	99.8	103207	104.8	84.5	3615
10500	2.601	26.2	98.3	108367	102.6	84.5	3710
11000	2.550	25.7	96.8	113527	100.3	84.5	3810
11500	2.500	25.2	95.0	118688	97.7	84.3	3890
12000	2.420	24.3	93.2	123848	94.1	84.0	3950
12500	2.337	23.5	91.6	129008	90.6	83.4	3985
13000	2.225	22.4	89.9	134169	85.6	82.0	4000
13300			88.5	137265	81.5	79.5	4008

Table D5A. Rated Process Conditions Direct From OEM for N=0.857 (8143 RPM)

Vol. Flow Rate m^3/h	Press. Ratio PR	Disch. Pressure bara	Disch. Temp °C	Mass Flow kg/h	Polytrop Head kJ/kg	Polytrop Efficiency %	Comp Shaft Power kW
6800			89.8	70181	86.8	82.8	2077

7000	2.270	22.8	89.2	72245	86.4	83.0	2115
7500	2.250	22.6	87.8	77405	85.8	83.9	2231
8000	2.200	22.1	86.3	82565	83.8	84.3	2315
8500	2.170	21.8	85.0	87726	82.6	84.5	2400
9000	2.120	21.3	83.4	92886	80.0	84.5	2469
9500	2.081	20.9	82.0	98046	77.4	84.5	2538
10000	2.028	20.4	80.6	103207	74.1	83.5	2608
10500	1.950	19.6	79.0	108367	70.6	82.0	2638
11000	1.860	18.7	77.2	113527	66.8	80.0	2692

Table D6A. Rated Process Conditions Direct From OEM for N=0.762 (7238 RPM)

Vol. Flow Rate m^3/h	Press. Ratio PR	Disch. Pressure bara	Disch. Temp °C	Mass Flow kg/h	Polytrop Head kJ/kg	Polytrop Efficiency %	Comp Shaft Power kW
6000	1.840	18.5	75.0	61924	65.6	83.0	1385
6500	1.810	18.2	74.0	67084	64.4	83.8	1462
7000	1.770	17.8	72.9	72245	62.7	84.2	1538
7500	1.730	17.4	71.5	77405	61.4	84.3	1600
8000	1.690	17.0	70.2	82565	57.9	83.8	1650
8500	1.640	16.5	68.6	87726	55.2	82.7	1692
9000	1.580	15.9	67.0	92886	51.8	81.0	1725

Table D7A. Rated Process Conditions Direct From OEM for N=0.667 (6334 RPM)

Table D8 below summarizes the gas inlet conditions as supplied by OEM used in the analysis. It may be noted that it is a pure coincident that a single set of OEM compressor data (One of the OEM Case References) resembles the compressor site conditions in Table D1.

Parameter	Rated Performance Data By OEM (OEM Ref Case 17 of Table D15)
Mol. Wt	24.88

Inlet P / kPaa	1006
Inlet T /K	303.85
Suction Z	0.960
Sp. Ht. Ratio	1.236

Table D8. OEM Supplied Compressor Data chosen for analysis

D.2 Compressor Data Analysis

D.2.1 Referring of OEM Performance Data

The OEM performance curves are supplied from the vendor for the rated conditions based on a set of predefined compressor inlet conditions and physical properties of throughput gas. However, the gas physical, gas inlet and environmental conditions at site as well as the rotational speed hardly ever matches with the OEM base data; therefore the OEM performance data and performance curves need to be modified to enable comparison with the site conditions. The most common condition of gas inlet to the site compressor is nominally chosen as the datum or Referred conditions. The closest available set of OEM data (Table D15) to the referred conditions is the Site Base Case 1 (see Table D1) and these are listed in Table D9.

	Referred Conditions (site base case 1, Table D1)	**Rated OEM Conditions** (OEM Ref Case 17 of Table D15)
Gas Handled	Site Gas	Specific Gas
Mol. Weight	24.60	24.88
Suction Pressure, kPaa	1070	1006
Intake Temperature, K	315.30	303.85
Compressibility	0.959	0.960
Cp/Cv	1.210	1.236

Table D9 Basis of Conditions for generation of Referred OEM Performance Curves

D.2.1.1 Sample Calculation for the Determination of Referred Values for the OEM and Site Data

Reference to the equations stated and developed under Chapter 4.1 in Chapter 4, the following equations are used:

Theta (θ) = T_1/ T_{ref} (Dimensionless) (1)

Delta (δ) = P_1/ P_{ref} (Dimensionless) (2)

The subscript "1" refers to compressor inlet conditions. T_{ref} and P_{ref} are arbitrary chosen values as a base temperature and base pressure upon which all the operating variables either from OEM or site are compared. It is normal to set reference values same as the most common site compressor inlet conditions for temperature, pressure and the molecular weight controlling the

mass flow. For an “n” set of site cases, there will be an “n” set of Thetas (θ) and Deltas (δ).

The flowchart for the methodology of the performance scaling is shown in chart 1 in Chapter 4.

The following are the equations used to refer the OEM and test data:

$T_{referred} = T_n / \theta$ (3)

$P_{referred} = P_n / \delta$ (4)

$m_{referred} = W * \sqrt{(\theta)} / \delta$ (5)

$PW_{referred} = PW / (\delta * \sqrt{(\theta)})$ (6)

$N_{referred} = N / \sqrt{(\theta)}$ (7)

$EEP_{referred} = EEP / 1$ (8)

Where, n=1, 2

In this work, subscript “1” refers to inlet of compressor and “2” refers to the compressor outlet.

The Referring of OEM Data

Referring to equations (1) and (2) above:

Theta, $\theta = T_1 / T_{ref}$

Delta, $\delta = P_1 / P_{ref}$

Now,

T_1 = 303.85 K (from Table D8)

T_{ref} = 315.3 (Base Case 1, from Table D1)

Therefore:

θ = 303.85/315.3

θ = 0.964

And,

P_1 = 1006 kPaa (from Table D8)

P_{ref} = 1070 kPaa (Base Case 1, from Table D1)

δ = 1006/1070

δ = 0.940

Other cases follow suit. The Theta and Delta for OEM data are shown in Table D10.

Scaling Parameter	Value for OEM
θ	0.964
δ	0.940

Table D10. Theta and Delta for OEM data

Note that for n set of cases there will be expected to be an n set of Theta and Delta values. But here there is only one OEM case suitably close to all available compressor inlet conditions at site. This is why there is one unique θ and one unique δ.

By using Equations (3) to (9), these are the calculation procedures to obtain the referred values for OEM data:

From Table D8 for rated OEM data at the compressor inlet:

Mol. Wt : 24.88

Inlet P / kPaa: 1006

Inlet T /K : 303.85

From Table D2A:

N=1 (9500 RPM),

q=10,000 m3/hr

PR=3.83

Outlet T= 132.0 C (405.15 K)

EEP=82.0%

We need to change volume flow into mass flow; using equation (9) for the mass flow rate:

Mass Flow, w = 10,000 x (1006 x 24.88) / (0.960 x 8.314 x 303.85) = 103, 207 kg/hr

Outlet P = Inlet P x PR = 1006 x 3.83 = 3853 kPaa (or 38.5 Bara)

Now, from Table D10 :

θ = 0.964

δ = 0.940

By applying the values of θ and δ above into equations 3-8, the corresponding referred values are obtained:

Referred Mass Flowrate = 103, 207 * √ (0.964) / 0.94 * (24.6/24.88) = 106,548 kg/hr

The last term in the equation is the correction for molecular weight change from OEM to the referred value.

Referred Outlet T = 405.15 / 0.964 = 420.4 K

Referred Outlet P = 3853 / 0.94 = 4090 kPaa

Referred Shaft Power = 5400/ [0.94 * √ (0.964)] = 5851 kW

Referred N = 1 / √ (0.964) = 1.019

Referred EEP = 82 / 1 = 82.0 (Note that referred polytropic efficiency is same as OEM [Ref. 56])

Having shown the sample calculation the referred values for each OEM case are developed and tabulated in Tables D2B-D7B. These referred Tables correspond to Tables D2A-D7A which are the untreated or uncorrected OEM data.

Table D2B. Corrected or Referred parameters of OEM data for N=1 (based on Table D2A)

Referred Mass Flow kg/hr	Referred Discharge T K	Referred Discharge P Bara	Referred Pressure Ratio -	Referred Shaft Power kW	Referred Polytropic Eff %	Referred N -
106548	420.4	40.9	3.827	5851	82.0	1.0187
111876	418.8	40.8	3.817	6040	82.7	1.0187
117203	417.2	40.5	3.787	6221	83.3	1.0187
122531	415.6	40.2	3.757	6409	84.0	1.0187
127858	414.3	39.8	3.718	6582	84.5	1.0187
133185	412.6	39.4	3.678	6755	84.5	1.0187
138513	411.1	38.7	3.618	6923	84.5	1.0187
143840	409.5	38.1	3.559	7048	84.5	1.0187
149167	408.0	37.3	3.489	7140	84.5	1.0187
153110	406.4	36.7	3.429	7194	84.5	1.0187
154495	405.9	36.5	3.410	7216	84.5	1.0187
159822	403.8	35.4	3.310	7281	84.5	1.0187
165149	401.7	34.1	3.191	7335	84.5	1.0187
170477	399.5	32.5	3.042	7362	84.0	1.0187

175804	396.6	30.7	2.873	7384	81.0	1.0187
181132	393.4	28.9	2.704	7378	77.5	1.0187

Table D3B. Corrected or Referred parameters of OEM data for N=0.952 (based on Table D3A)

Referred Mass Flow kg/hr	Referred Discharge T K	Referred Discharge P Bara	Referred Pressure Ratio -	Referred Shaft Power kW	Referred Polytropic Eff %	Referred N -
101221	409.8	36.5	3.410	5016	81.7	0.9698
106548	408.4	36.5	3.407	5179	82.9	0.9698
111876	406.9	36.3	3.393	5331	83.7	0.9698
117203	405.4	36.2	3.380	5477	84.3	0.9698
122530	403.9	35.5	3.320	5591	84.4	0.9698
127858	402.5	35.1	3.281	5699	84.4	0.9698
133185	400.9	34.5	3.228	5797	84.5	0.9698
138513	399.2	33.9	3.171	5889	84.5	0.9698
143840	397.4	33.2	3.104	5954	84.5	0.9698
149167	395.6	32.4	3.030	6024	84.5	0.9698
153110	394.3	31.6	2.950	6062	84.5	0.9698
154495	393.9	31.4	2.930	6078	84.5	0.9698
159822	391.6	30.2	2.820	6127	83.6	0.9698
165150	389.3	28.9	2.700	6160	82.0	0.9698
170477	386.7	27.3	2.550	6176	79.5	0.9698
175804	-	25.5	2.385	-	-	-

Table D4B. Corrected or Referred parameters of OEM data for N=0.941 (based on Table D4A)

Referred Mass Flow	Referred Discharge T	Referred Discharge P	Referred Pressure Ratio	Referred Shaft Power	Referred Polytropic Eff	Referred N

kg/hr	K	Bara	-	kW	%	-
95893	408.2	35.8	3.350	4670	80.5	0.9586
101220	406.7	35.5	3.320	4811	81.8	0.9586
106548	405.4	35.3	3.300	4962	83.0	0.9586
111876	403.8	35.0	3.270	5136	83.7	0.9586
117203	402.6	34.7	3.241	5287	84.4	0.9586
119547	401.8	34.5	3.221	5342	84.4	0.9586
122531	401.0	34.1	3.191	5417	84.4	0.9586
127858	399.7	33.6	3.141	5526	84.5	0.9586
133185	398.1	32.9	3.072	5634	84.5	0.9586
138513	396.6	32.1	3.002	5732	84.5	0.9586
140537	395.7	31.9	2.982	5753	84.5	0.9586
143840	394.5	31.2	2.913	5797	84.5	0.9586
149167	392.4	30.3	2.833	5851	84.5	0.9586
154495	390.1	28.9	2.704	5905	83.7	0.9586
159822	387.7	27.7	2.584	5943	82.6	0.9586
165149	384.9	25.8	2.416	5959	80.4	0.9586
170477	382.0	24.1	2.256	5959	78.0	0.9586

Table D5B. Corrected or Referred parameters of OEM data for N=0.857 (based on Table D5A)

Referred Mass Flow kg/hr	Referred Discharge T K	Referred Discharge P Bara	Referred Pressure Ratio -	Referred Shaft Power kW	Referred Polytropic Eff %	Referred N -
82042	393.4	-	-	3292	82.0	0.8730
85239	392.4	29.6	2.770	3375	82.5	0.8730
90566	390.9	29.3	2.736	3521	83.3	0.8730
95893	389.8	29.0	2.710	3667	84.0	0.8730
101221	388.4	28.7	2.680	3792	84.3	0.8730

106548	387.0	28.2	2.640	3917	84.5	0.8730
111876	385.4	27.8	2.601	4020	84.5	0.8730
117203	383.9	27.3	2.550	4128	84.5	0.8730
122530	382.0	26.8	2.500	4215	84.3	0.8730
127858	380.2	25.9	2.420	4280	84.0	0.8730
133185	378.4	25.0	2.337	4317	83.4	0.8730
138513	376.7	23.8	2.225	4334	82.0	0.8730
141709	375.3	-	-	4342	79.5	0.8730

Table D6B. Corrected or Referred parameters of OEM data for N=0.762 (based on Table D6A)

Referred Mass Flow kg/hr	Referred Discharge T K	Referred Discharge P Bara	Referred Pressure Ratio -	Referred Shaft Power kW	Referred Polytropic Eff %	Referred N -
72453	376.6	-	-	2250	82.8	0.7762
74584	376.0	24.3	2.270	2292	83.0	0.7762
79911	374.6	24.1	2.250	2417	83.9	0.7762
85239	373.0	23.5	2.200	2509	84.3	0.7762
90566	371.6	23.2	2.170	2600	84.5	0.7762
95893	370.0	22.7	2.120	2675	84.5	0.7762
101221	368.5	22.3	2.081	2750	84.5	0.7762
106548	367.1	21.7	2.028	2825	83.5	0.7762
111876	365.4	20.9	1.950	2859	82.0	0.7762
117203	363.6	19.9	1.860	2917	80.0	0.7762

Table D7B. Corrected or Referred parameters of OEM data for N=0.667 (based on Table D7A)

Referred Mass Flow kg/hr	Referred Discharge T K	Referred Discharge P Bara	Referred Pressure Ratio -	Referred Shaft Power kW	Referred Polytropic Eff %	Referred N -

63929	361.3	19.7	1.840	1500	83.0	0.6795
69256	360.2	19.4	1.810	1584	83.8	0.6795
74584	359.1	18.9	1.770	1667	84.2	0.6795
79911	357.6	18.5	1.730	1734	84.3	0.6795
85239	356.3	18.1	1.690	1788	83.8	0.6795
90566	354.6	17.5	1.640	1834	82.7	0.6795
95893	353.0	16.9	1.580	1869	81.0	0.6795

The Referring of Site Performance Data

The determination of Theta and Delta for the Site Base Cases will follow the same format as OEM described above and these are listed in Table D11below.

Theta (θ) and Delta (δ) will be unity for the base case 1 because this case was used as reference.

For site Base Case 2,

T_1 = 307.2 K (from Table D1)

T_{ref} = 315.3 (from Table D9)

Therefore for Site Base case 2,

θ = 307.2/315.3

θ = 0.9743

And,

P_1 = 1090 kPaa (from Table D1)

P_{ref} = 1070 kPaa (from Table D9)

δ = 1090/1070

δ = 1.0187

It may be noted that Theta and Delta are always unity for the datum values.

	Base case 1	Base case 2	Base case 3
θ	1.0000	0.9743	0.9410

δ	1.0000	1.0187	1.0000

Table D11. Theta and Delta for Site data

By using Equations (3) to (8) and applying the values in Tables D10 and D11, the following referred values are obtained for Site data in Table D12. It is to be noted that the inlet conditions are the same for all cases.

Parameter	Base Case 1	Base Case 2	Base Case 3	Unit
Inlet T	315.3			K
Inlet P	1070			kPaa
Mol. Wt.	24.6			kg/kmol
Outlet T	398.2	394.6	401.9	K
Outlet P	3130	2955	3200	kPaa
PR	2.93	2.76	2.99	-
Flow rate	150,400	140,499	122,227	kg/hr
Power	6784	6075	5775	kW
Rot Speed	0.996	0.942	0.928	-

Table D12. Corrected or Referred Site Test Data

D.2.3 Referred OEM data interpolation and deduction of scale factors

The numerical referred OEM speeds do not match the site referred speeds. From Table D12 the referred speeds are 0.996, 0.942 and 0.928. We do not have referred OEM speeds for these referred site speeds. Therefore the site and OEM speeds are required to be made the same. In order to do this, interpolate is needed, as described in Chapter 4, between the appropriate speeds that fall above and below the referred OEM speed and these are the details how the interpolation is accurately carried out:

Look at TWO referred OEM speeds that encompass the site referred speed, case by case. For Site Base Case 1 (Table D1), there is a referred speed of 0.996. We do not have a referred OEM speed of 0.996 but there is a performance curve for OEM referred speed of 1.0187 (Table D2B) and another curve for OEM $N_{referred}$ value of 0.9698 (Table D3B). Thus the site N_{ref} of 0.996 falls between these two OEM values and OEM curves are generated by dividing the space between two OEM curves into quality lines one of which matched the site referred speed of 0.996. A Scale Factor is deduced by comparing the Site referred pressure ratio with OEM referred pressure ratio for the same referred speeds of OEM and Site and this scale factor is then applied to the whole of the OEM referred curve to establish the site PR versus

referred mass flow curve. The referred OEM speed curves lower than 0.996 are shifted by the same scale factor.

For Pressure Ratios and Polytropic efficiencies the scale factors are summarized in Table D13 and Table D14 respectively.

	Site base case 1	Site base case 2	Site base case 3
Referred N	0.996	0.942	0.928
Scale Factor	0.896	1.118	1.116

Table D13. Pressure Ratio Scale Factors for site and OEM data matching

	Site base case 1	Site base case 2	Site base case 3
Referred N	0.996	0.942	0.928
Scale Factor	1.024	1.032	1.005

Table D14. Polytropic Efficiency Scale Factors for site and OEM data matching

D2.4 Performance Adaptation by Successive Iteration

Reference to Chart 2 in Chapter 4, it is stated that for performance adaptation by successive iteration the scale factor need to be obtained (by comparing actual to ideal performance at the prevailing conditions) starting from the highest referred speed in the first iteration, and shift all the performance maps accordingly. Going to the second highest speed in the second iteration, the 1st speed curve remains fixed and the 2nd speed curve and all the lower curves are shifted down by the scale obtained in the 2nd iteration. In the 3rd iteration, the 1st and second speed curve stays fixed and the 3rd and lower speeds are shifted by the scale factor obtained from the 3rd highest speed. This is repeated until all referred test data are completed. At the end, there will be a set of performance curves on the referred and modified OEM curves with the test points falling exactly on the curves giving a much accurate prediction of actual performance

The same procedure is applied to other site data and variables versus referred mass flow rate and the overall performance fro pressure ratio is shown in Graph D1.

Applying the same procedures above to polytropic efficiencies, Graph D2 is obtained representing the polytropic efficiency versus referred mass flow rate for the referred test site speeds as well as predictions for the lower speeds.

Graph D3 illustrates the superimposition of extreme winter and extreme summer case on the referred PR versus referred mass flow. As expected, there is good overlap of referred performance curves because regardless of

environmental conditions, it is still the same compressor performing and small differences are contributed to differences in referred RPMs and tolerances in performance predictions. The superimposition of extreme cases is for illustration purposes only and it is recommended that the datum OEM data chosen to establish theta and delta should be carefully chosen such that differences between the site inlet conditions and the referred case or datum are as close to each other as possible.

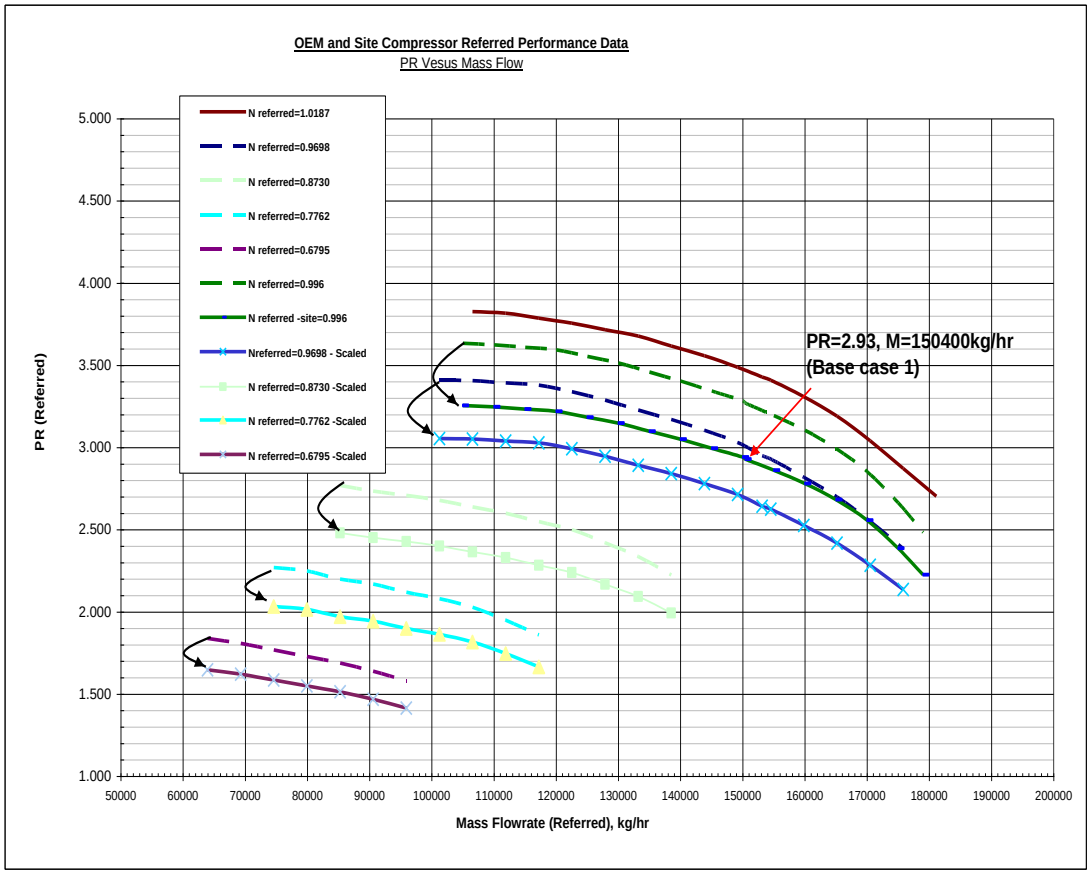

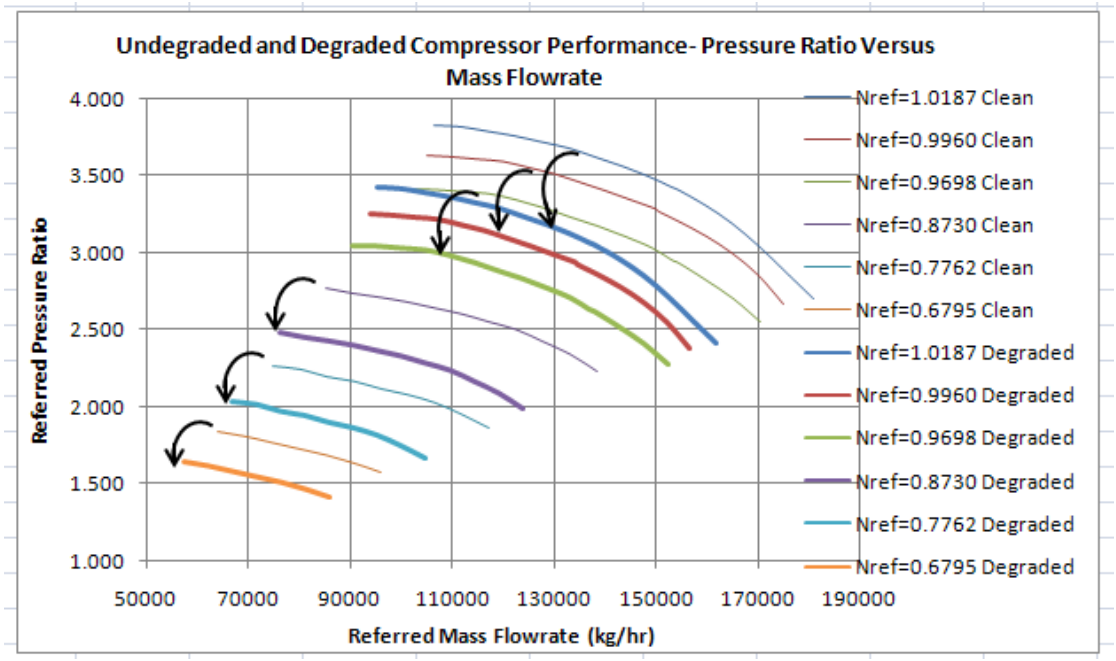

Graph D1. Performance Adaptation by Successive Iteration for Pressure Ratio

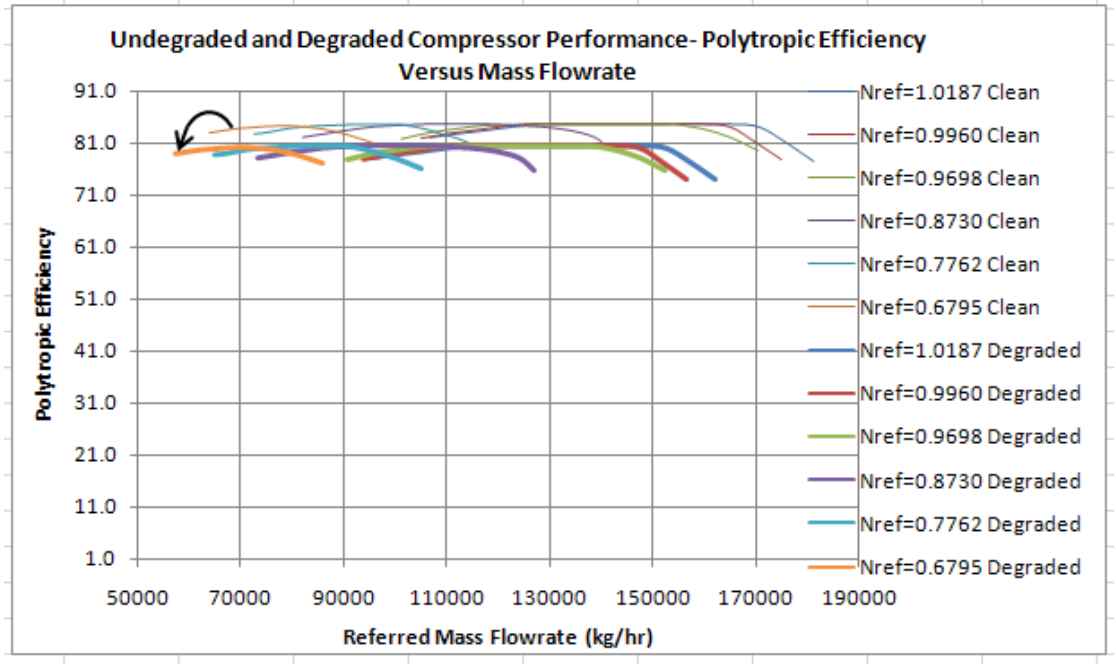

Graph D2. Performance Adaptation by Successive Iteration for Polytropic Efficiency

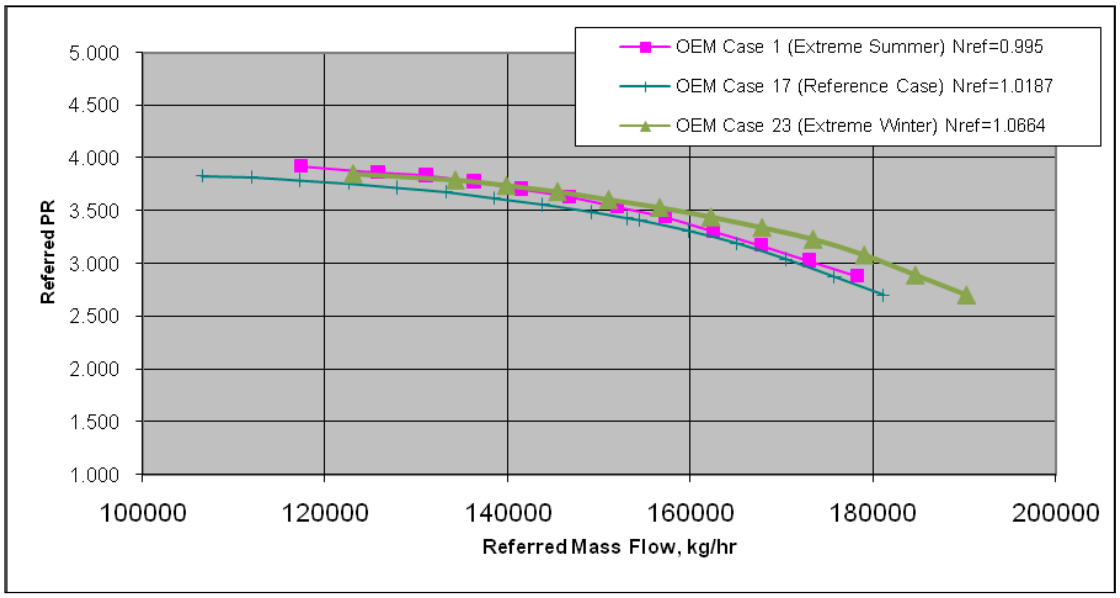

Graph D3. Referred values obtained from extreme summer and extreme winter OEM data (reference Table D15, below) superimposed on data derived for OEM reference case.

Table D15. The Conditions At Which Predicted Performance Curves Are Available From OEM For The Site Compressor

OEM Case Ref.	Graph Indicator	Time	M	Intake Press	Intake Temp	Z @ Suction	Cp/Cv	SPEED RPM CURVES BY OEM					
No.	Case No.			Bara	C			A	B	C	D	E	F
1	1	summer 04	27.24	11.31	45.3	0.953	1.213	9500	9048	8671	8142	7238	6333
2	11	summer 05	26.27	10.01	40.2	0.96	1.222	9500	9048	8824	8143	7238	6334
3	3	winter 04	25.71	10.42	17	0.949	1.239	9500	9048	8604	8142	7238	6333
4	4	summer 04	27.42	10.3	44.6	0.956	1.21	9500	9048	8526	8142	7238	6333
5	5	winter 11	24.59	9.43	6.1	0.952	1.251	9500	9048	8870	8142	7238	6333
6	6	winter 11	26.29	10.12	25.2	0.951	1.227	9500	9048	8523	8142	7238	6333
7	7	summer 04	27.57	11.06	47.4	0.953	1.209	9500	9048	8768	8142	7238	6333
8	8	summer 04	26.77	11.13	44.6	0.955	1.216	9500	9048	8671	8142	7238	6333
9	9	summer 04	27.52	11.1	46.7	0.953	1.21	9429	8980	8795	8081	7184	6285
10	10	summer 04	27.68	11.05	47.3	0.953	1.209	9492	9040	8763	8135	7232	6327
11	11	summer	26.02	9.32	40.1	0.963	1.222	9500	9188	9048	8142	7238	6333
12	11	winter	23.33	8.79	3.7	0.96	1.264	9500	9463	9048	8142	7238	6333
13	1	summer 04	28.24	11.77	45.5	0.947	1.207	9500	9048	8180	7238	6334	
14	2	winter 04	25.18	10.28	19.4	0.954	1.243	9500	9048	8677	8143	7238	6334
15	3	winter 04	26.92	11.1	20.5	0.941	1.23	9500	9048	8180	7238	6334	
16	4	summer 11	27.69	10.86	43.1	0.952	1.21	9500	9048	8224	7238	6334	
17	5	winter 11	24.88	10.06	30.7	0.96	1.236	9500	9048	8936	8143	7238	6334
18	6	winter 11	26.84	10.99	23.9	0.943	1.225	9500	9048	8143	8033	7238	6334
19	7	summer 04	28.26	11.75	45.5	0.947	1.207	9500	9048	8210	7238	6334	
20	8	summer 04	28.15	11.8	45.4	0.947	1.208	9500	9048	8208	7238	6334	
21	9	summer 04	26.92	11.79	47	0.953	1.215	9500	9048	8349	8143	7238	6334
22	10	summer 04	28.24	11.77	45.4	0.947	1.207	9500	9048	8208	7238	6334	
23	11	winter	23.48	9.4	4.1	0.957	1.264	9500	9135	9048	8143	7238	6334